5-2010

Chromatographic Studies of Drug-Protein Binding in Diabetes

Kathryn (Krina) S. Joseph
krina.joseph@huskers.unl.edu

CHROMATOGRAPHIC STUDIES OF DRUG-PROTEIN BINDING IN DIABETES

By

Kathryn (Krina) S. Joseph

A DISSERTATION

Presented to the Faculty of

The Graduate College at the University of Nebraska

In Partial Fulfillment of Requirements

For the Degree of Doctor of Philosophy

Major: Chemistry

Under the Supervision of Professor David S. Hage

Lincoln, Nebraska

May, 2010

CHROMATOGRAPHIC STUDIES OF DRUG-PROTEIN BINDING IN DIABETES

K.S. Joseph, Ph.D.

University of Nebraska, 2010

Advisor: David S. Hage

Drug-protein binding can have a dramatic impact on the distribution and metabolism of a drug. This manuscript describes the use of high-performance affinity chromatography to examine the binding of various compounds to human serum albumin (HSA) in normal and diabetic disease states.

The first study examined the use of four coumarin compounds as possible alternatives to warfarin as a probe for Sudlow site I on HSA. High-performance affinity chromatography and immobilized HSA columns were used to compare and evaluate the binding properties of these probe candidates. It was found from this group that 4-hydroxycoumarin was the best alternative to warfarin for drug-protein binding studies on HSA.

The primary portion of this manuscript examined the binding of sulfonylurea drugs to HSA as the glycation level of HSA was increased. This work was performed by using high-performance affinity chromatography to determine the binding regions, affinities, and the number of binding sites on HSA for sulfonylureas. The first part of this study examined the binding of two sulfonylureas to non-glycated HSA. Frontal analysis and competition studies indicated that the sulfonylureas had two major classes of binding

sites on HSA, with strong interactions occurring at both Sudlow sites I and II. The second part of this study examined the binding of two probe compounds, warfarin and L-tryptophan, to HSA as glycation levels of this protein increased. This study found no significant difference in the binding of warfarin to glycated HSA but observed some increases in the binding constant of L-tryptophan. The third part of the study examined the binding of the sulfonylureas to HSA with increasing levels of glycation. Minor alterations in binding were observed as the level of glycation increased. Lastly, theoretical studies were also performed to elucidate the appropriate analyte concentrations necessary for examining multi-site binding systems, such as those observed for some drug-protein interactions.

ACKNOWLEDGEMENTS

There have been so many people that have helped me on my journey through graduate school. I would like to begin by expressing my sincere gratitude to Dr. Hage for his patience and guidance over the last five years. Thank you for allowing me the freedom to explore my creativity and widen my scientific knowledge and thank you for always answering my stupid questions without laughing too hard! I would also like to thank my supervisory committee Dr. James Carr, Dr. Jody Redepenning, Dr. Barry Cheung and Dr. Julie Stone for all of their support and direction throughout my time at UNL.

I am also grateful to the Hage lab members who shared in life's ups and downs; we laughed, we cried, we vented, and we learned. I learned things from each one of you that I will carry with me for the rest of my life. A special thanks to Annette for her guidance in learning the ropes when I was just a "newbie" and to John for inadvertently continuing my training after Annette graduated. Jeanethe, I hope that I have imparted some sort of wisdom to you; just remember, don't do as I do, do as I say! Thank you, Michelle for all the good conversation that kept me grounded and sane these last few years and to the rest of the Hage lab that helped me learn along the way, especially Corey, Rangan, Efthimia, Mandi, Omar, Tong, Abby, and Erika.

Most of all I want to thank my family that put up with me through classes, teaching, research, RUI, OPO, and writing this manuscript. Thank you, Albie and Sammie, the two most wonderful dogs in the world, for always being the most happy and uplifting friends a girl could ever hope for. Thank you, Ed, Theresa, and Tony for being

such supportive in-laws. Your support and enthusiasm are always so welcoming and appreciated and your constant reminders to do what makes me happy will always be my own little mantra. Mom and Joe, what can I say? You have always stood behind me, lifting me up when I feel down, you have always stood beside me, whispering words of love and encouragement in my ears, and you have always stood in front of me, pulling me forward to do my best. I love you guys. Thanks for everything! To my wonderful and adoring husband, I always said "thank God that I'm married to a psychiatrist so he can either supply good drugs or have me committed when I finally crack under all the pressure." Luckily, all I needed was sleep… lots of sleep! Just think, Tom, if we can make it through grad school and residency together, we survive anything! You are my strength and my love. Thank you. I love you! Thank you, God, for getting me through. You are my rock and my salvation. "I can do everything through him who gives me strength" (Phil. 4:13). "This is the day the Lord has made; let us rejoice and be glad in it!" (Psalm 118:24).

TABLE OF CONTENTS

CHAPTER 2

THE EVALUATION OF WARFARIN PROBE ALTERNATIVES FOR HUMAN SERUM ALBUMIN

CHAPTER 3

THE BINDING OF SULFONYLUREAS TO NORMAL HSA

CHAPTER 5

THE BINDING OF SULFONYLUREAS TO GLYCATED HSA

CHAPTER 6

CHAPTER 7

CHAPTER 1

GENERAL INTRODUCTION

Diabetes

Diabetes is a growing problem in the United States and around the world. In 2000, when the International Diabetes Federation released its first volume of the *Diabetes Atlas*, the global population suffering from the disease was 151 million. The estimate for 2010 has almost doubled to 285 million people and the estimate for 2030 has continued increasing to a staggering 438 million people around the world.[1] Today, more than 6% of the world's population suffers from diabetes. In the United States, 23.6 million children and adults have diabetes, with 1.6 million new cases being diagnosed each year.[2] In 2006, UN Resolution 61/225 recognized the epidemic by stating that "diabetes is a chronic, debilitating and costly disease associated with severe complications, which poses severe risks for families, Member States and the entire world…"[3] It is estimated that over 376 billion dollars will be spent on healthcare costs in 2010, over 11.6% of total healthcare expenditures.[1] The United States alone is projected to spend over 50% of the global expenditure.

Diabetes is classified as a group of heterogeneous disorders that pertain to insulin deficiency, insulin ineffectiveness, or a combination of the two, which result in glucose intolerance or hypoglycemia.[1] Diabetes can be classified into four main types: type 1, type 2, gestational, and other. The two most prevalent forms are type 1 and type 2.

Type 1 diabetes, formerly called juvenile diabetes, is typically diagnosed in children and young adults. This type of diabetes is actually an autoimmune disease

where the body has turned against itself to attack the insulin-producing beta cells in the pancreas.[1, 4] In type 1 diabetes, little to no insulin is produced and insulin injections are required for the patient to survive. Type 1 diabetes accounts for 5-10% of diagnosed diabetes cases.

The most common form of diabetes is type 2, or non-insulin dependent, diabetes. This type of diabetes accounts for 90-95% of the diagnosed cases of diabetes and it is typically associated with obesity, age, or a family history of the disease.[1, 4] In type 2 diabetes, a two-fold deficit occurs: insulin resistance and insulin deficiency. Type 2 diabetes was originally discovered by Yalow and Berson in 1960 when they observed that patients with type 2 diabetes often generate more insulin than a normal individual.[5] Although this is true for early stages of the disease, subsequent research found that the insulin levels of these patients eventually fell below normal levels. This led to the hypothesis that a degree of insulin resistance initially leads to an increase in insulin production in the body, where the pancreas produces excess insulin. Unfortunately, the pancreas cannot keep up with this demand and over time many of the beta cells decrease insulin production.

Symptoms of diabetes include increased thirst, frequent urination, constant hunger, weight loss, extreme fatigue, and blurred vision. While the appearance of type 1 diabetes is sudden and the associated symptoms appear quickly, type 2 diabetes can be asymptomatic for many years. Both types of diabetes can lead to severe complications including cardiovascular disease (heart disease/stroke), neuropathy (nerve damage), nephropathy (renal failure), and retinopathy (blindness). However, with proper treatment, many of these complications can be delayed or even prevented entirely.

Sulfonylureas

During the years of World War II, another threat was underway: typhoid fever. A French pharmacologist by the name of Marcel Janbon asked the French government to send him a drug that might act against the illness.[5, 6] He was sent a sulfonylurea. In 1942, during his animal testing, the animals displayed strange behavior that would sometimes end in death. It soon became evident that the behavior matched the symptoms of hypoglycemia. Janbon contacted a colleague, August Loubatiéres, and asked that he test the drug. Loubatiéres' studies also ended with the same result: the production of hypoglycemia in normal fasting dogs. However, he also observed that this drug did not affect dogs which had their pancreas previously removed. Further testing by the two led to the hypothesis that there was a type of diabetes, characterized by "sluggish insulin secretion" (type 2 diabetes), that could be treated with sulfonylureas.[6]

Since the work of Janbon and Loubatiéres, an entire line of sulfonylureas have been developed to aid in the treatment of type 2 diabetes. Sulfonylureas were the first class of oral medications used to treat diabetes and they have been used for over 50 years (i.e., since tolbutamide was first introduced in 1956).[6, 7] Tolbutamide, tolazamide, acetohexamide, and chlorpropamide are the first-generation sulfonylureas. Since then, second and third generation sulfonylureas have been developed that have an increase in potency and a decrease in drug interactions. Sulfonylureas are widely used due to their reliability, limited side effects, and low cost. They are often recommended alone or in combination with other therapies.[7]

Figure 1-1. Mechanism of insulin release during a diabetic disease state. Glucose regulates insulin secretion in the beta cell of the pancreas. Sulfonylureas can also stimulate the release of insulin by entering through the (SUR)-1 receptor, altering the ion channel activity and leading to insulin secretion. (*Adapted from*: Powers Alvin C, "Chapter 338. Diabetes Mellitus" (Chapter). Fauci AS, Braunwald E, Kasper DL, Hauser SL, Longo DL, Jameson JL, Loscalzo J: Harrison's Principles of Internal Medicine, 17e: http://www.accessmedicine.com.)

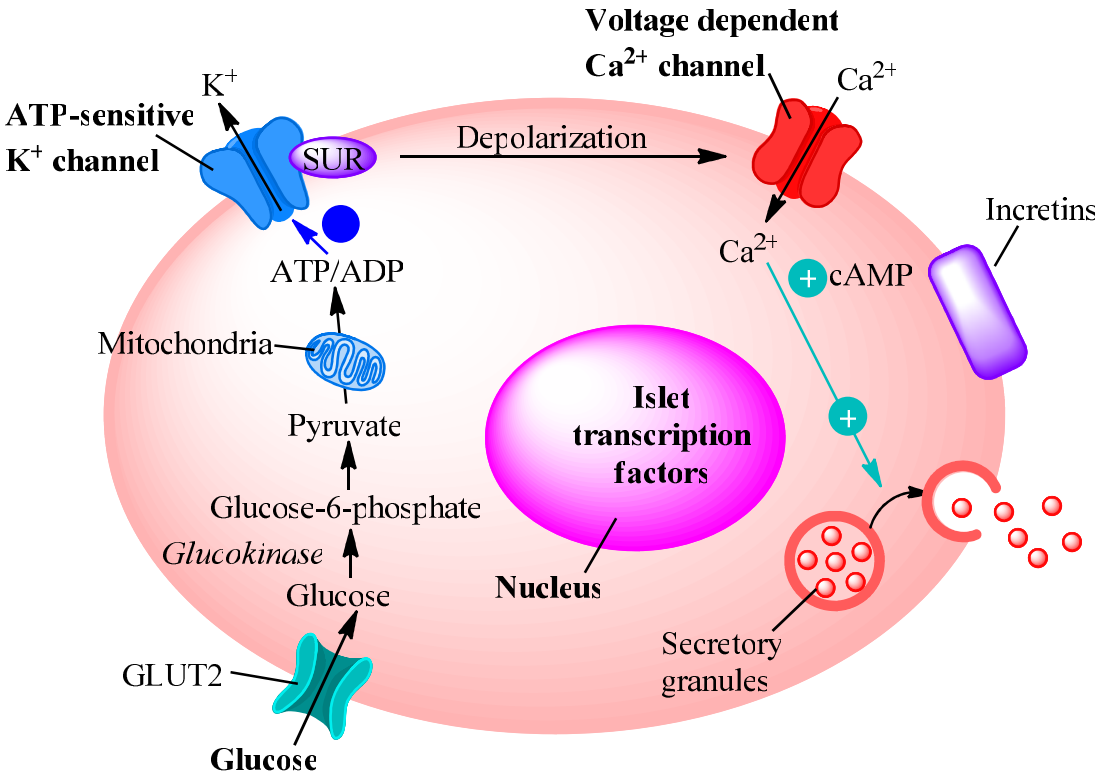
Voltage dependent
Ca2+ channel
Ca2+
K+
ATP-sensitive
K+ channel
SUR
Depolarization
Incretins
Ca2+
cAMP
ATP/ADP
Mitochondria
Pyruvate
Islet
transcription
factors
Glucose-6-phosphate
Glucokinase
Glucose
Nucleus
Secretory
granules
GLUT2
Glucose

Sulfonylureas work by stimulating insulin release from the beta cells in the pancreas (see Figure 1-1).[8-11] This occurs when a sulfonylurea binds to the sulfonylurea receptor unit (SUR)-1 of the adenosine-triphosphate (ATP)-sensitive potassium channels on the beta cell membrane. This closes the channels and reduces potassium efflux, leading to membrane depolarization. The voltage-dependent calcium channels then open, resulting in the influx of calcium ions which in turn stimulate the release of insulin from available storage granules in the cell.

Like many other drugs, sulfonylureas are mainly bound to serum proteins as they are distributed throughout the body. In fact, they bind primarily to human serum albumin (HSA). Sulfonylureas can bind to HSA at one or multiple binding sites, depending on the specific sulfonylurea. The binding affinity as well as the rate of displacement can also differ dramatically between different sulfonlyureas.[12-14]

Human Serum Albumin (HSA)

HSA is the most abundant protein in human plasma. It has a typical concentration of ~40-45 g/L and accounts for about 60% of the total protein in blood serum.[15-17] HSA is synthesized in the liver and exported as a single, non-glycosylated chain of 585 amino acids.[15, 18] It is a globular protein consisting of three domains (I, II, and III) that each contain two subdomains (A and B) connected by a random coil (Figure 1-2). These domains create a heart-shaped protein with a molecular weight of ~66,500 Da and an approximate size of 80 x 80 x 30 Å, with three lobes that correspond to each of the three homologous domains. The secondary structure is made up of 67% α-helices,

Figure 1-2. Structure of human serum albumin (HSA). The locations of Sudlow sites I and II are indicated. This structure was obtained from the Protein Data Bank (ID: 1AO6).

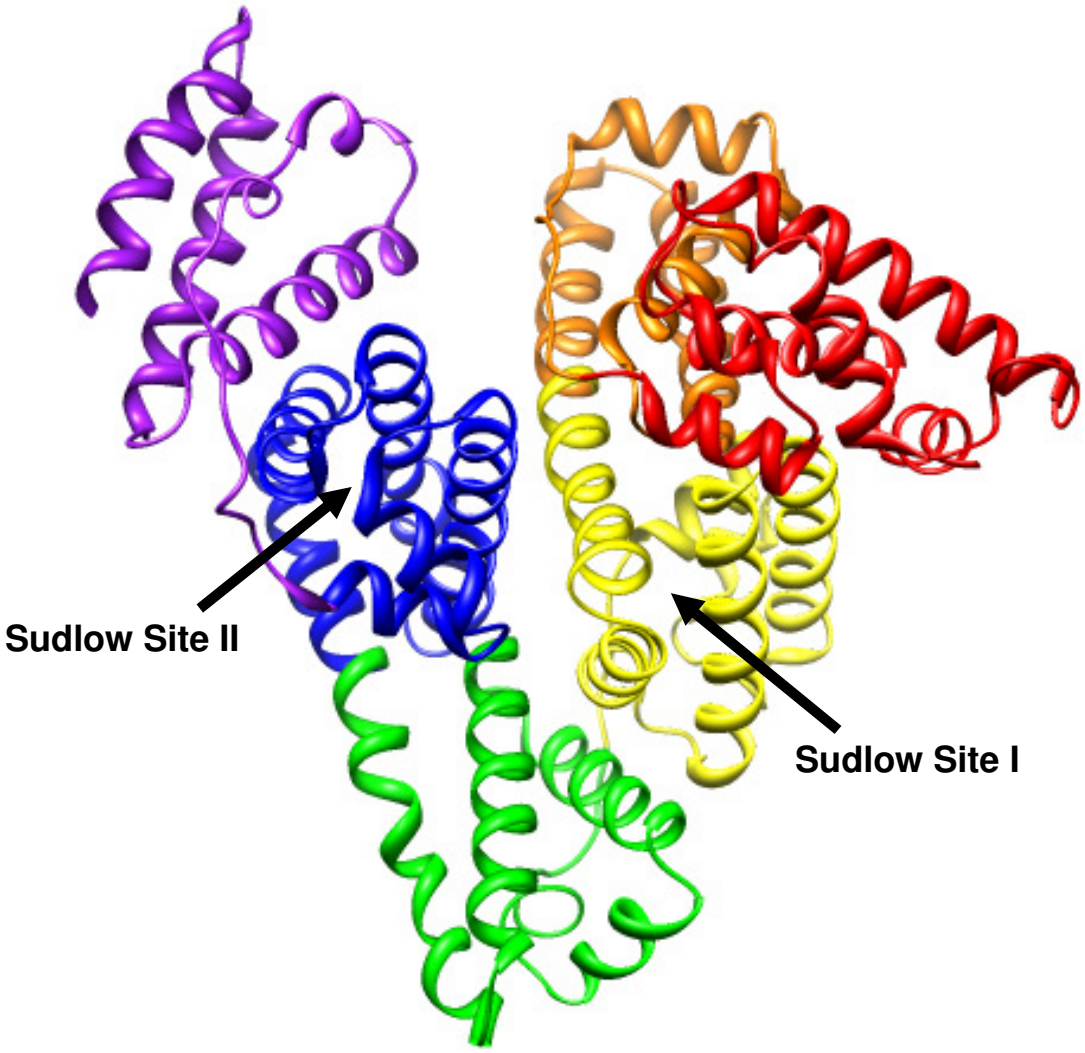
Sudlow Site II
Sudlow Site I

23% extended chain, and 10% β-turn, with the first six of ten total α-helices in each domain belonging to subdomain A and the last four to subdomain B.[16, 19, 20]

In 1975, Gillian Sudlow proposed that there are two high affinity binding sites on HSA for small heterocyclic or aromatic compounds.[21, 22] These sites are located on subdomains IIA and IIIA which are now often referred to as Sudlow sites I and II. Sudlow site I, or the warfarin-azapropazone site, is the binding site for bulky heterocyclic anions such as warfarin and salicylate, while Sudlow site II is the primary binding site for aromatic carboxylates like ibuprofen and indoles. At least two minor binding sites have also been proposed for compounds such as digitoxen and tamoxifen.[23, 24]

HSA is the most important nonspecific transporter protein in the circulatory system. It has an excellent binding capacity for many endogenous and exogenous compounds. The main role of HSA is to bind and transport unesterified fatty acids, making these compounds more soluble and evenly distributed throughout the body. HSA also binds other endogenous compounds such as bilirubin, bile salts, steroid hormones, hematin, tryptophan, thyroxine, and some vitamins and metal ions.[16] Yet one of the more remarkable attributes of HSA is its ability to transport a large number of drugs throughout the body. This ability gives HSA a primary role in pharmacokinetics (i.e. absorption, distribution, metabolism, and excretion). The distribution of the drugs to their receptor site ultimately occurs by first binding to HSA in order to be transported to their targets. A pharmaceutical compound could even be cut short in production if testing shows unfavorable binding with this protein.

The activity of a drug at the receptor site is often related to the amount of the unbound (or free) drug in circulation and the affinity of many drugs for HSA strongly

affects the free drug fraction in plasma. In most cases, it is the free drug fraction that has the ability to transfer into tissues in order to carry out its therapeutic activity. However, Herve, et. al. found that a small fraction of the bound drug can also be dissociated in capillaries and become available for drug transfer.[25] These two behaviors are referred to as *permissive* and *restrictive* binding.

Permissive and restrictive drug-protein interactions were originally seen in the liver when studies showed that although >90% of propanolol was bound to plasma proteins, >90% is also able to be extracted by the liver. This led to the conclusion that a significant amount of bound propanolol in the circulation was still available for drug transfer, a binding that was said to be "permissive" in nature.[25] In this type of binding, drugs have a high volume of distribution, always more than 0.6 L/kg (the volume of free body water), and drugs with higher values are not only distributed in body fluids but in tissues as well. In constrast, >99% of warfarin is bound in plasma and the extraction ratio of this drug was found to be extremely low (<0.3%) meaning that the bound portion of the drug cannot be used but rather the free fraction is necessary for drug transfer. This type of binding is said to be "restrictive" and the drug is almost completely contained within the compartment of distribution of its binding protein. This type of behavior was eventually extended to all tissues and found to be independent of drug-protein association constants. Any modification of the binding protein in this case could alter the free fraction of a drug, thereby altering the interaction the drug has at its target.

HSA has no sites for enzymatic glycosylation. However, it can undergo non-enzymatic glycosylation, also known as glycation. In fact, in average adults 6-13% of

Figure 1-3. The non-enzymatic glycation of a protein.

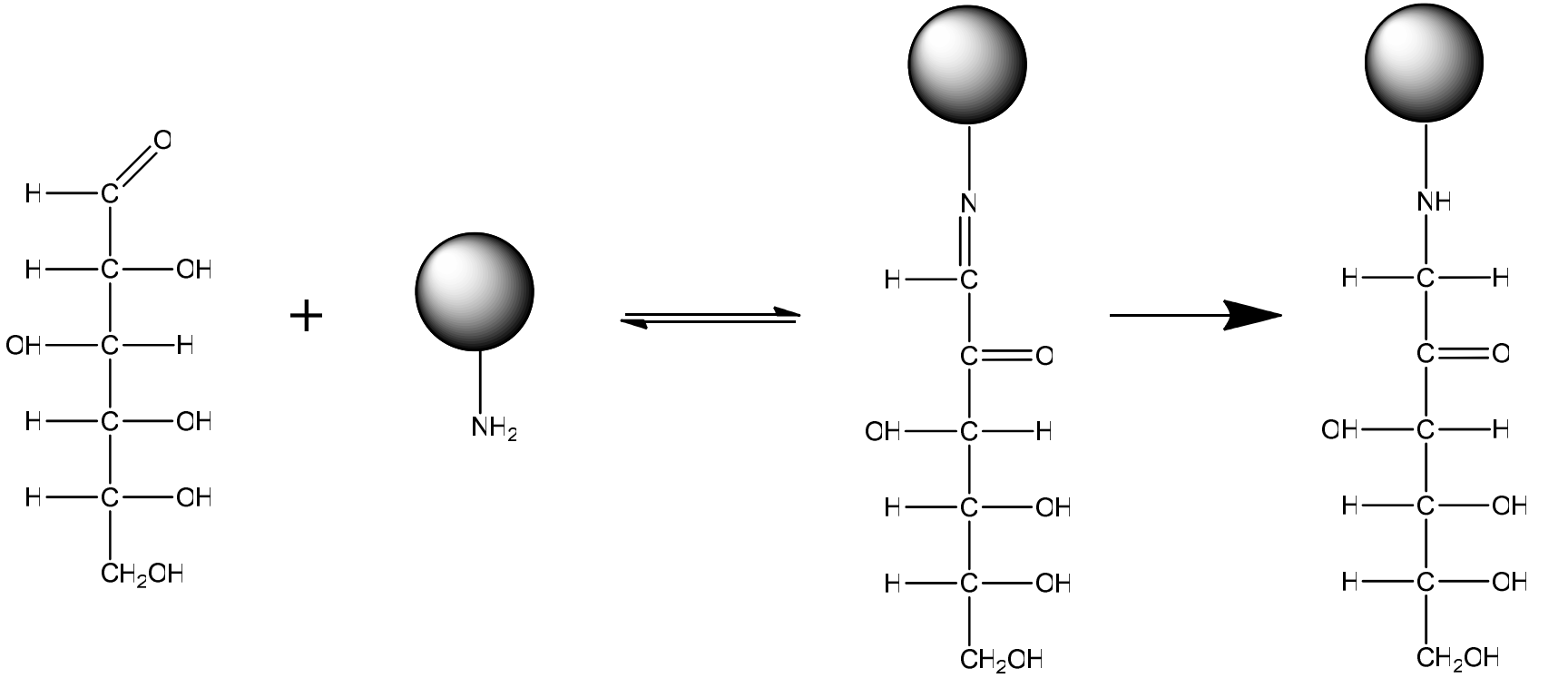
Glucose
Protein
Schiff Base
Amadori Product

HSA is glycated.[16, 26-28] This number can increase dramatically to 20-30% in people with diabetes.[26-28] Glycation takes place between a reducing sugar and a free amine group such as the α- or ε- amino groups on a protein.[28-30] This mechanism (see Figure 1-3) begins when the carbohydrate performs a neuclophilic attack on an amine group to form a Schiff base. The Schiff base can either dissociate or rearrange to form an irreversible ketoamine, also known as an Amadori product.[28, 30, 31] The Amadori product can then undergo a series of oxidative rearrangements and degradations to form a group of compounds known collectively as advanced glycation end-products (AGEs). The primary sites of glycation on HSA are lys-525, lys-199, lys-281, and lys-439[27-29, 32] but other residues are susceptible to glycation as well.[28, 32]

Glycation is thought to alter the secondary and tertiary structure of HSA, potentially leading to changes in the stability and biological properties of this protein. Changes in this protein due to glycation are also thought to affect drug-protein interactions, potentially resulting in a decreased or increased binding of drugs to HSA.[27] Some of the glycation sites on HSA are known to be at or near Sudlow sites I and II. For instance, lys-199 is known to be at the pocket entrance to Sudlow site I. Studies have already been performed to explore the structural changes induced in HSA by glycation[27, 28] as well as binding studies with various drugs including naproxen,[33] salicylic acid,[33] warfarin,[26, 27, 33] sulfonylureas,[34] L-tryptophan,[35] Bromocresol Purple and Phenol Red.[26] Drug binding studies have been performed by many methods, such as equilibrium dialysis, ultrafiltration, circular dichroism and fluorescence spectroscopy, the Hummel-Dreyer method, and fluorescence quenching. This dissertation will present data on drug-

binding studies by high-performance affinity chromatography (HPAC) using the methods of frontal analysis and zonal elution.

High-Performance Affinity Chromatography (HPAC)

Affinity chromatography (AC) is a type of liquid chromatography that uses a biological ligand as the stationary phase.[36] This technique has been used for decades for the purification and analysis of biologically-related samples. It uses reversible interactions that are found in biological systems, including the binding of an antigen to an antibody or a hormone to a protein. In this method, one of a pair of interacting compounds is immobilized onto a support for use as a stationary phase, while the other compound is contained within the injected sample or mobile phase. A common support for this application is a carbohydrate-based gel such as agarose or sepharose. These support materials are often used when purifying samples under gravity flow or using a peristaltic pump. These materials are easy and inexpensive to use, however, they are structurally stable only at low back-pressures.

High-performance affinity chromatography (HPAC) is a modification on this method in which the support material is made of small, rigid particles that are able to withstand high back-pressures.[36] Typical supports in HPAC include silica and polymeric monolith materials. The stability of these supports allows them to be used with typical HPLC equipment, including gradient pumps at high flow rates. Although this technique is more difficult to perform and more costly than traditional affinity chromatography due to the need for specialized equipment, the advantages of HPAC make this technique preferable in analytical applications.

One of the greatest advantages of HPAC is that the immobilized ligand can often be used for numerous sample applications in binding studies. This increases the precision of the experiments by reducing run-to-run variations. It also lowers costs by reducing the amount of ligand needed for binding studies. This is especially important when the ligand is an expensive monoclonal antibody or cell receptor.[37] This method also increases the speed of the experiments by allowing for a wider range of flow-rates to be employed.

One common application for HPAC is in studying the binding equilibrium and thermodynamics of biological systems. This is most often performed by the methods of frontal analysis or zonal elution.

Frontal Analysis

Frontal analysis was originally used as a purification technique. However, it has grown into a popular method for gathering equilibrium data on the affinities and binding sites of various analyte-ligand systems. Kasai and Ishii were the first to explore the use of frontal analysis and affinity columns for this purpose in 1975 when they used a low-performance affinity column to study the affinity of trypsin for a mixture of oligopeptides obtained from a tryptic digest of protamine.[38] The use of silica columns for biointeraction studies began about a decade later,[39] with other HPLC media such as monoliths and capillary systems also now being employed for such work.[40-42]

General Principles

Frontal analysis is performed when an analyte is continuously applied to a column containing an immobilized ligand (see Figure 1-4). As the analyte interacts with the ligand, the binding sites slowly become saturated. Upon saturation, excess analyte leaves the column and forms a characteristic breakthrough curve (see Figure 1-5). If fast association and dissociation kinetics are present for this system, the center of this breakthrough curve can be related to the concentration of applied analyte, the number of binding sites within the column, and the affinity to which the analyte binds to the ligand.

The advantages of using frontal analysis and affinity chromatography for biointeraction studies are its speed, precision, and automation along with the small amounts of sample required to run an experiment. Although frontal analysis requires a larger volume of sample than zonal elution, a technique that will later be discussed in greater detail, this method also provides more information per analysis. The main advantage of frontal analysis is that equilibrium constants and binding capacities can be obtained separately, making it possible to characterize both binding affinities and column properties. These experiments can also be carried out using a standard HPLC system with the addition of a temperature controller. Applications of frontal analysis include binding studies, competition studies, and temperature and solvent studies. Frontal analysis has also been used in recent years to screen the binding of a ligand against mixtures of compounds. The following sections provide more details on each of these applications.

Figure 1-4. A typical frontal analysis experimental system is composed of the following components: (A) mobile phase reservoir, (B) isocratic pump, (C) valve, (D) column oven, (E) column, (F) detector, (G) computer with data collection software, and (H) lines going to excess.

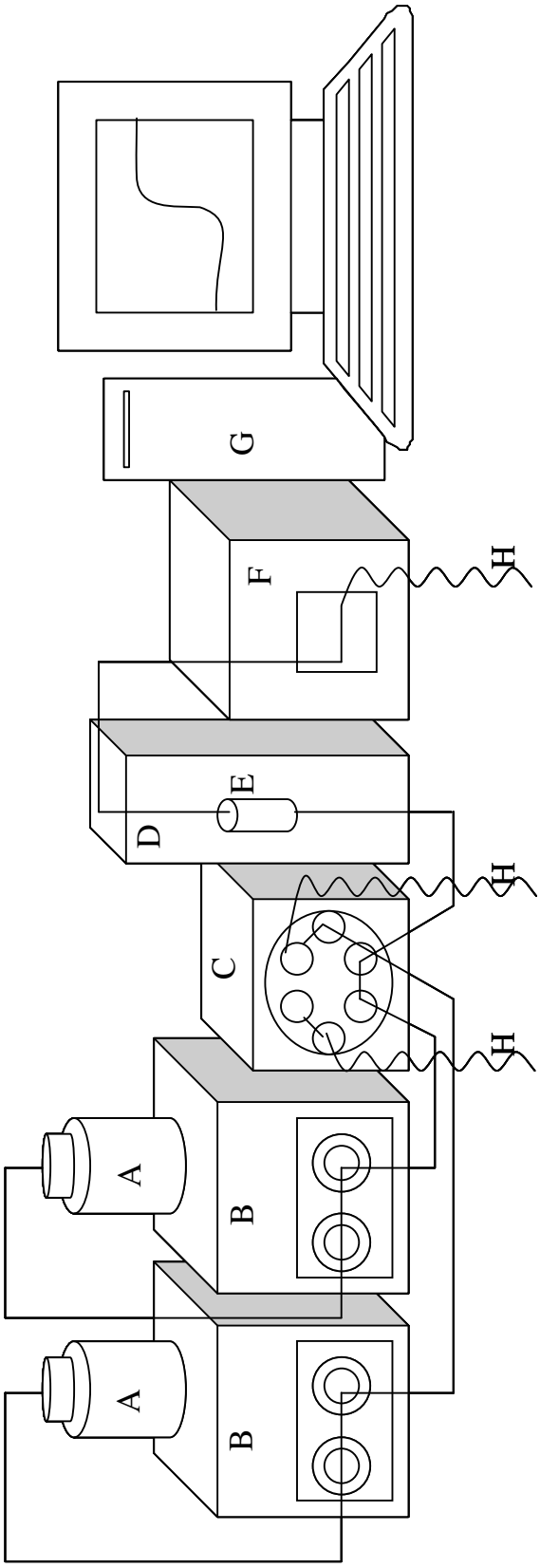
A
B
A
B
C
D
E
F
G
H
H
H

Figure 1-5. Example of frontal analysis experiments examining the binding of 7-hydroxycoumarin to immobilized HSA. The frontal analysis curves were obtained for the application of solutions that contained (from left-to-right) of 10, 7.5, 5.0, 2.5, or 1.0 μM 7-hydroxycoumarin.

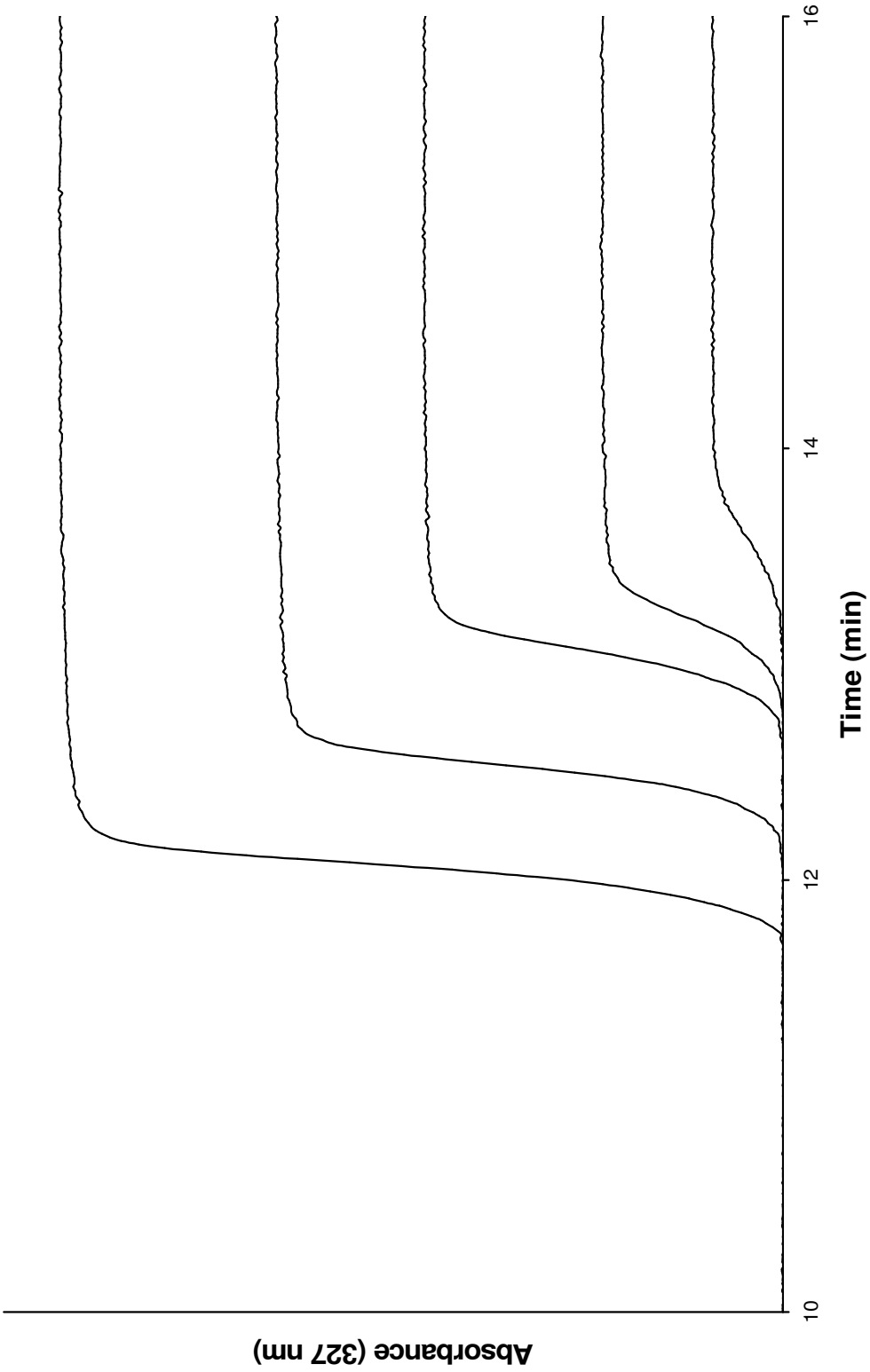
Absorbance (327 nm)
10
12
14
16
Time (min)

Binding Studies

One of the most common uses of frontal analysis is in the determination of the affinity and binding capacity of an analyte with an immobilized ligand. This can be accomplished by measuring the breakthrough time or breakthrough volume of the analyte that has been continuously applied to a column containing an immobilized ligand. Once obtained, the breakthrough time or volume can be related to the apparent number of moles of analyte needed to saturate the column, m_{Lapp}. For instance, if an analyte binds reversibly to the immobilized ligand at only one type of site, Equations 1-1 and 1-2 can be used to relate the measured value of m_{Lapp} to the parameters that describe the affinity of this interaction (as represented by K_a) and the amount of binding sites in the column (as represented by m_L).[43]

$$m_{Lapp} = \frac{m_L K_a [\mathrm{A}]}{1 + K_a [\mathrm{A}]} \qquad (1\text{-}1)$$

or

$$\frac{1}{m_{Lapp}} = \frac{1}{K_a m_L [\mathrm{A}]} + \frac{1}{m_L} \qquad (1\text{-}2)$$

Equivalent expressions can be written in terms of the breakthrough volume, as will be discussed later. For a system with 1:1 binding, Equation 1-2 can be used to find the values of both K_a and m_L if a plot is made of $1/m_{Lapp}$ versus 1/[A]. An example of such a plot is shown in Figure 1-6. Alternatively, Equation 1-1 and a non-linear fit can also be used to analysis such data.

If, however, more than one binding site is involved in the interaction of the applied analyte with the immobilized ligand, a negative deviation will occur at high

Figure 1-6. (a) Single-site binding of coumarin and (b) multi-site binding of 4-hydroxycoumarin to an immobilized HSA column, as examined by frontal analysis and Equation 1-2.

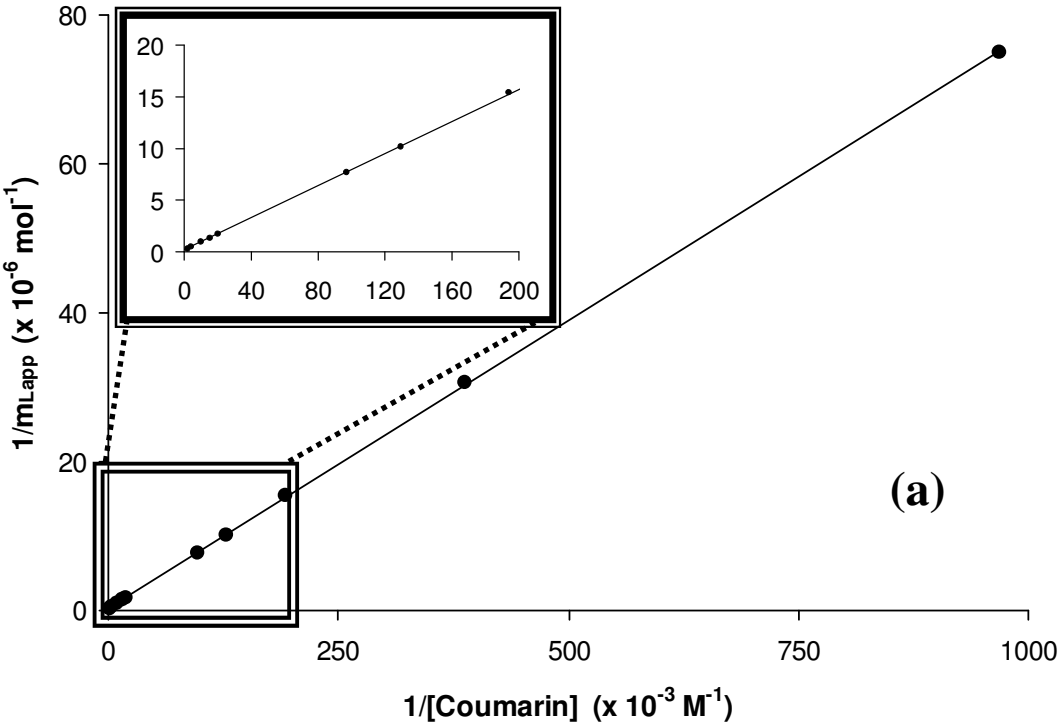
80
60
40
20
0
0
250
500
750
1000
1/mLapp (x 10-6 mol-1)
1/[Coumarin] (x 10-3 M-1)
20
15
10
5
0
0
40
80
120
160
200
(a)

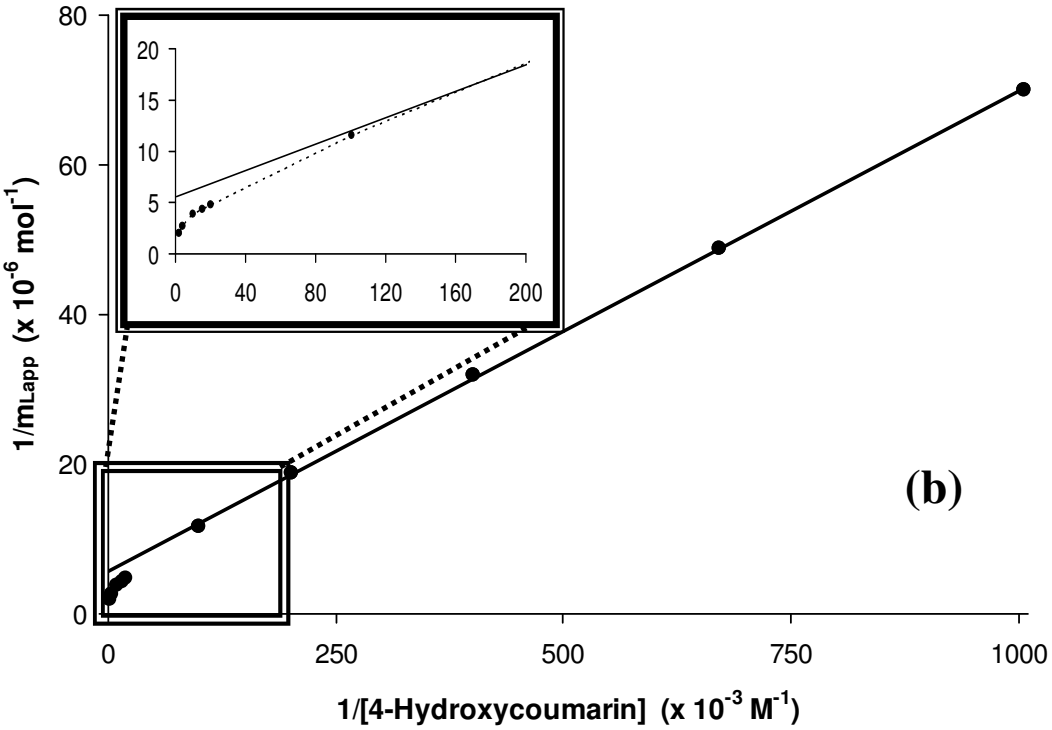
80
60
40
20
0
0
250
500
750
1000
1/mLapp (x 10-6 mol-1)
1/[4-Hydroxycoumarin] (x 10-3 M-1)
20
15
10
5
0
0
40
80
120
160
200
(b)

analyte concentration (or lower 1/[A] values), as shown in Figure 1-6b. These deviations indicate that multi-site binding is present, which requires the use of expanded forms of Equations 1-1 or 1-2. As an example, the following equations would be used to model a system that has two-site binding,[44]

$$m_{Lapp} = \frac{m_{L1}K_{a1}[\mathrm{A}]}{(1+K_{a1}[\mathrm{A}])} + \frac{m_{L2}K_{a2}[\mathrm{A}]}{(1+K_{a2}[\mathrm{A}])} \qquad (1\text{-}3)$$

or

$$\frac{1}{m_{Lapp}} = \frac{1+K_{a_1}[\mathrm{A}]+\beta_2 K_{a_1}[\mathrm{A}]+\beta_2 K_{a_1}{}^2[\mathrm{A}]^2}{m_L\{(\alpha_1+\beta_2-\alpha_1\beta_2)K_{a_1}[\mathrm{A}]+\beta_2 K_{a_1}{}^2[\mathrm{A}]^2\}} \qquad (1\text{-}4)$$

where $\beta_2 = K_{a2}/K_{a1}$ and $\alpha_1 = m_{L1}/m_{L2}$, and all other terms are as defined previously.

Because frontal analysis can provide information on both the number of binding sites and association equilibrium constants for an interaction, this is a valuable method for biointeraction studies. A number of studies have been done in this area, as has been discussed in previous reviews.[36, 45] More recent examples have included work examining the binding of HSA with carbamazepine,[46] α_1-acid glycoprotein (AGP) with oxybutynin[47] and R- and S-propranolol,[48] quinidine carbamate with naproxen,[49] and BSA with berberine chloride. [50]

Competition Studies

Competition studies can also be performed by frontal analysis through the use of a competing agent that is added to the mobile phase. An example of this is the competition of sulphamethizole with salicylic acid performed by Nakano, et. al.[51] Typically, a shift to shorter breakthrough times is seen in these studies as the amount of competing analyte is

increased. The degree of competition, including positive or negative allosteric effects, can also be observed using this method.

Over the last decade there has been a large amount of work in the use of frontal analysis and affinity chromatography in screening mixtures of compounds for any targets that might bind to a given immobilized ligand. The combination of these tools with mass spectrometry, a method commonly known as frontal affinity chromatography-mass spectrometry (FAC-MS), has been of particular interest.[52] This approach has been shown to be able to screen mixtures of compounds in a relatively short amount of time. As a mixture of analytes flows through the column, the individual analytes bind to the ligand based on their affinity for this agent. Using mass spectrometry as the detection method allows for a multitude of analytes to be evaluated simultaneously, as shown by the example in Figure 1-7 for a mixture of eight solutes that were injected onto a column containing immobilized sorbitol dehydrogenase. Selective detection at the characteristic mass-to-charge (m/z) value for each compound makes it possible to generate separate breakthrough curves for each of these analytes. This information is then used to evaluate and rank the relative affinity of each compound in the mixture for the ligand in the affinity column.[42]

An expression that is often used with breakthrough volume measurements in these competition studies to evaluate binding affinity is given in Equation 1-5,[42] which is equivalent to the mass relationship that was given earlier in Equation 1-1.

$$V_A - V_M = \frac{B_t}{[\mathrm{A}] + K_D} \qquad (1\text{-}5)$$

In this alternative expression, V_A is the measured breakthrough volume, V_M is the column void volume, [A] again represents the concentration of applied analyte, B_t is the total amount of immobilized active ligand, and K_D is the dissociation equilibrium constant for the interaction (where $K_D = 1/K_a$).

One variation of this approach is to make sequential injections of the analytes starting with the lowest concentrations and finishing at the highest concentrations. These injections are performed without washing steps in between infusions. The breakthrough volumes that are measured are then related to the applied concentrations of the analyte by using the following equation,[42]

$$[\mathrm{A}]_j + y_j = B_t\left[\frac{1}{V_{Aj} - V_M}\right] - K_D \qquad (1\text{-}6)$$

where

$$y_j = \frac{\sum_{i-1}^{j-1}([\mathrm{A}]_i - [\mathrm{A}]_{i-1})(V_{Aj} - V_M)}{V_{Aj} - V_M} \qquad (1\text{-}7)$$

for the *j*th injection in a series. A plot of the analyte concentration versus the corrected breakthrough volume is then used to give a graph where the slope is equal to the column capacity and the negative of the intercept is equal to the dissociation equilibrium constant.

Examples of systems that have recently been studied using this approach include galactosaminoglycans as a ligand for galectins,[53] jacalin as a ligand for various glycopeptides,[54] HSA with thyroxine,[55] and high-throughput lectin-oligosaccharide systems.[56] A number of articles have been published using this method in the past few years and more detailed information can be found in the literature.[42, 53, 54, 56-63]

Figure 1-7. Use of FAC/MS to examine the binding by eight compounds in a library to an immobilized sorbitol dehydrogenase column (with permission from D.C. Schriemer, *Anal. Chem.* 76 (2004) 440A).[42]

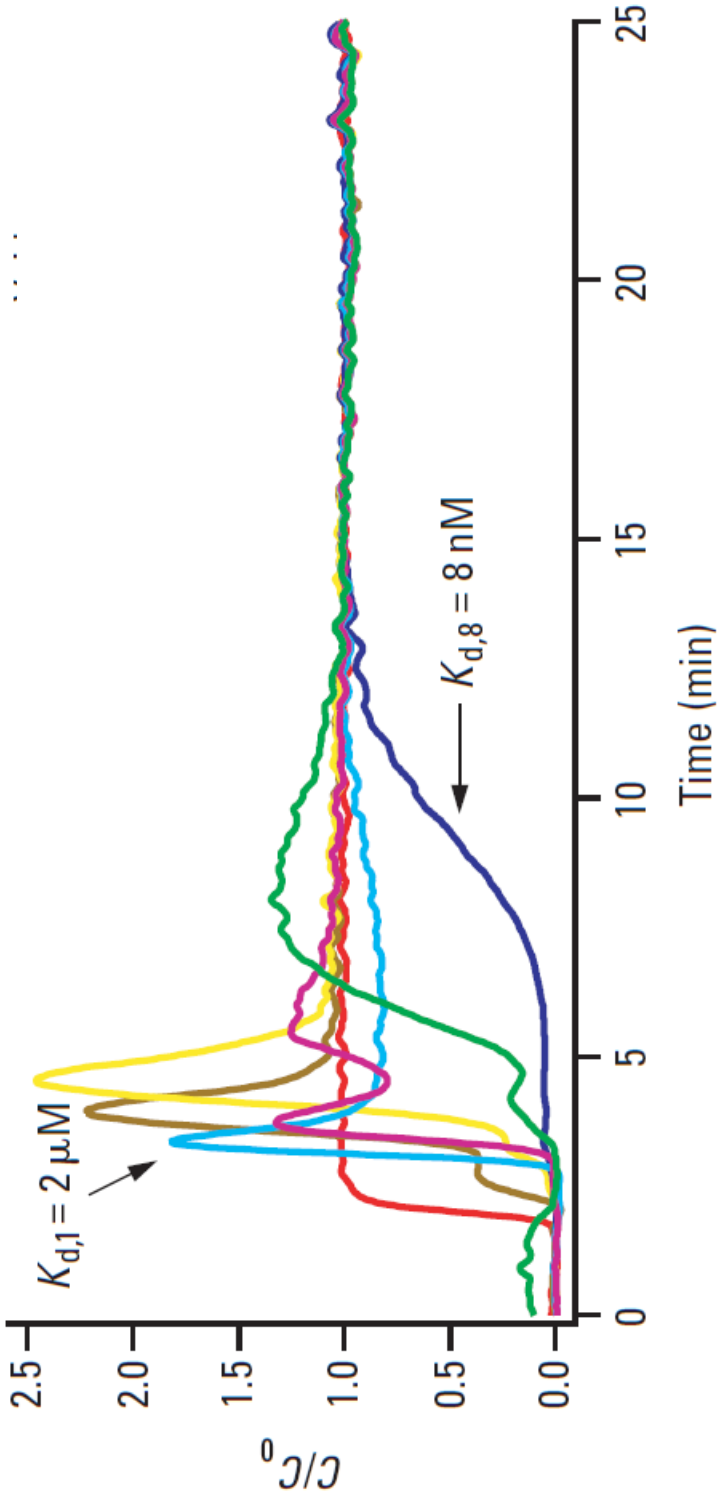
$K_{d,1} = 2\,\mu M$
$K_{d,8} = 8\,nM$
C/C_0
Time (min)
0.0
0.5
1.0
1.5
2.0
2.5
0
5
10
15
20
25

Temperature and Solvent Studies

The ability to measure both the amount of binding sites and affinity is a useful feature of frontal analysis in examining how changes in temperature or other conditions alter biological interactions. Temperature studies have been performed with this technique with systems such as HSA with R- and S-warfarin,[64] carbamazepine,[46] D- and L-tryptophan,[65] aptamers with adenosine,[66] and BSA with berberine chloride.[50] In these studies, it has been shown that the shifts in retention with temperature can correspond to a change in the number of available binding sites[46, 50, 64, 65] as well as the binding affinity of the compound.[50, 64-66] Figure 1-8 is an example of such a study, showing how the retention, activity, and affinity constant for berberine chloride change under various conditions when using an immobilized BSA column. Frontal analysis has also been used to examine how changes in solvent composition affect solute-ligand binding, as has been used for systems such as quinidine carbamate with naproxen,[49] and HSA with D- and L-tryptophan[65] and carbamazepine.[46]

Practical Considerations

Many of the practical factors that should be considered in the use of frontal analysis are the same as those that will be further described for zonal elution. The key differences in these methods are the approaches they use for sample application and data analysis. In the case of binding studies that are performed by frontal analysis, it is necessary to have an observable shift in the breakthrough curve as the concentration of analyte is varied. It is possible to determine the optimum analyte concentrations to use

Figure 1-8. Observed changes as a function of temperature in (a) the retention factor, (b) moles of active binding sites, and (c) and association equilibrium constant for berberine chloride on an immobilized BSA column (with permission from Lei, G., et. al. *Chromatographia*, 66, 847-852, 2007).[50]

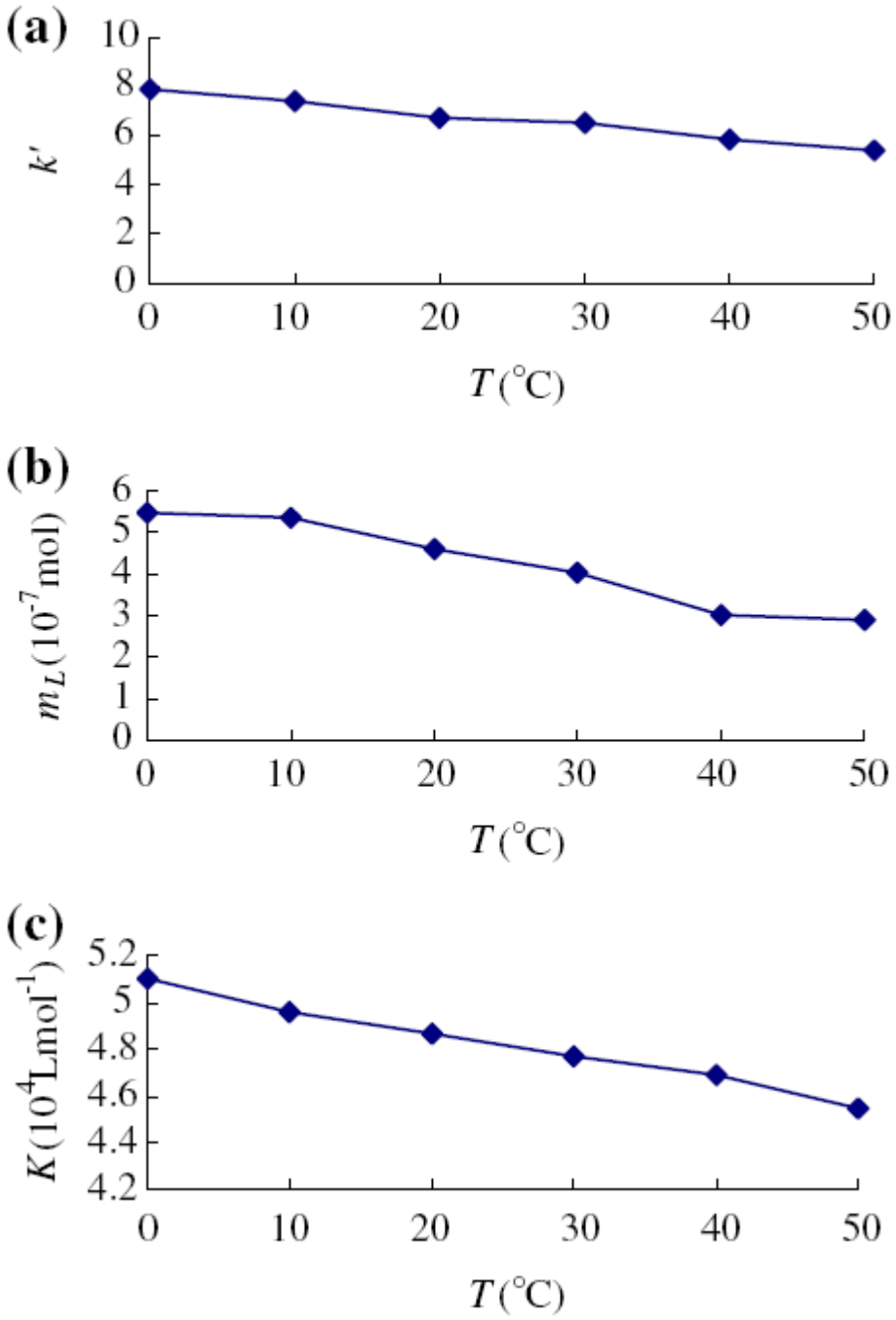
(a)
k′
10
8
6
4
2
0
0
10
20
30
40
50
T (°C)
(b)
m_L(10^-7 mol)
6
5
4
3
2
1
0
0
10
20
30
40
50
T (°C)
(c)
K(10^4 Lmol^-1)
5.2
5
4.8
4.6
4.4
4.2
0
10
20
30
40
50
T (°C)

for this experiment by using an expression like Equation 1-8, which has been previously derived for systems with 1:1 interactions between the analyte and ligand.[67]

$$\frac{m_{Lapp}}{m_L} = \frac{K_a[\mathrm{A}]}{1 + K_a[\mathrm{A}]} \tag{1-8}$$

According to this expression, as the analyte concentration [A] ranges from zero to infinity, the fraction of binding sites that are occupied by the analyte at equilibrium (as given by the ratio m_{Lapp}/m_L) will be between zero and one, respectively. It is at some intermediate analyte concentration that this ratio will have its greatest change with analyte concentration. For a 1:1 binding system, this occurs when [A] = $1/K_a$, with concentrations both above and below this optimum then being used for binding studies. Somewhere within these values, the analyte will have a concentration range that will show its greatest shift in retention. Analyte solubility and detectability must also be considered in choosing the range of analyte concentrations to be used in these studies.

It is relatively easy to analyze and determine the breakthrough time of a simple, symmetrical frontal analysis curve. In this situation, the point that is halfway between the baseline and plateau would be the breakthrough time. Unfortunately, many breakthrough curves are not perfectly symmetrical in shape and, therefore, the analysis approach has to be slightly altered. One approach is to find the point at which the areas below the front portion of the curve and above the latter half of the curve are equal. An equivalent approach for analyzing a breakthrough curve is to take the first derivative of the curve and then determine the central moment of this derivative.[36] This second approach can be easily handled with the correct data analysis software.

Zonal Elution

Zonal elution is currently the most common way in which binding studies are conducted through the use of affinity chromatography.[36] Zonal chromatography is typically used in affinity chromatography and in HPLC to separate compounds by injecting a small plug of sample onto a column. However, this method can also be used to obtain information on the binding equilibria and thermodynamic properties of the analyte as it interacts with the stationary phase (i.e., the immobilized ligand in the case of an affinity column). This type of experiment is usually performed under linear elution conditions to simplify the analysis,[67] although some work under non-linear conditions has also been reported.[68, 69]

The first reported use of zonal elution for thermodynamic studies in affinity chromatography was in 1974 when a low-performance Sepharose column containing thymidine-5'-phosphate-3'-aminophenylphosphate was used to characterize the binding by the enzyme staphylococcal nuclease to soluble thymidine biphosphate.[70] Over the last few decades, this method has been used to examine interactions in numerous systems and has been used in both low- and high-performance systems with affinity columns. Examples of these applications can be found in Table 1-1 and in previous reviews that have appeared on this topic.[43, 45, 71-73]

General Principles

In zonal elution, a small plug of analyte is injected onto a column in the presence of a mobile phase with a known composition that is being applied at a constant flow-rate. The mobile phase is often a buffer with a physiological pH but may also contain a known

Table 1-1

Applications of Affinity Chromatography in Equilibrium and Thermodynamic Studies

Method	Ligand	Analyte
Zonal Applications	Serum Proteins	Warfarin;[64] coumarins;[74, 75] benzodiazepines, triazole derivatives;[75] carbamazepine;[46] phenytoin, ibuprofen;[76] *for a more complete list see*[36]
Frontal Applications	Serum Proteins	Carbamazepine;[46] oxybutinin;[47] propanolol;[48] berberine chloride;[50] salicylic acid;[51] thyroxine;[55] warfarin;[64] tryptophan[65]
	Enzymes/Receptors	Nicotine, β-estradiol;[42] enzyme inhibitors;[57, 77] *for a more complete list see*[42]
	Lectins	Glycopeptides;[54] oligosaccarides;[56, 61] glycosaminoglycans[53]
	Aptamers	Adenosine[66]
	Quinidine Carbamate	Naproxen[49]

concentration of a salt, organic modifier or a competing agent that is known to bind at a specific site on the immobilized ligand. As the analyte interacts with the immobilized ligand, it is retained by the column. The retention time or volume of the analyte can be measured either on-line or off-line by using an appropriate detector. Information on analyte retention can be obtained by examining the changes in mobile phase composition. This technique can also be used to explore changes in the system due to alterations in temperature, pH, or mobile phase conditions.

An example of a typical zonal elution study is shown in Figure 1-9. In this example, racemic warfarin was used as a competing agent in the mobile phase while 7-hydroxycoumarin was injected as the analyte of interest.[74] The column contained immobilized HSA as the ligand. These studies were performed to examine the binding of 7-hydroxycoumarin with respect to warfarin. The 7-hydroxycoumarin peaks shifted to the left as the concentration of warfarin increased, indicating that some type of direct or allosteric competition was occurring between these two compounds and HSA. The advantages that have been noted for this type of experiment include its high precision, small sample requirements, and the ability to perform this method on a standard HPLC system with the addition of a device for temperature control.[36]

Zonal elution has been used in a large assortment of studies to gain information on analyte-ligand systems.[36, 45] A majority of these studies focus on binding in order to determine the strength and location of the bound analyte to the ligand. Other studies look at how those interactions change as conditions are altered. These studies often look at temperature, pH, or mobile phase variations. Yet other studies look at altering the ligand itself by mutations or structural changes. More details on these applications will follow.

Figure 1-9. Example of zonal elution experiments examining the binding of 7-hydroxycoumarin to immobilized HSA. The results were obtained through competition studies performed by injecting samples of 5.0 μM 7-hydroxycoumarin in the presence of mobile phases that contained (from top-to-bottom) 20, 15, 10, 5.0, 1.0, or 0 μM racemic warfarin as a competing agent.

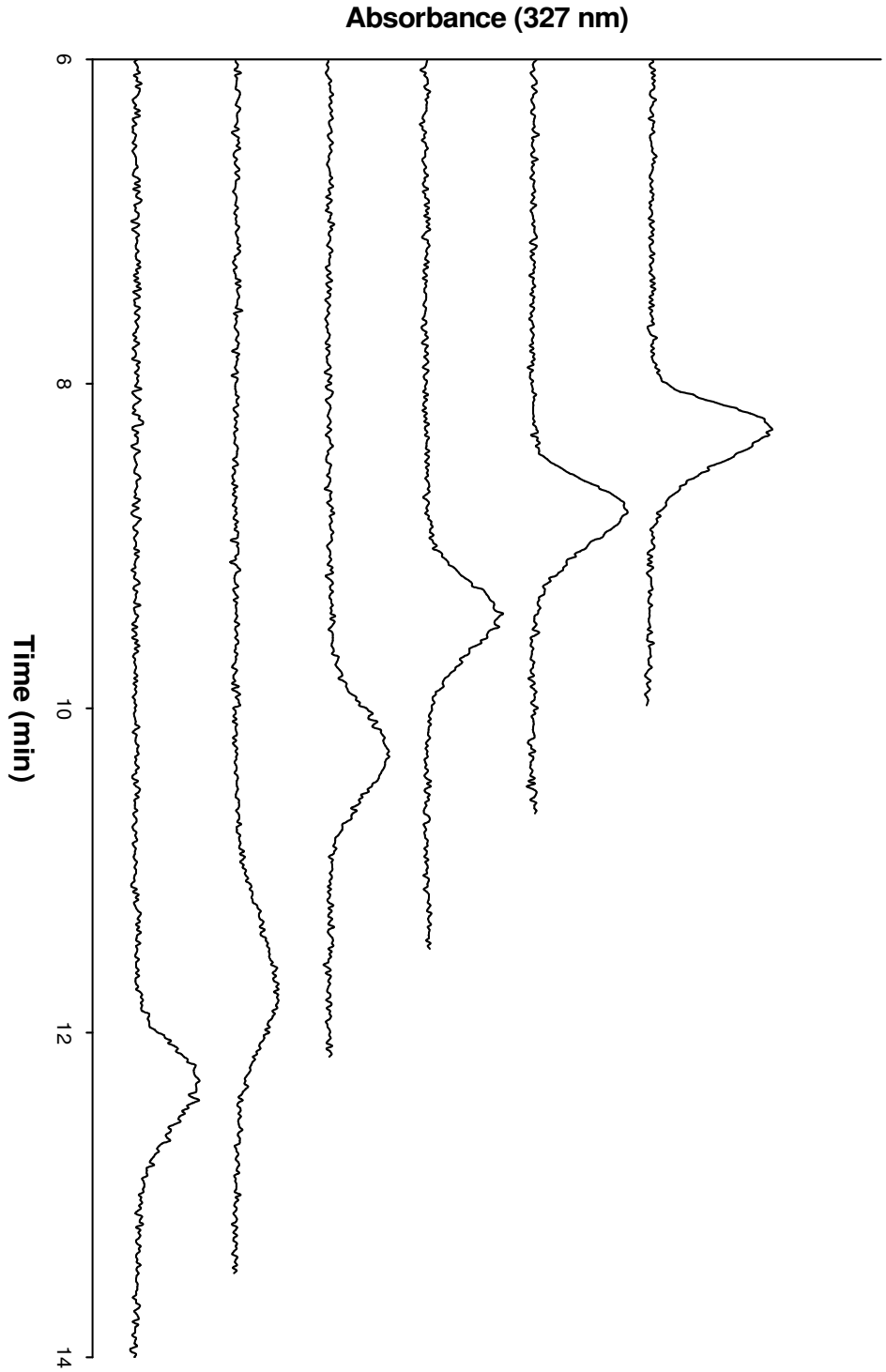
Absorbance (327 nm)
Time (min)
6
8
10
12
14

All of these applications rely on the same foundation: the analyte will have some reversible interaction with the immobilized ligand within the column. The extent of this interaction can be examined by measuring the retention factor (k) of the analyte as it passes through the column, as defined below.

$$k = \frac{t_R - t_M}{t_M} = \frac{V_R - V_M}{V_M} \quad (1\text{-}9)$$

In this equation, t_R is the retention time of the analyte of interest while t_M is the elution time of a non-retained compound (i.e., the void time). V_R is the corresponding retention volume and V_M is the void volume. The retention factor that is calculated according to Equation 1-9 for an affinity column can also be related by Equation 1-10 to the number of binding sites within the column as well as the binding affinity to each site.[78]

$$k = \frac{(K_{a1}n_1 + ... + K_{an}n_n)m_L}{V_M} \quad (1\text{-}10)$$

The terms K_{a1} through K_{an} in this equation represent the association equilibrium constants at binding sites 1 through n within the column, and n_1 through n_n represent the fraction of each type of individual site in the column. The term m_L represents the total moles of binding sites within the column. It can be seen from this equation that a change in the binding strength, location of binding, or number of binding sites within the column could significantly alter the retention factor for the analyte.

Binding and Competition Studies

One of the primary applications for zonal elution in biointeraction studies is to examine the extent of binding between an analyte and the immobilized ligand. One way this can be done is to relate the retention factor of an injected analyte to the ligand bound

fraction of the analyte (b) and free fraction of analyte in solution (f) at the center of the analyte's peak. This can be done under linear elution conditions for a system with fast association/dissociation kinetics by using Equation 1-11.

$$k = \frac{\mathrm{b}}{\mathrm{f}} \tag{1-11}$$

The sum of bound and free analyte fractions must equal one (i.e., b + f = 1), which means Equation 1-11 can be rearranged so that either the bound or free fraction of the analyte at equilibrium can be calculated from the measured retention factor.[75]

$$\mathrm{b} = \frac{k}{1+k} \tag{1-12}$$

Binding studies in this area have been used to explore a variety of analyte-ligand systems. Examples of such work include the binding of groups of benzodiazepines, coumarins, and triazole derivatives to HSA.[75] The retention factors of two solutes can also be compared if they bind to the same site on a ligand. If the binding site is identical for the two solutes and they each interact at only a single specific region on the ligand, the ratio of their two retention factors should also be equal to the ratio of the association equilibrium constants. These values cannot be compared, however, if the analytes bind to the ligand at multiple sites or if their binding sites are slightly different from one another. This latter situation occurs because binding regions on an immobilized ligand may lose activity to slightly different extents when covalent immobilization methods are employed.[43, 79]

The most prevalent application for zonal elution is in competition studies. This application can be used to see if the binding site for one solute is also a binding site for a second solute. This type of experiment is performed by continuously passing through the

affinity column a mobile phase with a known amount of competing agent I, which represents one of the two solutes being compared, while injecting a small plug of the second solute or analyte A onto the column. If A and I compete for the same sites on the ligand and both have fast association/dissociation kinetics, the following equation can be used to describe the observed change in the retention factor for A as it competes with I for binding sites in the column.[36, 51]

$$\frac{1}{k} = \frac{K_{aI} V_{\mathrm{M}} [\mathrm{I}]}{K_{aA} m_L} + \frac{V_{\mathrm{M}}}{K_{aA} m_L} \qquad (1\text{-}13)$$

The terms K_{aI} and K_{aA} in this equation represent the association equilibrium constants for the ligand with the competing agent and analyte, respectively, at their site of competition in the column. Similar equations can also be derived for more complex models, such as those that involve more than one binding site, non-specific interactions or allosteric effects.[36]

Relationships like the one in Equation 1-13 can be valuable tools in determining the nature of the competition that occurs between the analyte and mobile phase additive.[46, 74, 76] For example, if a plot of $1/k$ versus [I] that is made according to Equation 1-13 gives a linear relationship, then A and I are following a model in which they have competition at a single class of binding sites on the immobilized ligand. If this plot shows only random variations in the value of $1/k$ (or k) as [I] is increased, this behavior indicates that the analyte and competing agent are not binding at a common site nor do they have any allosteric interactions with one another. If the response of the plot is non-linear with a positive slope, the analyte is either binding to multiple sites or there are negative allosteric effects occurring between the analyte and the competing agent. If

a non-linear plot is obtained with a negative slope, this is an indication that positive allosteric effects are present between A and I as they interact with the ligand.[36]

Advantages of this method are the rapid speed of the experiments, the good run-to-run precision, and the need for only a small amount of analyte per run. Once an appropriate model has been found to describe the retention data (e.g., the use of Equation 1-13 for a system with single site binding), it is possible to also determine the association equilibrium constants for the competing agent and/or analyte with the ligand from these experiments. The precision of these measurements is typically in the range of 5-10% using a standard HPLC system, with a long-term change in ligand activity resulting in only a small variation in the association equilibrium constants that are determined by this approach.[43]

Zonal elution has been used in many past studies in a quantitative fashion to examine direct competition between solutes and to estimate the association equilibrium constants for these interactions. It has also been shown more recently how quantitative information can be obtained from zonal elution and competition studies to look at allosteric effects between two compounds. Allosteric effects occur when the binding of an analyte to a ligand at one binding site interferes with the binding of a second analyte to the ligand at a different binding site. This interference can either hinder or promote the binding of the analytes to the ligand. The effect of these interactions during a zonal elution study can be described by the following equation,[76] where k_0 is the retention factor for the ligand in the absence of any competing agent in the mobile phase.

$$\frac{k_0}{k - k_0} = \frac{1}{\beta_{I \to A} - 1} \times \left(\frac{1}{K_{aI}[\mathrm{I}]} + 1 \right) \qquad (1\text{-}14)$$

Figure 1-10. Allosteric effect of *R*- and *S*-ibuprofen on the binding of *S*-lorazepam acetate to an immobilized HSA, as analyzed according to Equation 1-14 (with permission from Chen, J., and D.S. Hage, *Nat. Biotechnol*., 22, 1445-1448, 2004).[76]

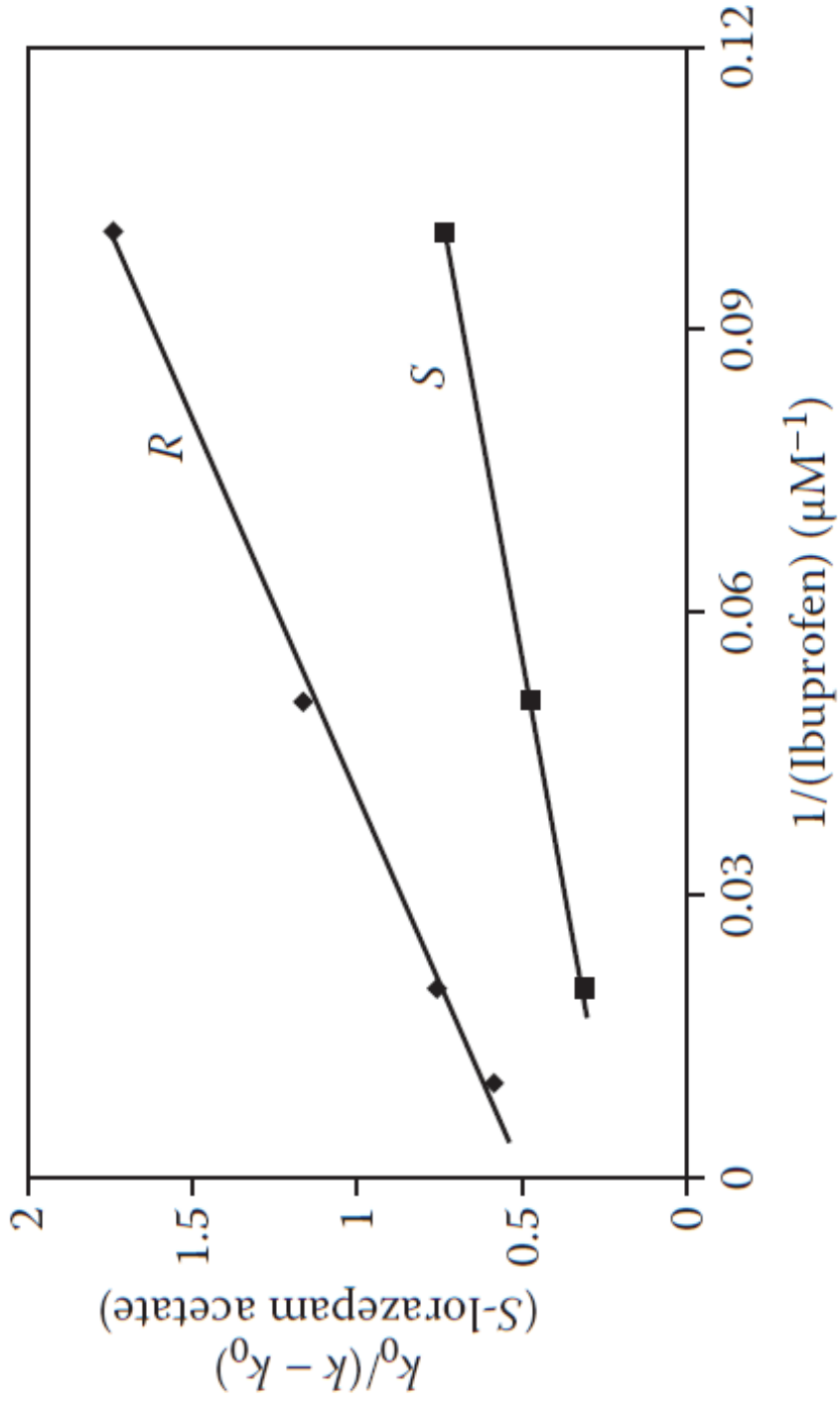
2
1.5
1
0.5
0
0
0.03
0.06
0.09
0.12
R
S
$k_0/(k - k_0)$
(S-lorazepam acetate)
1/(Ibuprofen) (μM^{-1})

In this equation, the ligand is viewed as having at least two binding sites, one for the injected analyte (A) and one for the competing agent in the mobile phase (I). The binding of A with the ligand is altered as I also binds to the ligand, which causes the association equilibrium constant for A with the ligand to change from K_{aL} to K_{aL}'. This change is represented in the above equation by the coupling constant $\beta_{I\rightarrow A}$, which is equal to the ratio K_{aL}'/K_{aL}. Equation 1-14 predicts that a plot of $k_0/(k-k_0)$ versus 1/[I] will give a linear relationship for a simple allosteric interaction and that, through this relationship, the values of $\beta_{I\rightarrow A}$ and K_{aI} can be obtained.[76] An example of such a plot is shown in Figure 1-10. Studies on drug-protein systems have been performed to examine the allosteric effects occurring between competing agent, such as the interactions between *R*- or *S*-ibuprofen with *S*-lorazepam or the enantiomers of oxazepam on HSA, as well as the interactions between L-tryptophan and phenytoin on HSA.[76]

Temperature and Solvent Studies

Zonal elution can also be used to see how a biological interaction will change as one varies the conditions under which this interaction takes place. For instance, altering the temperature of a system has been shown to have an effect on the association equilibrium constants for a variety of compounds with HSA.[46, 64, 65] This relationship can be described for a system with single site binding and over a reasonably narrow temperature range by using the following equation,

$$\ln K_a = \frac{-\Delta H}{RT} + \frac{\Delta S}{R} \qquad (1\text{-}15)$$

in which ΔH is the change in enthalpy of the reaction, ΔS in the change in entropy, T is the absolute reaction temperature, and R is the gas law constant. Preparing a plot of ln K_a versus $1/T$ in this situation would be expected to result in a graph where the slope is equal to $-\Delta H/R$ and the intercept is equal to $\Delta S/R$. Using this information, it is possible to calculate the overall change in enthalpy and entropy of the reaction. The total change in free energy (ΔG) can also be calculated using Equation 1-16.

$$\Delta G = -RT \ln K_a \tag{1-16}$$

This information can be used to determine what force has the greatest contribution to the free energy on the binding of an analyte to a ligand.[64]

Three other factors that can be altered during zonal elution experiments are the pH, ionic strength, and content of organic modifier in the mobile phase. Figure 1-11 shows examples of experiments in which these parameters were varied during a zonal elution study. Increasing the ionic strength of a buffer solution, for instance, tends to decrease coulombic interactions in this particular example by a creating a shielding effect that occurs due to the increase in ion concentration. However, increasing the ionic strength also tends to increase the adsorption of non-polar solutes onto the column. A change in pH can alter the conformation of the ligand and the overall net charge of the ligand, which will also change coulombic interactions. Adding organic modifier can disrupt the analyte-ligand binding. For example, if the ligand is a protein, the non-polar bonds could be affected as well as the protein conformation by adding only a small amount of organic solvent.

Figure 1-11. Shift in the retention factor of carbamazepine on an immobilized HSA column with changes in pH (a), ionic strength (b), or organic content of the mobile phase additive (with permission from Kim, H.S., and D.S. Hage, *J. Chromatogr. B*, 816, 57-66, 2005).[46]

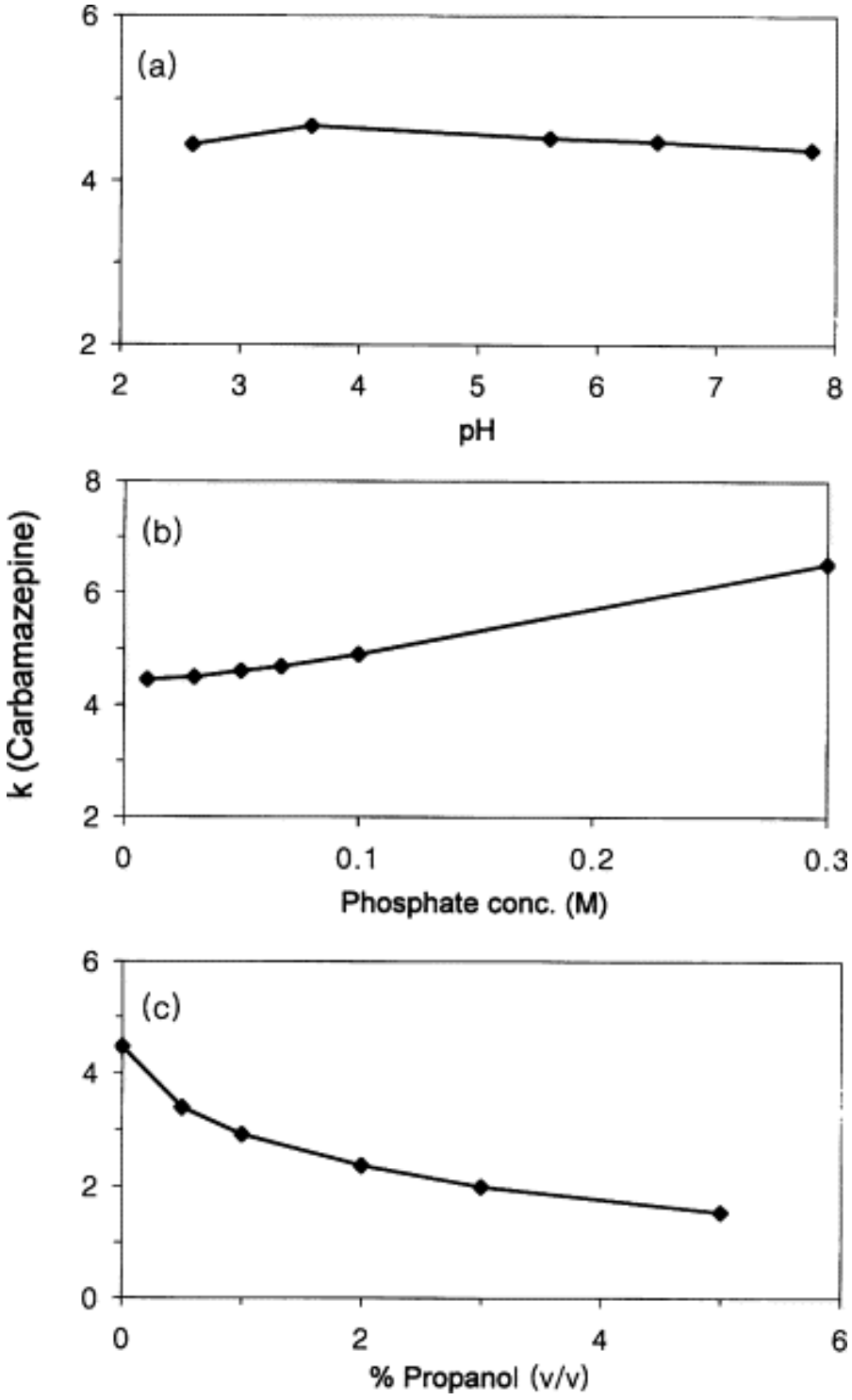
(a)
6
4
2
2
3
4
5
6
7
8
pH
(b)
k (Carbamazepine)
8
6
4
2
0
0.1
0.2
0.3
Phosphate conc. (M)
(c)
6
4
2
0
0
2
4
6
% Propanol (v/v)

Characterization of Binding Sites

Zonal elution-based competition studies are often used as a way to characterize and determine the location of an analyte's binding site on a ligand. In these studies, competing agents with known binding sites on the ligand are used to determine whether they compete with an analyte for interactions with the ligand. This type of competition experiment not only allows the binding site to be identified for the analyte, but also provides the association equilibrium constant for the analyte at this specific binding site, such as is obtained through the use of Equation 1-13 or related expressions.

Another way to map out the binding sites for a particular analyte is by chemically altering these binding regions and then using zonal elution to determine if there are any resulting changes in the retention of the analyte. This approach has been used along with the modification of specific residues on HSA that are thought to lie within one of its major binding sites. One such study examined the binding of drugs to the Sudlow site II of HSA by altering Tyr-411 on this protein; the resulting affinity column was shown to have altered binding for a number of compounds when compared to normal HSA in zonal elution studies.[80] Similar results were obtained for analytes that could bind to Sudlow site I when Trp-214 on HSA was modified and the resulting ligand was compared to normal HSA in zonal elution and frontal analysis studies.[81]

Practical Considerations

While zonal elution is an easy method with which to work, it does have a number of factors that must be considered to ensure that this approach is properly performed. For example, the choice of affinity column must be considered and reported. Items that

should be noted include the column dimensions, the support within the column and the immobilized ligand. The support within the column should be chosen based upon factors such as the mobile phase pH that will be used, the desired flow rate range for the experiments, the allowed column backpressure, and the degree of non-specific binding that can be tolerated.[82] If the experiments will be using high-flow rates, for example, the backpressure that would be created with a porous silica column might be too high and a more suitable approach might involve the use of a monolithic column.[41, 82] Some supports such as silica have a limited range of pH stability, which must also be considered. For example, silica will start to dissolve above a pH of approximately 8.0 or below 2.0. This pH range of stability can be increased by several means, such as incorporating zirconium or aluminum on to the silica surface which might improve its stability under these alkaline conditions.[40]

When a new column has been created with unknown binding properties, it should be tested using an analyte with known binding properties to ensure that the column, support, and immobilized ligand have all been chosen properly for upcoming studies. Also, when measuring analyte retention, it is crucial that the true center of the peak be determined. Due to peak tailing, this is typically not the tallest point of the peak but rather the point at which the two areas of the peak would be equal if the peak were to be split in half vertically. It is recommended that this be done with computer software to obtain the most accurate results.

If the analyte has high retention, a low-capacity column might be desirable to produce shorter retention times. The easiest way to solve this problem is to simply use a smaller column. This could mean shortening the column length, decreasing the inner

diameter of the column, or both. Whenever a column containing an immobilized ligand is created, a control column that was made following the same procedure (minus the addition of the ligand) should be used to account for any non-specific binding that might occur. One precaution that must be followed when reducing column size during binding studies is that it must be ensured that conditions are still present that allow a local equilibrium to be established as the true center of the analyte's peak. This is true if consistent results are still being obtained in the retention factor as the column size is altered.

Another point to consider when performing zonal elution studies is the concentration range that should be used for the competing agent or additive in the mobile phase. It is important to be able to observe a shift in analyte retention, and in order to do so the appropriate concentration range must be chosen for the competing agent. This can be done by looking at the shift in k as it moves between its maximum (k_{max}) and its minimum (k_{min}), as shown in Figure 1-12. The following equation can be used to describe this relationship for an analyte and a competing agent that engage in direct competition for a single binding site.[36]

$$\frac{k - k_{min}}{k_{max} - k_{min}} = \frac{1}{1 + K_{aI}[I]} \qquad (1\text{-}17)$$

It is important to note in this particular case that the shift in retention is due only to the concentration and association equilibrium constant of the competing agent ([I] and K_{aI}, respectively). The ideal range for this experiment is when the mobile phase concentration of the competing agent gives the greatest change in $(k\text{-}k_{min})/(k_{max}\text{-}k_{min})$. This occurs between values of 0.1 and 0.9 for this term in Figure 1-12. However, other

Figure 1-12. Relative shift in analyte retention as a function of competing agent concentration for a zonal elution experiment in which there is direct competition between A and I at a single site on an immobilized ligand, as predicted by Equation 1-13.

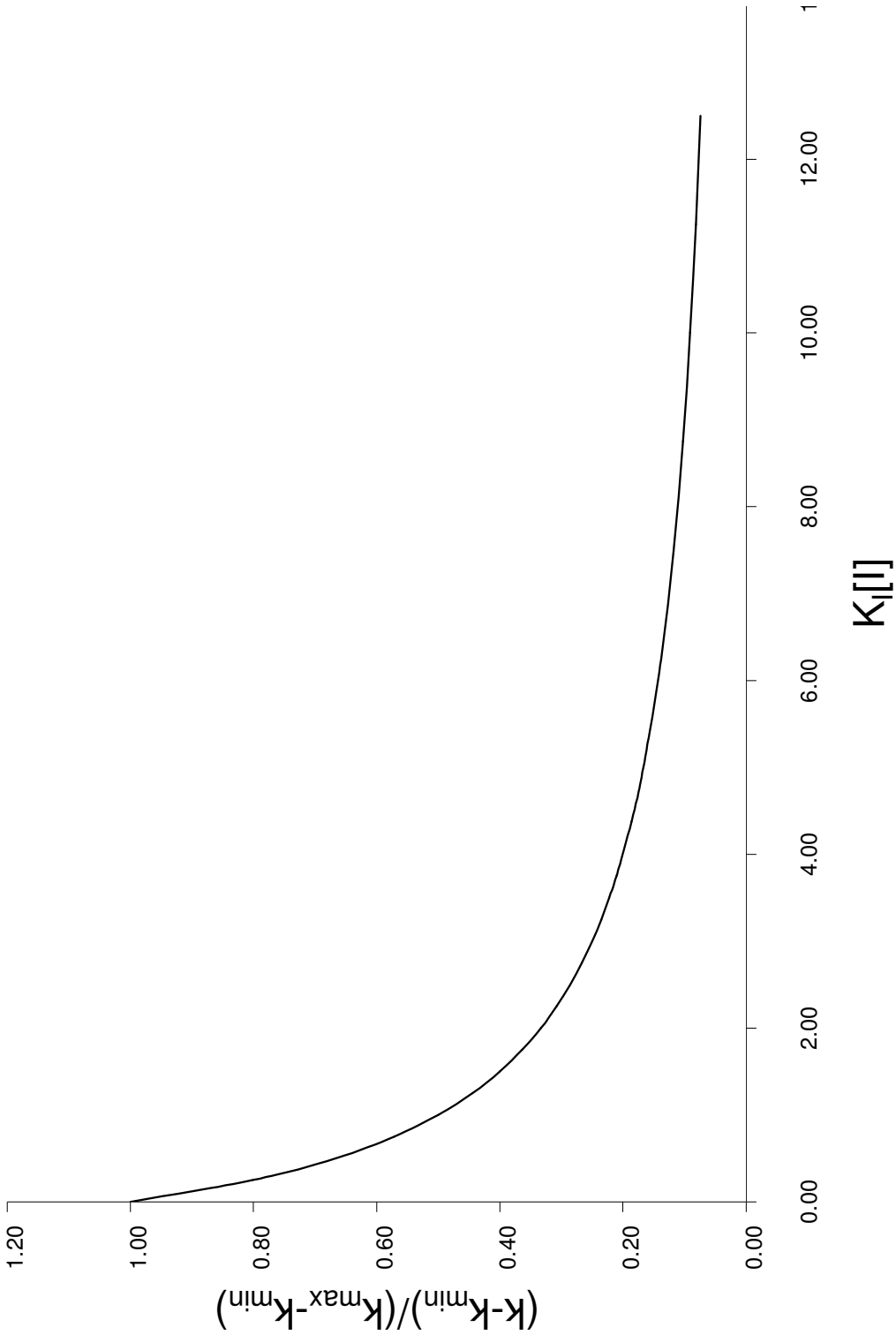
1.20
1.00
0.80
0.60
0.40
0.20
0.00
(k-k$_{min}$)/(k$_{max}$-k$_{min}$)
0.00
2.00
4.00
6.00
8.00
10.00
12.00
1
K$_I$[I]

concentrations above or below this optimum level should also be used to ensure that the correct model is being used to describe the biological interaction.[36]

Although it is possible to work under non-linear elution conditions,[68, 69] zonal elution studies are usually performed under linear elution conditions. This is the region where the concentration of analyte is small compared to the amount of immobilized active ligand within the column. Columns containing larger ligands, such as proteins, often have a smaller capacity than traditional small molecule columns, thus making it more difficult to stay within this region. Fortunately, testing for linear elution conditions simply involves injecting a range of analyte concentrations and observing whether there is any shift in retention. Samples concentrations are then selected over which no significant change in retention occurs. The concentration conditions often vary from one compound to the next, so it is important to test this feature with each new compound that is to be examined by zonal elution methods.[65]

Other factors to consider are the solubility and response or detectability of the analyte. Solubility will place an upper limit on the concentration range that can be used for the analyte, while the detector response and analyte detectability will place a lower limit on this range. Solubilizing agents such as cyclodextrins can often be used to increase the solubility of an analyte. However they require the use of more complex models to describe how the retention of an analyte will vary with the concentrations of both the competing agent and solubilizing agent.[83] Absorbance detectors are often used for zonal elution studies, but if there are issues with the detectability of the analyte then a more sensitive detection mode can be employed.

Overall Goals and Summary of Dissertation

The overall goal of this dissertation is to use HPAC to examine the binding of drugs (e.g., sulfonylurea compounds and others) with HSA and determine the influence of protein glycation on these binding processes. Chapter 2 will examine the possible use of four coumarin compounds (i.e., coumarin, 4-hydroxycoumarin, 7-hydroxycoumarin, and 7-hydroxy-4-methylcoumarin) as alternatives to warfarin, as Sudlow site I probes in drug-protein binding studies with HSA. HPAC will be used in this work to compare and evaluate the binding properties of each probe candidate. Frontal analysis studies will be performed in order to examine the binding constants for each of the compounds. The data will be fitted to single- and multi-site models to determine the overall binding relationship of each compound with HSA. Competition experiments based on the method of zonal elution will be used to observe the binding interactions between these compounds and warfarin. The results from these studies will then be used to determine which of these compounds might be useful as probes for Sudlow site I.

The work in chapter 3 will assess the binding of two sulfonylurea drugs (i.e., acetohexamide and tolbutamide) to normal HSA using HPAC. The method of frontal analysis will be used to estimate the overall binding parameters for each drug with HSA, while competition studies and zonal elution experiments will be used with *R*-warfarin and L-tryptophan as site-selective probes to examine the locations of these interactions on HSA. The data will be fitted to a number of different models, including single-site, two-site, three-site, and modified three-site models, to obtain a better understanding of these drug-protein binding interactions. These studies will also be used to illustrate how frontal

analysis and zonal elution studies can be used to compliment each other in obtaining information about the interactions that can take place between a drug and a protein.

Chapter 4 will explore how the binding of site-specific probes for Sudlow site I (warfarin) and Sudlow site II (L-tryptophan) are affected by an increase in HSA glycation. This investigation will be performed using HPAC and the method of frontal analysis. Association equilibrium constants and binding capacities for the given probe compounds will be measured and compared as glycation levels on HSA increase. The results will be used to clarify how such binding parameters might change within this system as a result of HSA glycation.

The work in chapter 5 will investigate the drug-protein binding that occurs between sulfonylureas drugs (i.e., acetohexamide and tolbutamide) and HSA as the degree of glycation is increased on this protein. In these studies, glycated HSA that has been prepared *in vitro* will be used to obtain a range of glycation levels for HPAC columns. Frontal analysis will then be used to look at the binding for each drug on each set of glycated HSA columns to determine how the binding parameters for these drugs are altered as the level of glycation for HSA is increased. Competition experiments will be performed to further explore how the binding interactions for these drugs are affected at Sudlow sites I and II on HSA.

Chapter 6 will examine how ligand heterogeneity may affect the results that are obtained in HPAC studies. These studies will examine the analyte concentrations and conditions that are necessary to see shifts in analyte-protein binding due to multi-site interactions in frontal analysis work. Computer modeling and the use of chromatographic theory will be used in this work to determine the conditions that are best

suited for studying changes in analyte-ligand interactions when modifications such as glycation are occurring in the immobilized ligand.

References

1. Diabetes Atlas. Fourth ed.; Unwin, N.; Whiting, D.; Gan, D.; Jacqmain, O.; Ghyoot, G., Eds. International Diabetes Federation: 2009. www.diabetesatlas.org.
2. National Diabetes Fact Sheet: General Information and National Estimates on Diabetes in the United States, 2007. U. S. Department of Health and Human Services; Centers for Disease Control and Prevention: Atlanta, GA, 2008.
3. In *61/225. World Diabetes Day*, United Nations General Assembly, United Nations: 2007.
4. National Diabetes Information Clearinghouse, Diabetes Overview. U. S. Department of Health and Human Services, National Institute of Health: Bethesda, 2008.
5. Patlak, M., New Weapons to Combat an Ancient Disease: Treating Diabetes. In *Breakthroughs in Bioscience*, Biology, Federation of American Societies for Experimental Biology; FASEB: Bethesda, 2002.
6. Skillman, T. G.; Feldman, J. M., *Am. J. Med.* **1981,** *70*, 361-372.
7. Prato, S. D.; Pulizzi, N., *Metabolism.* **2006,** *55* (Suppl 1), S20-S27.
8. Green, J. B.; Feinglos, M. N., *Curr. Diab. Rep.* **2006,** *6*, 373-377.
9. *Drug Information for the Health Care Professional*. The US Pharmacopeial Convention, Inc.: 1997; Vol. 1.
10. Krentz, A. J.; Bailey, C. J., *Drugs* **2005,** *65* (3), 385-411.
11. Fauci, A. S.; Kasper, D. L.; Braunwald, E.; Hauser, S. L.; Longo, D. L.; Jameson, J. L.; Loscalzo, J., Harrison's Principles of Internal Medicine. 17th ed. http://www.accessmedicine.com (accessed January 2010).

12. Crooks, M. J.; Brown, K. F., *J. Pharm. Pharmacol.* **1974,** *26*, 304-311.

13. Jakoby, M. G.; Covey, D. F.; Cistola, D. P., *Biochem.* **1995,** *34*, 8780-8787.

14. Brown, K. F.; Crooks, M. J., *Can. J. Pharm. Sci.* **1974,** *9* (3), 75-77.

15. Ascenzi, P.; Bocedi, A.; Notari, S.; Fanali, G.; Fesce, R.; Fasano, M., *Mini-Rev. Med. Chem.* **2006,** *6*, 483-489.

16. Colmenarejo, G., *Med. Res. Rev.* **2003,** *23* (3), 275-301.

17. Dockal, M.; Carter, D. C.; Ruker, F., *J. Biol. Chem.* **1999,** *274* (41), 29303-29310.

18. Fasano, M.; Curry, S.; Terreno, E.; Galliano, M.; Fanali, G.; Narciso, P.; Notari, S.; Ascenzi, P., *IUBMB Life* **2005,** *57* (12), 787-796.

19. Ascoli, G. A.; Domenici, E.; Bertucci, C., *Chirality* **2006,** *18*, 667-679.

20. Otagiri, M., *Drug Metab. Pharmacokinet.* **2005,** *20* (5), 309-323.

21. Sudlow, G.; Birkett, D. J.; Wade, D. N., *Mol. Pharmacol.* **1975,** *11*, 824-832.

22. Sudlow, G.; Birkett, D. J.; Wade, D. N., *Mol. Pharmacol.* **1976,** *12*, 1052-1061.

23. Sengupta, A.; Hage, D. S., *Anal. Chem.* **1999,** *71*, 3821-3827.

24. Hage, D. S.; Sengupta, A., *J. Chromatogr. B* **1999,** *724* (1), 91-100.

25. Herve, F.; Urien, S.; Albengres, E.; Duche, J.-C.; Tillement, J.-P., *Clin. Pharmacokinet.* **1994,** *26* (1), 44-58.

26. Fitzpatrick, G.; Duggan, P. F., *Biochem. Soc. Trans.* **1987,** *15* (2), 267-268.

27. Nakajou, K.; Watanabe, H.; Kragh-Hansen, U.; Maruyama, T.; Otagiri, M., *Biochim. Biophys. Acta* **2003,** *1623*, 88-97.

28. Mendez, D. L.; Jensen, R. A.; McElroy, L. A.; Pena, J. M.; Esquerra, R. M., *Arch. Biochem. Biophys.* **2005,** *444*, 92-99.

29. Marashi, S.-A.; Safarian, S.; Moosavi-Movahedi, A. A., *Med. Hypotheses* **2005,** *64* (4), 881.

30. Garlick, R. L.; Mazer, J. S., *J. Biol. Chem.* **1983,** *258* (10), 6142-6146.

31. Lapolla, A.; Fedele, D.; Seraglia, R.; Traldi, P., *Mass Spectrom. Rev.* **2006,** *25*, 775-797.

32. Iberg, N.; Fluckiger, R., *J. Biol. Chem.* **1986,** *261* (29), 13542-13545.

33. Koizumi, K.; Ikeda, C.; Ito, M.; Suzuki, J.; Kinoshita, T.; Yasukawa, K.; Hanai, T., *Biomed. Chromatogr.* **1998,** *12*, 203-210.

34. Koyama, H.; Sugioka, N.; Uno, A.; Mori, S.; Nakajima, K., *Biopharm. Drug Dispos.* **1997,** *18* (9), 791-801.

35. Barzegar, A.; Moosavi-Movahedi, A. A.; Sattarahmady, N.; Hosseinpour-Faizi, M. A.; Aminbakhsh, M.; Ahmad, F.; Saboury, A. A.; Ganjali, M. R.; Norouzi, P., *Protein Peptide Lett.* **2007,** *14*, 13-18.

36. Hage, D. S., *J. Chromatogr. B* **2002,** *768*, 3-30.

37. Schiel, J. E.; Joseph, K. S.; Hage, D. S., Biointeraction Affinity Chromatography. In *Adv. Chromatogr.*, Grinsberg, N.; Grushka, E., Eds. Taylor & Francis: New York, 2010; Vol. 48.

38. Kasai, K.; Ishii, S., *J. Biochem.* **1975,** *78*, 653-662.

39. Muller, A. J.; Carr, P. W., *J. Chromatogr.* **1984,** *284*, 33-51.

40. Schiel, J. E.; Mallik, R.; Soman, S.; Joseph, K. S.; Hage, D. S., *J. Sep. Sci.* **2006,** *29*, 719-737.

41. Mallik, R., *J. Sep. Sci.* **2006,** *29*, 1686-1704.

42. Schriemer, D. C., *Anal. Chem.* **2004,** *76* (23), 440A-448A.

43. Loun, B.; Hage, D. S., *J. Chromatogr.* **1992,** *579*, 225-235.

44. Tweed, S. A.; Loun, B.; Hage, D. S., *Anal. Chem.* **1997,** *69*, 4790-4798.

45. Winzor, D. J., *J. Chromatogr. A* **2004,** *1037*, 351-367.

46. Kim, H. S.; Hage, D. S., *J. Chromatogr. B.* **2005,** *816*, 57-66.

47. Kimura, T.; Shibukawa, A.; Matsuzaki, K., *Pharm. Res.* **2006,** *23* (5), 1038-1042.

48. Mallik, R.; Xuan, H.; Guiochon, G.; Hage, D. S., *Anal. Biochem.* **2008,** *376*, 154-156.

49. Asnin, L.; Kaczmarski, K.; Guiochon, G., *J. Chromatogr. A* **2008,** *1192*, 62-73.

50. Lei, G.; Yang, R.; Zeng, X.; Shen, Y.; Zheng, X.; Wei, Y., *Chromatographia* **2007,** *66*, 847-852.

51. Nakano, N. I.; Shimamori, Y.; Yamaguchi, S., *J. Chromatogr.* **1982,** *237*, 225-232.

52. Schriemer, D. C.; Bundle, D. R.; Li, L.; Hindsgaul, O., *Angew. Chem. Int. Ed.* **1998,** *37*, 3383-3387.

53. Iwaki, J.; Minamisawa, T.; Tateno, H.; Kominami, J.; Suzuki, K.; Nishi, N.; Nakamura, T.; Hirabayashi, J., *Biochem. Biophys. Res. Commun.* **2008,** *373*, 206-212.

54. Tachibana, K.; Nakamura, S.; Wang, H.; Iwasaki, H.; Tachibana, K.; Maebara, K.; Cheng, L.; Hirabayashi, J.; Narimatsu, H., *Glycobiology* **2006,** *16* (1), 46-53.

55. Kimura, T.; Nakanishi, K.; Nakagawa, T.; Shibukawa, A.; Matsuzaki, K., *Pharm. Res.* **2005,** *22* (4), 667-675.

56. Nakamura-Tsuruta, S.; Uchiyama, N.; Hirabayashi, J., *Methods Enzymol.* **2006,** *415*, 311-325.

57. Kovarik, P.; Hodgson, R. J.; Covey, T.; Brook, M. A.; Brennan, J. D., *Anal. Chem.* **2005,** *77*, 3340-3350.

58. Chan, N.; Lewis, D.; Kelly, M.; Ng, E. S. M.; Schriemer, D. C., Frontal affinity chromatography-mass spectrometry for ligand discovery and characterization. In *Mass Spectrometry in Medicinal Chemistry*, Wanner, K. T.; Hofner, G., Eds. WILEY-VCH Verlag GmbH & Co. KGaA: Weinhein, 2007; pp 217-246.

59. Slon-Usakiewicz, J. J.; Dai, J.-R.; Ng, W.; Foster, J. E.; Deretey, E.; Toledo-Sherman, L.; Redden, P. R.; Pasternak, A.; Reid, N., *Anal. Chem.* **2005,** *77*, 1268-1274.

60. Ng, E. S. M.; Yang, F.; Kameyama, A.; Palcic, M. M.; Hindsgaul, O.; Schriemer, D. C., *Anal. Chem.* **2005,** *77*, 6125-6133.

61. Arata, Y.; Ishii, N.; Tamura, M.; Nonaka, T.; Kasai, K.-i., *Biol. Pharm. Bull.* **2007,** *30* (11), 2012-2017.

62. Kimura, T.; Nakanishi, K.; Nakagawa, T.; Shibukawa, A.; Matsuzaki, K., *J. Pharm. Biomed. Anal.* **2005,** *38*, 204-209.

63. Itakura, Y.; Nakamura-Tsuruta, S.; Kominami, J.; Sharon, N.; Kasai, K.-i.; Hirabayashi, J., *J. Biochem.* **2007,** *142*, 459-469.

64. Loun, B.; Hage, D. S., *Anal. Chem.* **1994,** *66* (21), 3814-3822.

65. Yang, J.; Hage, D. S., *J. Chromatogr. A* **1996,** *725*, 273-285.

66. Ruta, J.; Ravelet, C.; Désiré, J.; Décout, J.-L.; Peyrin, E., *Anal. Bioanal. Chem.* **2008,** *390*, 1051-1057.

67. Hage, D. S.; Chen, J., Quantitative affinity chromatography: Practical aspects. In *Handbook of Affinity Chromatography*, Hage, D. S., Ed. Taylor and Francis: New York, 2006.

68. Vidal-Madjar, C.; Jaulmes, A.; Racine, M.; Sebille, B., *J. Chromatogr.* **1988,** *458*, 13-25.

69. Arnold, F. H.; Schofield, S. A.; Blanch, H. W., *J. Chromatogr.* **1986,** *355*, 1-12.

70. Dunn, B. M.; Chaiken, I. M., *Proc. Natl. Acad. Sci. U. S. A.* **1974,** *71*, 2382-2385.

71. Sebille, B.; Thuaud, N., *J. Chromatogr.* **1978,** *167*, 159-170.

72. Dalgaard, L.; Hansen, J. J.; Pedersen, J. L., *J. Pharm. Biomed. Anal.* **1989,** *7*, 361-368.

73. Fitos, I.; Visy, J.; Simonyi, M.; Hermansson, J., *J. Chromatogr.* **1992,** *609* (163-171).

74. Joseph, K. S.; Moser, A. C.; Basiaga, S.; Schiel, J. E.; Hage, D. S., *J. Chromatogr. A* **2009,** *1216*, 3492-3500.

75. Noctor, T. A. G.; Diaz-Perez, M. J.; Wainer, I. W., *J. Pharm. Sci.* **1993,** *82*, 675-676.

76. Chen, J.; Hage, D. S., *Nat. Biotechnol.* **2004,** *22* (11), 1445-1448.

77. Ng, E. S. M.; Yang, F.; Kameyama, A.; Palcic, M. M.; Hindsgaul, O.; Schriemer, D. C., *Anal. Chem.* **2005,** *77*, 6125-6133.

78. Hage, D. S.; Tweed, S. A., *J. Chromatogr. B* **1997,** *699*, 499-525.

79. Yang, J.; Hage, D. S., *J. Chromatogr.* **1993,** *645*, 241-250.

80. Noctor, T. A. G.; Wainer, I. W., *Pharm. Res.* **1992,** *9*, 480-484.

81. Chattopadhyay, A.; Tian, T.; Kortum, L.; Hage, D. S., *J. Chromatogr. B* **1998,** *715*, 183-190.

82. Gustavsson, P.-E.; Larsson, P.-O., Support Materials for Affinity Chromatography. In *Handbook of Affinity Chromatography*, 2 ed.; Hage, D. S., Ed. Taylor & Francis: New York, 2006.

83. Hage, D. S.; Sengupta, A., *Anal. Chem.* **1998,** *70*, 4602-4609.

CHAPTER 2

THE EVALUATION OF WARFARIN PROBE ALTERNATIVES FOR HUMAN SERUM ALBUMIN

Introduction

The analysis of drug binding to plasma proteins is important in the pharmaceutical industry for characterizing the pharmacokinetics and pharmacological effects of drugs.[1-6] One plasma protein that has been extensively investigated during such work is human serum albumin (HSA).[7] HSA is the most abundant protein in plasma, with a concentration that ranges from 35-50 g/L or 0.6-0.7 mM.[1, 6-10] This protein is involved in transporting and distributing many drugs within the body and also binds to a variety of endogenous and exogenous compounds to aid in their transport and to improve their solubility.[8-12]

Numerous techniques have been utilized to look at HSA and drug-protein interactions, including ultrafiltration,[13] ultracentrifugation,[14] equilibrium dialysis,[15-17] fluorescence,[18, 19] UV/Vis absorption,[19] circular dichroism,[20-23] capillary electrophoresis,[24-27] surface plasmon resonance,[28, 29] and nuclear magnetic resonance (NMR) spectroscopy.[30, 31] Another technique that has been popular for some time in this type of application is high-performance affinity chromatography (HPAC).[32-36] HPAC is a specialized form of HPLC that makes use of an immobilized biological ligand (e.g., HSA) as the stationary phase.[32, 33, 37-39] It has been previously shown that columns containing immobilized HSA are effective models for soluble HSA in drug binding studies, making it possible to rapidly obtain accurate and precise estimates of the

association equilibrium constants and number of binding sites for drugs on HSA, while also providing a means for studying drug-drug competition for this protein.[32, 33, 39] These properties make HPAC and HSA columns appealing for the high throughput screening of drug binding to HSA.

Both the number of binding sites and affinity of a drug are important in determining the interaction of such an agent with HSA.[40] This protein is known to contain two major binding sites for drugs (i.e., Sudlow site I and II),[41, 42] as well as several minor binding sites.[43] One way the binding of a drug at a particular site on HSA can be identified is by determining if this drug has direct competition with a specific probe for that site. Warfarin (i.e., 3-(α-acetonylbenzyl)-4-hydroxycoumarin) is an anti-coagulant drug that is frequently used as a probe for Sudlow site I (also often called the warfarin-azapropazone site of HSA).[44] Warfarin has a relatively high affinity for HSA and well-characterized interactions with this protein.[42] There are, however, several disadvantages to using warfarin in binding studies. For instance, the strong binding of warfarin to HSA can lead to long retention times for this drug on HPAC columns that contain immobilized HSA.[45] In addition, although the two enantiomers of warfarin have the same binding region but slightly different affinities for HSA,[44, 45] it can be expensive to use these separate enantiomers in binding studies (see Table 2-1); this has lead to the frequent use of racemic warfarin as a probe in many past investigations of solute interactions with HSA.[32, 33, 37, 45] In addition, recent studies have shown that warfarin undergoes a slow conversion in aqueous solution that can lead to measurable shifts in its binding to HSA over time.[44]

Table 2-1. Relative cost of warfarin and selected probe candidates for Sudlow site I of HSA.

Analyte	Relative Cost (U.S. dollars per gram)[a]
***R*-Warfarin**	$72,800
***S*-Warfarin**	$74,800
Racemic Warfarin	$8.38
Coumarin	$0.31
7-Hydroxycoumarin	$1.32
7-Hydroxy-4-methylcoumarin	$0.35
4-Hydroxycoumarin	$0.35

[a]These numbers are based on 2007/2008 list prices from Sigma-Aldrich.

Figure 2-1. Structures of warfarin and compounds that were examined as possible alternative probes for Sudlow site I on HSA.

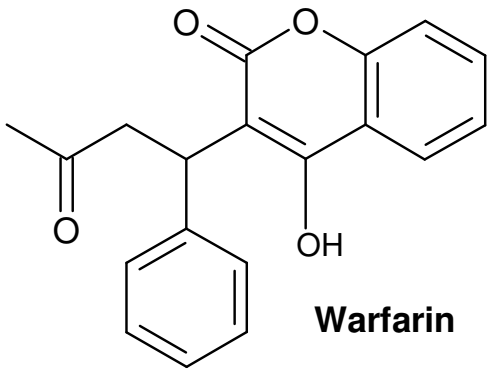

Warfarin

Coumarin

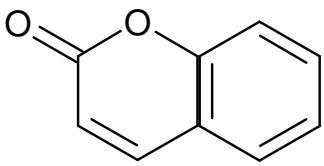

4-Hydroxycoumarin

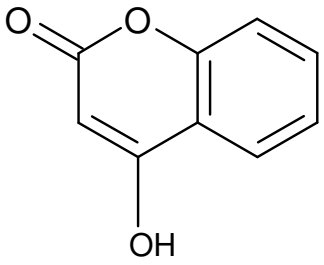

7-Hydroxy-4-methylcoumarin

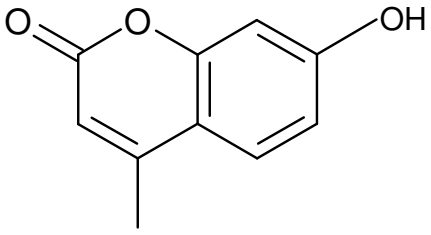

7-Hydroxycoumarin

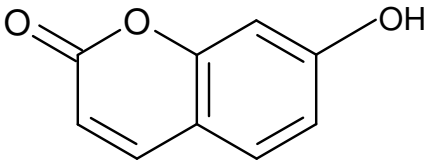

The purpose of this study is to examine several compounds that are closely-related to warfarin in structure with the goal of determining if these might be used as alternative probes for Sudlow site I in drug-protein binding studies. Ideally, a suitable warfarin replacement for high throughput studies should be specific for Sudlow site I and have few non-specific interactions with HSA or the analysis system. This probe should also have a good long-term stability in aqueous solution and be present in only a single form in solution. Figure 2-1 shows the various coumarin compounds that will be examined in this study as possible probes for Sudlow site I. These compounds are all achiral, which avoids the possibility of having any differences in binding by separate chiral forms; this property also makes these compounds more cost-effective to use (as illustrated in Table 2-1) and easier to obtain than the separate enantiomers of warfarin. In this study, the stability for each of these compounds will be examined by NMR spectroscopy. This will be followed by an evaluation of their binding properties for HSA by using HPAC. From the results it will be possible to compare these compounds and determine which might be suitable replacements for warfarin for use in high throughput screening of drug interactions with HSA. The data obtained in this study should also provide clues as to how the various structural features of warfarin and related coumarin compounds contribute to their binding to Sudlow site I.

Theory

Frontal Analysis

The method of frontal analysis (or frontal affinity chromatography) will be used to determine the number of binding sites and association equilibrium constants for each

probe candidate examined in this study. This technique is carried out by continuously applying a solution with a known concentration of the analyte (e.g., a probe candidate) to a column that contains an immobilized ligand (e.g., HSA). As the analyte binds to the ligand, the binding sites in the column become saturated, forming a breakthrough curve like the one shown in Figure 2-2(a). If fast association and dissociation kinetics are present, the mean position of this breakthrough curve can be directly related to the concentration of the applied analyte [A], the total moles of active binding sites in the column for the analyte (m_L), and the association equilibrium constant (K_a) for analyte-ligand binding. The following two equivalent equations can be used to relate these terms for a system where the analyte binds to a single type of site on a ligand.[32, 37]

$$m_{Lapp} = \frac{m_L K_a [\mathrm{A}]}{(1 + K_a [\mathrm{A}])} \tag{2-1}$$

$$\frac{1}{m_{Lapp}} = \frac{1}{(K_a m_L [\mathrm{A}])} + \frac{1}{m_L} \tag{2-2}$$

In these equations m_{Lapp} is the apparent moles of analyte that are required to reach the mean position of the breakthrough curve at any given concentration of applied analyte, [A]. According to Equation 2-2, a plot of $1/m_{Lapp}$ versus 1/[A] for a system with 1:1 binding will make it possible to determine both the binding capacity of the column and the association equilibrium constant by finding the inverse of the intercept and the ratio of the intercept divided by the slope, respectively.

If multi-site binding occurs between the analyte and ligand, a plot prepared according to Equation 2-2 will result in a non-linear relationship and produce negative deviations from a linear response at high analyte concentrations (i.e., low values for 1/[A]).[46] To deal with this situation, Equations 2-1 and 2-2 can be expanded into the

Figure 2-2. (a) Frontal analysis curves for 7-hydroxycoumarin at concentrations (from left-to-right) of 10, 7.5, 5.0, 2.5 or 1.0 μM. (b) Zonal elution competition studies performed with warfarin in the mobile phase while samples of 5.0 μM 7-hydroxycoumarin were injected; the concentration for warfarin in the mobile phase (from top-to-bottom) was 20, 15, 10, 5.0, 1.0 or 0 μM.

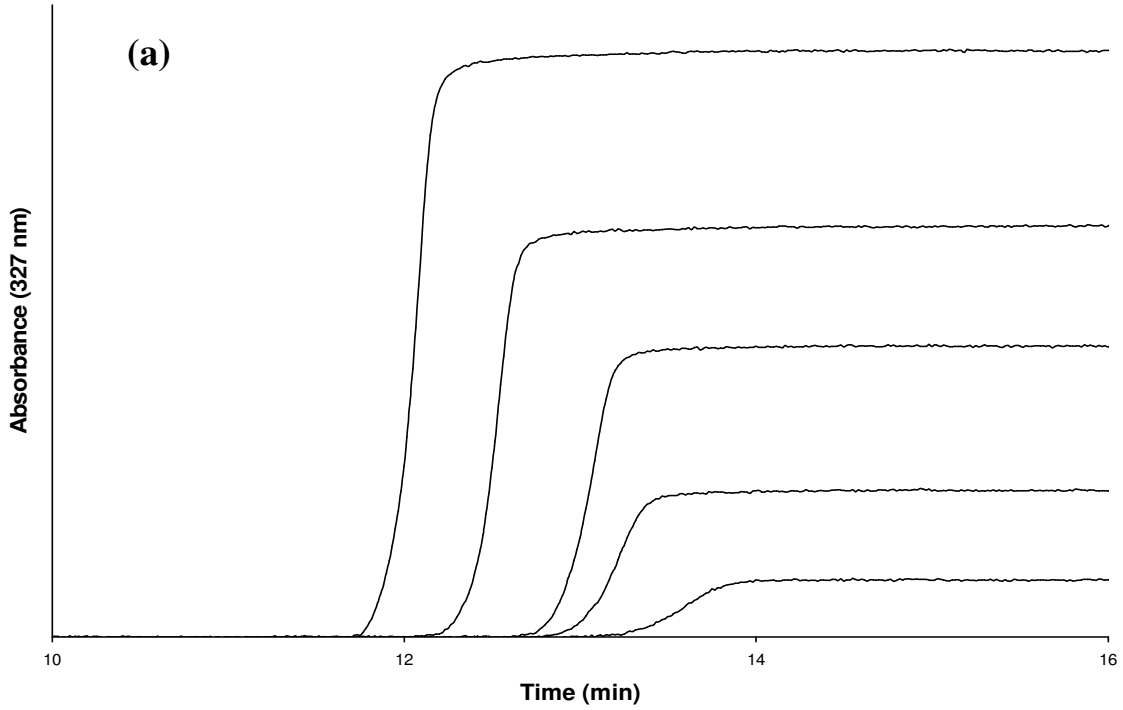
(a)
Absorbance (327 nm)
10
12
14
16
Time (min)

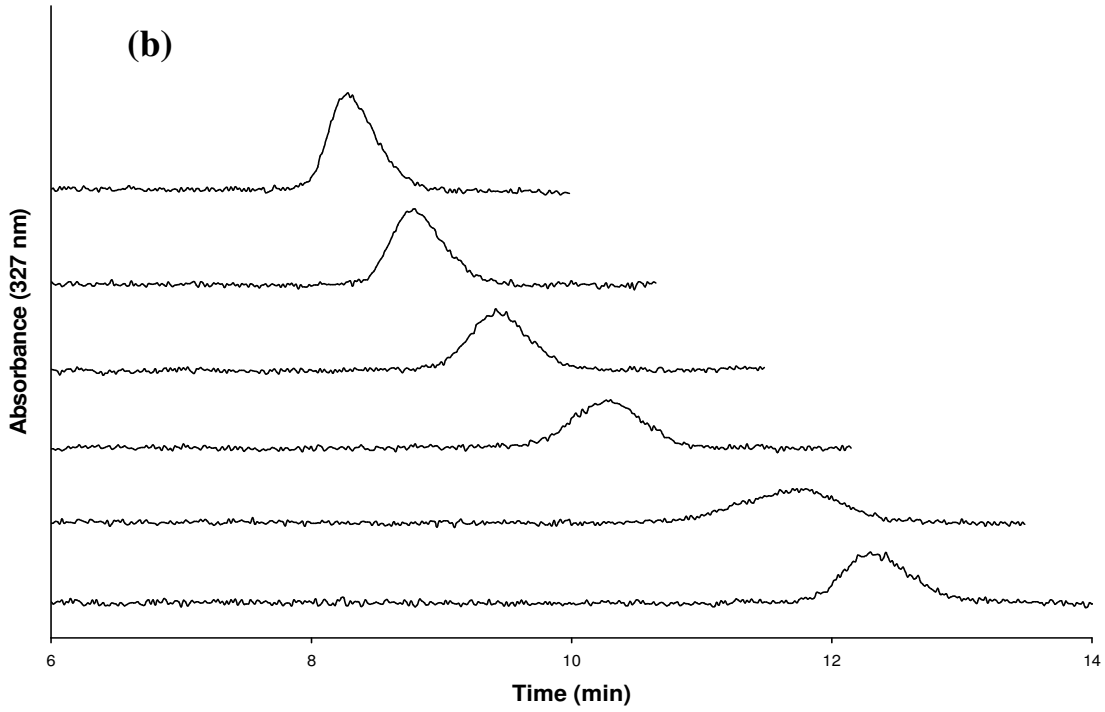
(b)
Absorbance (327 nm)
6
8
10
12
14
Time (min)

following forms for the case in which an analyte has two different groups of binding sites within a column.[32, 46]

$$m_{Lapp} = \frac{m_{L1}K_{a1}[\mathrm{A}]}{(1+K_{a1}[\mathrm{A}])} + \frac{m_{L2}K_{a2}[\mathrm{A}]}{(1+K_{a2}[\mathrm{A}])} \qquad (2\text{-}3)$$

$$\frac{1}{m_{Lapp}} = \frac{1+K_{a1}[\mathrm{A}]+\beta_2 K_{a1}[\mathrm{A}]+\beta_2 K_{a1}^2[\mathrm{A}]^2}{m_{Ltot}\{(\alpha_1+\beta_2-\alpha_1\beta_2)K_{a1}[\mathrm{A}]+\beta_2 K_{a1}^2[\mathrm{A}]^2\}} \qquad (2\text{-}4)$$

In these expanded equations, K_{a1} is the association equilibrium constant for the binding site with the highest affinity for the analyte, and K_{a2} is the association equilibrium constant for the site with weaker binding, where $0 < K_{a2} < K_{a1}$. The term α_1 is the fraction of all binding sites for the analyte that belong to the first group of sites (where $\alpha_1 = m_{L1,tot}/m_{Ltot}$), and β_2 is the ratio of the association equilibrium constants for the low affinity binding sites versus the high affinity sites (where $\beta_2 = K_{a2}/K_{a1}$). Similar expressions can be written for systems with more than two classes of binding sites for an analyte.[46]

Zonal elution

The method of zonal elution was utilized in this study to examine the competition of warfarin with each probe candidate on HSA columns. This type of experiment is performed by continuously passing a competing agent (I) with a known concentration of [I] through a column that contains the immobilized ligand of interest (e.g., HSA). A small plug of the analyte (A) is then injected onto the column, as demonstrated in Figure 2-2(b). If A and I compete for a single class of binding sites on the ligand and have fast

association/dissociation kinetics for their binding, the following relationship can be used to describe how the retention of A will be affected by the presence of I.[32, 37]

$$\frac{1}{k} = \frac{K_{aI} V_M [I]}{K_{aA} m_L} + \frac{V_M}{K_{aA} m_L} \qquad (2\text{-}5)$$

In this equation, k is the observed retention factor for the analyte, as given by $k = (t_R - t_M)/t_M$ where t_R is the measured retention time for the injected analyte and t_M is the column void time (i.e., the retention time for a non-retained compound). Also included in Equation 2-5 are the association equilibrium constants for the competing agent and the analyte with the ligand (K_{aI} and K_{aA}, respectively) and the column void volume (V_M). Equation 2-5 is useful in studying drug-drug competition because it indicates that a plot of $1/k$ versus [I] should result in a linear relationship if there is direct competition between the competing agent and analyte at a single common binding site on the immobilized ligand, provided the analyte has no other separate binding sites in the column. Non-linear behavior in this plot will be seen for allosteric competition and negative deviations at low values of [I] will be noted for multi-site interactions.[32]

Experimental

Reagents

The coumarin, 4-hydroxycoumarin, 7-hydroxycoumarin and 7-hydroxy-4-methylcoumarin were purchased from Aldrich (Milwaukee, WI, USA); all of these compounds were of analytical grade (>97% pure). The racemic warfarin (98%) was purchased from Sigma (St. Louis, MO, USA). The HSA (>96%, essentially fatty acid free) was also from Sigma. The Nucleosil Si-300 silica (7 μm particle diameter, 300 Å

pore size) was from Macherey-Nagel (Düren, Germany). Reagents used in the bicinchoninic acid (BCA) protein assay were from Pierce (Rockford, IL, USA). All aqueous solutions were prepared using water obtained from a NANOpure system (Barnstead, Dubuque, IA, USA) and were filtered using 0.20 µm GNWP nylon membranes from Millipore (Billerica, MA, USA).

Apparatus

NMR studies were carried out on a DRX 500 MHz NMR (Bruker, Billerica, MA, USA) equipped with a cryoprobe. All ^{1}H NMR spectra were acquired in D_2O using 128 scans per sample. The chromatographic system consisted of a Waters 590 pump (Milford, MA, USA) and a Beckman 118 Solvent Module (Fullerton, CA, USA). While both of these components were used in the frontal analysis experiments, only the Waters 590 pump was required for the zonal elution experiments. The chromatographic system also contained a Jasco UV-975 UV/Vis absorbance detector (Tokyo, Japan) and a six-port Rheodyne Advantage PF valve (Cotati, CA, USA) equipped with a 20 µL sample loop during the zonal elution experiments. An Isotemp water bath from Fisher (Pittsburgh, PA, USA) was used in conjunction with a column water jacket (Alltech, IL, USA) to maintain a temperature of 37 (± 0.1) ºC during all binding studies. The chromatographic data were collected and processed using LabView 5.1 or LabView 8.0 software (National Instruments, Austin, TX, USA). The BCA protein assay was carried out using a UV 160U spectrophotometer (Shimadzu, Kyoto, Japan) and the diol assay was performed on a P/ACE MDQ capillary electrophoresis system (Beckman, Fullerton, CA, USA).

Methods

^{1}H NMR spectroscopy was used to monitor the stability of each probe candidate in a pH 7.4, 0.067 M potassium phosphate buffer. These studies were conducted using an approach identical to that described previously to examine the stability of warfarin in this same buffer.[44] The photosensitivity of each candidate probe was examined by using split samples in which one set was stored in the dark and the other set was continuously exposed to ordinary laboratory light. Both sets of samples were stored at 25°C throughout the duration of the stability studies.

The Nucleosil Si-300 silica was converted into a diol form according to the literature.[47] The diol content of the resulting material was 250 (± 20) μmol per gram silica (1 S.D.), as determined in triplicate by an iodometric capillary electrophoresis assay [48]. This diol silica was used along with the Schiff base method for the immobilization of HSA.[49] This immobilization was carried out by placing two 0.55 g portions of the diol silica into two separate 20 mL test tubes and combining each of these portions with 0.55 g sodium periodate. A 10 mL portion of a 90:10 acetic acid/water solution was then added to each test tube and mixed for 2 h at room temperature. The silica in each test tube was washed six times by centrifugation and resuspension in water. After the final washing step, 10 mL of pH 6.0, 0.10 M potassium phosphate buffer was added to each silica sample and the resulting slurries were degassed for approximately 5 min under vacuum. A 0.055 g portion of HSA was added to one of the silica slurries while the slurry in the other test tube was used as control with no HSA being added. Approximately 0.03 g of sodium cyanoborohydride was added to the slurry in each test tube, with these test tubes then being tightly covered and placed in a rocking shaker at

4ºC for 6 days. The silica in each test tube was later washed three times by centrifugation and resuspended in pH 8.0, 0.10 M potassium phosphate buffer. A total of 0.1375 g sodium borohydride was slowly added in three portions to each of these test tubes over 90 min while the silica slurry was being shaken. The silica was then washed as described earlier, including three washes with pH 8.0, 0.10 M potassium phosphate buffer that contained 0.5 M sodium chloride, followed by four more washings with pH 7.4, 0.067 M potassium phosphate buffer. The final HSA silica and control support with no HSA added were then stored in pH 7.4, 0.067 M potassium phosphate buffer at 4ºC until use.

The HSA silica and control silica were packed into separate 5.0 cm x 4.6 mm I.D. stainless steel columns. These columns were downward slurry packed at 3000 psi (0.21 Mbar) using pH 7.4, 0.067 M potassium phosphate buffer as the packing solution. A small amount of the remaining HSA silica was dried overnight in a vacuum oven and analyzed by using a BCA assay to determine its protein content. This assay was performed in triplicate using soluble HSA as the standard and the control support as the blank, giving a protein content of 40 (± 2) mg HSA per g silica, or 600 (± 30) nmol per g silica.

All samples and competing agent solutions for the chromatographic studies were prepared in pH 7.4, 0.067 M phosphate buffer. This same buffer was used as the application buffer and isocratic elution buffer during the chromatographic studies. The mobile phases were stored at 4ºC and were degassed for at least 20 min prior to use. All chromatographic studies were carried out at 37ºC using a flow rate of 0.5 ml/min. A six-port valve was used to change between the buffer and analyte solutions during the frontal analysis studies.

Frontal analysis studies were performed by applying to the HSA column and control column buffered solutions that consisted of the mobile phase or a known concentration of the desired probe candidate dissolved in the mobile phase. UV/Vis absorbance detection was used to monitor the eluting analyte, with the detection wavelength being adjusted during the study to ensure that the signal was always within the linear response range of the detector. The concentrations of the probe candidates ranged from 1-500 μM and the detection wavelengths were as follows: 1-10 μM coumarin, 275 nm; 50-500 μM coumarin, 241 nm; 1-100 μM 7-hydroxycoumarin, 327 nm; 250-500 μM 7-hydroxycoumarin, 260 nm; 1-10 μM 7-hydroxy-4-methylcoumarin, 327 nm; 50-500 μM 7-hydroxy-4-methylcoumarin, 258 nm; 1-50 μM 4-hydroxycoumarin, 286 nm; and 65-500 μM 4-hydroxycoumarin, 325 nm. The retained analyte was eluted and the column was regenerated by changing the mobile phase to a pH 7.4, 0.067 M potassium phosphate buffer. Breakthrough times for each probe compound on the HSA column and control column were determined by using the equal area method.[32] The breakthrough times for the control column were subtracted from those for the HSA column to correct for non-specific binding by each probe candidate to the support. The association equilibrium constants and binding capacities for each probe candidate on the HSA column were then determined by analyzing the data according to Equations 2-1 through 2-4.

Competition studies were performed through the use of zonal elution experiments by injecting 20 μL samples of the probe compounds onto the HSA or control column in the presence of a known concentration of warfarin in the mobile phase. Racemic warfarin was acceptable for use as a probe for Sudlow site I in this particular case

because both *R*- and *S*-warfarin bind to Sudlow site I with only slightly different affinities for these interactions,[44, 45] and the primary goal of this competition study was to identify if each achiral probe candidate could compete with warfarin for binding at this specific site. Racemic warfarin is also of general interest for such studies because it is the form of warfarin that is commonly used in therapeutic preparations. The detection wavelengths used in the competition studies were as follows: coumarin, 277 nm; 7-hydroxycoumarin, 325 nm; 7-hydroxy-4-methylcoumarin, 325 nm; and 4-hydroxycoumarin, 286 nm. A 5 μM sample of each probe candidate was injected; no significant change in the retention factors were noted by using lower concentration samples, indicating that these conditions allowed work to be performed under linear elution conditions. The concentration of warfarin that was added to the mobile phase ranged from 1-20 μM. This concentration range was determined in advance to be within the optimum range needed to observe a shift in analyte retention based on the known association equilibrium constant of warfarin with HSA.[32] The retention factors for the analyte peaks were found by using their central moments[32] using PeakFit 4.12 (Jandel Scientific Software, San Rafael, CA, USA). After correcting the data for the retention observed on the control column, the resulting retention factors were plotted according to Equation 2-5 to determine the type of competition that was present for each probe candidate with warfarin.

Results and Discussion

NMR stability studies

A previous study examined the stability of warfarin in pH 7.4, 0.067 M phosphate buffer by using ^{1}H NMR spectroscopy.[44] It was found in this earlier report that warfarin

Figure 2-3. ^{1}H NMR spectra for 7-hydroxycoumarin when stored in pH 7.4, 0.067 M phosphate buffer for various lengths of time at 25º C. The same results were obtained for samples that were stored in the dark or in the presence of normal laboratory lighting.

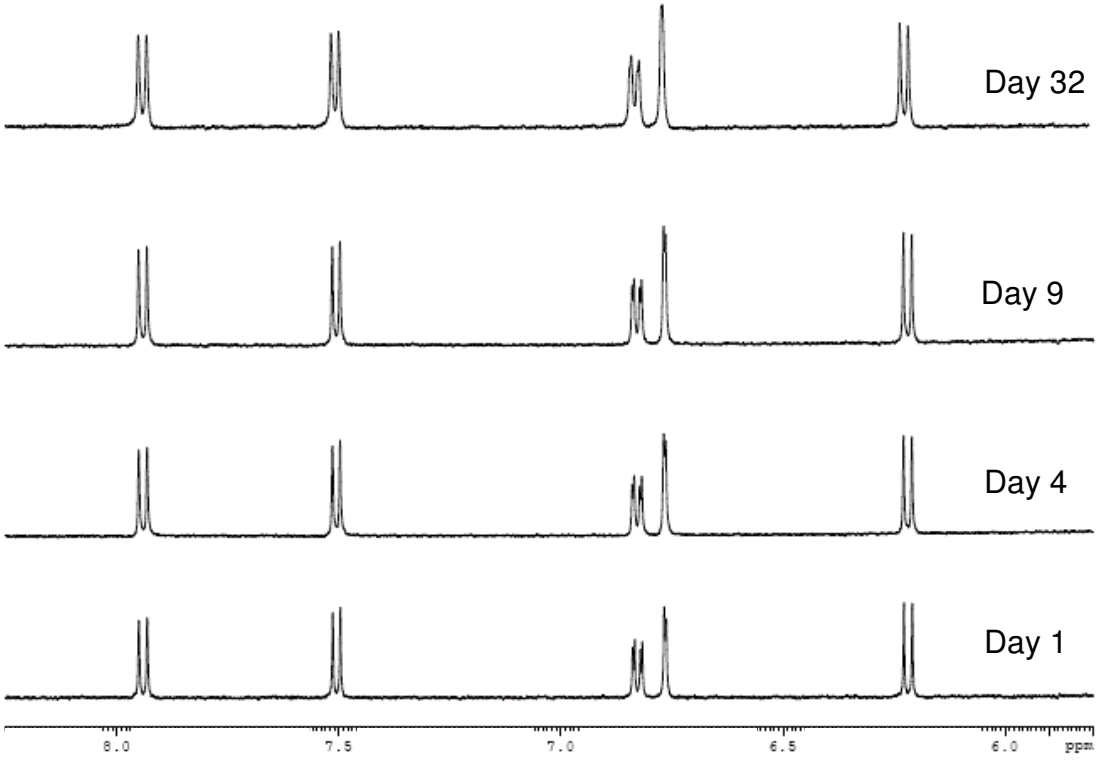
Day 32
Day 9
Day 4
Day 1
8.0
7.5
7.0
6.5
6.0
ppm

has a slow conversion in structure from one form to another over time. It is believed that this conversion involves a change in warfarin between one cyclic epimer and another due to the presence of two chiral centers in the cyclic form of warfarin (Note: although warfarin is generally drawn in an open chain form, it is known to exist as a cyclic hemiketal in solution).[50] This slow change in structure is temperature-dependent and follows a first-order decay process that has a rate constant of 0.0086 h^{-1} (2.39 x 10^{-6} s^{-1}) at 25°C.[44]

Similar experiments were conducted in this current report to examine the stability of each candidate probe. Some typical results are shown in Figure 2-3 for 7-hydroxycoumarin, which gave no observable change in its ^{1}H NMR spectrum over the course of four weeks in pH 7.4, 0.067 M phosphate buffer. Similar results were obtained for all of the other candidate probes in both the presence and absence of normal laboratory lighting. These results indicated that each of these probe candidates had better long-term stability than warfarin in a pH 7.4, 0.067 M phosphate buffer. This greater stability was not surprising because none of these probe candidates are capable of forming a cyclic hemiketal in solution, the feature believed to create a change in the dominant structure of warfarin over time when present in an aqueous solution.[44] These results indicated that all of these probe candidates were stable for at least one month when stored in a pH 7.4, 0.067 M phosphate buffer. This feature is useful because this is the same buffer that is commonly used in drug binding studies with HSA.

Frontal analysis studies

Frontal analysis was performed using HPAC and an immobilized HSA column to

determine the number of binding sites and association equilibrium constants for each probe candidate with HSA. Figure 2-2(a) shows some typical frontal analysis breakthrough curves that were obtained for the binding of 7-hydroxycoumarin to the HSA column. The breakthrough curves in this type of experiment shifted to the left, and to smaller breakthrough times, as the concentration of the analyte was increased. Similar results were obtained for the other probe candidates and in work performed with the control column.

Each of the probe compounds showed some non-specific binding to the support in the control column. This binding ranged from a corrected breakthrough time at 0.5 ml/min of 0.3-1.2 min (when using a void time of 1.5 min). The non-specific binding was low for most of the probe candidates and made up only 6-15% of the total binding noted on the HSA column when applying a 1.0 μM solution of the given probe candidate. The only exception was coumarin, for which non-specific binding to the support made up 48% of the capacity measured on the HSA column under the given experimental conditions. This higher level of non-specific binding may limit the usefulness of coumarin as an alternative probe to warfarin when working with columns that are based on silica supports; however, it is possible that coumarin might still be usable with HPAC columns that are prepared using other support materials.

Equation 2-2 was initially used to examine the frontal analysis data. Double reciprocal plots of $1/m_{Lapp}$ versus 1/[A] that were obtained are shown in Figure 2-4 for 7-hydroxycoumarin, coumarin, and 7-hydroxy-4-methylcoumarin at applied concentrations that ranged from 1-500 μM. These plots had correlation coefficients that ranged from 0.9983-0.9998 (n = 10), but they did show some negative deviations at high analyte

Figure 2-4. Double reciprocal plot of frontal analysis data obtained for (a) 7-hydroxycoumarin, (b) coumarin, and (c) 7-hydroxy-4-methylcoumarin on an HSA column. The error bars represent a range of ± 1 S.D. The best-fit lines were obtained by using Equation 2-2. The inset shows an expanded view of the negative deviations that occur at high analyte concentrations (i.e., low values for 1/[analyte]).

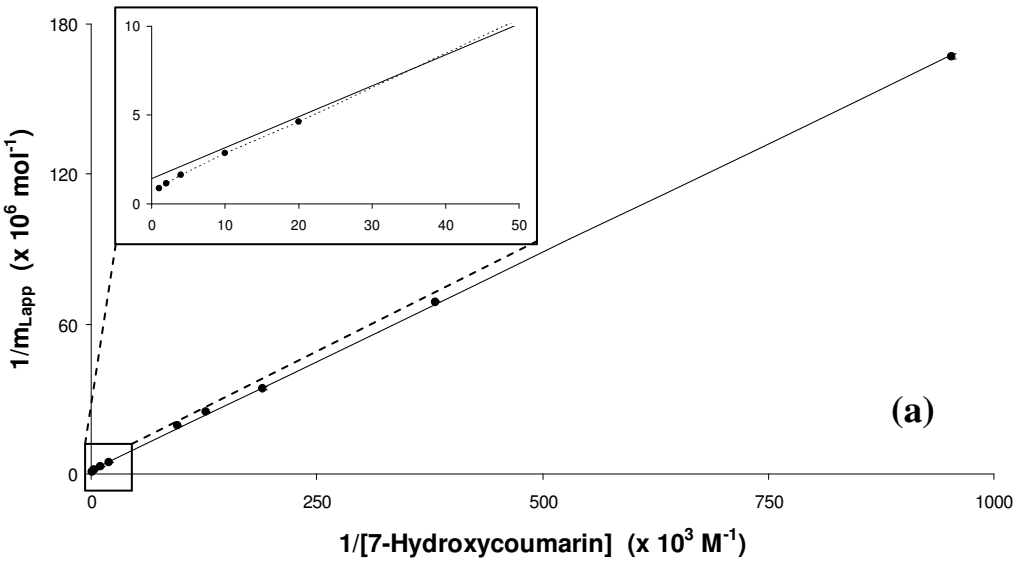
180
120
60
0
0
250
500
750
1000
10
5
0
0
10
20
30
40
50
1/m_Lapp (x 10^6 mol^-1)
1/[7-Hydroxycoumarin] (x 10^3 M^-1)
(a)

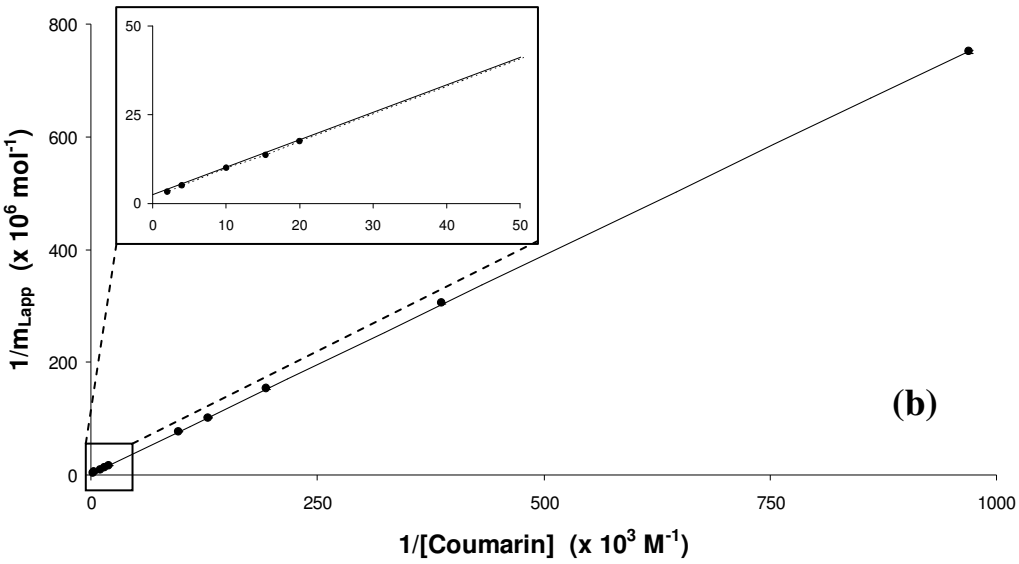
800
600
400
200
0
0
250
500
750
1000
50
25
0
0
10
20
30
40
50
1/m_Lapp (x 10^6 mol^-1)
1/[Coumarin] (x 10^3 M^-1)
(b)

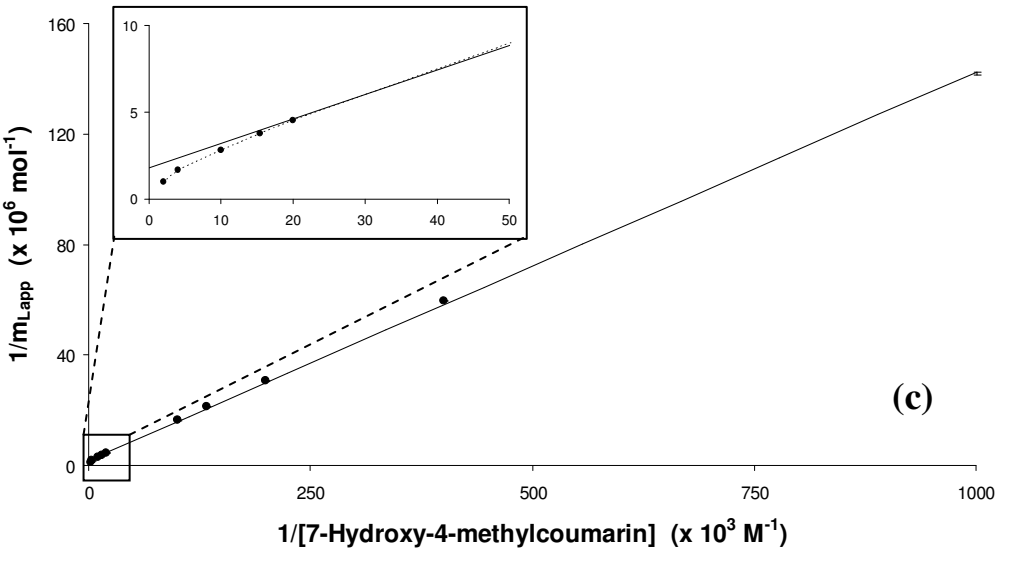
160
120
80
40
0
0
250
500
750
1000
10
5
0
0
10
20
30
40
50
1/m_Lapp (x 10^6 mol^-1)
1/[7-Hydroxy-4-methylcoumarin] (x 10^3 M^-1)
(c)

concentrations (i.e., above 30-50 μM, as demonstrated by the inset in Figure 2-4). These results suggested that these three compounds each had a single major class of binding sites on HSA (creating the good linearity seen at low-to-moderate concentrations of these analytes), as well as a group of weaker binding sites (producing the negative deviations observed at high analyte concentrations). The same conclusion was reached for 4-hydroxycoumarin, which showed more apparent deviations from linearity at higher concentrations.

Figure 2-5 shows the results that were obtained when plots of m_{Lapp} versus the concentration of the applied analyte were prepared for 4-hydroxycoumarin and examined according to a one-site or two-site model. These data were found to produce the best fit to the two-site model described by Equation 2-3, giving a correlation coefficient of 0.9998 (n =10) and only random variations in the corresponding residual plot, with an absolute residual sum of squares that was equal to 6.3×10^{-17} (see graph in lower part of Figure 2-5). When the same plot was analyzed according to a one-site model described by Equation 2-1, the correlation coefficient was 0.9890 and non-random deviations were noted in the residual plot at both low and high analyte concentrations; this residual plot also showed a much larger absolute residual sum of squares (5.3×10^{-15}) than that obtained with the two-site model. The other probe candidates also gave better fits to a two-site model than a one-site model for such plots, with correlation coefficients of 0.9997-0.9999, smaller absolute residual sum of squares, and only random deviations in the residual plots for the two-site model.

Table 2-2 summarizes the association equilibrium constants and binding capacities that were estimated from these plots based on a two-site model. The term "Site

Figure 2-5. Fit of frontal analysis data for 4-hydroxycoumarin to a (a) one-site model or a (b) two-site binding model and the corresponding residual plots for these graphs (see inserted figures). The best-fit parameters for the two-site model are given in Table 2-2. The values of the residuals in the inserted graphs were calculated by taking the difference between the actual and predicted values for m_{Lapp} at each given concentration of [4-hydroxycoumarin].

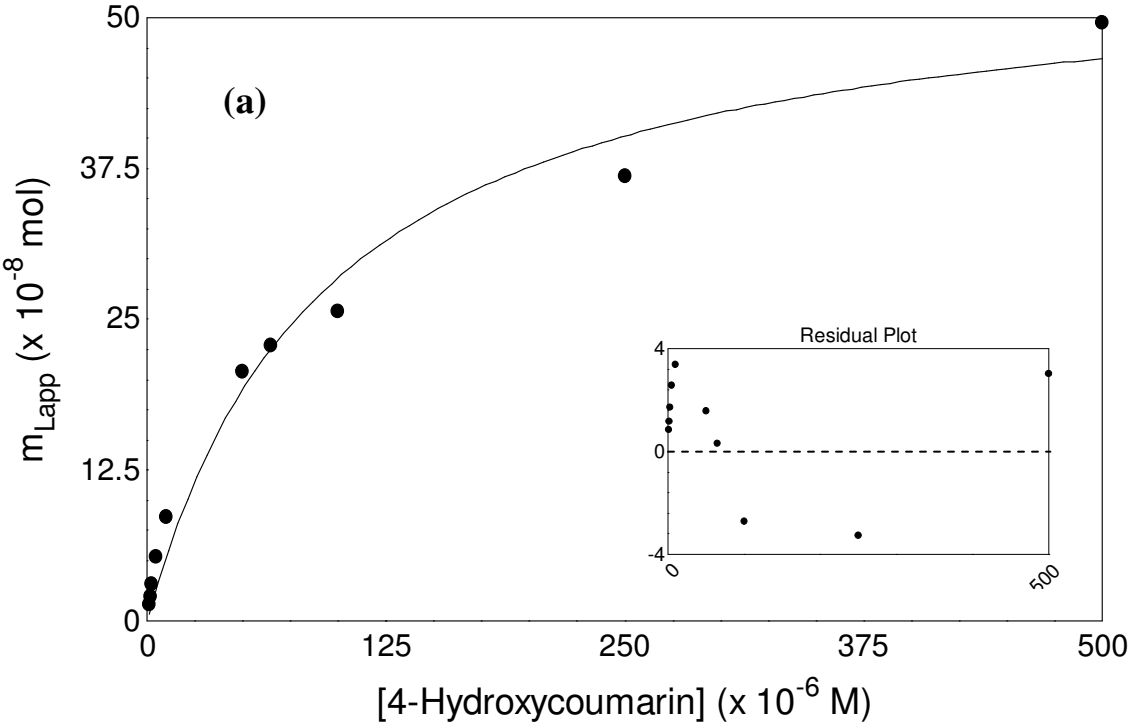
(a)
50
37.5
25
12.5
0
m_{Lapp} (x 10^{-8} mol)
0
125
250
375
500
[4-Hydroxycoumarin] (x 10^{-6} M)
Residual Plot
4
0
-4
0
500

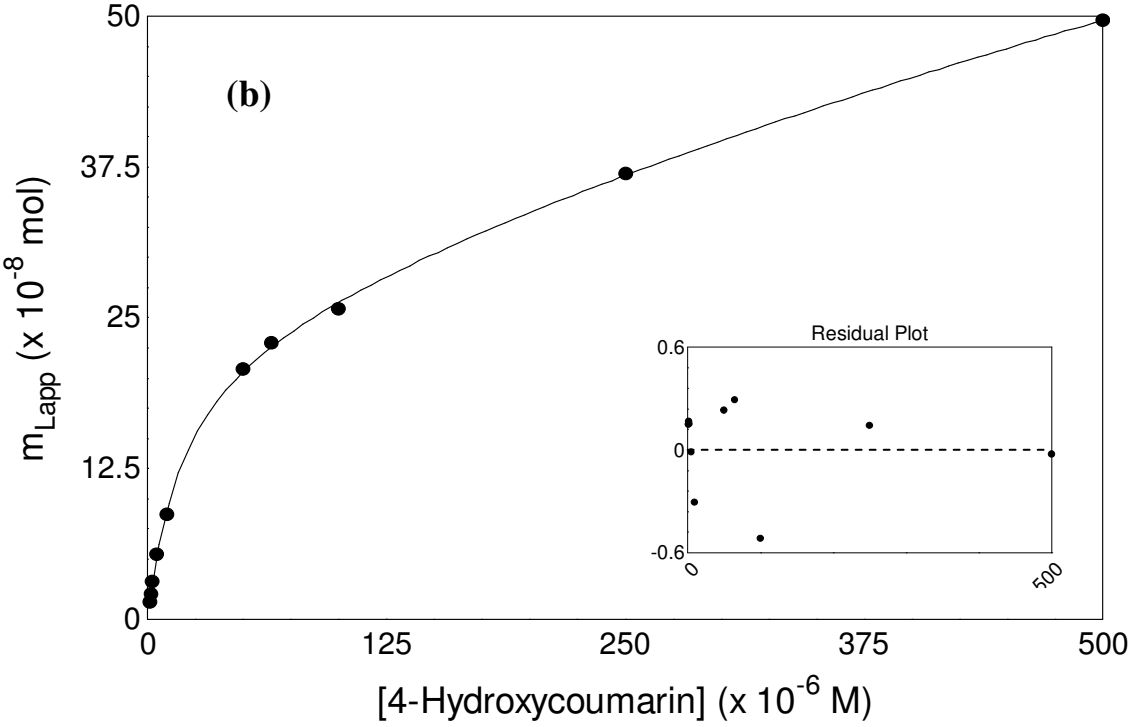
(b)
50
37.5
25
12.5
0
m_{Lapp} (x 10^{-8} mol)
0
125
250
375
500
[4-Hydroxycoumarin] (x 10^{-6} M)
Residual Plot
0.6
0
-0.6
0
500

Table 2-2. Association equilibrium constants (K_a) and binding capacties (m_L) measured for each of the tested probe candidates on an HSA column using a two-site model.

Analyte	K_a (M^{-1})	m_L (mol)
Coumarin	*Site 1:* 6.4 (± 5.1) x 10^3	*Site 1:* 1.2 (± 1.6) x 10^{-7}
	Site 2: 7.3 (± 8.1) x 10^2	*Site 2:* 7.8 (± 2.6) x 10^{-7}
7-Hydroxycoumarin	*Site 1:* 8.2 (± 0.9) x 10^3	*Site 1:* 5.3 (± 0.7) x 10^{-7}
	Site 2: 8.6 (± 1.4) x 10^2	*Site 2:* 1.5 (± 0.1) x 10^{-6}
7-Hydroxy-4-methyl-coumarin	*Site 1:* 2.2 (± 0.8) x 10^4	*Site 1:* 2.8 (± 0.8) x 10^{-7}
	Site 2: 3.8 (± 30) x 10^1	*Site 2:* 3.7 (± 0.3) x 10^{-5}
4-Hydroxycoumarin	*Site 1:* 5.5 (± 0.5) x 10^4	*Site 1:* 2.4 (± 0.1) x 10^{-7}
	Site 2: 4.4 (± 2.5) x 10^2	*Site 2:* 1.5 (± 0.6) x 10^{-6}

The values in parenthesis represent a range of ± 1 SD. All of these measurements were made at 37ºC in the presence of pH 7.4, 0.067 M potassium phosphate buffer.

1" in this table refers to the higher affinity binding region for each probe candidate, while "Site 2" refers to the weaker binding regions that were detected. The high affinity sites had association equilibrium constants for these probe candidates that ranged from 6.4 x 10^3 M^{-1} (for coumarin) up to 5.5 x 10^4 M^{-1} (for 4-hydroxycoumarin) at 37° C and pH 7.4. These values were approximately 4.5- to 40-fold lower than the average association equilibrium constant of 2.5 x 10^5 M^{-1} that has been reported for warfarin enantiomers with HSA under similar conditions.[44, 45] It is interesting to note that the probe candidate with the closest similarity to warfarin in its structure also gave the largest association equilibrium constant for its high affinity site. This observation fits with a model in which at least some of these probe candidates were binding to Sudlow site I of HSA.

The binding capacities obtained for the high affinity site of each probe compound were compared to the amount of HSA in the HPAC column to give the specific activities for these sites. The total number of moles of HSA in this column was calculated to be 224 (± 11) nmol based on the known protein content of the HSA support, the packing density of this material and the total column void volume. The resulting specific activities of the high affinity site for coumarin, 7-hydroxy-4-methylcoumarin and 4-hydroxycoumarin were in the range of 0.5-1.2 mol probe/mol HSA, as would be expected for interactions at a single binding region on HSA.[44, 45] The specific activity obtained for 7-hydroxycoumarin was 2.3 mol/mol HSA, suggesting that this probe candidate might have interacted with two sites on HSA that had similar association equilibrium constants; such a feature would limit the usefulness of this particular compound if the goal is to use it as a specific probe for only Sudlow site I.

The weak affinity regions for these probe candidates had apparent association equilibrium constants in the range of only 38-860 M^{-1} at 37°C and pH 7.4. These interactions probably represent non-specific binding of these compounds to the structure of HSA. This conclusion is supported by the binding capacities that were estimated for these regions, which gave specific activities that ranged from 3.4-16 mol/mol HSA. These large specific activities agree with what would be expected for a group of non-selective interactions between a solute and a protein rather than binding at a specific binding site. A similar set of low affinity interactions at secondary sites has been noted between warfarin and HSA, with a reported association equilibrium constant of 1.4×10^4 M^{-1} at 25°C.[51]

Competition studies

Zonal elution studies were carried out to determine if the probe candidates could compete directly with warfarin for Sudlow site I on HSA. These studies were performed by adding various known concentrations of racemic warfarin to the mobile phase while a small and fixed amount of each candidate was injected onto the column. Figure 2-2(b) shows how the retention of 7-hydroxycoumarin changed with increasing concentrations of warfarin in the mobile phase. Figure 2-6 shows the results that were obtained when the data of such studies were analyzed according to Equation 2-5. Coumarin, 7-hydroxycoumarin, and 7-hydroxy-4-methylcoumarin (see Figure 2-6(a)-(c)) gave a linear response at warfarin concentrations of at least 5 μM or higher, along with a small negative deviation from this linear behavior at lower warfarin concentrations or when no

Figure 2-6. Zonal elution competition studies for injections of (a) coumarin, (b) 7-hydroxycoumarin, (c) 7-hydroxy-4-methylcoumarin, and (d) 4-hydroxycoumarin in the presence of racemic warfarin on an HSA column. The best-fit lines in (a)-(d) were found by using Equation 2-5 along with data obtained at warfarin concentrations of 1-20 μM for plot (a), and 5-20 μM for plots (b)-(d). The equations for these best-fit lines were as follows: (a) $y = 3.08 (\pm 0.10) \times 10^4 x + 0.906 (\pm 0.013)$;

(b) $y = 3.21 (\pm 0.06) \times 10^3 x + 0.144 (\pm 0.001)$;

(c) $y = 4.48 (\pm 0.24) \times 10^3 x + 0.135 (\pm 0.003)$;

(d) $y = 6.05 (\pm 0.07) \times 10^3 x + 0.0236 (\pm 0.0010)$.

The correlation coefficients for all of these plots were in the range of 0.9971-0.9998 (n = 4-5). Values in parentheses represent ± 1 SD.

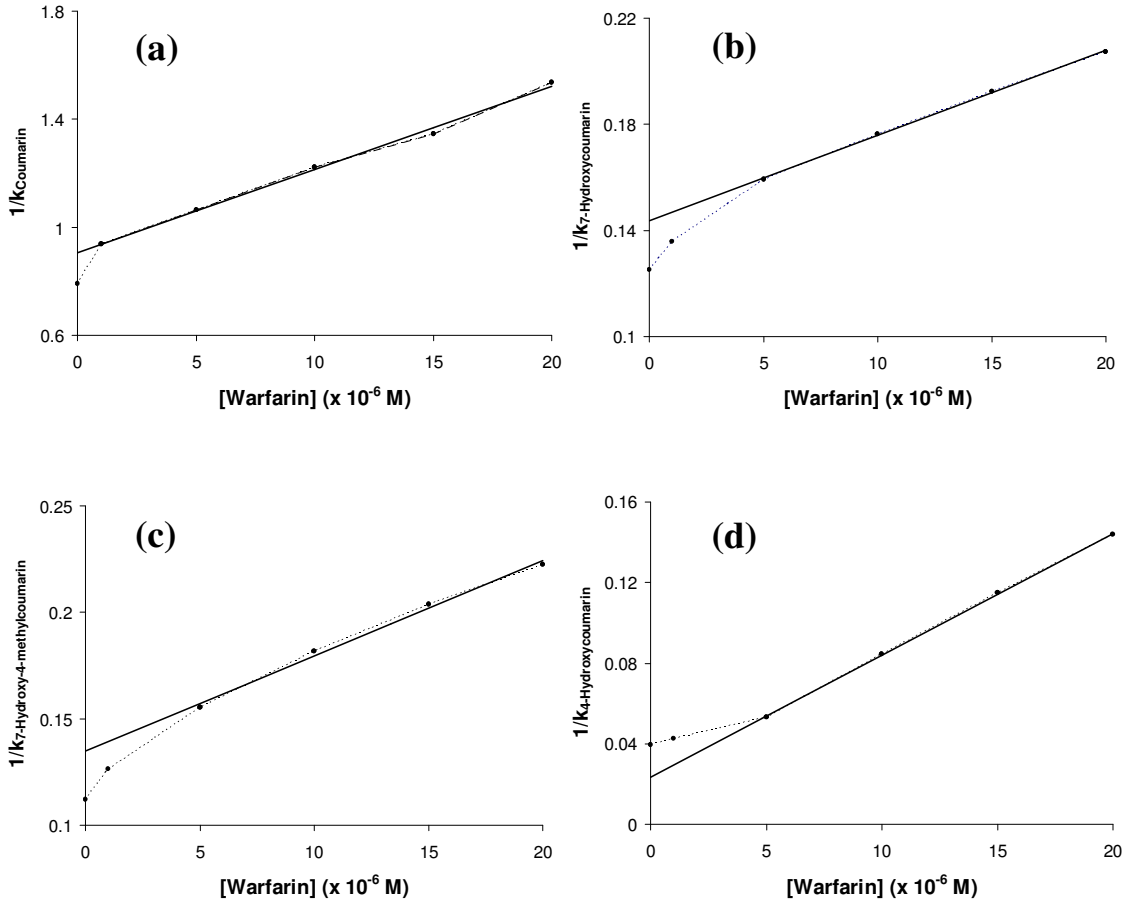
(a)
1.8
1.4
1
0.6
1/kCoumarin
0
5
10
15
20
[Warfarin] (x 10-6 M)
(b)
0.22
0.18
0.14
0.1
1/k7-Hydroxycoumarin
0
5
10
15
20
[Warfarin] (x 10-6 M)
(c)
0.25
0.2
0.15
0.1
1/k7-Hydroxy-4-methylcoumarin
0
5
10
15
20
[Warfarin] (x 10-6 M)
(d)
0.16
0.12
0.08
0.04
0
1/k4-Hydroxycoumarin
0
5
10
15
20
[Warfarin] (x 10-6 M)

warfarin was present. The relative difference in the retention factors calculated from the best-fit intercept and actual intercept for each of these plots was in the range of 12.8 to 16.7%. 4-Hydroxycoumarin gave slightly different behavior, with a linear response being seen in Figure 2-6(d) at warfarin concentrations above 5 μM and a slight positive deviation being noted at lower warfarin concentrations.

For each probe candidate, the intercept of the best-fit line was consistent with the value predicted for the high affinity site by using the data in Table 2-2 and Equation 2-5. This result indicated that competition between warfarin and the probe candidates at their high affinity sites was the dominant interaction being observed in the linear regions of these plots. In addition, the difference in the actual intercept and the best-fit intercept from the linear region for plots with negative deviations was consistent with the level of retention predicted from Table 2-2 for the weak affinity regions of these probe candidates. The relative size of the contributions of the weak sites to retention in the absence of any warfarin (i.e., at the *y*-intercept in Figure 2-6) was estimated from the data in Table 2-2 to be about 5% for 4-hydroxycoumarin, 23% for 7-hydroxycoumarin and 19% for 7-hydroxy-4-methylcoumarin. The relative contribution of the weak sites to retention was 43% for coumarin, which again suggested that this candidate would have limited usefulness as a site-specific probe for HSA.

The behavior observed for coumarin, 7-hydroxycoumarin and 7-hydroxy-4-methylcourmin for plots like those in Figure 2-6 is consistent with a model in which direct competition is occurring between warfarin and these probe candidates at both their high and weak affinity sites. Competition at the high affinity sites was noted to dominate at moderate-to-high concentrations of warfarin (creating the linear response seen in this

region), while both the weak and high affinity sites had significant contributions to retention at lower warfarin concentrations. Similar behavior has been noted previously for other solute systems with competition at two groups of sites on HSA.[32] The results for 4-hydroxycoumarin are consistent with a slightly different model. For this probe candidate, it appears that 4-hydroxycoumarin and warfarin were again competing for the high affinity site of this probe at moderate-to-low concentrations of warfarin. However, the positive deviations seen when only small concentrations of warfarin were present suggest that at least some of the weak affinity sites for 4-hydroxycoumarin were showing little or no binding for warfarin under these conditions.

The ratio of the slope and intercepts for the best-fit lines in these plots were used along with Equation 2-5 to estimate the value of warfarin's association equilibrium constant at its site of competition with each probe candidate. It was found that warfarin had an association equilibrium constant of 2.6 (± 0.1) x 10^5 M^{-1} as it underwent binding at the high affinity site for 4-hydroxycoumarin. This value is statistically identical to the average association equilibrium constant of 2.5 x 10^5 M^{-1} that has been reported for *R*- and *S*-warfarin at Sudlow site I of HSA, thus confirming that the high affinity site of 4-hydroxycoumarin was the same as this binding region.[44, 45] Thus, it appeared from this result that 4-hydroxycoumarin could indeed be used as a replacement for warfarin as a probe for examining the binding of other solutes at Sudlow site I.

The association equilibrium constants determined for racemic warfarin at its site of competition with the other probe candidates were about an order of magnitude lower than the full value for warfarin at Sudlow site 1. These calculated values were as follows: competition with coumarin, 3.4 (± 0.1) x 10^4 M^{-1}; competition with 7-

hydroxycoumarin, 2.23 (± 0.05) x 10^4 M^{-1}; and competition with 7-hydroxy-4-methylcoumarin, 3.3 (± 0.2) x 10^4 M^{-1}. Because warfarin has only one major binding site on HSA, these results indicate that these probe candidates are binding to and competing with warfarin at only part of this site. A similar effect has been noted in the competition of octanoic acid with various drugs for binding to HSA.[36] This scenario is consistent with the fact that each of these three probe candidates contains only part of the structure of warfarin (i.e., as is the case for coumarin) or contain additional groups that are not present in warfarin (e.g., the 7-hydroxyl group in 7-hydroxycoumarin and 7-hydroxy-4-methylcoumarin). This would also explain why the association equilibrium constant calculated for warfarin during its competition with 4-hydroxycoumarin was essentially the same as the full value reported for warfarin at Sudlow site I because this particular probe candidate has the closest structure to that of warfarin and the best chance for fully competing with warfarin at Sudlow site I.

Effects of Coumarin Structure on Binding to Sudlow Site I

Although the main goal of this study was to identify alternatives to warfarin as probes for Sudlow site I, the results that were obtained in the frontal analysis and zonal elution studies do provide some information on the nature of the binding of warfarin and related compounds to HSA. It is known that many solutes like warfarin that bind at Sudlow site I are bulky heterocyclic compounds that also contain anionic groups near a central location of the molecule.[51, 52] This general model was confirmed in this current report by the fact that the probe with the greatest similarity to warfarin in its affinity for Sudlow site I was 4-hydroxycoumarin, a compound which contains the same type of

heterocyclic ring and anion-forming, acidic hydroxyl group that appears in warfarin. Removal of the hydroxyl group from this structure (leaving only the coumarin backbone) produced a decrease in K_a of 8.5-fold, as noted in Table 2-2 when comparing the results at Site 1 for 4-hydroxycoumarin and coumarin.

It is also clear from the data in Table 2-2 that the structure shared by 4-hydroxycoumarin and warfarin is only partly responsible for the high affinity of warfarin at Sudlow site I. This result is demonstrated by the 4.5-fold difference in affinity at this site that was measured for 4-hydroxycoumarin versus the average K_a value of 2.5 x 10^5 M^{-1} that has been reported for warfarin enantiomers under equivalent conditions.[44, 45] This comparison indicates that the 3-(α-acetonylbenzyl) group on warfarin (see lower left portion of the warfarin structure in Figure 2-1) plays a significant role in contributing to the high affinity of this drug at Sudlow site I.

The positions of the hydroxyl group and other side chains about the coumarin ring were also found to affect the affinity of the tested probe compounds for HSA. Table 2-2 indicates that moving the hydroxyl group from the 4- to 7-position created a 6.7-fold lower affinity for 7-hydroxycoumarin versus 4-hydroxycoumarin as these compounds were bound by Sudlow site I. Placing a methyl group in the 4-position regained some of this affinity, as shown in Table 2-2 by the 2.7-fold increase in the association equilibrium constant at Site 1 when going from 7-hydroxycoumarin to 7-hydroxy-4-methylcoumarin.

Conclusions

This study examined the binding of four coumarin compounds to HSA using HPAC. It was determined by frontal analysis that all of the probe candidates had

interactions with HSA that followed a two-site model, including a high affinity site and a second group of weak, non-specific binding regions. It was found in zonal elution competition studies that all of these probe candidates gave direct competition with warfarin at their high affinity sites, as well as either direct competition or no competition at their weak affinity sites (the latter behavior been noted in the case of 4-hydroxycoumarin). The results of this study not only allowed new probes for HSA to be identified, but also provided information on how the coumarin ring, hydroxyl group and 3-(α-acetonylbenzyl) group that are part of warfarin each contribute to the binding of this drug at Sudlow site I.

Of the various probe candidates that were examined, 4-hydroxycoumarin was found to be the best alternative for warfarin in its binding to Sudlow site I of HSA. Some advantages of using 4-hydroxycoumrin for this purpose include its good long term stability in a pH 7.4 phosphate buffer and its ability to be obtained in an inexpensive and single form for binding studies. 4-Hydroxycoumarin also has slightly weaker binding than warfarin to HSA, which would avoid the need for long elution times when working with such an agent in HPAC.

The other tested probes had several limitations. Coumarin had high non-specific binding to silica supports and a relatively large contribution by its weak affinity sites on HSA to its overall binding to this protein. In addition, coumarin, 7-hydroxycoumarin and 7-hydroxy-4-methylcoumarin all appeared to compete with warfarin for only part of Sudlow site I. 7-Hydroxycoumarin and 7-hydroxy-4-methylcoumarin did have small non-specific interactions with the support and with HSA, which may make them useful in some situations as probes for drug binding studies. However, binding capacity

measurements did suggest that 7-hydroxycoumarin may have more than one high affinity site on HSA. Thus, 4-hydroxycoumarin was found to be the best overall alternative to warfarin as a probe for Sudlow site I of HSA.

References

1. Colmenarejo, G., *Med. Res. Rev.* **2003,** *23* (3), 275-301.
2. Finlay, G. J.; Baguley, B. C., *Cancer Chemother. Pharmacol.* **2000,** *45*, 417-422.
3. Berezhkovskiy, L. M., *J. Pharmacokin. Pharmacodyn.* **2006,** *33* (5), 595-608.
4. Otagiri, M., *Drug Metab. Pharmacokinet.* **2005,** *20* (5), 309-323.
5. Liu, Z.; Li, F.; Huang, Y., *Biomed. Chromat.* **1999,** *13*, 262-266.
6. Wan, H.; Bergstrom, F., *J. Liq. Chrom. Rel. Technol.* **2007,** *30*, 681-700.
7. Fasano, M.; Curry, S.; Terreno, E.; Galliano, M.; Fanali, G.; Narciso, P.; Notari, S.; Ascenzi, P., *IUBMB Life* **2005,** *57* (12), 787-796.
8. Ascenzi, P.; Bocedi, A.; Notari, S.; Fanali, G.; Fesce, R.; Fasano, M., *Mini-Rev. Med. Chem.* **2006,** *6*, 483-489.
9. Bocedi, A.; Notaril, S.; Narciso, P.; Bolli, A.; Fasano, M.; Ascenzi, P., *IUBMB Life* **2004,** *56* (10), 609-614.
10. Ghuman, J.; Zunszain, P. A.; Petitpas, I.; Bhattacharya, A. A.; Otagiri, M.; Curry, S., *J. Mol. Biol.* **2005,** *353*, 38-52.
11. Ascoli, G. A.; Domenici, E.; Bertucci, C., *Chirality* **2006,** *18*, 667-679.
12. Petitpas, I.; Bhattacharya, A. A.; Twine, S.; East, M.; Curry, S., *J. Biol. Chem.* **2001,** *276* (25), 22804-22809.
13. Heinze, A.; Holzgrabe, U., *Int. J. Pharm.* **2006,** *311* (1-2), 108-112.
14. Matsushita, Y.; Moriguchi, I., *Chem. Pharm. Bull.* **1985,** *33* (7), 2948-2955.
15. Aarons, L. J.; Schary, W. L.; Rowland, M., *J. Pharm. Pharmacol.* **1979,** *31* (5), 322-330.
16. Bowmer, C. J.; Lindup, W. E., *J. Pharmacol. Exp. Ther.* **1979,** *210* (3), 440-445.

17. Coulson, C. J.; Smith, V. J., *Methodological Surveys* **1981,** *10*, 210-213.

18. Seedher, N.; Agarwal, P., *Ind. J. Pharm. Sci.* **2006,** *68* (3), 327-331.

19. Xie, M.; Long, M.; Liu, Y.; Qin, C.; Wang, Y., *Biochim. Biophys. Acta* **2006,** *1760* (8), 1184-1191.

20. Russeva, V.; Rakovska, R.; Stavreva, N.; Mihailova, D.; Berova, N., *Pharmazie* **1994,** *49* (7), 519-522.

21. Detrich, H. W. I.; Williams, R. C. J.; Macdonald, T. L.; Wilson, L.; Puett, D., *Biochem.* **1981,** *20* (21), 5999-6005.

22. Sjoholm, I.; Sjodin, T., *Biochem. Pharmacol.* **1972,** *21* (22), 3041-3052.

23. Chignell, C. F., *Mol. Pharmacol.* **1970,** *6* (1), 1-12.

24. Shiwang, L.; Zhang, L.; Zhang, X., *Anal. Sci.* **2006,** *22* (12), 1515-1518.

25. Zhongjiang, J., *Curr. Pharm. Anal.* **2005,** *1* (1), 41-56.

26. Xiaocui, Z.; You, T.; Liu, J.; Sun, X.; Yan, J.; Yang, X.; Wang, E., *Electrophoresis* **2004,** *25* (20), 3422-3426.

27. Thormann, W.; Wey, A. B.; Lurie, I. S.; Gerber, H.; Byland, C.; Malik, N.; Hochmeister, M.; Gehrig, C., *Electrophoresis* **1999,** *20* (15-16), 3203-3236.

28. Day, Y. S. N.; Myszka, D. G., *J. Pharm. Sci.* **2003,** *92* (2), 333-343.

29. Frostell-Karlsson, A.; Remaeus, A.; Roos, H.; Andersson, K.; Borg, P.; Haemaelaeinen, M.; Karlsson, R., *J. Med. Chem.* **2000,** *43* (10), 1986-1992.

30. Sulkowska, A.; Bojko, B.; Rownicka, J.; Rezner, P.; Sulkowski, W. W., *J. Mol. Struct.* **2005**, 744-747, 781-787.

31. Li, C.; Liu, M., *Am. Biotech. Lab.* **2000,** *18* (11), 36.

32. Hage, D. S., *J. Chromatogr. B* **2002,** *768*, 3-30.

33. Patel, S.; Wainer, I. W.; Lough, W. J., Chromatographic Studies of Molecular Recognition and Solute Binding to Enzymes and Plasma Proteins. In *Handbook of Affinity Chromatography*, Hage, D. S., Ed. CRC Press Taylor & Francis Group: Boca Raton, 2006; Vol. 92, pp 663-683.

34. Noctor, T. A. G.; Diaz-Perez, M. J.; Wainer, I. W., *J. Pharm. Sci.* **1993,** *82*, 675-676.

35. Domenici, E.; Bertucci, C.; Salvadori, P.; Felix, G.; Cahagne, I.; Motellier, S.; Wainer, I. W., *Chromatographia* **1990,** *29*, 170-176.

36. Winzor, D. J., *J. Chromatogr. A* **2004,** *1037*, 351-367.

37. Kim, H. S.; Hage, D. S., *J. Chromatogr. B* **2005,** *816*, 57-66.

38. Schiel, J. E.; Mallik, R.; Soman, S.; Joseph, K. S.; Hage, D. S., *J. Sep. Sci.* **2006,** *29* (6), 719-737.

39. Patel, S.; Wainer, I. W.; Lough, W. J., Affinity-Based Chiral Stationary Phases. In *Handbook of Affinity Chromatography*, Hage, D. S., Ed. CRC Press Taylor & Francis Group: Florida, 2006; Vol. 92, pp 571-592.

40. Garten, S.; Wosilait, W., *Comp. gen. Pharmac.* **1972,** *3*, 83-88.

41. Sudlow, G.; Birkett, D. J.; Wade, D. N., *Mol. Pharmacol.* **1975,** *11*, 824-832.

42. Sudlow, G.; Birkett, D. J.; Wade, D. N., *Mol. Pharmacol.* **1976,** *12*, 1052-1061.

43. Sengupta, A.; Hage, D. S., *Anal. Chem.* **1999,** *71*, 3821-3827.

44. Moser, A. C.; Kingsbury, C.; Hage, D. S., *J. Pharm. Biomed. Anal.* **2006,** *41*, 1101-1109.

45. Loun, B.; Hage, D. S., *Anal. Chem.* **1994,** *66*, 3814-3822.

46. Tweed, S. A.; Loun, B.; Hage, D. S., *Anal. Chem.* **1997,** *69*, 4790-4798.

47. Ruhn, P. F.; Garver, S.; Hage, D. S., *J. Chromatogr. A* **1994,** *669*, 9-19.

48. Ruhn, P. F.; Garver, S.; Hage, D. S., *J. Chromatogr. A* **1994,** *669* (1-2), 9-19.

49. Loun, B.; Hage, D. S., *J. Chromatogr. A* **1992,** *579* (2), 225-235.

50. Giannini, D. D.; Chan, K. K.; Roberts, J. D., *Proc. Natl. Acad. Sci. U.S.A.* **1974,** *71*, 4221-4223.

51. Dockal, M.; Chang, M.; Carter, D. C.; Ruker, F., *Protein Sci.* **2000,** *9*, 1455.

52. Peters, T., *All About Albumin: Biochemistry, Genetics and Medicinal Applications*. Academic Press: New York, 1996.

CHAPTER 3

THE BINDING OF SULFONYLUREAS TO NORMAL HSA

Introduction

Sulfonylureas are a group of drugs used to treat type II diabetes (i.e., adult onset or non-insulin dependent diabetes). These drugs stimulate acute insulin release from the beta cells of pancreatic islet tissue.[1] Tolbutamide and acetohexamide are two common "first-generation" sulfonylurea drugs (see Figure 3-1).[1-3] These agents have been widely used since the introduction of tolbutamide in 1956.[2, 4] All sulfonylureas bind tightly to serum proteins, with human serum albumin (HSA) being the main protein that is believed to be involved in these interactions.[2]

HSA is the most prevalent plasma protein.[5, 6] This protein is composed of a single peptide chain and has a typical concentration in blood of 35-50 mg/ml (i.e., 0.6-0.7 mM).[5-9] HSA is known to act as a transport protein that binds to a wide variety of compounds, including many drugs, hormones, bilirubin, and fatty acids.[5-8] In this role, HSA and its interactions with drugs can have a strong influence on the free concentrations of drugs in plasma[6, 7, 10] and the pharmacologic and pharmacokinetic properties of a drug.[5-8, 11] For instance, this binding can affect drug adsorption, distribution, metabolism and excretion.[5, 12]

Previous studies have been conducted to investigate the binding of both acetohexamide[4, 13-15] and tolbutamide[3, 13-19] to HSA using equilibrium dialysis, dynamic dialysis, equilibrium gel filtration, fluorescence quenching, ultrafiltration, isothermal titration calorimetry, heteronuclear 2-D NMR, and reversed-phase liquid

Figure 3-1. Structures of acetohexamide and tolbutamide.

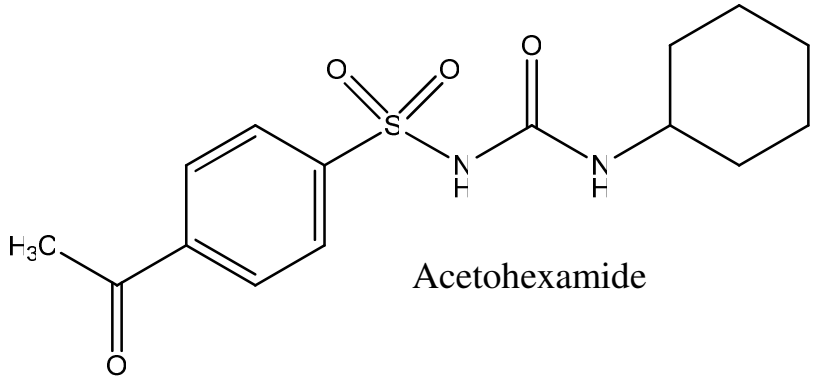

Acetohexamide

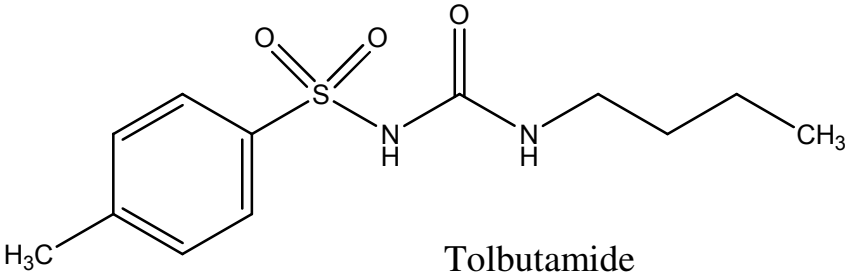

Tolbutamide

chromatography. However, the binding constants that have been obtained in these studies have ranged by almost ten-fold for both acetohexamide ([0.4 to 4.1] x 10^5 M^{-1})[4, 15] and tolbutamide ([0.4 to 3.0] x 10^5 M^{-1}).[15-20] It is also not yet apparent as to whether one or several major sites on HSA are involved in these interactions.[4, 16-18]

This current report will use the method of high-performance affinity chromatography (HPAC) to obtain more detailed information on the strength and location of the binding sites on HSA for acetohexamide and tolbutamide. This method has previously been used to examine the binding of HSA to many other drugs and small solutes, such as coumarins,[20-22] indoles,[23] carbamazepine,[20, 24, 25] ibuprofen and benzodiazepines.[22, 26] The benefits of HPAC over traditional methods like ultrafiltration and equilibrium dialysis include its use of smaller amounts of sample, its better reproducibility and precision, and its ease of automation.[27-29]

The combined use of HPAC with frontal analysis (i.e., frontal affinity chromatography) and immobilized HSA columns will first be used in this study to estimate the total number of binding sites and association equilibrium constants of acetohexamide and tolbutamide with HSA. Zonal elution and competition with site-selective probe compounds for HSA will then be used to examine the binding of these two sulfonylurea drugs at the major binding regions for drugs on this protein (i.e., Sudlow site I and II).[30, 31] The results will be compared to previous observations made in the literature and should provide a more complete picture of how these drugs bind with HSA and are transported by this protein in the circulation. This work will also be used to illustrate how HPAC and several tools available in this method (e.g., equations for

examining multi-site interactions or allosteric effects)[26] can be utilized to examine relatively complex drug-protein interactions.

Experimental

Reagents

The acetohexamide, tolbutamide (≥ 99.9 %), warfarin (≥ 97%), and L-tryptophan (98%) were purchased from Sigma-Aldrich (St. Louis, MO, USA). The buffer salts and HSA (essentially fatty acid free, ≥ 96%) were also obtained from Sigma-Aldrich. The Nucleosil Si-300 (7 micron particle diameter, 300 Å pore size) was from Macherey-Nagel (Düren, Germany). Reagents used in the bicinchoninic acid (BCA) protein assay were from Pierce (Rockford, IL, USA). All solutions were made using water obtained from a NANOpure system (Barnstead, Dubuque, IA, USA). Prior to use, all aqueous solutions were filtered through a 0.20 μm GNWP nylon membrane from Millipore (Billerica, MA, USA).

Apparatus

The chromatographic system consisted of a DG-2080-53 three-solvent degasser, two PU-2080 isocratic HPLC pumps, a UV-2075 absorbance detector, and a AS-2055 autosampler (Jasco, Tokyo, Japan), along with a Rheodyne Advantage PF 6-port valve (Cotati, CA, USA). A Jasco CO-2060 column oven was used to control the column temperature. All of the chromatographic components were controlled through EZChrom Elite software v3.2.1 (Scientific Software, Inc., Pleasanton, CA, USA) via Jasco LC Net hardware. In-house programs written in Labview 5.1 (National Instruments, Austin, TX,

USA) were used to determine the analyte breakthrough times in the frontal analysis experiments. PeakFit 4.12 (Jandel Scientific Software, San Rafael, CA, USA) was used to determine the peak central moments in the zonal elution studies.

Methods

Nucleosil Si-300 silica was modified to produce diol silica by using a previously-published procedure.[32] This diol silica was then used to immobilize HSA by the Schiff base method, also according to previous methods.[21, 33] A control support was made in the same manner without any added HSA. A small amount of the HSA immobilized support and the control support was dried overnight in a vacuum oven, and a bicinchoninic acid (BCA) assay was used to determine the final protein content of this material. This assay was performed in triplicate using soluble HSA as the standard and the control support as the blank. The amount of immobilized HSA was estimated to be 38 (± 3) mg/g silica, or approximately 600 (± 30) nmol HSA/g silica. Separate 2.0 cm x 2.1 mm ID stainless steel columns containing either the HSA silica or the control support were downward slurry packed with the silica at 3000 psi (20.7 MPa) using pH 7.4, 0.067 M potassium phosphate buffer as the packing solution. These columns were stored in pH 7.4, 0.067 M potassium phosphate buffer at 4 ºC when not in use. Experiments were performed over a period of eleven months and over the course of less than 500 sample applications or injections; similar HSA columns have been shown to maintain good stability in drug binding studies under these conditions.[34]

All aqueous solutions of samples and competing agents were prepared using pH 7.4, 0.067 M potassium phosphate buffer. This buffer was used as the application and

regeneration buffer during the frontal analysis and zonal elution studies (note: no elution buffer was needed in this work because the drugs and competing agents that were applied to the HSA columns could later be eluted under isocratic conditions by this same buffer). All solutions were filtered through a 0.2 μm nylon filter and degassed under vacuum for at least 15 min prior to use. A flow rate of 0.5 ml/min was used throughout this work for sample application and injection. This flow rate has been shown in previous work to obtain reproducible binding capacities and retention factors for other drugs or small solutes on similar HSA columns.[35] During frontal analysis, the application of either the pH 7.4, 0.067 M phosphate buffer or the desired drug solution was made by alternating between these solutions through the use of a six-port valve. The application of samples in the zonal elution experiments was controlled through the autosampler and was carried out by using an injection volume of 20 μL.

Frontal analysis studies were performed by first equilibrating the HSA column in the presence of pH 7.4, 0.067 M potassium phosphate buffer at 37 ºC. A switch was then made from this buffer to the same buffer that also contained a known concentration of the analyte of interest (i.e., fifteen concentrations of acetohexamide ranging from 1 to 1000 μM, and nine concentrations of tolbutamide ranging from 1 to 200 μM). Once the analyte had saturated the column and created a breakthrough curve, the system was switched back to applying only the pH 7.4 buffer to elute the retained analyte from the column. Elution of the analyte was monitored using a UV/Vis detector, with the wavelength of detection being adjusted at high concentrations to ensure that a linear change in signal with concentration was always present. Acetohexamide was monitored at 248 nm for applied concentrations of 1-20 μM and at 315 nm for concentrations of 30-

1000 μM. Tolbutamide was monitored at 250 nm for all of its applied concentrations. These runs were performed in triplicate on both the HSA column and the control column. Breakthrough times were determined using the equal area method[27] and were corrected for non-specific binding to the support by subtracting the values for the control column for those measured on the HSA column at each given concentration of the analyte (e.g., interactions with the support made up 33% of the total binding noted for 1 μM tolbutamide and 21% for 1 μM acetohexamide on the HSA columns, but a correction for these non-specific interactions could be effectively made in this manner, as demonstrated for other analytes in previous studies with HSA columns).[20-22] The resulting data were analyzed according to various binding models, as described in the Results and Discussion section. Linear regression was performed using Microsoft Excel 2003 (Microsoft Corporation, Redmond, WA, USA). Non-linear regression was carried out using DataFit 8.1.69 (Oakdale Engineering, PA, USA).

The competitive binding, zonal elution studies were performed using *R*-warfarin and L-tryptophan as the injected agents. These compounds have been shown in the past to bind to Sudlow sites I and II, respectively, and are often used as probes in drug-binding studies.[30, 31] Additions of 20 μL samples containing 5 μM *R*-warfarin or L-tryptophan were injected onto a column equilibrated with a mobile phase that contained a known concentration of the drug of interest. The injected agent was always kept at a concentration of 5 μM, a value found in additional experiments to provide linear elution conditions for the HSA columns used in this study,[23, 36] while the analyte in the mobile phase (acetohexamide or tolbutamide) was applied at concentrations that ranged from 0 to 20 μM. These studies were performed at 37 ºC on both the HSA and control columns.

A pH 7.4, 0.067 M potassium phosphate buffer was used as the mobile phase and to prepare all solutions of the injected analytes and competing agents. The elution of *R*-warfarin and L-tryptophan was monitored at 308 and 280 nm, respectively. The central moments of the resulting peaks were determined by using PeakFit v.4.12 and an exponentially-modified Gaussian curve fit. The resulting values were used along with the measured void time of the system, as determined by injecting 20 μL of 20 μM sodium nitrate (i.e., a non-retained solute on HSA columns), to obtain the retention factors for each probe compound. Sodium nitrate was monitored at 205 nm.

Results and Discussion

Frontal analysis studies using acetohexamide

In these studies, frontal analysis was used to estimate the association equilibrium constants (K_a) for acetohexamide and the number of binding sites of this drug with HSA by using HPAC and columns that contained immobilized HSA. This was done by measuring the binding capacity of this column (m_L) as the concentration of acetohexamide that was applied to the column was varied. Some typical breakthrough curves that were obtained in these experiments are shown in Figure 3-2. If fast association/dissociation kinetics are present for the binding of the applied analyte with the immobilize protein (i.e., as is typically present during drug-HSA interactions), the mean position of the resulting breakthrough curve can be related to K_a, m_L, and the applied concentration of the analyte [A].[27, 28] For an analyte that binds to only a single type of site within the column, the following equations can be used to describe this relationship.[24, 27]

Figure 3-2. Breakthrough curves for acetohexamide on an immobilized HSA column at applied concentrations (from left to right) of 10, 7.5, 5, 2.5, and 1 μM. Alternative detection wavelengths were used for some of the higher concentrations of analyte solutions to maintain a linear response in absorbance versus concentration during these studies, as described in the Experimental Section. Other conditions are given in the text.

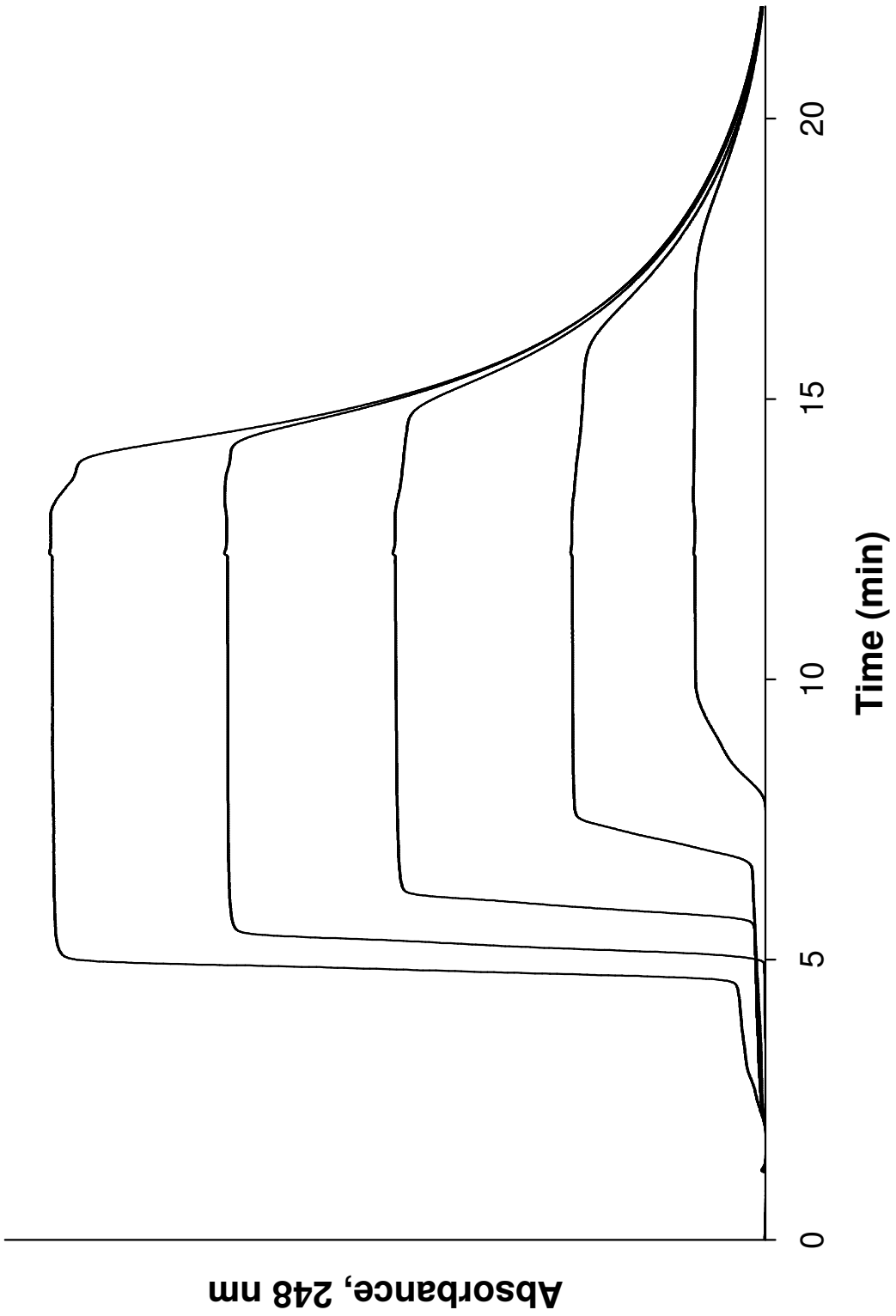
Absorbance, 248 nm
0
5
10
15
20
Time (min)

$$\frac{1}{m_{Lapp}} = \frac{1}{(K_a m_L[\mathrm{A}])} + \frac{1}{m_L} \qquad (3\text{-}1)$$

or

$$m_{Lapp} = \frac{m_L K_a[\mathrm{A}]}{(1 + K_a[\mathrm{A}])} \qquad (3\text{-}2)$$

In these equations, m_{Lapp} is the apparent moles of analyte required to saturate the column at a particular concentration. Equation 3-1 indicates for a system with a single type of binding site that a plot of $1/m_{Lapp}$ versus 1/[A] should provide a linear relationship from which the values of K_a and m_L can be determined from the slope and intercept. If multi-site binding is present, such a plot should approach a linear response at low concentrations (i.e., high values for 1/[A]) and give a curved response and negative deviations at high analyte concentrations (i.e., low values for 1/[A]), as illustrated in Figure 3-3.

In the case of multi-site binding, Equation 3-1 can be expanded to allow for more than one class of binding sites. For example, a system containing two binding sites would have the following relationship,[24, 27]

$$\frac{1}{m_{Lapp}} = \frac{1 + K_{a1}[\mathrm{A}] + \beta_2 K_{a1}[\mathrm{A}] + \beta_2 K_{a1}^2[\mathrm{A}]^2}{m_{Ltot}\{(\alpha_1 + \beta_2 - \alpha_1\beta_2)K_{a1}[\mathrm{A}] + \beta_2 K_{a1}^2[\mathrm{A}]^2\}} \qquad (3\text{-}3)$$

where K_{a1} is the association equilibrium constant for the binding site with the highest affinity (L_1) and α_1 is the fraction of all binding regions that make up the high affinity binding sites (i.e., $\alpha_1 = m_{L1,tot}/m_{Ltot}$). The term β_2 is the ratio of the association equilibrium constants for any lower affinity site (e.g., K_{a2}) versus the highest affinity site, where $\beta_2 = K_{a2}/K_{a1}$ and $0 < K_{a2} < K_{a1}$. Equation 3-3 can also be written in a non-reciprocal form, as given below.[24, 27]

$$m_{Lapp} = \frac{m_{L1}K_{a1}[\mathrm{A}]}{(1+K_{a1}[\mathrm{A}])} + \frac{m_{L2}K_{a2}[\mathrm{A}]}{(1+K_{a2}[\mathrm{A}])} \qquad (3\text{-}4)$$

Using this latter equation it is possible to find both K_a and m_L values for an analyte by plotting m_{Lapp} versus [A], from which the values of the individual association equilibrium constants and binding capacities for each site can be obtained by non-linear regression. Although Equation 3-3 would be expected to produce a non-linear response throughout a broad range of concentrations, it is known at low analyte concentrations that a linear response can still be observed even for a system with multi-site binding, as demonstrated by the following equation.[37]

$$\lim_{[\mathrm{A}]\to 0} \frac{1}{m_{Lapp}} = \frac{1}{m_{Ltot}(\alpha_1 + \beta_2 - \alpha_1\beta_2)K_{a1}[\mathrm{A}]} + \frac{\alpha_1 + \beta_2{}^2 - \alpha_1\beta_2{}^2}{m_{Ltot}(\alpha_1 + \beta_2 - \alpha_1\beta_2)^2} \qquad (3\text{-}5)$$

Equation 3-5 indicates that a linear relationship will be approached even for a multi-site system for a plot of $1/m_{Lapp}$ versus. 1/[A] at low analyte concentrations, or high values for 1/[A].[37] The values of m_{Ltot} and K_{a1} in this relationship will now be a function of the relative amount of each type of binding site in the column and their relative affinities for the analyte, as described by the terms α_1 and β_2 in the Equation 3-5. However, it has also been shown in previous theoretical studies that the ratio of the intercept versus slope for this plot can still be used to provide a good estimate of K_{a1} (i.e., the association equilibrium constant for the highest affinity sites).[37]

From the breakthrough curves that were obtained for acetohexamide (see examples in Figure 3-2), double-reciprocal plots were first made of $1/m_{Lapp}$ versus 1/[A]

Figure 3-3. A double-reciprocal plot for frontal analysis studies examining the binding of acetohexamide to an immobilized HSA column. When comparing this response to the linear relationship that is predicted by Equation 3-1, it was apparent that negative deviations occurred at high analyte concentrations (i.e., low values of 1/[A]), indicating that multiple binding regions for acetohexamide were present. The dashed line shows the linear response that was obtained for the data at relatively low analyte concentrations (i.e., high 1/[A] values), which can still be used in such a case to estimate the association equilibrium constant for the highest affinity binding sites in such a system.

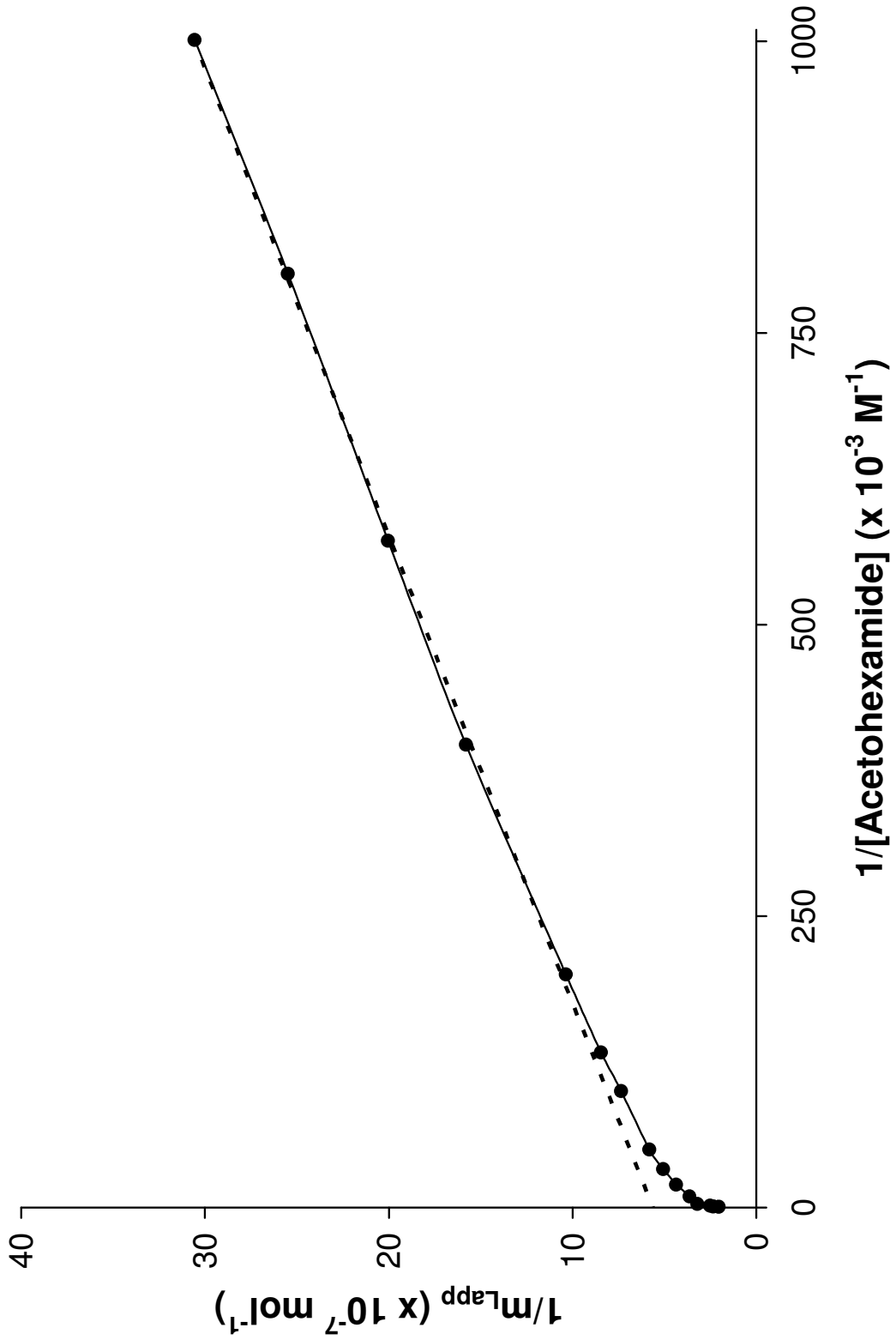
1/mLapp (x 10-7 mol-1)
0
10
20
30
40
0
250
500
750
1000
1/[Acetohexamide] (x 10-3 M-1)

and compared to the responses predicted by Equations 3-1 and 3-3. Some curvature was noted at high analyte concentrations (i.e., low values for 1/[A]), indicating that more than one type of binding site was present for acetohexamide on HSA (Figure 3-3). In addition, a linear response was approached at high values of 1/[A], as predicted by Equation 3-5. By using the best-fit line to the linear region of this data set (as occurred at 1-10 μM acetohexamide), an estimate of 2.0 (± 0.1) x 10^5 M^{-1} was obtained for the association equilibrium constant for the highest affinity sites (K_{a1}) in this system with an m_L value of 1.9 (± 0.1) x 10^{-8} mol.[37]

The frontal analysis data for acetohexamide were also examined by using a non-reciprocal plot. Figure 3-4 shows the results that were obtained when these results were compared to the best-fit response predicted by Equation 3-4 for a two-site binding model. Using a two-site model, acetohexamide was found to have a relative high affinity group of sites with an average K_a of 1.3 (± 0.2) x 10^5, as well as a group of low affinity sites with an average K_a of 3.5 (± 2.9) x 10^2 M^{-1}. The corresponding best-fit values of m_L for these sites were 2.4 (± 0.1) x 10^{-8} and 9.3 (± 5.5) x 10^{-8} mol, respectively. The result for the high-affinity binding site in this two-site model showed good agreement with the estimate of K_a made for the high affinity site using the linear region of Figure 3-3 when this previous plot was examined according to Equation 3-5.

For the sake of comparison, the acetohexamide data in the non-linear plot given in Figure 3-4 were also analyzed directly according to a one-site binding model. As expected for the results in Figures 3-3 and 3-4, the two-site model gave a higher correlation coefficient versus the one-side model (i.e., r = 0.998 versus 0.964 for n = 15) and a smaller sum of the square of the residuals (i.e., 1.2 x 10^{-17} versus 2.2 x 10^{-16}). In

Figure 3-4. Non-linear regression of the acetohexamide frontal analysis data using a two-site binding model, as described by Equation 1-4. The data used in this plot were the same as utilized for the double-reciprocal plot in Figure 3-3.

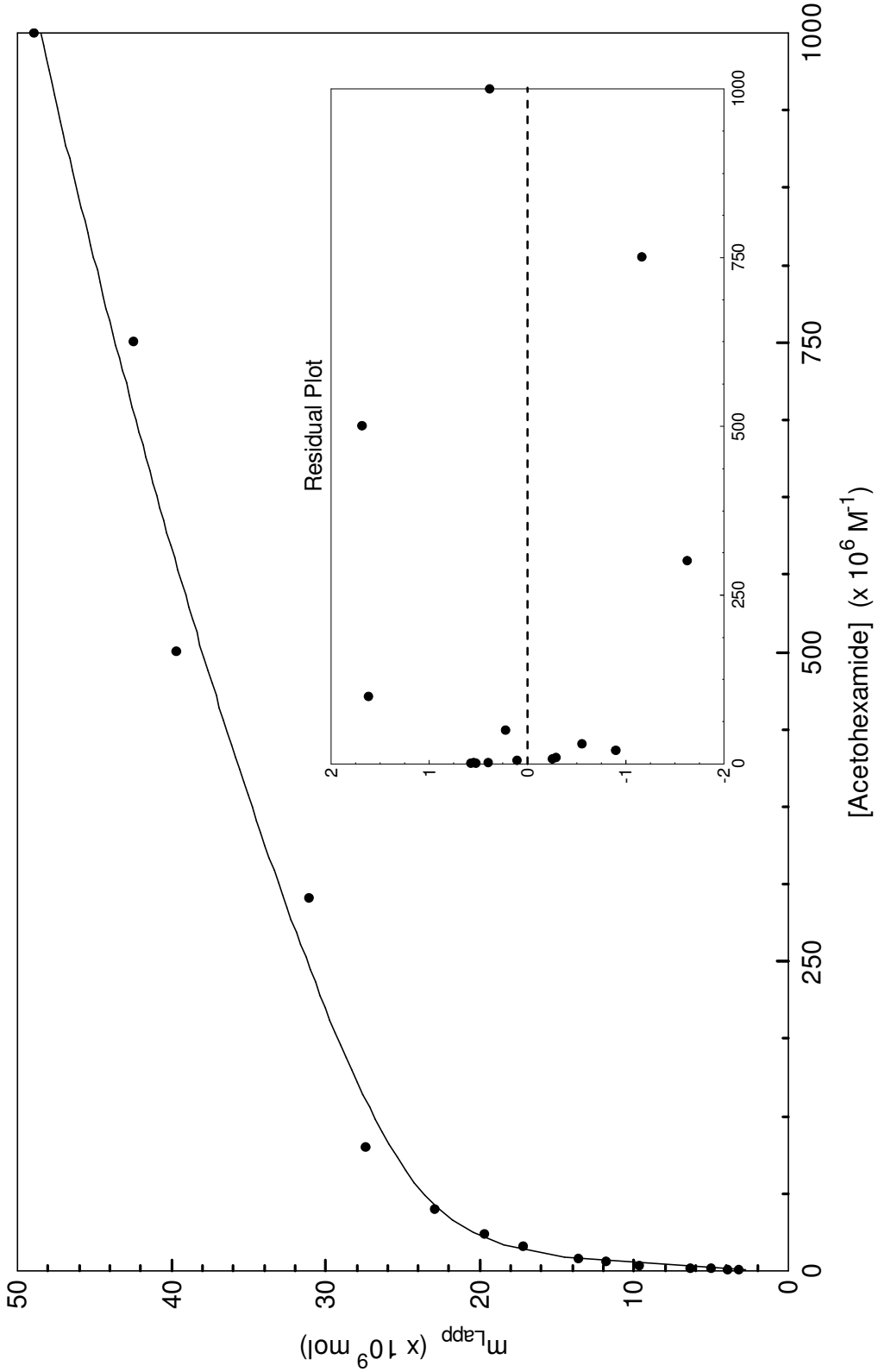
m_{Lapp} (x 10^9 mol)
[Acetohexamide] (x 10^6 M^{-1})
Residual Plot
0
10
20
30
40
50
250
500
750
1000
-2
-1
1
2

addition, a residual plot that was prepared for the fit of these data to a two-site model appeared to give only random variations about the predicted best-fit response, while the residuals for the one-site fit followed a non-random pattern. All of these results indicated that acetohexamide was binding to HSA through at least two general groups of sites: a set of high affinity regions and a set of low affinity regions. This conclusion fits with the fact that many sulfonylurea drugs are known to bind to more than one binding site on HSA and bovine serum albumin (BSA) simultaneously (e.g., as noted when using equilibrium dialysis methods to examine the binding of acetohexamide).[4, 38] This overall result also gave good agreement with previous ultrafiltration studies performed at pH 7.4 and 37°C with soluble HSA, which identified a general group of high affinity sites on HSA for acetohexamide (K_{a1} = 5.9 (± 1.9) x 10^4 M^{-1}) and a group of lower affinity sites (K_{a2} = 3.4 (± 3.3) x 10^3 M^{-1}).[39]

A comparison of the measured binding capacities with the known protein content of the column, 1.78 (± 0.09) x 10^{-8} mol HSA, indicated that each of the two groups of binding sites actually involved more than one region of interaction for acetohexamide with HSA. For example, the best-fit value of m_L for the high affinity sites represented a relative activity of 1.35 (± 0.08) mol acetohexamide/HSA, which suggested that at least two regions contributed to this group of interactions (e.g., this might correspond to two sites each with relative activities of 0.55-0.8, as is often seen with HSA columns).[39] In the same manner, the weak affinity sites had a binding capacity that gave a relative activity of 5.2 (± 3.1) mol/mol HSA, a result which is similar to results that have been obtained when examining the non-specific binding regions for other drugs with this protein.[39]

Based on the binding capacity data, an attempt was made to re-examine the frontal analysis data to test the fit of a three-site binding model to see if any distinction could be made between multiple high affinity sites. The corresponding equation that was employed for this model is shown in Equation 3-6.

$$m_{Lapp} = \frac{m_{L1} K_{a1}[\mathrm{A}]}{(1 + K_{a1}[\mathrm{A}])} + \frac{m_{L2} K_{a2}[\mathrm{A}]}{(1 + K_{a2}[\mathrm{A}])} + \frac{m_{L3} K_{a3}[\mathrm{A}]}{(1 + K_{a3}[\mathrm{A}])} \qquad (3\text{-}6)$$

At first glance, the three-site model appeared to give a reasonable fit to the data. The correlation coefficient (r = 0.998) was comparable to that of the two-site model and the sum of the square of the residuals was slightly smaller (i.e., 9.2 x 10^{-18} versus 1.2 x 10^{-17}). However, the best-fit parameters for the three-site model had high levels of uncertainty associated with them. For instance, the K_a values obtained with this model were 3.6 (± 5.9) x 10^5, 4.9 (± 6.5) x 10^4, and 4 (± 39) x 10^1 M^{-1} with corresponding m_L values of 9.0 (± 15.4) x 10^{-9}, 1.9 (± 1.3) x 10^{-8}, and 5 (± 44) x 10^{-7} mol (see Table 3-1). This greater uncertainty indicated that, if more than one type of high affinity sites were present, the difference in the binding parameters for these sites could not be reliably determined by using the frontal analysis results alone. This issue was examined again later after additional information had been obtained on these interactions through site-selective zonal elution experiments (see *Zonal elution studies using acetohexamide*).

Frontal analysis studies using tolbutamide

Frontal analysis studies with tolbutamide were conducted in the same fashion as the work described for acetohexamide in the previous section to estimate the total the number of binding sites and affinities of this drug with HSA. When these tolbutamide

Table 3-1. Binding parameters obtained by frontal analysis for acetohexamide with HSA

	One-Site Model	Two-Site Model	Three-Site Model
K_{a1} (M^{-1})	2.0 (± 0.1) x 10^{5}	1.3 (± 0.2) x 10^{5}	3.6 (± 5.9) x 10^{5}
m_{L1} (mol)	1.9 (± 0.1) x 10^{-8}	2.4 (± 0.1) x 10^{-8}	9.0 (± 15.4) x 10^{-8}
K_{a2} (M^{-1})		3.5 (± 3.0) x 10^{2}	4.9 (± 6.5) x 10^{4}
m_{L2} (mol)		9.3 (± 5.5) x 10^{-8}	1.9 (± 1.3) x 10^{-8}
K_{a3} (M^{-1})			4 (± 39) x 10^{1}
m_{L3} (mol)			5 (± 44) x 10^{-7}

The values in parentheses represent a range of ± 1 S.D.

results were examined according to a double-reciprocal plot, deviations at high analyte concentrations (or low values of 1/[A]) were again seen, indicating that multiple binding sites were present (data now shown). When the linear region of this plot was analyzed according to Equation 3-5, the estimate obtained for K_a of the high affinity sites was 8.2 (± 0.4) x 10^4 M^{-1} with a corresponding m_L value of 2.4 (± 0.1) x 10^{-8} mol (r = 0.999, n = 6).

These data were next examined by using non-reciprocal plots and fits to both one-site and two-site models according to Equations 3-2 and 3-4. Using a single-site model, this type of regression gave a K_a value of 4.7 (± 0.4) x 10^4 M^{-1} and an m_L of 3.2 (± 0.1) x 10^{-8} mol. Fitting the data to a two-site model, tolbutamide had a K_a value for its major binding site of 8.7 (± 0.6) x 10^4 M^{-1} and a value of 8.1 (± 1.8) x 10^3 M^{-1} for the second set of binding sites; the corresponding m_L values for tolbutamide at these sites were 2.0 (± 0.1) x 10^{-8} and 1.8 (± 0.1) x 10^{-8} mol, respectively. This model gave a correlation coefficient of 0.999 with randomly distributed residuals and a sum of the square of the residuals of 4.3 x 10^{-20}, (versus values of r = 0.998 and 3.9 x 10^{-18} for the fit of the one-site model). The K_a estimated for the high affinity binding site when using either model were within the range of 0.4 to 3.0 x 10^5 M^{-1} that has been reported in the literature for this interaction.[15-20]

The binding capacities estimated for these sites were compared to the protein content of the HSA column. A relative activity of 1.12 (± 0.08) mol tolbutamide/mol HSA was calculated for the higher affinity binding sites. Given the fact that not all of the binding sites on HSA are probably active,[39] this result suggested that more than one group of binding sites was involved in these particular interactions. The lower affinity

regions gave a relative activity of 1.01 (± 0.08) mol tolbutamide/mol HSA. This latter result indicated that only a few regions on HSA were taking part in these weaker interactions.

The use of a three-site model was also attempted for tolbutamide but gave results similar to those for acetohexamide. The sum of the square of the residuals decreased slightly in going from the two-site to three-site model (i.e., decreasing from 4.3 x 10^{-20} to 2.9 x 10^{-20}), but the correlation coefficient of 0.999 was comparable to that found for the two-site binding model. The K_a values found using the three-site binding model were 1.1 (± 0.9) x 10^5, 2.6 (± 6.5) x 10^4, and 5 (±149) x 10^2 M^{-1} with m_L values of 1.3 (± 2.0) x 10^{-8}, 1.7 (± 0.6) x 10^{-8}, and 4 (± 97) x 10^{-8} mol (see Table 3-2). The variations in many of these parameters were again quite large, which indicated that if more than two groups of sites were present they could not be differentiated with just the frontal analysis data. These data were again examined with a three-site model later in this study once additional information had been collected on site-specific interactions by using the method of zonal elution (see *Zonal elution studies using tolbutamide*).

Zonal elution studies using acetohexamide

Competition studies using zonal elution were next performed to determine the specific binding regions on HSA that were interacting with each of these tested drugs. In this technique a mobile phase containing a known concentration of competing agent ([I]) was applied to the column while a small plug of analyte was injected onto the column (see Figure 3-5). The retention time for the analyte was then measured and used to calculate the retention factor (k), where $k = (t_R - t_M)/t_M$, t_R is the retention time of the

Table 3-2. Binding parameters obtained by frontal analysis for tolbutamide with HSA

	One-Site Model	Two-Site Model	Three-Site Model
K_{a1} **(M^{-1})**	8.2 (± 0.4) x 10^4	8.7 (± 0.6) x 10^4	1.1 (± 0.9) x 10^5
m_{L1} **(mol)**	2.4 (± 0.1) x 10^{-8}	2.0 (± 0.1) x 10^{-8}	1.3 (± 2.0) x 10^{-8}
K_{a2} **(M^{-1})**		8.1 (± 1.7) x 10^3	2.6 (± 6.5) x 10^4
m_{L2} **(mol)**		1.8 (± 0.1) x 10^{-8}	1.7 (± 0.6) x 10^{-8}
K_{a3} **(M^{-1})**			5 (± 149) x 10^2
m_{L3} **(mol)**			4 (± 97) x 10^{-8}

The values in parentheses represent a range of ± 1 S.D.

Figure 3-5. Competition studies based on zonal elution for the injection of (a) L-tryptophan or (b) *R*-warfarin as site-selective probes onto HSA columns and in the presence of various concentrations of tolbutamide in the mobile phase. The concentration of tolbutamide in these examples (from left to right) was 20, 15, 10, 5, or 1 μM. The injected concentration of each probe, L-tryptophan and *R*-warfarin, was 5 μM and the injection volume was 20 μL. Other conditions are given in the text.

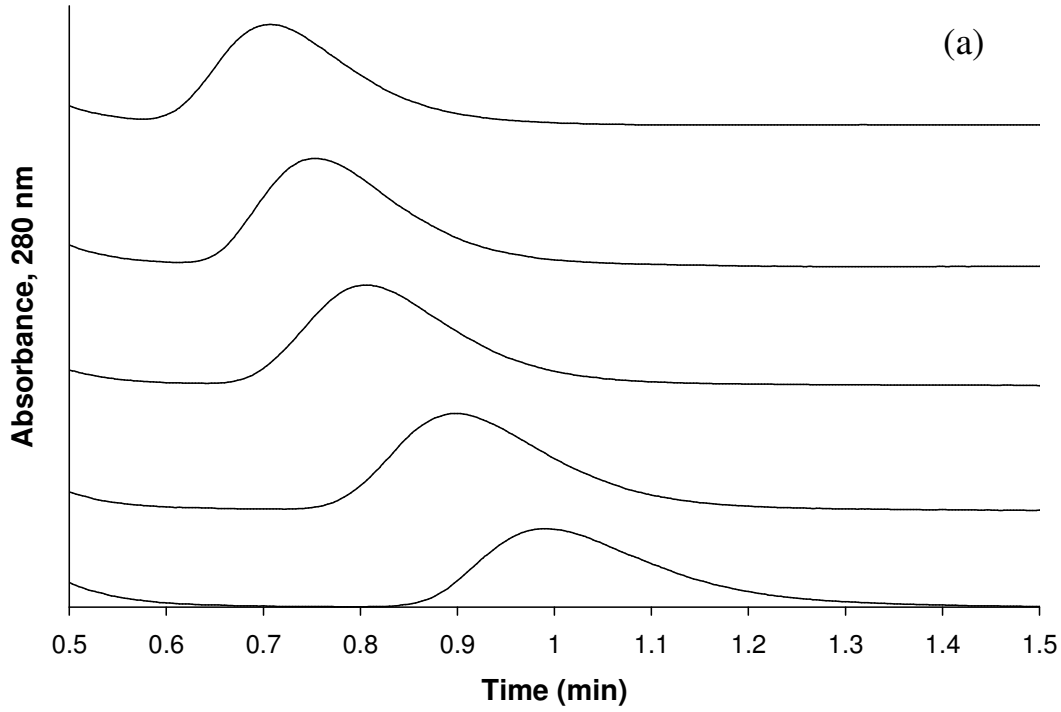
(a)
Absorbance, 280 nm
0.5
0.6
0.7
0.8
0.9
1
1.1
1.2
1.3
1.4
1.5
Time (min)

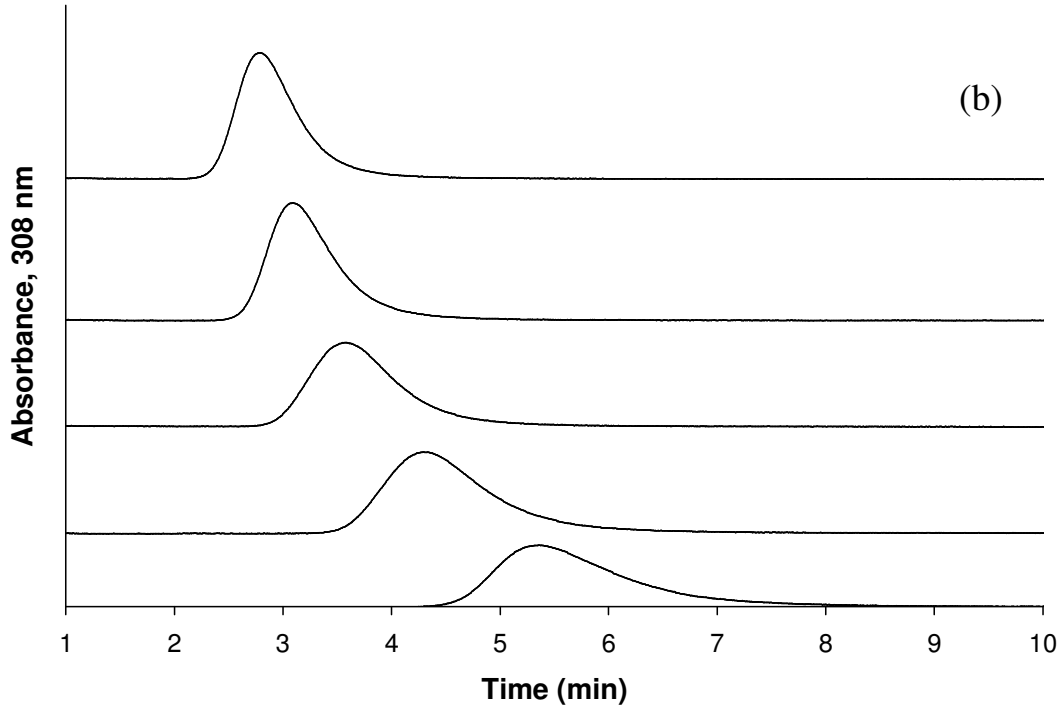
(b)
Absorbance, 308 nm
1
2
3
4
5
6
7
8
9
10
Time (min)

injected solute's peak, and t_M is the retention time of a non-retained solute (e.g., sodium nitrate). The results are often first examined by making a plot of 1/k versus [I]. The following equation predicts that such a plot will give a linear response if A and I compete at a single type of site on the immobilized protein and I has no other types of binding sites with the column.[27, 28]

$$\frac{1}{k} = \frac{K_{aI} V_M [\mathrm{I}]}{K_{aA} m_L} + \frac{V_M}{K_{aA} m_L} \qquad (3\text{-}7)$$

In this equation, K_{aA} and K_{aI} are the association equilibrium constants for the analyte and the competing agent, respectively, at their site of competition and V_M is the void volume. According to Equation 3-7, if a plot of $1/k$ versus [I] is linear, the association equilibrium constant for I at the site of competition can then be calculated from the ratio of the slope versus the intercept of this plot. This is a useful tool in that it can allow information to be obtained on site-selective interactions and local association equilibrium constants for analytes that may have multiple binding sites to an immobilized ligand.[27]

In the competition studies that were conducted in this study, *R*-warfarin was used as a site-selective probe for Sudlow site I and L-tryptophan was used as a site-selective probe for Sudlow site II, as employed in previous studies examining the binding of HSA with other drugs and solutes.[21, 23, 24, 36] It was found in these experiments when using acetohexamide as the competing agent that plots of $1/k$ versus [I] gave a linear response for the injection of both *R*-warfarin and L-tryptophan (see Figure 3-6), with correlation coefficients of 0.991 and 0.996, respectively ($n = 6$).

The predicted value of k (as calculated by taking the inverse of the intercept) for *R*-warfarin when no acetohexamide was present in the mobile phase was 54.3 (± 1.7),

Figure 3-6. Plots of 1/*k* versus [Acetohexamide] for competition studies performed by zonal elution using (a) L-tryptophan or (b) *R*-warfarin as site-selective probes injected onto HSA columns in the presence of various concentrations of acetohexamide as a competing agent. The equations for the best-fit lines in these plots are as follows: (a) y = 18,100 (± 800) x + 0.137 (± 0.009), with a correlation coefficient of 0.996 (n = 6); and (b) y = 780 (± 50) x + 0.0184 (±0.0006), with a correlation coefficient of 0.991 (n = 6).

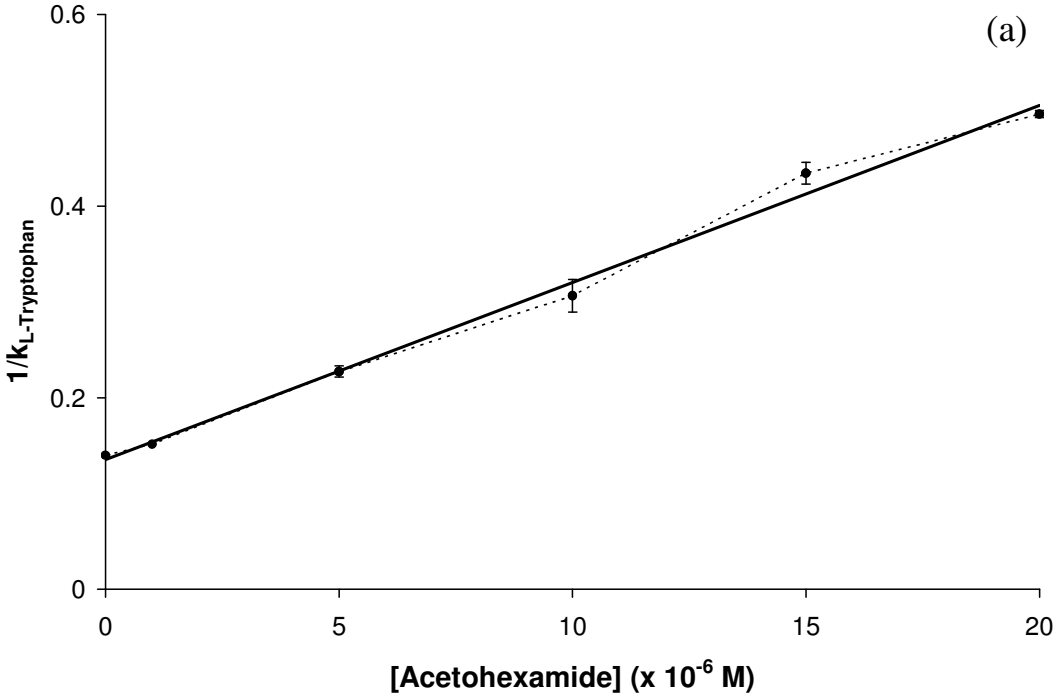
(a)
0.6
0.4
0.2
0
1/k L-Tryptophan
0
5
10
15
20
[Acetohexamide] (x 10-6 M)

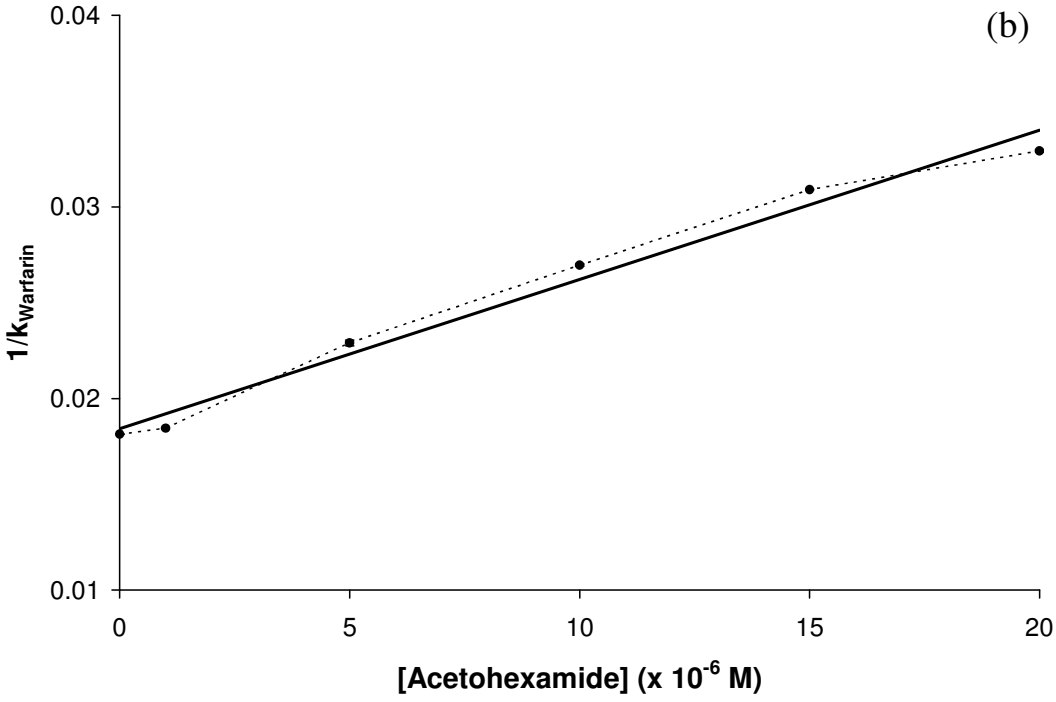
(b)
0.04
0.03
0.02
0.01
1/k Warfarin
0
5
10
15
20
[Acetohexamide] (x 10-6 M)

which showed good agreement with the actual measured value of 55.1 (± 0.1). The retention factor for L-tryptophan when no competing agent is present in the mobile phase is 7.13 (± 0.02), while the predicted value is 7.31 (± 0.47). The relative difference in retention factors between the predicted value (i.e., as obtained from the best-fit intercept) and the actual value (i.e, *k* when no competing agent was present in the mobile phase) was only 1.6% for *R*-warfarin and 2.4% for L-tryptophan showing little difference between predicted and actual values. The agreement of these results is a further indication that acetohexamide had direct competition with both R-warfarin and L-tryptophan, indicating that acetohexamide also had binding to both Sudlow sites I and II of HSA. It was possible to use the best-fit lines to the plots in Figure 3-6 along with Equation 3-5 to determine the site-specific association equilibrium constants for acetohexamide at Sudlow sites I and II. The K_a values that were obtained through this process were 4.2 (± 0.3) x 10^4 M^{-1} and 1.3 (± 0.1) x 10^5 M^{-1}, respectively. It was noted that the K_a value found by this approach for Sudlow site II was similar to that for the highest affinity site when using a two-site model to examine the frontal data.

Zonal elution studies using tolbutamide

Competition studies in zonal elution experiments were also carried out for tolbutamide (see Figure 3-5). The results that were obtained when injections of L-tryptophan were made in the presence of tolbutamide are shown in Figure 3-7(a). The resulting plot of 1/*k* versus [Tolbutamide] gave a linear relationship with a correlation coefficient of $r = 0.998$ ($n = 6$). This result indicated that direct competition was taking place between tolbutamide and L-tryptophan at Sudlow site II. By using Equation 3-5 to

Figure 3-7. Plots of $1/k$ versus [Tolbutamide] for competition studies performed by zonal elution using (a) L-tryptophan or (b) *R*-warfarin as site-selective probes injected onto HSA columns in the presence of various concentrations of tolbutamide as a competing agent. The equations for the best-fit lines shown in these plots are as follows: (a) $y = 8400\ (\pm\ 300)\ x + 0.157\ (\pm\ 0.003)$, with a correlation coefficient of 0.998 ($n = 6$); (b) $y = 1070\ (\pm\ 30)\ x + 0.0194\ (\pm\ 0.0004)$, with a correlation coefficient of 0.999 ($n = 4$).

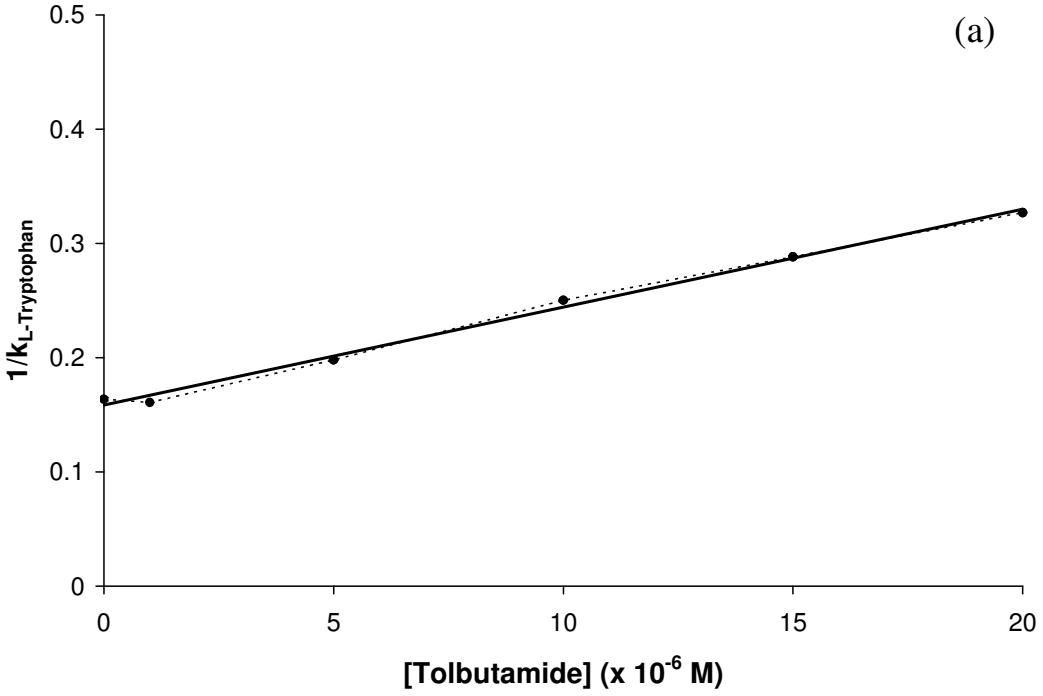
(a)
0.5
0.4
0.3
0.2
0.1
0
1/k L-Tryptophan
0
5
10
15
20
[Tolbutamide] (x 10-6 M)

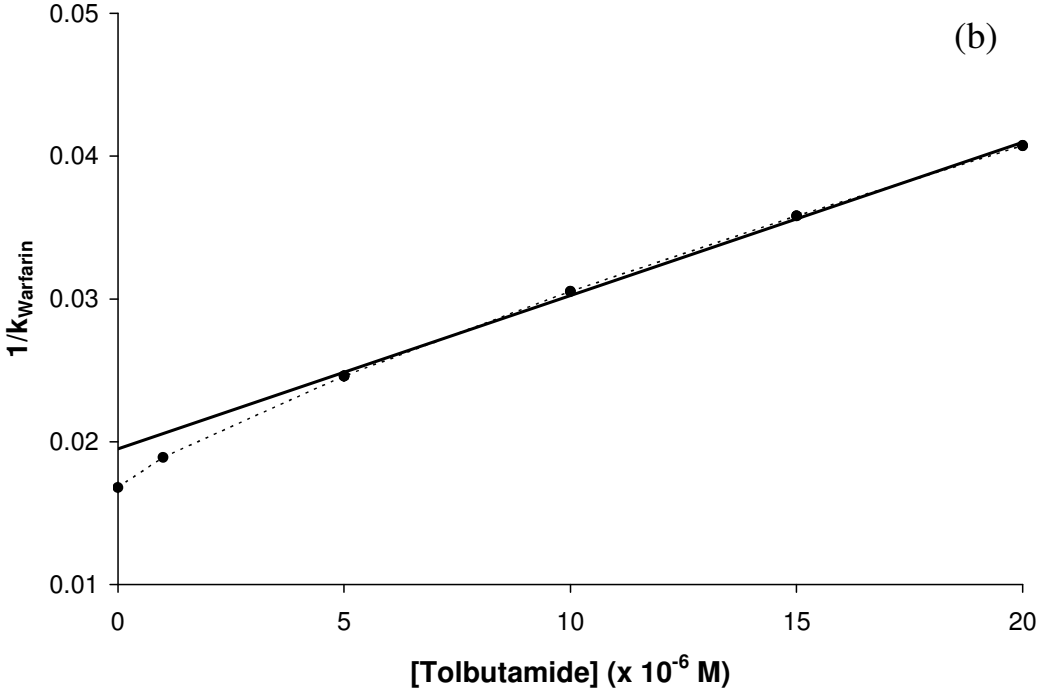
(b)
0.05
0.04
0.03
0.02
0.01
1/k Warfarin
0
5
10
15
20
[Tolbutamide] (x 10-6 M)

analyze this plot (see Table 3-3), it was determined that the association equilibrium constant for tolbutamide at this site was 5.3 (± 0.2) x 10^4 M^{-1}, which is similar to the value calculated for the high-affinity binding site of tolbutamide with HSA when using frontal analysis.

The plot of 1/*k* versus [Tolbutamide] that was generated when *R*-warfarin was the injected probe compound is shown in Figure 3-7(b). This plot appeared to be linear at high tolbutamide concentrations but did have some deviations from linearity at tolbutamide concentrations below 5 μM. One way this behavior may be produced is if some competition were present between *R*-warfarin and tolbutamide at both Sudlow site I and at a few of the weaker affinity regions for tolbutamide on HSA. For instance, the behavior seen in Figure 3-7(b) is predicted by the following equation that has been previously derived to predict the response that would be obtained for a plot of 1/*k* versus [I] in a system with two groups of bindings sites.[37]

$$\frac{1}{k} = \frac{V_m(1 + K_{II}[I] + \gamma_2 K_{II}[I] + \gamma_2 K_I^2[I]^2}{m_{Ltot} K_{a1}\{(\alpha_1 + \beta_2 - \alpha_1\beta_2) + K_{II}[I](\gamma_2\alpha_1 + \beta_2 - \alpha_1\beta_2)\}} \qquad (3\text{-}7)$$

In Equation 3-7, K_{a1} is the association equilibrium constant for the injected analyte binding to the highest affinity site of the ligand and K_{II} is the association equilibrium constant for the competing agent at that site. The terms α_1 again represents the fraction of active sites in the column that is due to the high affinity binding sites, and β_2 is again the ratio of the association equilibrium constant for the lower affinity site vs. the highest affinity region ($\beta_2 = K_{a2}/K_{a1}$). The term γ_2 in this equation is similar to β_2 but now represents the ratio of the association equilibrium constant for the competing agent at the

Table 3-3. Binding constants obtained by zonal elution and competition studies for acetohexamide and tolbutamide with HSA

	Sudlow Site I (*R*-warfarin) (x 10^4 M^{-1})	**Sudlow Site II (L-tryptophan) (x 10^4 M^{-1})**
Acetohexamide	4.2 (± 0.4)	13 (± 1)
Tolbutamide	5.5 (± 0.2) *	5.3 (± 0.2)

The values in parentheses represent a range of ± 1 S.D. *Some curvature was noted at low competing agent concentrations in a plot prepared according to Equation 3-5 when examining the competition of *R*-warfarin with tolbutamide. The linear region of this plot was used to obtain the result given here, based on behavior predicted by Equation 3-8.

site with the lower affinity for the injected analyte vs. the highest affinity for the injected analyte ($\gamma_2 = K_{I2}/K_{I1}$).

At reasonably high values of [I], the response of Equation 3-7 will approach a linear relationship, which is described by Equation 3-8.

$$\lim_{[I]\to\infty} \frac{1}{k} = \frac{V_m K_{I1}[I]\gamma_2}{m_{Ltot} K_{a1}(\gamma_2\alpha_1 + \beta_2 - \alpha_1\beta_2)} + \frac{V_m(\beta_2 + \alpha_1\gamma_2^2 - \alpha_1\beta_2)}{m_{Ltot} K_{a1}(\gamma_2\alpha_1 + \beta_2 - \alpha_1\beta_2)^2} \qquad (3\text{-}8)$$

In this relationship, the slope and intercept are now a function of the relative amount and affinity of each binding site (as described by the terms α_1, β_2, and γ_2) as well as the values for V_m, K_{a1} and m_{Ltot}. However, it has been demonstrated in theoretical studies that the use of the slope versus intercept ratio from this linear region can still be used to provide a reasonable estimate of K_{I1} in a system with multisite interactions. A linear fit was made to the data for tolbutamide and warfarin in Figure 3-7(b) at tolbutamide ranging from 5-20 μM, this approach gave an estimate for K_{I1} of 5.5 (± 0.2) x 10^4 M^{-1}, which would represent the binding of tolbutamide at its highest affinity site of competition with *R*-warfarin. This value is similar to the value calculated for the high-affinity binding site when using frontal analysis, and direct binding by tolbutamide at Sudlow site I is consistent with previous information reported in the literature.[3, 30] It is interesting to note that this value is also quite close to the association equilibrium constant that was determined for tolbutamide at Sudlow site II. This later observation explains why a two-site model using only a single group of higher affinity sites plus a group of weaker affinity sites appeared to give a good fit in the frontal analysis work described for tolbutamide with HSA in the frontal analysis studies. Even when the results of these zonal studies were combined with the previous frontal analysis data, no

further distinction between the interactions of tolbutamide at the two proposed high affinity sites could be made when using the overall binding isotherm because of the similarity in these values. This behavior demonstrates the value of using both frontal analysis and site-selective competition studies in zonal elution to examine such interactions.

Another possible explanation for the deviations from linearity that were noted in Figure 3-7(b) is that some allosteric effects were occurring between *R*-warfarin at Sudlow site I and some other region that was interacting with tolbutamide. This possibility was explored by using the following that has been developed in previous work to describe such an interaction.[40]

$$\frac{k_0}{k - k_0} = \frac{1}{\beta_{I \to A} - 1} \times \left(\frac{1}{K_{IL}[\mathrm{I}]} + 1 \right) \qquad (3\text{-}9)$$

This equation includes the retention factor k that is observed for the injected analyte A, the mobile phase concentration of the competing agent ([I]) and the association equilibrium constant K_{IL} for the binding of competing agent I to the immobilized ligand L. Other terms in this equation include k_0, which is the retention factor for A in the absence of any competing agent, and $\beta_{I \to A}$, which is the coupling constant for the allosteric interaction, as given by $\beta_{I \to A} = K_{aL'}/K_{aL}$ (where K_{aL} is the initial association equilibrium constant for A with L, and $K_{aL'}$ is the association equilibrium constant for A with I after I has been bound to L, also resulting in a change in the binding of A to L). Equation 3-9 predicts that a plot of $k_0/(k - k_0)$ will give a linear relationship for a simple allosteric interaction, where the intercept is equal to $1/(\beta_{I \to A} - 1)$ and the slope is $1/[(\beta_{I \to A} - 1) K_{IL}]$. From the slope and intercept it is possible to determine the values of $\beta_{I \to A}$ and

Figure 3-8. Change in the retention of *R*-warfarin in the presence of tolbutamide during zonal elution studies, as examined according to Equation 1-9. The best-fit line shown in this plot is described by the equation y = [7.60 (± 0.17) x 10^{-6}] x – 1.44 (± 0.08) and had a correlation coefficient of 0.999 (n = 5). The error bars represent a range of ±1 S.D.

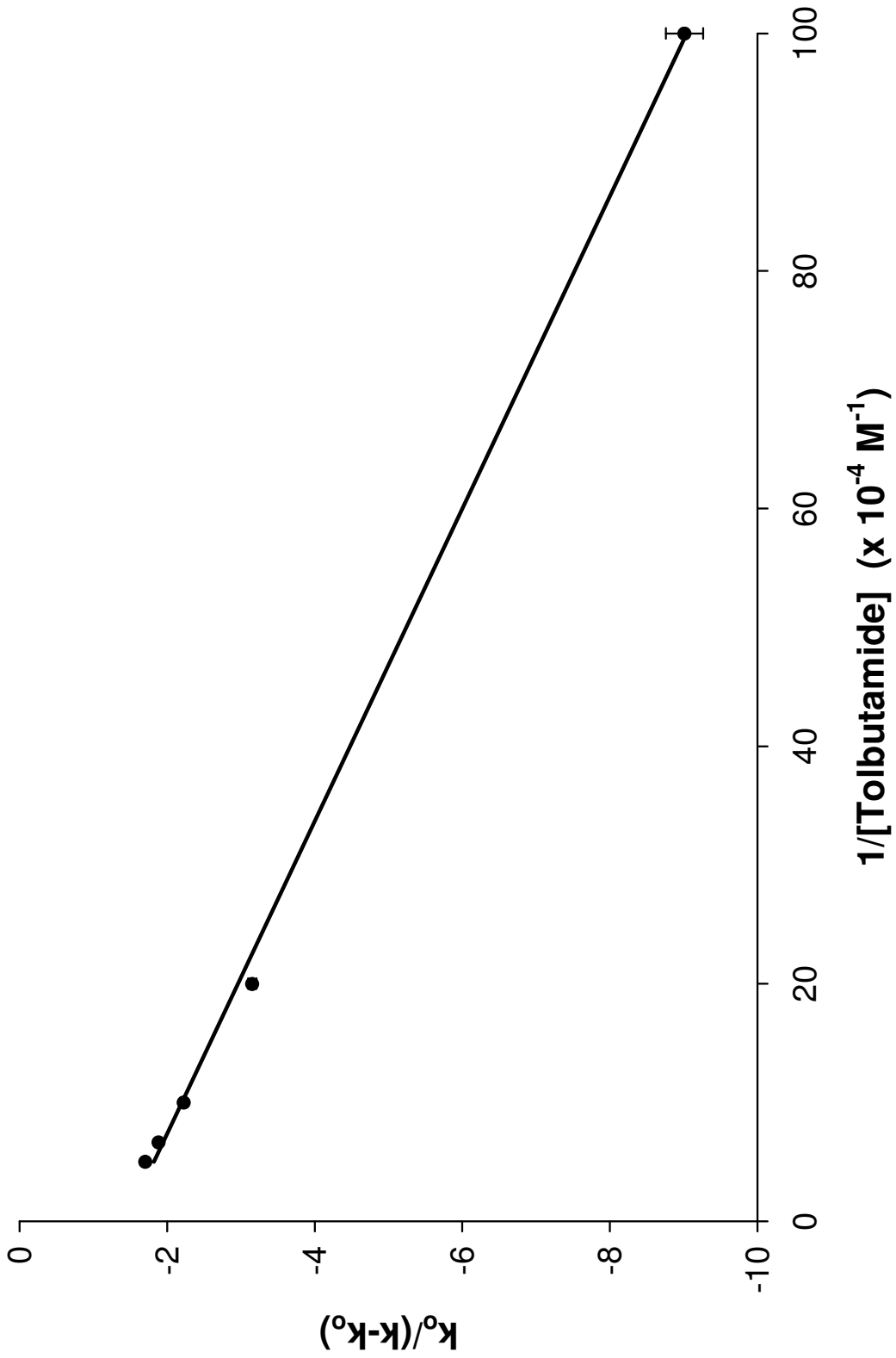
0
-2
-4
-6
-8
-10
$k_o/(k-k_o)$
0
20
40
60
80
100
1/[Tolbutamide] (x 10^{-4} M^{-1})

K_{IL}. A value of $\beta_{I\rightarrow A} > 1$ will occur if positive allosteric effects are present between I and A and a value of $0 < \beta_{I\rightarrow A} < 1$ will occur if negative allosteric effects are taking place. If $\beta_{I\rightarrow A}$ is equal to zero, then direct competition is taking place between I and A, while a value of one for $\beta_{I\rightarrow A}$ indicates that there is no effect of *I* on *A* as these agents bind to L.

A plot of $k_0/(k-k_0)$ versus. 1/[I] was prepared according to Equation 3-9 to further explore the observed change in retention for *R*-warfarin by HSA in the presence of tolbutamide. The result that was obtained is shown in Figure 3-8. This plot appeared to have a good correlation coefficient for a linear fit (r =0.999, n = 5); however, some curvature did appear to be present in this plot. If these deviations were ignored, a $\beta_{I\rightarrow A}$ value of 0.31 (± 0.02) would be obtained for the coupling constant, which would represent a negative allosteric effect for tolbutamide on the binding of *R*-warfarin at Sudlow site I. The value of K_{IL} that would be obtained from the same fit is 1.9 (± 0.1) x 10^5 M^{-1} for the binding of tolbutamide to HSA. This latter result is similar to some previously reported values for the binding of tolbutamide with HSA,[15-18] but is higher than the K_a value for the high affinity site that was determined in this current work when using frontal analysis. Based on these observations, the curved behavior noted for the plot in Figure 3-8, and the results that were obtained for acetohexamide, it was concluded that a multi-site model was a more likely explanation than allosteric interactions for the curvature seen in Figure 3-7(b).

Conclusion

These studies showed that frontal studies and zonal studies compliment each other as a means for gleaning a better understanding of the overall binding of drugs such as

sulfonylureas to proteins like HSA. Using frontal analysis alone, it was initially determined that acetohexamide was interacting with HSA at two general classes of binding sites, including a set of higher affinity regions and a group of weaker affinity regions (Note: this binding can occur simultaneously at both classes of sites). The use of more detailed competitive binding studies and zonal elution studies indicated that acetohexamide was binding with a relatively high affinity to both Sudlow sites I and II. It was also possible through these measurements to obtain site-selective equilibrium constants for these interactions (1.3 (± 0.1) x 10^5 and 4.3 (± 0.3) x 10^4 M^{-1}) and to combine the zonal elution and frontal analysis data to further refine the overall binding model and estimates of the weak affinity interactions of acetohexamide with HSA.

Tolbutamide was also determined by frontal analysis to bind with HSA at both high affinity and lower affinity regions. Zonal elution studies and work with site-selective probes indicated that the high affinity interactions probably involved binding at both Sudlow sites I and II, with interactions that were quite similar in strength. The K_a values estimated for tolbutamide at Sudlow sites I and II were 5.5 (± 0.2) x 10^4 and 5.3 (± 0.2) x 10^4 M^{-1}, respectively, and were again used with the frontal analysis results to refine a model for describing the overall binding of this drug to HSA. This study demonstrates that using both frontal analysis and zonal elution can be extremely valuable in obtaining a good quantitative description of how drugs such as sulfonylureas are interacting with HSA. The same approach should also be useful when employing HPAC to examine other complex drug-protein interactions.

References

1. *Drug Information for the Health Care Professional*. The US Pharmacopeial Convention, Inc.: 1997; Vol. 1.
2. Skillman, T. G.; Feldman, J. M., *Am. J. Med.* **1981,** *70*, 361-372.
3. Jakoby, M. G.; Covey, D. F.; Cistola, D. P., *Biochem.* **1995,** *34*, 8780-8787.
4. Imamura, Y.; Kojima, Y.; Ichibagase, H., *Chem. Pharm. Bull.* **1985,** *33* (3), 1281-1284.
5. Colmenarejo, G., *Med. Res. Rev.* **2003,** *23* (3), 275-301.
6. Kragh-Hansen, U.; Chuang, V. T. G.; Otagiri, M., *Biol. Pharm. Bull.* **2002,** *25* (6), 695-704.
7. Fasano, M.; Curry, S.; Terreno, E.; Galliano, M.; Fanali, G.; Narciso, P.; Notari, S.; Ascenzi, P., *IUBMB Life* **2005,** *57* (12), 787-796.
8. Ascenzi, P.; Bocedi, A.; Notari, S.; Fanali, G.; Fesce, R.; Fasano, M., *Mini-Rev. Med. Chem.* **2006,** *6*, 483-489.
9. Dockal, M.; Carter, D. C.; Ruker, F., *J. Biol. Chem.* **1999,** *274* (41), 29303-29310.
10. Otagiri, M., *Drug Metab. Pharmacokinet.* **2005,** *20* (5), 309-323.
11. Wan, H.; Bergstrom, F., *J. Liq. Chromatogr. Rel. Technol.* **2007,** *30*, 681-700.
12. Ascoli, G. A.; Domenici, E.; Bertucci, C., *Chirality* **2006,** *18*, 667-679.
13. Tsuchiya, S.; Sakurai, T.; Sekiguchi, S.-i., *Biochem. Pharmacol.* **1984,** *33* (19), 2967-2971.
14. Judis, J., *J. Pharm. Sci.* **1973,** *62* (2), 233-237.
15. Koyama, H.; Sugioka, N.; Uno, A.; Mori, S.; Nakajima, K., *Biopharm. Drug Dispos.* **1997,** *18* (9), 791-801.

16. Yoshitomi, H.; Goto, S., *Chem. Pharm. Bull.* **1981,** *29* (8), 2374-2379.

17. Crooks, M. J.; Brown, K. F., *J. Pharm. Pharmacol.* **1974,** *26*, 304-311.

18. Brown, K. F.; Crooks, M. J., *Can. J. Pharm. Sci.* **1974,** *9* (3), 75-77.

19. Koizumi, K.; Ikeda, C.; Ito, M.; Suzuki, J.; Kinoshita, T.; Yasukawa, K.; Hanai, T., *Biomed. Chromatogr.* **1998,** *12*, 203-210.

20. Kim, H. S.; Wainer, I. W., *J. Chromatogr. B* **2008,** *870*, 22-26.

21. Joseph, K. S.; Moser, A. C.; Basiaga, S.; Schiel, J. E.; Hage, D. S., *J. Chromatogr. A* **2009,** *1216*, 3492-3500.

22. Noctor, T. A. G.; Diaz-Perez, M. J.; Wainer, I. W., *J. Pharm. Sci.* **1993,** *82*, 675-676.

23. Conrad, M. L.; Moser, A. C.; Hage, D. S., *J. Sep. Sci.* **2009,** *32*, 1145-1155.

24. Kim, H. S.; Hage, D. S., *J. Chromatogr. B.* **2005,** *816*, 57-66.

25. Yoo, M. J.; Hage, D. S., *J. Sep. Sci.* **2009,** *32*, 2776-2785.

26. Chen, J.; Fitos, I.; Hage, D. S., *Chirality* **2006,** *18*, 24-36.

27. Hage, D. S., *J. Chromatogr. B* **2002,** *768*, 3-30.

28. Schiel, J. E.; Joseph, K. S.; Hage, D. S., Biointeraction Affinity Chromatography. In *Adv. Chromatogr.*, Grinsberg, N.; Grushka, E., Eds. Taylor & Francis: New York, 2010; Vol. 48.

29. Schriemer, D. C., *Anal. Chem.* **2004,** *76* (23), 440A-448A.

30. Sudlow, G.; Birkett, D. J.; Wade, D. N., *Mol. Pharmacol.* **1975,** *11*, 824-832.

31. Sudlow, G.; Birkett, D. J.; Wade, D. N., *Mol. Pharmacol.* **1976,** *12*, 1052-1061.

32. Ruhn, P. F.; Garver, S.; Hage, D. S., *J. Chromatogr. A* **1994,** *669* (1-2), 9-19.

33. Loun, B.; Hage, D. S., *J. Chromatogr.* **1992,** *579*, 225-235.

34. Yang, J.; Hage, D. S., *J. Chromatogr. A* **1997,** *766*, 15-25.

35. Loun, B.; Hage, D. S., *Anal. Chem.* **1994,** *66* (21), 3814-3822.

36. Moser, A. C.; Kingsbury, C.; Hage, D. S., *J. Pharm. Biomed. Anal.* **2006,** *41*, 1101-1109.

37. Tweed, S. A. Effects of Heterogeneity on the Characterization of Chromatographis Stationary Phases. Thesis, University of Nebraska, Lincoln, 1997.

38. Goro, S.; Yoshitomi, H.; Kishi, M., *Yakugaku Zasshi* **1977,** *97* (11), 1219-1227.

39. Anguizola, J. Analysis of Drug Binding to serum proteins in diabetes. Thesis, University of Nebraska, Lincoln, 2009.

40. Chen, J.; Hage, D. S., *Nature Biotech.* **2004,** *22* (11), 1445-1448.

CHAPTER 4

THE BINDING OF WARFARIN AND L-TRYPTOPHAN TO GLYCATED HSA

Introduction

Diabetes is a growing problem in the United States. In 2007, over 23 million people within the U.S. (7.8% of the population) were reported to have this disease, with over 1 million people being diagnosed every year.[1] The most common form of diabetes is type 2 (non-insulin dependent) diabetes, where the body suffers from a shortage of insulin. Diabetes is characterized by an elevated level of glucose in the blood. This glucose can form covalent adducts with proteins in blood through a non-enzymatic process known as glycation.[2-4] For example, glycated hemoglobin is now commonly used by physicians to monitor the long-term control of diabetes by a patient.[2] However, many other blood proteins also become glycated including human serum albumin (HSA). Because HSA has a shorter half-life than hemoglobin in blood, monitoring the extent of HSA glycation has been considered as a way to look at short-term diabetes management.[2]

HSA is the most prominent protein in human plasma. This protein is synthesized in the liver and contains 585 amino acids with a total molar mass of 66,438 Da.[5-7] Two-thirds of HSA is made up of α-helix structures while 10% of the protein contains β-turns. This protein has three homologous domains (I, II, and III) that each contain two subunits (A and B). Approximately 6-13% of this protein is glycated in normal individuals,[2-5] but this level can increase to over 20-30% in individuals with diabetes.[2, 3, 5] Glycation occurs by a condensation reaction of glucose with a lysine residue or the *N*-terminus of HSA to first form a Schiff base.[3, 6-8] Rearrangements of this product create a ketoamine (i.e., an

Amadori product).[3, 6, 8] Further rearrangements of this adduct can create advanced glycation end-products (AGEs). Increased levels of these adducts and products can lead to severe health complications in diabetic individuals.[3]

HSA is a major transport protein in blood for carrying various endogenous and exogenous compounds throughout the body. It greatly influences drug distribution and can play a major role in affecting drug absorption, distribution, metabolism, and excretion.[4, 9-11] Binding to HSA also allows hydrophobic drugs to be more soluble in blood and increases the overall lifetime of a drug before it is metabolized.[4, 11] It has previously been determined that HSA has two major binding sites for drugs (i.e., Sudlow sites I and II, located in subunits IIA and IIIB of HSA), as well as additional minor binding sites.[12-14] Sudlow site I binds anti-coagulant drugs such as warfarin and anti-inflammatory drugs such as azapropazone, phenylbutazone, and salicylate. Sudlow site II binds drugs such as ibuprofen, fenoprofen, ketoprofen, and benzodiazepines, along with the essential amino acid L-tryptophan.[9]

The purpose of this study was to see if the binding of HSA to warfarin and L-tryptophan (see structures in Figure 4-1) is altered as the level of HSA glycation is increased, as occurs in diabetes. Warfarin and L-trytophan were of interest to this work because they are often used as site-selective probes for Sudlow sites I and II, respectively, in examining the binding of other drugs to HSA at these sites.[15-17] Glycation has been noted in previous work to occur at locations that are near both Sudlow sites I and II.[2, 3, 8, 16, 17] It has been suggested in earlier studies that the binding of HSA to some drugs and other solutes,[5,18,19] including both warfarin[5] and L-tryptophan,[19] can be affected by modifications resulting from glycation. However, past studies examining the binding of

Figure 4-1. Structures of warfarin and L-tryptophan.

Warfarin

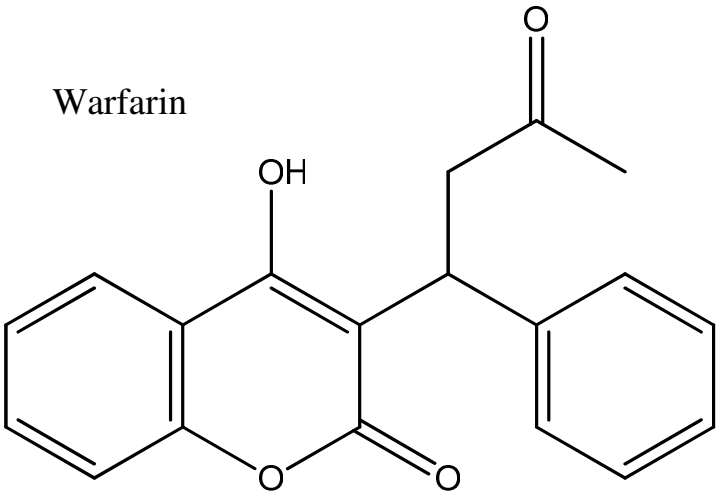

L-tryptophan

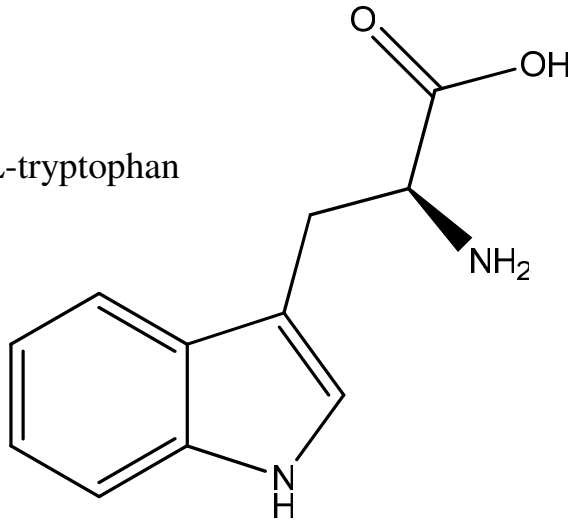

warfarin with glycated HSA have resulted in apparently conflicting results, in which some authors have reported an increase in binding while others reported a decrease.[2, 5] Previous work with L-tryptophan and glycated HSA have suggested that there may be a fluctuation in the binding constants for this interaction at 4ºC when increasing levels of glycation are present in HSA.[19] Thus, there is still a need for a clearer understanding of how glycation affects the binding of both warfarin and L-tryptophan with HSA, especially under physiological conditions (i.e., 37°C and pH 7.4).

The goal of this current study was to obtain binding information on these probe compounds by using high-performance affinity chromatography (HPAC). HPAC is a chromatographic technique that can make use of an immobilized protein (e.g., HSA) to provide a precise, reproducible, and convenient means of examining drug-protein binding, while also being capable of automation.[20] This approach has been utilized successfully in the past to obtain drug-protein binding data on interactions of both warfarin and L-tryptophan with normal HSA.[21-24] This current report employed HPAC to also examine the interactions of these solutes with *in vitro* glycated HSA. This was accomplished by preparing HPAC columns that contained HSA with various known levels of glycation. The binding parameters that were found with warfarin and L-tryptophan on these columns were then compared to those noted with normal HSA. Knowledge of how these interactions are affected by glycation should be valuable in future work that uses warfarin or L-tryptophan as probes to examine the binding of other drugs of solutes with glycated HSA. This information, in turn, could be important in the future in obtaining a better picture of how such compounds bind to serum proteins such

as HSA during diabetes and in how these interactions affect properties such as the metabolism, excretion and distribution of these drugs in this disease state.

Experimental

Reagents

Racemic warfarin (98% pure), L-tryptophan (98%), monobasic and dibasic potassium phosphate salts, D-(+)-glucose (99.5%), sodium azide (>95%), acetohexamide, sodium chloride, sodium nitrate, sodium phosphate salts, HSA (essentially fatty acid free albumin from human serum, ≥ 96%), and *in vitro* glycated HSA used to make the gHSA1 column (Lot 058K6087) were purchased from Sigma-Aldrich (St. Louis, MO, USA). Reagents used in the bicinchoninic acid (BCA) protein assay were from Pierce (Rockford, IL, USA). Nucleosil Si-300 silica (300 Å pore size, 7 micron particle diameter) was obtained from Macherey-Nagel (Düren, Germany). The enzymatic assay kits for fructosamine were from Diazyme Laboratories (San Diego, CA, USA). Sterilized 17 x 100 mm culture tubes were purchased from Fisher Scientific (Pittsburg, PA, USA). Slide-A-Lyzer 7K dialysis cassettes (7 kDa MW cutoff; 0.5-3, 3-12, and 12-30 ml sample volume) were acquired from Thermo Scientific (Rockford, IL, USA). Econo-Pac 10 DG disposable chromatography desalting columns were purchased from Bio-Rad Laboratories (Hercules, CA, USA). Solutions were made using water from a Nanopure system (Barnstead, Dubuque, IA, USA) and filtered with a 0.20 µm GNWP nylon membrane from Millipore (Billerica, MA, USA).

Apparatus

The chromatographic system consisted of a Jasco DG-2080-53 three-solvent degasser (Tokyo, Japan), two Jasco PU-2080 isocratic HPLC pumps, a Rheodyne Advantage PF six-port valve (Cotati, CA, USA), a Jasco AS-2055 autosampler, a Jasco CO-2060 column oven (i.e., to maintain a column temperature of 37 °C), and a Jasco UV-2075 UV/Vis detector. This chromatographic system hardware was controlled through EZChrom Elite software v3.2.1 (Agilent, CA, USA) and a Jasco LC Net component. The chromatographic data were analyzed using in-house programs written using Labview 5.1 software (National Instruments, Austin, TX, USA) or using Peakfit 4.12 (Jandel Scientific Software, San Rafael, CA, USA). Linear regression was performed using Excel 2003 (Microsoft Corporation, Redmond, WA, USA) and non-linear regression was performed using DataFit (Oakdale Engineering, PA, USA).

Methods

Studies were performed using three different glycated HSA samples. The first of which was purchased from a commercial source (Sigma-Aldrich), and the other two glycated HSA samples were made *in vitro* using a modified version of previously published methods.[21, 22] To perform *in vitro* glycation of the HSA samples, all glassware and spatulas that would come in contact with the glycated HSA solution were previously sterilized by autoclaving to prevent bacterial growth during the preparation of the glycated HSA. One liter of pH 7.4, 0.2 M potassium phosphate buffer was prepared and also sterilized by autoclaving to minimize bacterial growth during this process. Sodium azide (i.e., a strong antibacterial agent) was added to this buffer once it had cooled to

make a 1 mM solution of this agent. A 15 mM glucose solution was prepared using this sterilized sodium azide solution and 20 ml of this solution was then used to dissolve 840 mg of HSA to give a working solution with an HSA concentration of 42 g/L. This concentration of HSA was within the typical range (40-45 g/L) seen in humans under normal physiological conditions.[4, 23, 24]

This HSA solution was placed into a series of sterile culture tubes as 3-4 ml fractions, covered with the culture tube cap, further sealed with parafilm, and incubated in a water bath at 37 °C for four weeks.[21] After this incubation period, each glycated HSA solution was passed through a size-exclusion desalting column to separate the protein from any excess glucose and sodium azide in the solution. The collected protein fraction was dialyzed against water to remove any remaining glucose and buffer salts. The water used during dialysis was 200-500 times the volume of the sample. The sample was placed into a sterile dialysis cassette and allowed to dialyze for 2 h at room temperature, with gentle stirring using a magnetic stir bar. The water was then changed and the sample was dialyzed against water again for another 2 h under the same conditions. The water was changed one last time and the sample was allowed to dialyze, without stirring, at 4 °C overnight for approximately 14-18 h. The final samples were stored at -80 °C. Lyophilization was performed until samples were completely dry. Samples were again stored at -80 °C until use. This procedure was performed once for each HSA sample. The first time this procedure was carried out, the levels of glucose were kept around physiological levels. However, the second time a greater level of glycation was desired so the glucose concentration was increased to ~30 mM to increase glycation levels.

A commercial fructosamine assay from Diazyme was modified for use in determining the overall level of glycation of each batch of HSA that was used in this study. A 0.85% (w/v) saline solution was first prepared by dissolving 0.85 g sodium chloride in 100 ml of water. A pH 7.4, 0.025 M sodium phosphate buffer was also prepared. Although normal HSA concentrations in serum are around ~40 g/L, an HSA sample solution of ~20 g/L was prepared to stay within the linear range of the assay (i.e., 30-1354 μmol/L or 2-90 g/L). Each sample of glycated HSA for this assay was prepared by weighing out roughly 10 mg of this protein and adding 500 μL of pH 7.4, 0.025 M sodium phosphate buffer, followed by the solution then being placed on a vortex mixer for a short period of time. A temperature-controlled UV/vis spectrometer was used to perform the assay with the temperature held at 37 °C for the entire duration. A 300 μL portion of Reagent 1 from the kit was added to an empty cuvette. A 30 μL portion of the sample was then added, the resulting solution was mixed quickly, and placed into the spectrometer, with absorbance measurements being taken after 5 min at 600 and 700 nm. A 75 μL portion of Reagent 2 from the kit was then added to the cuvette and mixed quickly with the other contents, with this mixture then being allowed to react for 5 min before measurements were again taken at 600 and 700 nm. Each sample was run in duplicate or triplicate. A 0.85% (w/v) saline solution was used as a blank to subtract out the background while calibration standards and a control were measured during this assay; this procedure was repeated several times using these solutions in place of a 30 μL sample. The difference in the absorbance readings at 600 nm and 700 nm was calculated at each time, and the difference in the resulting values for the first and second 5 min readings was then also found. A calibration curve was made per the manufacturer's

instructions using a calibration standard included with the kit. This gave a plot that was used to find the μmol of fructosamine (i.e., a value equivalent to μmol hexose) in each protein sample.

Nucleosil Si-300 silica was used to prepare diol-bonded silica according to a previously published procedure.[25] Glycated HSA was immobilized to the resulting support by using the Schiff-base method, as previously discussed for normal HSA; and a control support was made in the same manner but with no glycated HSA being added during the immobilization step.[26] A BCA assay was performed in triplicate to determining the content of each support, using soluble glycated HSA as the standard and the control support as the blank. The protein content of gHSA 1, 2, and 3 samples were found by this method to be 29 (± 4), 47 (± 8), and 40 (± 3) mg HSA/g silica, respectively (see Table 4-1). Each glycated HSA silica sample was downward slurry-packed into a separate 2.0 cm x 2.1 mm I.D. columns at 3500 psi (24.1 MPa) using pH 7.4, 0.067 M potassium phosphate buffer as the packing solution. A column with the same dimensions but packed with the control support was also prepared. All columns were stored at 4 °C in pH 7.4, 0.067 M potassium phosphate buffer and were used over the course of one year and for fewer than 500 sample applications or injections per column. HSA columns have been shown in previous studies to retain good stability for drug-protein binding studies under such conditions.[27]

The warfarin, L-tryptophan and all other sample solutions for the chromatographic studies were prepared in pH 7.4, 0.067 M potassium phosphate buffer. The same pH 7.4, 0.067 M potassium phosphate buffer was used for application and elution in the chromatographic studies. All solutions were filtered through a 0.2 μm

nylon filter and degassed under vacuum for at least 15 min prior to use. Solutions of L-tryptophan have been found to decrease in stability over 2-9 days (depending on storage conditions),[16] so for this work the L-tryptophan solutions were made fresh daily prior to use. Racemic warfarin has been shown to have a slow structural conversion over time from its minor cyclic hemiketal to its major cyclic hemiketal.[28] When stored at 5 °C, a 5% conversion occurs in 45-52 hours whereas 95% conversion occurs between 109-127 days. Warfarin solutions were stored at 4 °C and used within 10 days for these experiments. All chromatographic experiments described in this report were performed at 37.0 (± 0.1) °C. Wavelengths of 308 and 280 nm were used to detect *R*-warfarin and L-tryptophan, respectively, while sodium nitrate (i.e., a non-retained solute) was monitored at 205 nm.

The competition studies described later in this report were conducted by using zonal elution on the columns containing normal HSA or glycated HSA. These studies were conducted using varying concentrations of acetohexamide (0-20 μM) in the mobile phase while 20 μL of *R*-warfarin or L-tryptophan were injected on to the column at a concentration of 5 μM. These studies were performed for the HSA or gHSA columns and corresponding control columns. Sodium nitrate was used to determine the void time of the columns and the system by injecting 20 μL of 20 μM sodium nitrate onto each column and injecting it onto the system with a zero-volume union. A pH 7.4, 0.067 M potassium phosphate buffer was used to make all solutions. PeakFit v.4.12 and an exponentially-modified Gaussian curve fit were used to determine the central moments of the eluting peaks.

All frontal analysis experiments were carried out at 0.5 ml/min. This flow rate has been shown in similar studies to obtain reproducible binding capacities with the given analytes and on columns containing normal HSA.[29, 30] The concentrations for the applied analyte solutions ranged from 1 and 10 μM. A six-port injection valve was used to switch between the mobile phases (i.e. sample application and elution/column regeneration). The column was first equilibrated using pH 7.4, 0.067 M potassium phosphate buffer. When performing the frontal analysis experiments, the six-port valve was programmed to switch from this buffer to the given analyte solution after one minute from time zero to ensure an initial steady baseline for data analysis. Once the analyte had fully saturated the column and a breakthrough curve had been obtained, the six-port valve was switched back to the original pH 7.4 phosphate buffer to wash the retained analyte from the column and re-equilibrate the column before the next run. All experiments were performed at each analyte concentration on both the glycated HSA columns and the control column. The resulting breakthrough curves were analyzed using by Labview 5.1 or Peakfit v.4.12 and were corrected for non-specific binding by the analytes to the support by subtracting control column data from data for the glycated HSA columns.

Results and Discussion

Preparation and Initial Studies of Glycated HSA

The *in vitro* glycated HSA used to make the gHSA1 column was determined to have 1.31 (± 0.05) mol hexose/mol HSA according to a fructosamine assay (see Table 4-1). The *in vitro* glycated HSA used to make the gHSA2 column had a glycation level of 2.34 (± 0.13) mol hexose/mol HSA, and the glycated HSA used to make the gHSA3

Table 4-1. Protein content and level of glycation of HSA supporsts

	gHSA1	**gHSA2**	**gHSA3**
Protein Content of the Column (mg HSA/g silica)	29 (± 4)	47 (± 8)	40 (± 3)
mol Hexose per mol HSA	1.31 (± 0.05)	2.34 (± 0.13)	3.35 (± 0.14)

Reported errors represent ± 1 S.D.

column contained 3.35 (± 0.14) mol hexose/mol HSA. Separate protein assays indicated that the amount of glycated HSA for all of these samples was comparable to that typically seen for normal HSA.[17, 28] The protein content of the columns ranged from 29 to 47 mg protein/g silica, or roughly 440 to 710 nmol glycated HSA/g silica.

Preliminary competition studies were first conducted with these supports using the method of zonal elution. In these studies, similar retention factors (when corrected for differences in column protein content) were noted to be present for *R*-warfarin and L-tryptophan in the absence of any competing agents. An example of such a study is shown in Figure 4-2 for columns containing HSA or glycated HSA. In this type of study, the retention of these site-selective probe compounds was being examined while varying the concentration of a mobile phase additive and possible competing agent (i.e., acetohexamide, in this case). In this type of experiment, Equation 4-1 describes the predicted change in retention of the injected analyte (A) if it has competition at a single type of site on an immobilized ligand with the competing agent (I).

$$\frac{1}{k} = \frac{K_{aI} V_M [\mathrm{I}]}{K_{aA} m_L} + \frac{V_M}{K_{aA} m_L} \qquad (4\text{-}1)$$

In this equation, the retention factor (k) is determined by using the retention time of the analyte (t_R) and the void time of the system (t_M), where $k = (t_R - t_M)/t_M$. K_{aA} and K_{aI} are the association equilibrium constants for the analyte and the competing agent, respectively, at their site of competition on the immobilized ligand and V_M is the void volume. If direct competition is present between A and I at a single type of binding site, a plot of $1/k$ versus [I] should be linear, as occurs for the plots in Figure 4-2. In addition, the value of k at the intercept will be directly related to the equilibrium constant and

Figure 4-2. (a) Competition studies for the injection of *R*-warfarin onto gHSA1 column with acetohexamide solutions in the mobile phase. Acetohexamide concentrations from left to right: 20, 15, 10, 5, and 1 μM. *R*-warfarin injections were 5 μM and the injection volume was 20 μL. (b) Plots of 1/*k* vs. [Acetohexamide] while injecting R-warfarin on to a normal HSA column (●) and gHSA1 column (■). The best-fit line for the normal HSA column was determined to be $y = 779\ (\pm 51)\ x + 0.0184\ (\pm 0.0006)$, r = 0.991. The equation for the glycated HSA column was calculated to be $y = 1075\ (\pm 72)\ x + 0.0183\ (\pm 0.0008)$, r = 0.991.

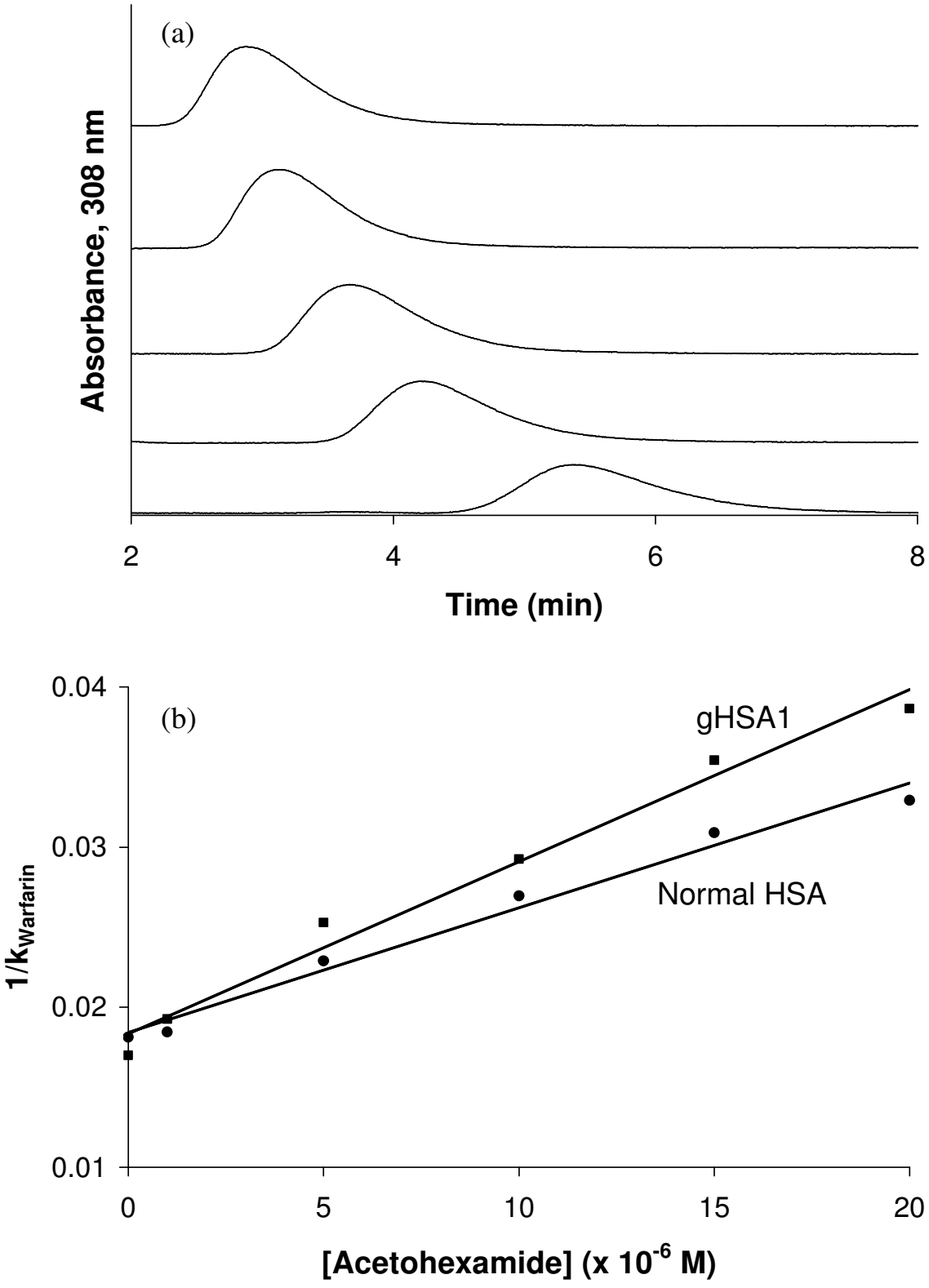
(a)
Absorbance, 308 nm
2
4
6
8
Time (min)
(b)
gHSA1
Normal HSA
0.04
0.03
0.02
0.01
1/k Warfarin
0
5
10
15
20
[Acetohexamide] (x 10-6 M)

relative activity of the immobilized ligand for the injected analyte (i.e., at [I] = 0, $1/k = V_M/\{K_{aA}\, m_L\}$ or $k = K_{aA}\, m_L/V_M$).

The similarities of the retention factors noted when [I] = 0 in plots such as Figure 4-2 for the normal HSA and glycated HSA columns suggested that warfarin and L-tryptophan (data not shown) had relatively consistent binding to Sudlow sites I and II, respectively. This appeared to be the case even though the competition of these probes with drugs like acetohexamide did create a change in the response of these plots. Additional studies based on frontal analysis were next undertaken (see following sections) to further examine the interactions of warfarin and L-tryptophan with these columns prior to more in depth studies using these compounds as probes in competition studies with additional drugs on glycated HSA.

Binding of Warfarin to Glycated HSA

Frontal analysis studies were performed to obtain a more detailed analysis of the binding parameters for glycated HSA with warfarin. This method is performed by continuously applying a solution with a known amount of analyte to a column with an immobilized ligand. As the analyte binds to the ligand, the column becomes saturated and a characteristic breakthrough curve is formed (Figure 4-3). A breakthrough time can be calculated when the area under the first half of the curve equals the area above the second half of the curve.[20] The middle point represents the breakthrough time. When fast association/dissociation kinetics are present, the breakthrough time can be related to the concentration of the analyte [A], the association equilibrium constant for the analyte-ligand system (K_a), and the moles of active binding sites on the column for the analyte

(m_L). The following equations show this relationship for a system where there is a single type of binding site on the ligand for the analyte (single-site model),[20]

$$m_{Lapp} = \frac{m_L K_a [\mathrm{A}]}{(1 + K_a [\mathrm{A}])} \tag{4-2}$$

$$\frac{1}{m_{Lapp}} = \frac{1}{(K_a m_L [\mathrm{A}])} + \frac{1}{m_L} \tag{4-3}$$

in which m_{Lapp} is the apparent moles of analyte that are required to reach the mean position of the breakthrough curve at any given concentration of applied analyte and [A] is the molar concentration of the applied analyte. Equation 4-3 would be expected to produce a linear relationship for a 1:1 binding model when a plot is made of $1/m_{Lapp}$ versus 1/[A], while a non-linear fit and a plot of m_{Lapp} versus [A] would be used when applying Equation 4-2 to the same data. Either type of fit make it possible to determine K_a and m_L simultaneously for the interaction, which can be used to provide information on how a change in the ligand might affect its affinity or relative activity for the applied analyte.[31] In this current study, this approach was used to monitor any changes that occurred in binding as the degree of glycation was varied for HSA.

Some typical frontal analysis results that were obtained for warfarin on the glycated HSA columns are shown in Figures 4-3 and 4-4. In each case, warfarin produced breakthrough curves that shifted to shorter breakthrough times as the concentration of the applied analyte was increased (see Figure 4-3). The data obtained from these breakthrough curves were then analyzed according to Equation 4-3. Some typical results are shown in Figure 4-4. It was found for each of the glycated HSA columns that there was good agreement with the linear behavior predicted by Equation 4-3 at the concentration range which was examined in this study. The correlation

Figure 4-3. Breakthrough curves for warfarin at applied concentrations 10, 5, 2.5, 1.5, and 1 μM (from left to right) on the gHSA1 column. Conditions for these studies are given in the text.

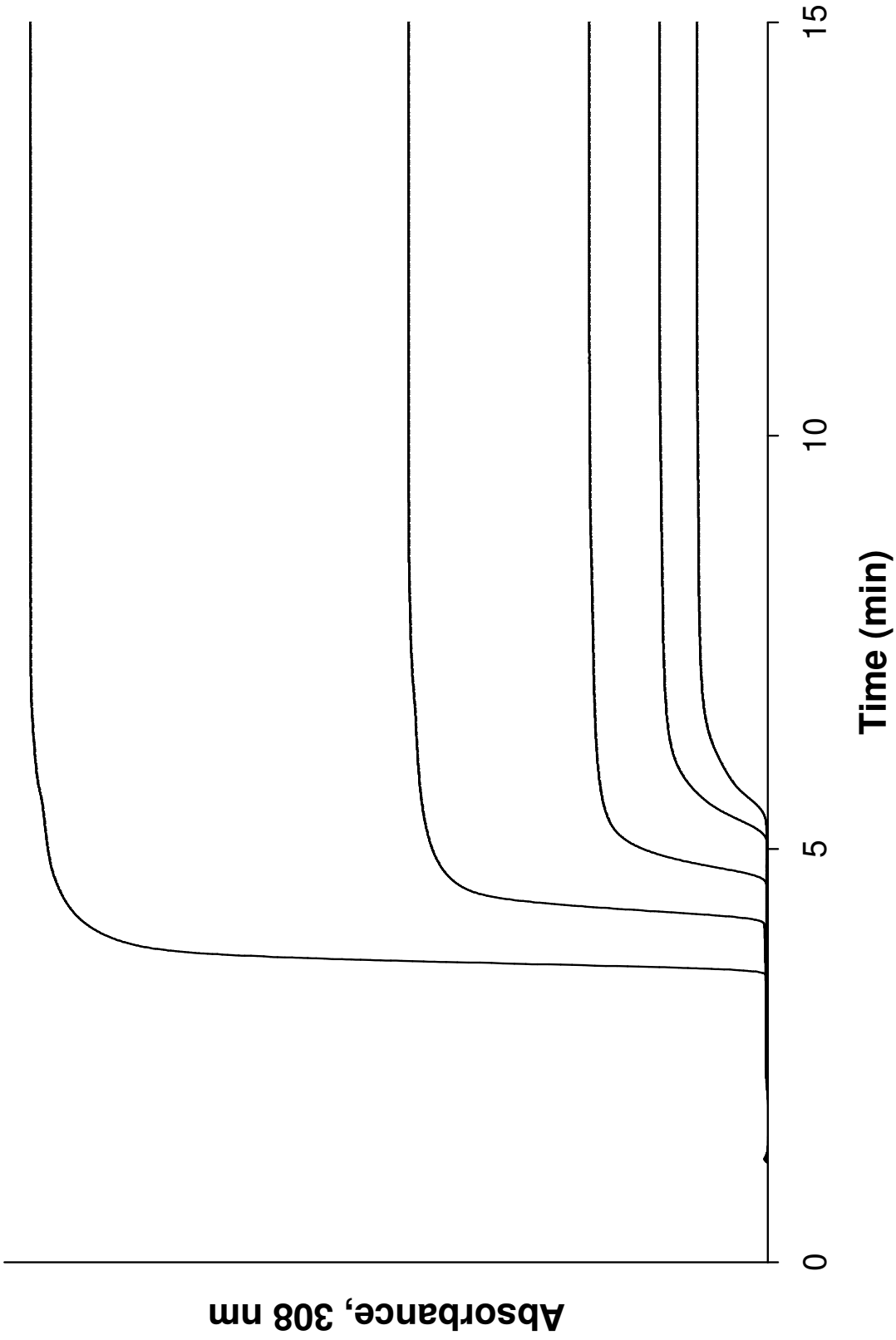
Absorbance, 308 nm
0
5
10
15
Time (min)

Figure 4-4. Double reciprocal plots of warfarin binding to affinity columns containing glycated HSA for the gHSA1 column (▲), gHSA2 column (■), and gHSA3 column (●). The solid line shows the best-fit line for each data set. The error bars represent a range of ± 1 S.D. The best-fit line for the gHSA1 column was determined to be y = 424 (± 15) x + [9.62 (± 0.87)] x 10^7, r = 0.998. The best-fit line for the gHSA2 column was determined to be y = 270 (± 10) x + [6.10 (± 0.56)] x 10^7, r = 0.998. The best-fit line for the gHSA3 column was determined to be y = 287 (± 13) x + [7.80 (± 0.77)] x 10^7, r = 0.997.

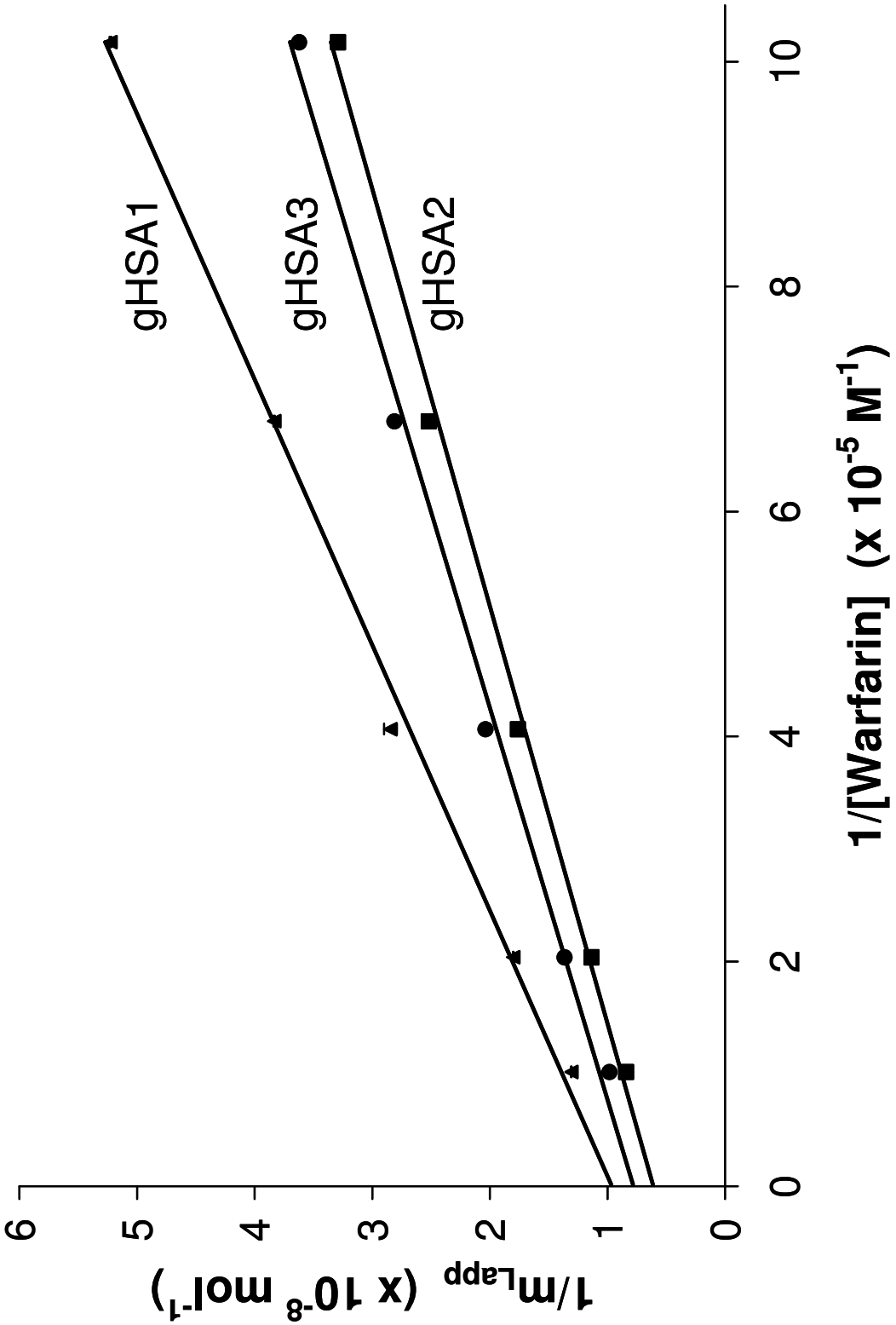
gHSA1
gHSA3
gHSA2
0
2
4
6
8
10
0
1
2
3
4
5
6
1/[Warfarin] (x 10-5 M-1)
1/mLapp (x 10-8 mol-1)

coefficients ranged from 0.997 to 0.998 (n = 5), with only random variations generally being noted in each of the plots about the best-fit line (Note: a small amount of curvature may have been present in the results for the gHSA3 column, but using a higher-order fit such as a two-site model did not give any further improvement in the quality of the overall fit to this set of results). Similar agreement between the data and a one-site binding model was obtained when fitting a plot of m_{Lapp} versus [A] according to Equation 4-2, as demonstrated in Figure 4-5.

Table 4-2 summarizes the association equilibrium constants that were obtained when plotting the data according to Equation 4-3 and using a single-site model. These values ranged from 2.3 x 10^5 M^{-1} to 2.7 x 10^5 M^{-1}, and had relative precisions of ± 9-10%. These results did not show any significant variations between the various glycated HSA columns that were examined in this study, with all K_a values agreeing within 17-20% and within ± 2 S.D. of any other K_a value for warfarin in this same data set. This range of values also agreed within an average association equilibrium constant of 2.35 x 10^5 M^{-1} that was determined based on previous results reported for the separate *R*- and *S*-enantiomers of warfarin on a similar column that contained normal HSA and using the same method of data analysis.[29] These results indicated that glycation did not have any observable effect on the average K_a that was measured for *R/S*-warfarin on these columns as the level of glycation of HSA was increased up to the level present in the gHSA column (i.e., 3.35 mol hexose/mol HSA, as shown in Table 4-1).

It was also possible from the results in Figure 4-4 to determine the binding capacity of each affinity column for warfarin. This information could then be combined with the known protein content to obtain the specific activity of each type of HSA for the

Figure 4-5. Plot of m_{Lapp} vs. [warfarin] using Equation 4-2 for the gHSA1 column (▲), gHSA2 column (■), and gHSA3 column (●). The best-fit line for the gHSA1 column was determined to be: $y = [\{1.81\ (\pm\ 0.15)\} \times 10^5 \times \{1.19\ (\pm\ 0.05) \times 10^{-8}\ x]\ /[1 + \{1.81\ (\pm\ 0.15)\} \times 10^5\ x]$, $r = 0.999$. The best-fit line for the gHSA2 column was determined to be: $y = [\{1.89\ (\pm\ 0.09)\} \times 10^5 \times \{1.83\ (\pm\ 0.05) \times 10^{-8}\ x]\ /[1 + \{1.89\ (\pm\ 0.09)\} \times 10^5\ x]$, $r = 0.999$. The best-fit line for the gHSA3 column was determined to be: $y = [\{2.01\ (\pm\ 0.20)\} \times 10^5 \times \{1.52\ (\pm\ 0.05) \times 10^{-8}\ x]\ /[1 + \{2.01\ (\pm\ 0.20)\} \times 10^5\ x]$, $r = 0.998$.

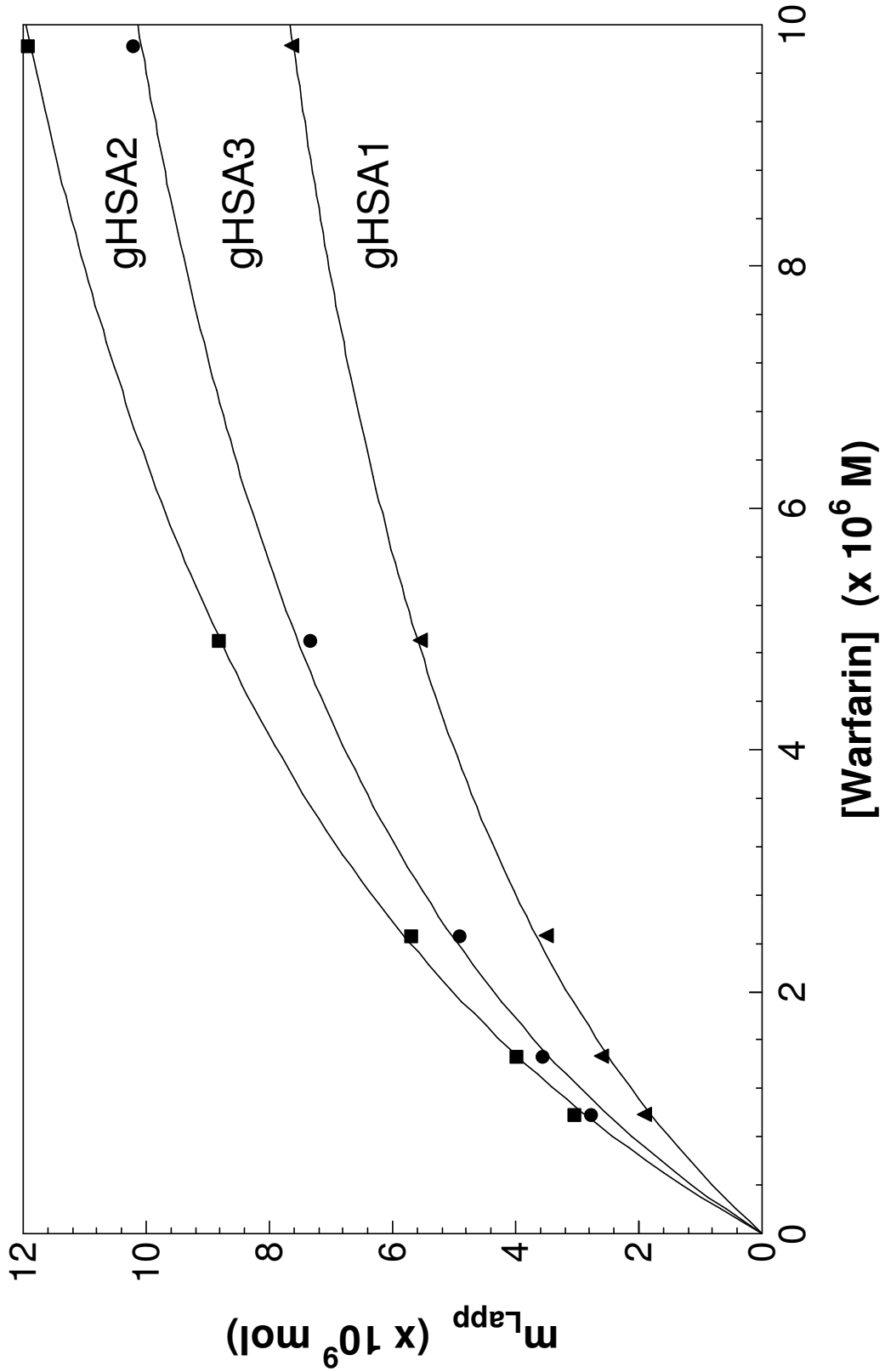
gHSA2
gHSA3
gHSA1
m_{Lapp} (x 10^9 mol)
[Warfarin] (x 10^6 M)
0
2
4
6
8
10
12

Table 4-2. Calculated binding constants for warfarin and L-tryptophan on each of the glycated HSA columns

Racemic Warfarin ***(Values using Eqn 4-3)***	**HSA**	**gHSA1**	**gHSA2**	**gHSA3**
K_a (x 10^5 M^{-1})	2.35 (± 0.35)[a]	2.27 (± 0.22)	2.26 (± 0.22)	2.72 (± 0.29)
m_L (x 10^{-8} mol)	1.29 (± 0.13)	1.04 (± 0.09)	1.64 (± 0.15)	1.28 (± 0.13)
Activity (%)	73 (± 9)	76 (± 12)	74 (± 14)	68 (± 9)
L-Tryptophan ***(Values using Eqn 4-3)***				
K_a (x 10^4 M^{-1})	1.1 (± 0.3)[b]	5.18 (± 0.92)	6.36 (± 1.66)	5.67 (± 0.54)
m_L (x 10^{-9} mol)	NA	5.0 (± 0.9)	6.7 (± 1.8)	5.8 (± 0.6)
Activity (%)	NA	36 (± 8)	30 (± 5)	31 (± 4)

[a] Value from Ref. 29.

[b] Value from Ref. 30; NA, not available.

All reported errors represent ± 1 S.D.

applied analyte. These results are also summarized in Table 4-2. When the binding capacities were normalized for the protein content, it was found that comparable specific activities were present on each of the columns for warfarin. These values ranged from 68 to 76% with the activities decreasing slightly with increasing levels of glycation. The precision of these measurements were ±12-19% of the reported activities while the activities were within 11% of one another. Although an initial decrease of activity was noted as glycation levels were increased, overall precision of these values reveal them to be comparable to each other. Calculations performed for the normal HSA column using the data collected from the competition studies between *R*-warfarin and acetohexamide and Equation 4-1 also shows an activity of 73 (± 9)% which is also well within the range of the measurements determined for the glycated HSA columns. Therefore, there does not seem to be a significant change in the binding constant or the activity as the level of glycation is increased.

Binding of L-Tryptophan to Glycated HSA

Similar frontal analysis studies were also done for L-tryptophan to examine the binding of this compound to Sudlow site II as glycation levels were increased. Frontal analysis studies were again performed at low concentrations of L-tryptophan because low concentrations offer only single-site binding to HSA. All columns produced characteristic breakthrough curves for L-tryptophan binding. The data were fit to Equation 4-2 with linear results obtained on all three glycated HSA columns and correlation coefficients of 0.999 (n = 5) for all data. These data also produced residual plots with random variation.

Table 4-2 again summarizes association constants and activities calculated for L-tryptophan binding to glycated HSA. Association constants for this compound ranged from 5.18 10^4 M^{-1} to 6.36 x 10^4 M^{-1} with precisions of ±9-26% (Figure 4-6). These results did not show any significant variations between the columns and were within 2 S.D.s of one another. These values did appear 5-6 times higher than the reported value for normal HSA determined using a similar column.[30] Studies done by Okabe and Hashizume also found that the binding of low concentrations of flufenamic acid, a compound that binds to site II, also increased its binding to glycated HSA.[32] However, they also found that the site II-ligands dansylproline and ibuprofen decreased in binding due to the glycation of HSA compared to non-glycated HSA. Nakajou et. al. also saw a decrease in binding of dansylsarcosine to glycated HSA.[2] Bohney and Feldhoff found no binding changes in L-tryptophan with increased levels of glycation on HSA[33] while Barzegar, et. al. reported a decrease followed by an increase of the binding constant as glycation increases.[19] It is possible that differences in experimental conditions led to variations in results. Also, although major glycation sites are close in proximity to Sudlow site I, no major glycation sites have been noted to be close to Sudlow site II. It is probable that the conformational changes that occur when HSA undergoes glycation affect the binding at site II. These changes could lead to differences in the binding of site specific compounds depending on how they bind in the binding pocket of that site. This was also suggested by Barzegar, et. al. who proposed that a small amount of glycation induces a change in the tertiary structure of HSA causing local unfolding of the protein around the binding site while higher levels of glycation are able to stabilize the protein structure in order to facilitate binding again.[19]

Figure 4-6. Double reciprocal plots of L-tryptophan binding to affinity columns containing glycated HSA. These results are for the gHSA1 column (▲), gHSA2 column (■), and gHSA3 column (●). The solid line shows the best-fit line for each data set. The error bars represent a range of ± 1 S.D. The best-fit line for the gHSA1 column was determined to be $y = [3.89 (\pm 0.06)] \times 10^3 x + [2.02 (\pm 0.36)] \times 10^8$, $r = 0.999$. The best-fit line for the gHSA2 column was determined to be $y = [2.34 (\pm 0.07)] \times 10^3 x + [1.49 (\pm 0.39)] \times 10^8$, $r = 0.999$. The best-fit line for the gHSA3 column was determined to be $y = [3.04 (\pm 0.04)] \times 10^3 x + [1.72 (\pm 0.16)] \times 10^8$, $r = 0.999$.

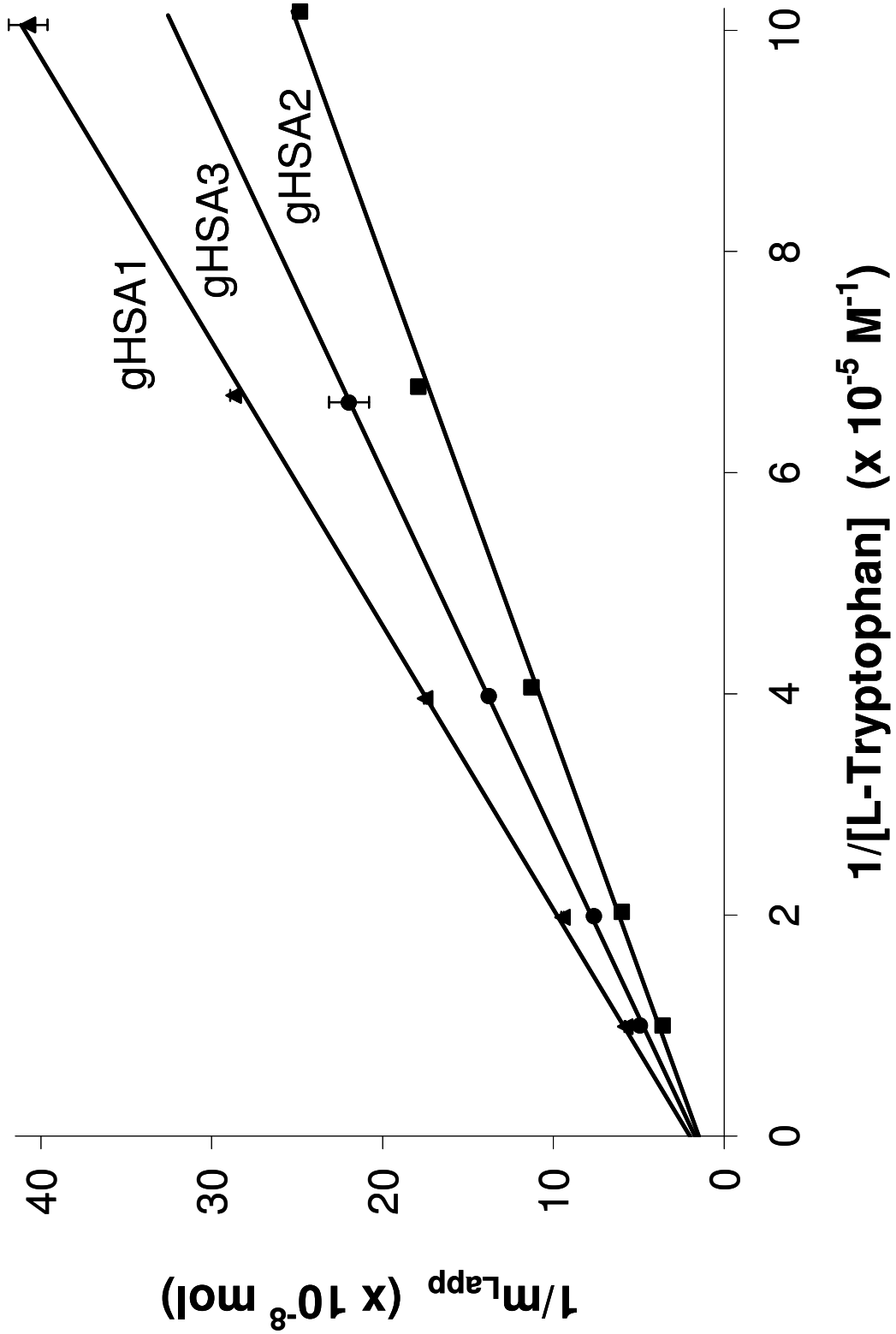
gHSA1
gHSA3
gHSA2
0
10
20
30
40
0
2
4
6
8
10
1/[L-Tryptophan] (x 10-5 M-1)
1/mLapp (x 10-8 mol)

The binding capacity and the protein content were used to determine the activity of L-tryptophan on each glycated HSA column. These values have also been summarized in Table 4-2. When the binding capacities had been normalized for the amount of protein on the column, the activities of L-tryptophan were comparable between the columns. The activities ranged from 30.5 to 36.5% with precisions of ±12-22%. The highest and the lowest values differed from each other by approximately 16% but were within 1 S.D. Although an initial decrease in activity appeared to be apparent, the precisions of these values show that they are statistically comparable at the 95% confidence level.

Conclusion

Uncontrolled diabetes increases blood sugar levels which facilitates a boost in the level of glycation that blood proteins undergo. This increase in glycation can potentially alter the binding of drugs to the protein thereby changing the transport of the drug around the body. These studies examined the binding of two drugs to the two major binding sites on HSA, Sudlow sites I and II. As glycation levels are increased, the association equilibrium constants of warfarin remain constant while the percent of bound drug decreases as glycation increases. However, when taking into account the standard errors associated with the activities, the values are in fact comparable. The association equilibrium constants for L-tryptophan appear to increase slightly but then return to normal as glycation levels are increased. Yet again, when taking into account the standard errors associated with the binding constants, the binding constants remain the same as glycation increases. L-Tryptophan also shows similar activities for the protein as

the levels of glycation are increased, with no appreciable difference in either the binding constants or the activity with glycation but higher binding constants for glycated HSA than for normal HSA. In general, both probe compounds show steady association equilibrium constants when glycation levels were increased and overall activities that were comparable when taking into account the standard errors for these values. These findings are important when determining drug binding to Sudlow sites I and II because it can help to identify the cause behind a change in binding to these sites. HPLC using the method of frontal analysis is a useful tool to examine these binding changes because it can differentiate between the two factors, K_a and m_L, that attribute to the binding of compounds to HSA using only one type of experiment.

References

1. National Diabetes Fact Sheet: General Information and National Estimates on Diabetes in the United States, 2007. U.S. Department of Health and Human Services, Centers for Disease Control and Prevention: Atlanta, GA, 2008.
2. Nakajou, K.; Watanabe, H.; Kragh-Hansen, U.; Maruyama, T.; Otagiri, M., *Biochim. Biophys. Acta* **2003,** *1623*, 88-97.
3. Mendez, D. L.; Jensen, R. A.; McElroy, L. A.; Pena, J. M.; Esquerra, R. M., *Arch. Biochem. Biophys.* **2005,** *444*, 92-99.
4. Colmenarejo, G., *Med. Res. Rev.* **2003,** *23* (3), 275-301.
5. Fitzpatrick, G.; Duggan, P. F., *Biochem. Soc. Trans.* **1987,** *15* (2), 267-268.
6. Garlick, R. L.; Mazer, J. S., *J. Biol. Chem.* **1983,** *258* (10), 6142-6146.
7. Marashi, S.-A.; Safarian, S.; Moosavi-Movahedi, A. A., *Med. Hypotheses* **2005,** *64* (4), 881.
8. Lapolla, A.; Fedele, D.; Seraglia, R.; Traldi, P., *Mass Spectrom. Rev.* **2006,** *25*, 775-797.
9. Ascoli, G. A.; Domenici, E.; Bertucci, C., *Chirality* **2006,** *18*, 667-679.
10. Dockal, M.; Carter, D. C.; Ruker, F., *J. Biol. Chem.* **1999,** *274* (41), 29303-29310.
11. Herve, F.; Urien, S.; Albengres, E.; Duche, J.-C.; Tillement, J.-P., *Clin. Pharmacokinet.* **1994,** *26* (1), 44-58.
12. Sudlow, G.; Birkett, D. J.; Wade, D. N., *Mol. Pharmacol.* **1975,** *11*, 824-832.
13. Sudlow, G.; Birkett, D. J.; Wade, D. N., *Mol. Pharmacol.* **1976,** *12*, 1052-1061.
14. Sengupta, A.; Hage, D. S., *Anal. Chem.* **1999,** *71*, 3824-3827.

15. Bertucci, C.; Andrisano, V.; Gotti, R.; Cavrini, V., *J. Chromatogr. B* **2002,** *768*, 147-155.

16. Conrad, M. L.; Moser, A. C.; Hage, D. S., *J. Sep. Sci.* **2009,** *32*, 1145-1155.

17. Joseph, K. S.; Moser, A. C.; Basiaga, S.; Schiel, J. E.; Hage, D. S., *J. Chromatogr. A* **2009,** *1216* 3492-3500.

18. Koyama, H.; Sugioka, N.; Uno, A.; Mori, S.; Nakajima, K., *Biopharm. Drug Dispos.* **1997,** *18* (9), 791-801.

19. Barzegar, A.; Moosavi-Movahedi, A. A.; Sattarahmady, N.; Hosseinpour-Faizi, M. A.; Aminbakhsh, M.; Ahmad, F.; Saboury, A. A.; Ganjali, M. R.; Norouzi, P., *Protein Peptide Lett.* **2007,** *14*, 13-18.

20. Hage, D. S., *J. Chromatogr. B* **2002,** *768*, 3-30.

21. Lapolla, A.; Fedele, D.; Reitano, R.; Arico, N. C.; Seraglia, R.; Traldi, P.; Marotta, E.; Tonani, R., *J. Am. Soc. Mass Spectrom.* **2004,** *15*, 496-509.

22. Ney, K. A.; Colley, K. J.; Pizzo, S. V., *Anal. Biochem.* **1981,** *118*, 294-300.

23. Fasano, M.; Curry, S.; Terreno, E.; Galliano, M.; Fanali, G.; Narciso, P.; Notari, S.; Ascenzi, P., *IUBMB Life* **2005,** *57* (12), 787-796.

24. Ascenzi, P.; Bocedi, A.; Notari, S.; Fanali, G.; Fesce, R.; Fasano, M., *Mini-Rev. Med. Chem.* **2006,** *6*, 483-489.

25. Ruhn, P. F.; Garver, S.; Hage, D. S., *J. Chromatogr. A* **1994,** *669* (1-2), 9-19.

26. Joseph, K. S.; Moser, A. C.; Basiaga, S.; Schiel, J. E.; Hage, D. S., *J. Chromatogr. A* **2008,** *submitted*.

27. Yang, J.; Hage, D. S., *J. Chromatogr. A* **1997,** *766*, 15-25.

28. Moser, A. C.; Kingsbury, C.; Hage, D. S., *J. Pharm. Biomed. Anal.* **2006,** *41*, 1101-1109.

29. Loun, B.; Hage, D. S., *Anal. Chem.* **1994,** *66* (21), 3814-3822.

30. Yang, J.; Hage, D. S., *J. Chromatogr.* **1993,** *645* (2), 241-250.

31. Chattopadhyay, A.; Tian, T.; Kortum, L.; Hage, D. S., *J. Chromatogr. B* **1998,** *715*, 183-190.

32. Okabe, N.; Hashizume, N., *Biol. Pharm. Bull.* **1994,** *17* (1), 16-21.

33. Bohney, J. P.; Feldhoff, R. C., *Biochem. Pharmacol.* **1992,** *43* (8), 1829-1834.

CHAPTER 5

THE BINDING OF SULFONYLUREAS TO GLYCATED HSA

Introduction

Human serum albumin (HSA) is the most abundant protein in human plasma. HSA is produced in the liver and exported as a single chain of 585 amino acids, reaching a serum concentration of ~40 g/L.[1-8] It is a globular protein made up of three homologous domains, I-III, each containing two subdomains, A and B.[3-7, 9] This protein is known to have two major binding sites for drugs (i.e., Sudlow sites I and II), which are found in subdomains IIA and IIIA, respectively.[10, 11] Sudlow site I, also known as the warfarin-azapropazone site, binds to bulky heterocyclic compounds such as coumarin compounds, sulfonamides, and salicylate.[3, 6, 8, 9] Sudlow site II, also known as the indole-benzodiazapine site, binds aromatic carboxylic acids and is known for binding profens such as ibuprofen and ketoprofen.[3, 6, 8, 9] HSA binds many endogenous and exogenous compounds, acting as the major transport protein for these compounds in the circulation.[8]

The binding of drugs to HSA can greatly affect the pharmacologic and pharmacokinetic properties of such drugs. This can influence the activity of a drug by altering the drug's free fraction in blood.[8, 12] It is commonly believed that this free fraction is the portion that interacts at receptor sites, allowing drug delivery and uptake by cells.[8, 13] The binding of drugs to HSA can be affected by competition for binding sites with co-administered drugs, fluctuations in endogenous compounds that bind to this protein, and post-translational modifications of HSA, such as glycation.[8, 14] Glycation occurs when a protein becomes non-enzymatically linked to sugar molecules. This

process is especially prevalent in diabetes, where blood sugar levels are elevated. The normal level of HSA glycation is around 6-13%, while a diabetic individual may have 20-30% of HSA glycated in the circulation.[1, 2, 8] Some of the primary glycation sites have been shown to be at or near Sudlow sites I and II, potentially creating interferences with drug-protein binding at these sites.[2, 15, 16]

Drugs such as sulfonylureas are often used to treat type II, or non-insulin dependent, diabetes. Sulfonylureas have been used since their discovery in 1942 in monotherapy and in combination therapy with other drugs to treat diabetes.[17-19] First-generation sulfonylureas include tolbutamide, chlorpropamide, acetohexamide, and tolazamide. These drugs are of particular interest in drug-binding studies because they are thought to be more easily displaced from HSA than their next-generation counterparts.[20] Displacement of these drugs could be particularly problematic due to their high degree of binding to HSA. For instance, tolbutamide is 90% bound to HSA at therapeutic levels and even a small change in the free fraction of this drug can lead to severe hypoglycemia.[8, 21]

This study used high-performance affinity chromatography (HPAC) to examine the binding of two first-generation sulfonylurea drugs, tolbutamide and acetohexamide, to HSA with various levels of glycation. Past studies using equilibrium gel filtration have found that the amount of sulfonylureas bound to glycated HSA decreases compared to binding of the same drugs with normal HSA.[22] Also, work with a fluorescence quenching method has shown that there is a decrease in the apparent binding constants of glycated HSA vs. normal HSA.[21] The benefits of using HPAC over these more traditional methods include the good precision and reproducibility of HPAC plus its small

sample requirements, and ease of automation. These current studies were performed to determine how the association equilibrium constants and binding capacities of sulfonylurea drugs on HSA were affected with increasing levels of glycation as determined by using frontal analysis.[23, 24] Zonal elution studies were also performed to examine the binding of these drugs at Sudlow sites I and II of HSA as the levels of glycation were increased. The knowledge gained from these studies should aid in the development of personalized medicine for patient drug therapy regiments in diabetes.

Theory

Frontal Analysis

The method of frontal analysis was used to determine the association equilibrium constant(s), K_a, and moles of binding sites, m_L, for acetohexamide and tolbutamide on glycated HSA. If fast association/dissociation kinetics are present in a drug-protein system, the resulting breakthrough curve can be related to K_a, m_L, and the concentration of the applied analyte, [A].[23] Examples of breakthrough curves that were obtained for acetohexamide in this study are shown in Figure 5-1. The following equations can be used to describe the response in this method for a drug with a single type of binding site on an immobilized protein:[23, 24]

$$\frac{1}{m_{Lapp}} = \frac{1}{(K_a m_L[\mathrm{A}])} + \frac{1}{m_L} \qquad (5\text{-}1)$$

or

$$m_{Lapp} = \frac{m_L K_a[\mathrm{A}]}{(1 + K_a[\mathrm{A}])} \qquad (5\text{-}2)$$

In the above equations, m_{Lapp} is the apparent moles of analyte required to saturate the column at a given concentration of applied analyte. Using Equation 5-1, a plot of $1/m_{Lapp}$ vs. 1/[A] should give a linear relationship if the drug binds to only one type of binding site on the protein. The intercept divided by the slope of the best-fit line can be used to calculate K_a, while taking the inverse of the intercept will give m_L. Deviations from linearity at high concentrations (low 1/[A]) in this type of plot indicate that the drug is binding to more than one type of binding site on the protein in the column.[23]

Equations 5-1 and 5-2 can be expanded for systems with more than one type of binding site with a ligand. An expansion of Equation 5-1 for a two-site binding model is shown in Equation 5-3, while a similar expansion for Equation 5-2 is given in Equation 5-4:[23, 24]

$$\frac{1}{m_{Lapp}} = \frac{1 + K_{a1}[\mathrm{A}] + \beta_2 K_{a1}[\mathrm{A}] + \beta_2 K_{a1}^2[\mathrm{A}]^2}{m_{Ltot}\{(\alpha_1 + \beta_2 - \alpha_1\beta_2)K_{a1}[\mathrm{A}] + \beta_2 K_{a1}^2[\mathrm{A}]^2\}} \qquad (5\text{-}3)$$

$$m_{Lapp} = \frac{m_{L1}K_{a1}[\mathrm{A}]}{(1 + K_{a1}[\mathrm{A}])} + \frac{m_{L2}K_{a2}[\mathrm{A}]}{(1 + K_{a2}[\mathrm{A}])} \qquad (5\text{-}4)$$

In these equations, K_{a1} and K_{a2} are the association equilibrium constants of A at binding sites 1 and 2, and m_{L1} or m_{L2} are the binding capacities that correspond to these sites. The term α_1 is the fraction of all binding regions that make up the high affinity binding sites (i.e., $\alpha_1 = m_{L1,tot}/m_{Ltot}$), while β_2 is the ratio of the association equilibrium constants for any lower affinity site (e.g., K_{a2}) versus the highest affinity site, where $\beta_2 = K_{a2}/K_{a1}$ and $0 < K_{a2} < K_{a1}$. Equation 5-4 can be used to make of plot of m_{Lapp} vs. [A] in order to calculate binding constants for the two binding sites. Similar models can be used for systems with more than two binding sites.[24]

Using these equations, a non-linear plot of $1/m_{Lapp}$ vs. [A] would be expected throughout a broad range of concentrations for a system with multi-site binding. However, at low concentrations a linear response would still be observed. In this case, Equation 5-3 can be simplified and used to calculate binding constants for the highest affinity binding site, as occurs when using low concentrations of the analyte and as shown by the linear approximation in Equation 5-5.[25]

$$\lim_{[A]\to 0} \frac{1}{m_{Lapp}} = \frac{1}{m_{Ltot}(\alpha_1 + \beta_2 - \alpha_1\beta_2)K_{a1}[A]} + \frac{\alpha_1 + \beta_2{}^2 - \alpha_1\beta_2{}^2}{m_{Ltot}(\alpha_1 + \beta_2 - \alpha_1\beta_2)^2} \qquad (5\text{-}5)$$

A plot of $1/m_{Lapp}$ vs. 1/[A] according to Equation 5-5 has been shown in previous theoretical studies to provide a good estimate for K_{a1} and m_{Ltot} in multi-site systems.[25]

Zonal Elution

HPAC and the method of zonal elution were used to examine the binding of acetohexamide and tolbutamide to glycated HSA at specific binding sites. In this method, a competing agent I (in this case, acetohexamide or tolbutamide) is present in the mobile phase at a known concentration while a small plug of analyte A (either *R*-warfarin or L-tryptophan) is injected onto the column. This technique is often used to examine the binding interactions of the analyte and the competing agent. Observations can often be put into three categories for these interactions: 1) the pair directly competes for the same binding site, 2) the compounds affect the binding of one another through allosteric effects, or 3) no direct competition is observed. The retention time of the resulting analyte peaks can be used to determine the retention time of the analyte, t_R, which can then be used to calculate the retention factor k, where $k = (t_R\text{-}t_M)/t_M$) and t_M is the elution

time of a non-retained solute (e.g., sodium nitrate). The following equation can be used to describe the relationship between the retention factor of the analyte and the concentration of the competing agent, [I].[23, 24]

$$\frac{1}{k} = \frac{K_{aI} V_M [\mathrm{I}]}{K_{aA} m_L} + \frac{V_M}{K_{aA} m_L} \qquad (5\text{-}6)$$

In Equation 5-6, K_{aI} and K_{aA} are the association equilibrium constants for the competing agent and analyte, respectively, at their site of competition and V_M is the void volume. A plot of $1/k$ vs. [I] for this equation should yield a linear response if A and I have direct competition for one binding site on the ligand. The best-fit line for a system with these interactions can be used to determine the association equilibrium constant for the competing agent by dividing the slope by the intercept. This can be a useful tool to determine site-selective interactions for a compound at a particular binding site on a ligand.[23]

Experimental

Reagents

The acetohexamide, tolbutamide (≥ 99.9%), warfarin (≥ 97%), L-tryptophan (98%), monobasic and dibasic potassium phosphate salts, D-(+)-glucose (99.5%), sodium azide (>95%), sodium chloride, sodium phosphate salts, HSA (essentially fatty acid free, ≥ 96%), and commercial glycated HSA (Lot 058K6087) were purchased from Sigma-Aldrich (St. Louis, MO, USA). The Nucleosil Si-300 (7 micron particle diameter, 300 Å pore size) was purchased from Macherey-Nagel (Düren, Germany). Reagents used in the bicinchoninic acid (BCA) protein assay were from Pierce (Rockford, IL, USA). The

enzymatic assay kits for fructosamine (used here for glycated serum proteins) were from Diazyme Laboratories (San Diego, CA, USA). Sterilized 17 x 100 mm culture tubes were purchased from Fisher Scientific (Pittsburg, PA, USA). Slide-A-Lyzer 7K (7 kDa MW cutoff) dialysis cassettes with varying sample volume sizes (0.5-3, 3-12, and 12-30 ml) were acquired from Thermo Scientific (Rockford, IL, USA). The Econo-Pac 10 DG disposable chromatography 30 x 10 ml desalting columns were from Bio-Rad Laboratories (Hercules, CA, USA). All solutions were made using water from a NANOpure system (Barnstead, Dubuque, IA, USA) and filtered with a 0.20 µm GNWP nylon membrane from Millipore (Billerica, MA, USA).

Apparatus

The HPLC system consisted of a Jasco DG-2080-53 three-solvent degasser (Tokyo, Japan), two Jasco PU-2080 isocratic pumps, a Rheodyne Advantage PF six-port valve (Cotati, CA, USA), a Jasco AS-2055 autosampler, a Jasco CO-2060 column oven, and a Jasco UV-2075 UV/Vis detector. The HPLC system hardware was controlled by EZChrom Elite software v3.2.1 (Scientific Software, Inc., Pleasanton, CA, USA) via Jasco LC Net hardware. An in-house version of Labview 5.1 software (National Instruments, Austin, TX, USA) was used to analyze the frontal analysis breakthrough curves while PeakFit 4.12 (Jandel Scientific Software, San Rafael, CA, USA) was used to determine the central moments of peaks obtained from zonal elution experiments. Linear regression was performed using Excel 2003 (Microsoft Corporation, Redmond, WA, USA) and non-linear regression was performed using DataFit (Oakdale Engineering, PA, USA).

Methods

Diol silica was made using Nucleosil Si-300 silica and HSA was immobilized to the diol silica by the Schiff base method according to a previously-published procedures.[26-28] Control silica was also made using this method but with no added HSA. A BCA assay was performed in triplicate to determine the protein content of the supports, using soluble glycated HSA as the standard and the control support as the blank. These studies used three batches of HSA for immobilization, with each batch having a different level of glycation. The first HSA sample was purchased from Sigma (gHSA1), while the second and the third were made *in vitro* using low or medium levels of glucose (gHSA2 and gHSA3, respectively).

HSA was glycated *in vitro* using a modified version of previously-published methods.[29, 30] In order to make the gHSA2 sample, a 20 mL solution containing 1 mM sodium azide, 15 mM glucose, and 42 g/L HSA was made in sterile pH 7.4, 0.2 M potassium phosphate buffer. This solution was put into sterile culture tubes in 3-4 ml fractions, capped, sealed with parafilm and allowed to incubate in a water bath for 4 weeks at 37 °C. The solutions were then filtered using a size exclusion desalting column to remove excess glucose and sodium azide from the protein solution. The protein fraction was then dialyzed against water to remove buffer salts. This protein solution was placed into sterile dialysis cassettes and dialyzed against water at a volume 200-500x that of the sample for 2 h with gentle stirring at room temperature; the water outside of the cassettes was removed and replaced with fresh water, followed by another 2 h of dialysis under the same conditions. The water was again replaced with fresh water and dialysis was allowed to continue at 4 °C for ~14-18 h with no stirring. The resulting protein

solution was stored at -80 °C until further use. Lyophilization was performed on the protein solution until the protein was dry. The HSA was then stored at -80 °C until it was used for immobilization. The same procedure was used to make the gHSA3 sample but with the glucose levels being increased to ~30 mM during incubation to elevate the level of HSA glycation.

After immobilization, the glycated HSA supports were downward slurry-packed into separate 2.0 cm x 2.1 mm I.D. columns at 3500 psi (24 MPa) using pH 7.4, 0.067 M potassium phosphate buffer as the packing solution. The control supports for each gHSA sample were packed into separate columns under the same conditions. These columns were stored at 4 °C in the packing solution and used over a period of one year and fewer than 500 sample applications per column. Similar columns containing normal HSA have been found in previous studies to retain good stability for drug-protein binding studies under such conditions.[31]

A fructosamine assay kit from Diazyme Laboratories was used to determine the mol hexose (sugar)/mol HSA as a measure of glycation. This kit contained a calibrator, a control, Reagent 1, and Reagent 2. This assay is meant to be used for serum samples and was modified from the original instructions per the manufacturer's advice for use with the protein solution. A 20 g/L HSA solution was prepared from a glycated HSA sample by dissolving ~10 mg of protein in 500 μL of pH 7.4, 0.025 M potassium phosphate buffer. A 300 μL portion of Reagent 1 was placed into an empty cuvette and 30 μL of the protein solution was added to the cuvette. This mixture was stirred quickly and placed into a temperature-controlled UV/vis spectrometer at 37 °C for 5 min. Absorbance values were collected at 600 and 700 nm at this time. A 75 μL portion of

Reagent 2 was quickly added to the cuvette, mixed, and allowed to react for 5 more minutes, after which the absorbance values were again measured. This procedure was repeated for the control, calibration standard, and a saline solution sample in place of the protein sample. The assay was performed in duplicate or triplicate. A 0.85% sodium chloride saline solution was used as a blank for the calibration curve, while the assay kit provided a calibration standard of 613 μmol/L fructosamine for the second point of the curve. A control provided with this kit was used to test for the accuracy of the method. The original procedure called for only one absorbance reading to be taken at 600 nm, while this modified procedure required the use of a difference in absorbance readings at 600 and 700 nm. Other than this change, the assay followed the manufacturer's protocol. The value of mol hexose/mol HSA was calculated for each glycated HSA sample using the resulting data and calibration plot. The assay was repeated with fresh reagents and solutions when new batches of glycated HSA were analyzed.

The acetohexamide, tolbutamide, *R*-warfarin, and L-tryptophan solutions were made in pH 7.4, 0.067 M potassium phosphate buffer. This buffer was also used as the application and elution buffer in the chromatographic studies. All solutions were filtered through a 0.2 μM nylon filter and degassed for 10-15 min prior to use. A flow rate of 0.5 ml/min was used for both the frontal analysis and zonal elution studies. This flow rate has been shown in previous studies to give reproducible retention factors and binding capacities for drug binding studies conducted on similar columns containing normal HSA.[32, 33]

Frontal analysis studies were performed at 37 °C. In these experiments, the column was first equilibrated with pH 7.4, 0.067 M potassium phosphate buffer, with

equilibration being completed between each successive run. The solutions were switched quickly between the pH 7.4 buffer and sample solution using an automated six-port valve. Once the analyte had saturated the column and produced a breakthrough curve, the valve was switched again and buffer was used to elute the remaining analyte from the column. For the frontal analysis studies, the analyte solutions contained acetohexamide at a concentration of 1-1000 μM or tolbutamide at a concentration of 1-200 μM. The analyte was monitored using absorbance readings at 248 nm for acetohexamide at 1-7.5 μM, 315 nm for acetohexamide at 10-1000 μM, and 250 nm for tolbutamide at 1-200 μM. (Note: the wavelength was changed for acetohexamide in going from 1-7.5 μM to 10-1000 μM to keep the absorbance values within a linear range of response). Runs were performed in triplicate for each analyte concentration and the resulting breakthrough curves were analyzed using Labview 5.1 and the equal areas method.[23] Non-specific binding was corrected by subtracting the results for the control column from the protein column results.

Zonal elution competition studies were performed using two well-characterized probe compounds for HSA: *R*-warfarin, known to bind to Sudlow site I, and L-tryptophan, known to bind to Sudlow site II.[10, 11] Varying concentrations of acetohexamide or tolbutamide (ranging from 1-20 μM) were placed in the mobile phase. A series of 20 μL injections of 5 μM *R*-warfarin or L-tryptophan were made at 37 °C. The concentration of these samples has been shown in the past to be within linear elution conditions for similar HSA columns.[34, 35] The elution of *R*-warfarin and L-tryptophan was monitored at 308 and 280 nm, respectively. Injections of 20 μM sodium nitrate were also made at 20 μL under the same conditions using only the pH 7.4 buffer as the mobile

phase. Sodium nitrate was used as a non-retained solute to determine column and system void times, with the elution of sodium nitrate being monitored at 205 nm. The resulting peaks were analyzed using PeakFit v4.12 software and fit to an exponentially-modified Gaussian curve.

Results and Discussion

Preparation of Glycated HSA

A fructosamine assay was used to determine the amount of glycation present in each HSA sample. The first glycated HSA column (gHSA1) was determined to contain 1.31 (± 0.05) mol hexose/mol HSA. The second glycated HSA column (gHSA2) had HSA with a glycation level of 2.34 (± 0.13) mol hexose/mol HSA. The third column (gHSA3) was made with HSA that had a glycation level of 3.35 (± 0.14) mol hexose/mol HSA. The protein content of these columns was between 29 and 47 mg protein/g silica (or ~440-710 nmol HSA/g silica). These levels were comparable to protein levels previously noted for normal HSA supports prepared by the same method.[28] The protein content and glycation levels for each of the supports are summarized in Table 5-1.

Acetohexamide Binding to gHSA1

Breakthrough curves were collected for acetohexamide on each glycated HSA column. The first analysis was performed using the gHSA1 column (see Figure 5-1). Breakthrough times were calculated from the curves and m_{Lapp} values were determined at each analyte concentration. Double reciprocal plots were prepared according to Equation 5-1. Previous studies have indicated that acetohexamide binds to normal (non-glycated)

Table 5-1. Protein content and level of glycation of HSA supports

	gHSA1	**gHSA2**	**gHSA3**
Protein Content (mg HSA/g silica)	29 (± 4)	47 (± 8)	40 (± 3)
Level of glycation (mol Hexose per mol HSA)	1.31 (± 0.05)	2.23 (± 0.13)	3.22 (± 0.14)

The values in parenthesis represent ± 1 S.D.

Figure 5-1. Breakthrough curves for acetohexamide on the gHSA1 column. Concentrations from left to right: 1000, 500, 300, 100, 50 μM acetohexamide.

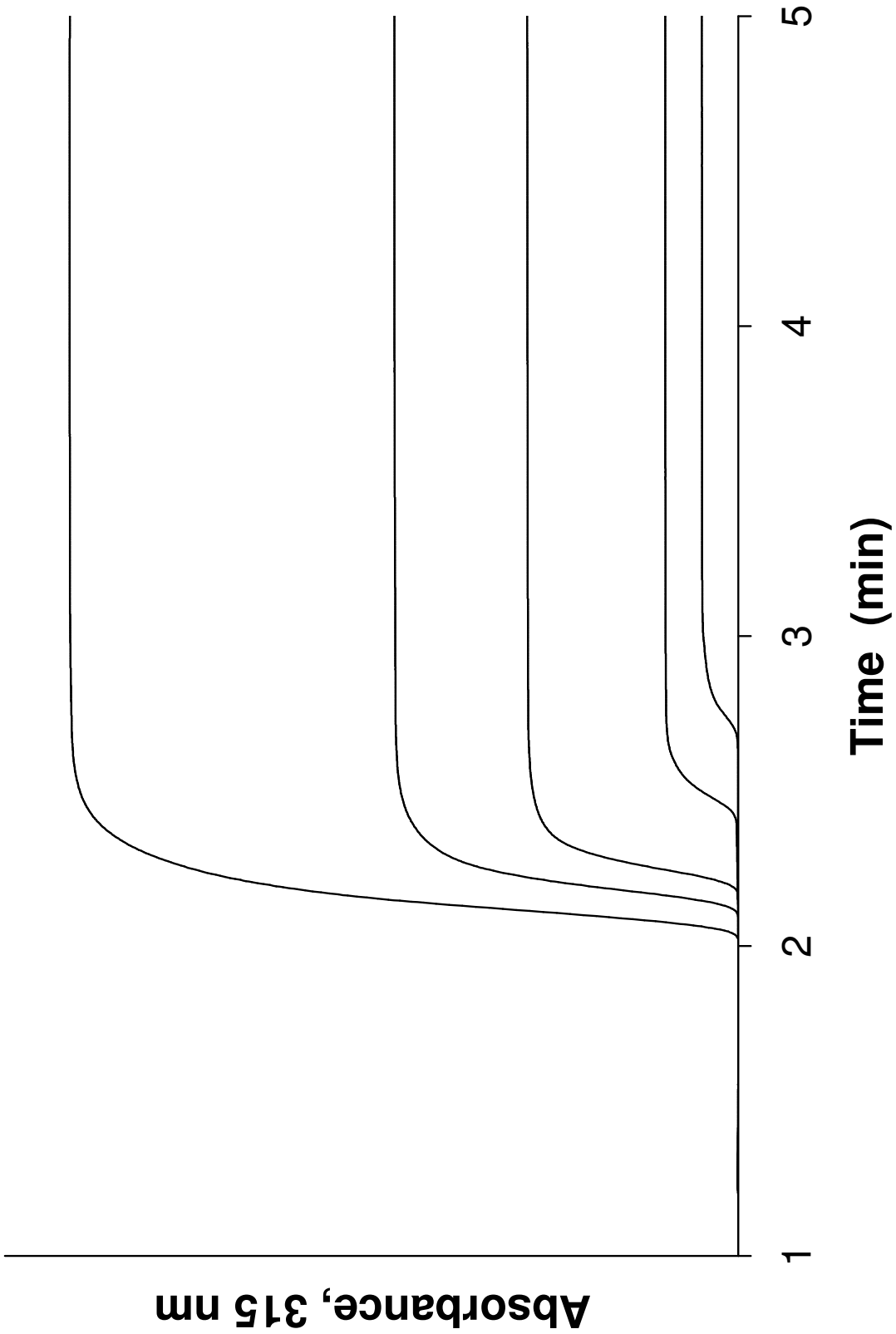
Absorbance, 315 nm
1
2
3
4
5
Time (min)

HSA at more than one type of binding site (see Chapter 3), so deviations from linearity at high concentrations were expected for this type of plot, as seen in Figure 5-2. The data over the linear range (acetohexamide concentrations 1-10 μM) were fit to Equation 5-5. From this linear region (r = 0.998, n = 7), K_{a1} and m_{L1} values for the high-affinity binding regions of acetohexamide with the glycated HSA were found to be 2.0 (± 0.2) x 10^5 M^{-1} and 1.35 (± 0.10) x 10^{-8} mol.

Due to the curvature of the results in Figure 5-2, the overall data in Figure 5-3 were also fit to a two-site model using Equation 5-4. The data fit well to this model and gave only random residuals and a small sum of square of the residuals. The K_a value for the high-affinity interactions was calculated from this fit to be 1.2 (± 0.2) x 10^5 M^{-1}, and these sites had an m_L value of 1.7 (± 0.1) x 10^{-8} mol. The second, lower-affinity binding sites gave a K_a value of 1.4 (± 0.8) x 10^3 M^{-1} and a corresponding m_L value of 1.7 (± 0.4) x 10^{-8} mol. The K_a value calculated for the group of high-affinity binding sites was similar to the value obtained when using Equation 5-5. The association equilibrium constant for the high-affinity sites is comparable to those obtained for acetohexamide on a normal HSA column, which had a K_a value of 1.3 (± 0.2) x 10^5 M^{-1}. The lower-affinity binding site appears to increase from 3.5 (± 0.3) x 10^2 M^{-1} on the normal HSA column to 1.4 (± 0.8) x 10^3 M^{-1} on the gHSA1 column; however, the error associated with these values makes them indistinguishable at the 95% confidence level. These results are summarized in Table 5-2.

A comparison of the binding capacity and protein content of the gHSA1 column was also made. This comparison was used to estimate the number of binding regions. Using the results from the two-site binding model, the high-affinity sites had a calculated

Figure 5-2. Reciprocal plot for acetohexamide using Eqn. (1). Best-fit line was calculated using concentrations 1-10 μM acetohexamide according to Eqn. (5): $y = 360\ (\pm\ 10)\ x + [7.4\ (\pm\ 0.5) \times 10^7]$, r = 0.998, n = 7. The error bars represent a range of ± 1 SD.

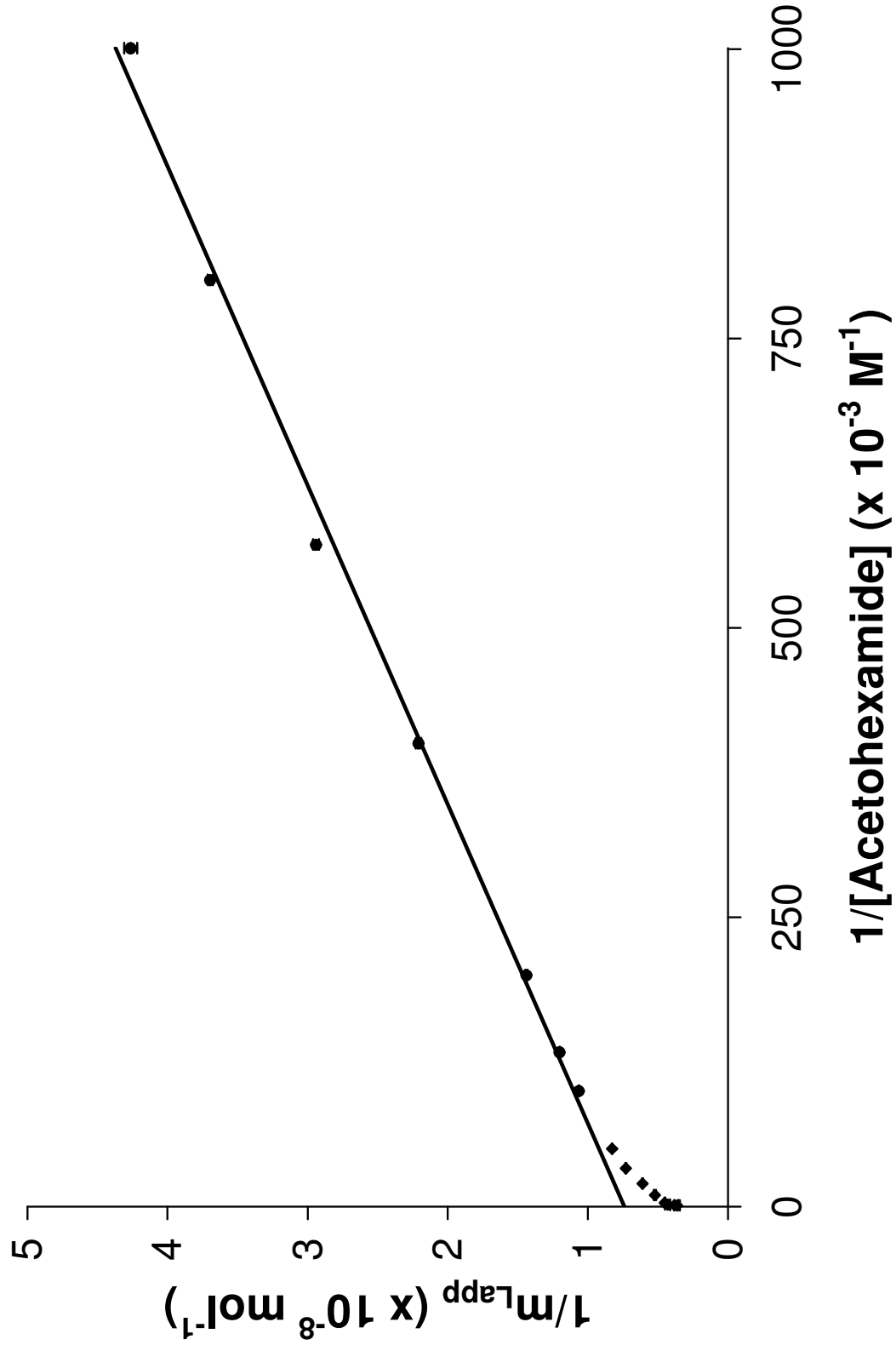
1/m$_{Lapp}$ (x 10^{-8} mol^{-1})
0
1
2
3
4
5
0
250
500
750
1000
1/[Acetohexamide] (x 10^{-3} M^{-1})

Figure 5-3. Plot of m_{Lapp} vs. [Acetohexamide] for the gHSA1 column with a fit using Eqn. (4).

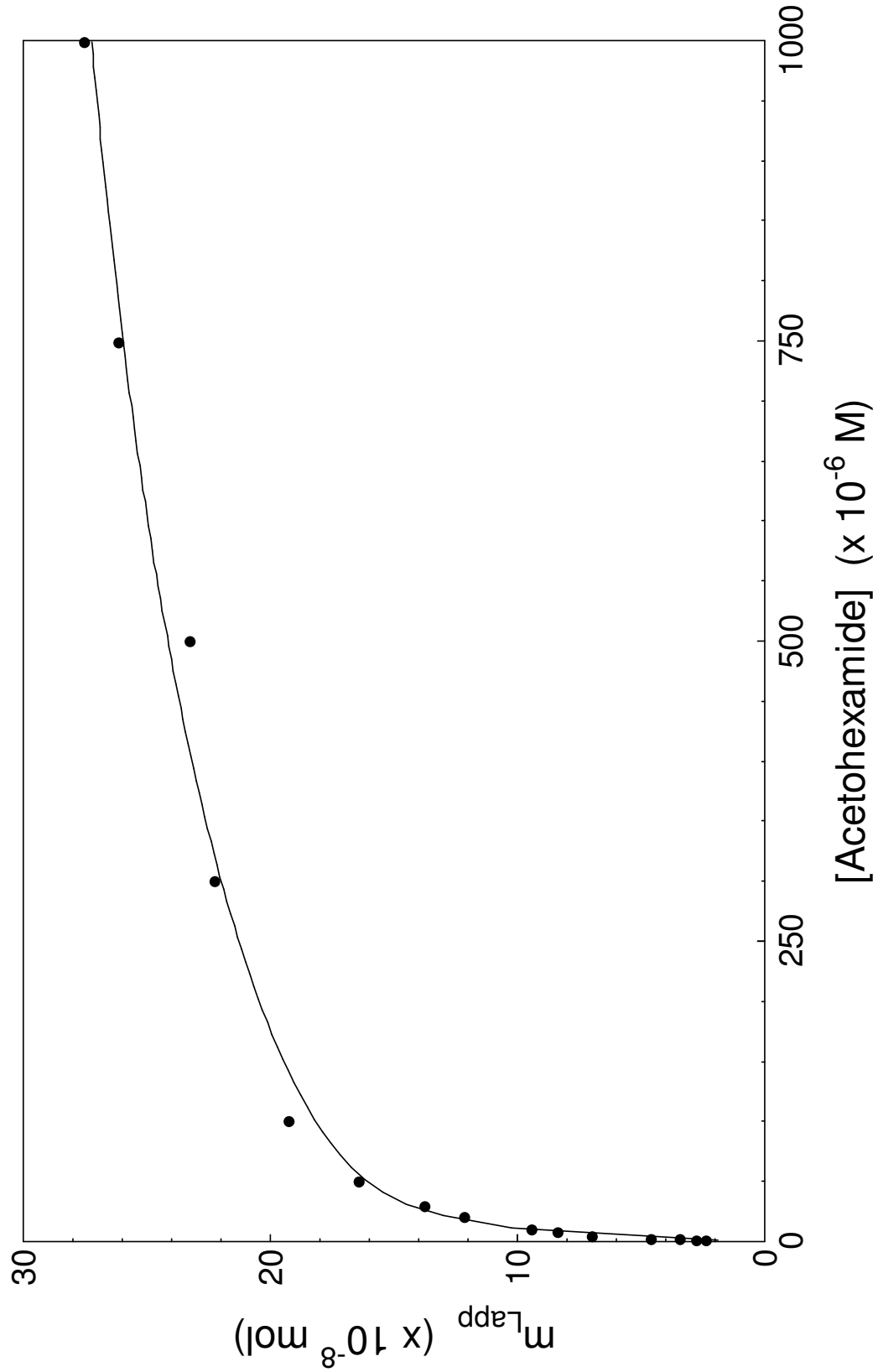
30
20
10
0
0
250
500
750
1000
m_{Lapp} (x 10^{-8} mol)
[Acetohexamide] (x 10^{-6} M)

Table 5-2. Binding constants calculated for acetohexamide and tolbutamide using frontal analysis and a two-site binding model.

Acetohexamide	K_{a1} (x 10^5 M^{-1})	m_{L1} (x 10^{-8} mol)	**Activity**	K_{a2} (x 10^3 M^{-1})	m_{L2} (x 10^{-8} mol)	**Activity**
Column						
HSA	1.3 (± 0.2)	2.4 (± 0.1)	1.3 (± 0.1)	0.35 (± 0.03)	9.3 (± 5.5)	5.2 (± 3.1)
gHSA1	1.2 (± 0.2)	1.7 (± 0.1)	1.3 (± 0.2)	1.4 (± 0.8)	1.7 (± 0.4)	1.3 (± 0.3)
gHSA2	2.0 (± 0.6)	1.8 (± 0.3)	0.80 (± 0.20)	11 (± 3)	2.4 (± 0.3)	1.1 (± 0.2)
gHSA3	2.0 (± 0.3)	1.5 (± 0.1)	0.80 (± 0.09)	4.1 (± 0.7)	3.0 (± 0.1)	1.6 (± 0.5)
Tolbutamide						
Column						
HSA	0.87 (± 0.06)	2.0 (± 0.1)	1.1 (± 0.1)	8.1 (± 1.7)	1.8 (± 0.1)	1.0 (± 0.1)
gHSA1	1.2 (± 0.2)	1.1 (± 0.2)	0.82 (± 0.18)	9.5 (± 3.2)	1.7 (± 0.1)	1.2 (± 0.2)
gHSA2	0.84 (± 0.16)	2.2 (± 0.4)	1.0 (± 0.3)	7.8 (± 5.1)	1.9 (± 0.2)	0.87 (± 0.18)
gHSA3	0.89 (± 0.06)	1.9 (± 0.1)	1.1 (± 0.1)	1.7 (± 1.1)	3.6 (± 1.4)	1.9 (± 0.8)

The values in parenthesis represent ± 1 S.D.

activity of 1.3 (± 0.2), while the lower-affinity sites had an activity of 1.3 (± 0.3). When compared to a typical value of 0.55-0.8 for single-site binding to immobilized HSA, these values suggest that at least two regions are involved in binding at each of these groups of sites. Similar results for the high-affinity sites were found for acetohexamide binding to normal HSA in previous studies.

Zonal elution competition studies were performed to examine binding at Sudlow sites I and II using the site-selective probe compounds *R*-warfarin (see Figure 5-4) and L-tryptophan, respectively. When plotting 1/*k* vs. [acetohexamide], a linear response was obtained for each probe compounds as seen in Figure 5-5. These plots gave a correlation coefficient of 0.991 for both L-tryptophan and *R*-warfarin, indicating there was direct competition of both these probe compounds with acetohexamide. Previous zonal elution competition studies performed using normal HSA also displayed direct competition of these probes with acetohexamide. This indicates that acetohexamide had binding at both Sudlow sites I and II on HSA when low levels of glycation were present.

The experimental retention factor for L-tryptophan determined by this method was 3.9 (± 0.1) when no competing agent was present in the system. A predicted value for the retention factor was also calculated by taking the inverse of the intercept from the best-fit line. This value was determined to be 3.7 (± 0.2). With a calculated 3.2% difference, the experimental value showed good agreement to the predicted value. The same was true for R-warfarin. This compound had an experimental retention factor of 59 (± 1) and a predicted value of 55 (± 2) in the absence of any acetohexamide. These values are within two standard deviations of one another, with only a slightly larger difference (7.3%) than seen with L-tryptophan.

Figure 5-4. Zonal elution competition studies for *R*-warfarin and acetohexamide on the gHSA1 column. *R*-Warfarin was injected onto the column while known amounts of acetohexamide were present in the mobile phase. Acetohexamide concentrations from top to bottom: 20, 15, 10, 5, and 1 μM. Injections were made using 20 μL of 5 μM *R*-warfarin.

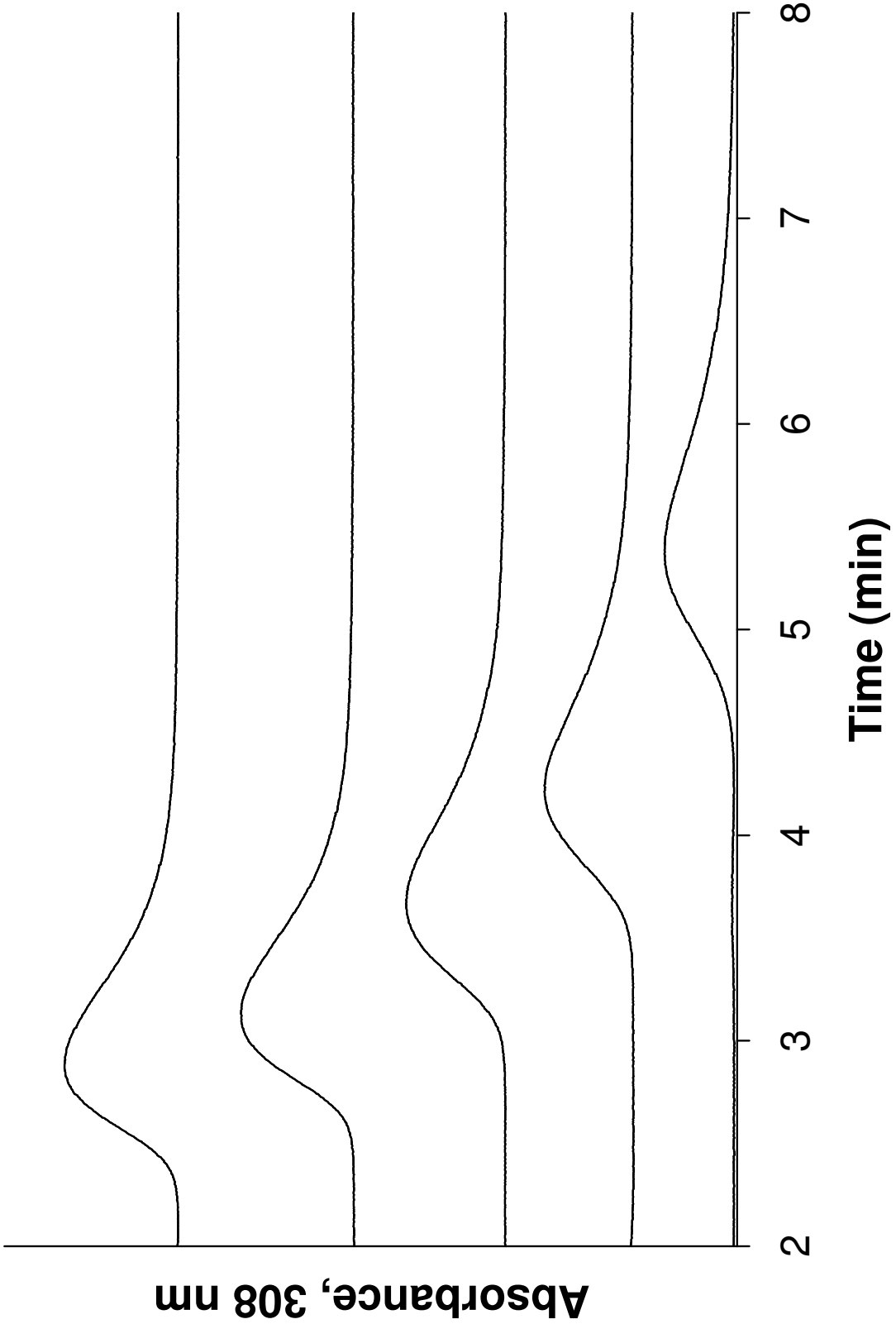
Absorbance, 308 nm
2
3
4
5
6
7
8
Time (min)

Figure 5-5. Determination of the (a) *R*-warfarin and (b) L-tryptophan retention on the gHSA1 column in the presence of acetohexamide as analyzed using Equation 5-6. The best-fit line for *R*-warfarin was $y = 1100\ (\pm\ 100)\ x + 0.018\ (\pm\ 0.001)$, $r = 0.991$, $n = 6$. The best-fit line for L-tryptophan was $y = [2.1\ (\pm\ 0.1)\ \text{x}\ 10^4]\ x + 0.27\ (\pm\ 0.02)$, $r = 0.991$, $n = 6$. The error bars represent a range of ± 1 SD.

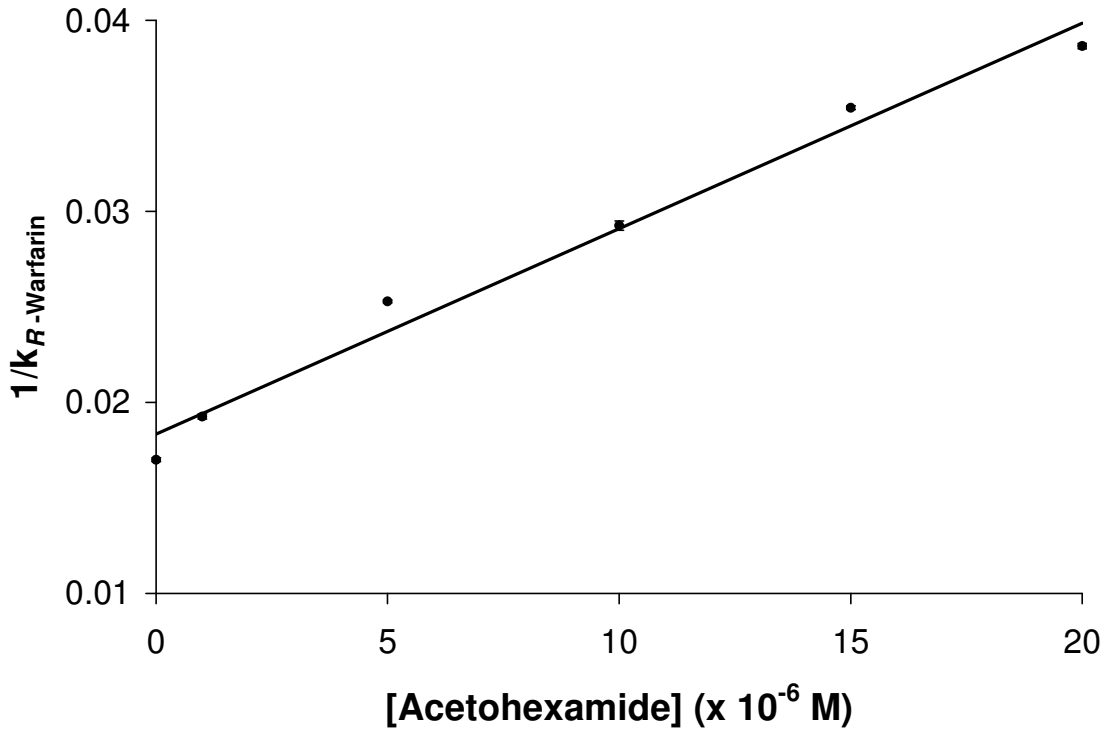
0.04
0.03
0.02
0.01
1/k R-Warfarin
0
5
10
15
20
[Acetohexamide] (x 10-6 M)

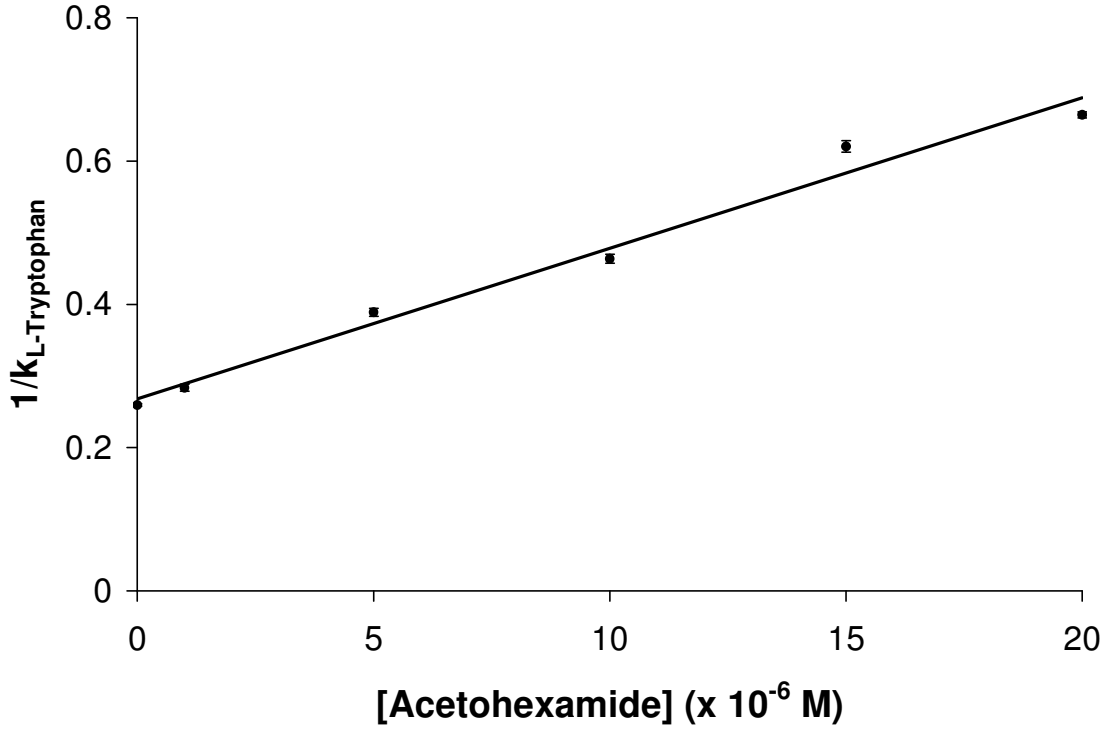
0.8
0.6
0.4
0.2
0
1/k L-Tryptophan
0
5
10
15
20
[Acetohexamide] (x 10-6 M)

The association equilibrium constants were calculated for acetohexamide at Sudlow sites I and II by taking the ratio of the slope to the intercept for plots of $1/k$ vs. [acetohexamide]. Values of 5.9 (± 0.5) x 10^4 M^{-1} and 7.9 (± 0.7) x 10^4 M^{-1} were calculated for the interactions at Sudlow site I and site II, respectively. It was noted that these values were both slightly lower than the high-affinity set of binding sites found for acetohexamide using frontal analysis, but much higher than the value for the lower-affinity sites. It is possible that frontal analysis was grouping both of these regions in the group of high-affinity sites.

Compared to a normal HSA column, the association equilibrium constant calculated for Sudlow site I increased from 4.2 (± 0.4) x 10^4 M^{-1} to 5.9 (± 0.5) x 10^4 M^{-1} on the gHSA1 column. This value remained within two standard deviations of the K_a for the normal HSA column. The opposite was true for the interactions at Sudlow site II, where the binding constant decreased from 1.3 (± 0.1) x 10^5 M^{-1} to 7.9 (± 0.7) x 10^4 M^{-1} in going from a normal HSA column to the gHSA1 column (see Table 5-3). Perhaps these opposing binding changes are why there was no apparent change in the overall K_a value at the high-affinity sites for these two columns when examined by frontal analysis.

Acetohexamide Binding to gHSA2

The HSA that had the next highest level of glycation was gHSA2. The same studies that were performed using the gHSA1 column were performed with a gHSA2 column. First, frontal analysis was performed to investigate the binding of acetohexamide to glycated HSA. A reciprocal plot of $1/m_{Lapp}$ vs. 1/[acetohexamide] was again made for these data and examined using a single-site binding model. Like the

Table 5-3. Binding constants for acetohexamide and tolbutamide determined using zonal elution competition studies

Acetohexamide	**Sudlow Site I (*R*-warfarin) (x 10^4 M^{-1})**	**Sudlow Site II (L-tryptophan) (x 10^4 M^{-1})**
Column		
HSA	4.2 (± 0.4)	13 (± 1)
gHSA1	5.9 (± 0.5)	7.9 (± 0.7)
gHSA2	3.8 (± 0.3)	11 (± 1)
gHSA3	4.1 (± 0.6)	12 (± 1)
Tolbutamide		
Column		
HSA	5.5 (± 0.2)	5.3 (± 0.2)
gHSA1	6.9 (± 0.2)	5.9 (± 0.3)
gHSA2	6.6 (± 0.5)	7.2 (± 0.3)
gHSA3	6.5 (± 0.2)	6.4 (± 0.3)

The values in parenthesis represent ± 1 S.D.

gHSA1 column, non-linear results were seen for this column at high concentrations (low 1/[A] values), implying that acetohexamide binds to the gHSA2 column at more than one type of binding site. Linear regression was performed for the lower acetohexamide concentrations (1-10 μM, r = 0.999, n = 6) using Equation 5-5 to estimate the binding constants for the high-affinity binding sites. This gave a K_a of 2.0 (± 0.2) x 10^5 M^{-1} and a corresponding m_L of 2.0 (± 0.1) x 10^{-8} mol. These results are similar to those calculated for the gHSA1 column for its high affinity sites.

The data were then fit to a two-site model using Equation 5-4. Association equilibrium constants of 2.0 (± 0.6) x 10^5 M^{-1} and 1.1 (± 0.3) x 10^4 M^{-1} were calculated for the high- and lower-affinity binding regions. The high-affinity binding regions showed strong agreement with the one-site model results using only low concentrations and Equation 5-5. This again supported the use of Equation 5-5 in determining binding constants for the high-affinity regions. Acetohexamide appeared to have stronger affinity to the lower-affinity binding sites with the gHSA2 column then with the gHSA1 column. Further investigation was done using zonal elution to explore these interactions.

The binding capacities for the high- and lower-affinity regions were 1.8 (± 0.3) x 10^{-8} mol and 2.4 (± 0.3) x 10^{-8} mol, respectively. At first glance, the high-affinity site seemed to have the same activity level as seen using the gHSA1 column, while the lower-affinity site appeared to increase. However, since the protein content was higher for the gHSA2 column than the gHSA1 column, the binding capacities alone can be misleading in this instance. In fact, the specific activities at both the high affinity and low affinity regions appeared to decrease for the gHSA2 column, with the high-affinity binding sites

having an activity of 0.79 (± 0.20) and the lower-affinity sites having an activity of 1.1 (± 0.2).

Zonal elution studies were performed to examine the binding of acetohexamide at Sudlow sites I and II for the gHSA2 column. Using Equation 5-6, plots of 1/*k* vs. [acetohexamide] were made for the competition of acetohexamide with *R*-warfarin and L-tryptophan. Both plots appeared to be linear when fit to Equation 5-6. The experimental retention factor for the competition of L-tryptophan and acetohexamide when no acetohexamide was present in the mobile phase was 5.6 (± 0.3), while the predicted value from the best-fit line was calculated to be 5.8 (± 0.1). These values were within two standard deviations of one another and had only a 5% difference. The competition between *R*-warfarin and acetohexamide had similar results, with an experimental retention factor of 64 (± 1) and a predicted value of 62 (± 2) in the absence of acetohexamide. These values only differed by 3% and were also within two standard deviations of one another. These retention factors were higher on the gHSA2 column than the gHSA1 column due to the increased protein content within the gHSA2 column.

Association constants for acetohexamide were also calculated using the zonal elution data. The competition with L-tryptophan produced a K_a value of 1.1 (± 0.1) x 10^5 M^{-1}, while the competition with *R*-warfarin resulted in a K_a of 3.8 (± 0.3) x 10^4 M^{-1}. These values both shifted from those calculated for the gHSA1 column. Using higher levels of glycation, it appears as though the K_a value at Sudlow site II increased while the K_a value at Sudlow site I decreased. These values were both lower than the frontal analysis estimate for the high-affinity binding site; however, the K_a value calculated for Sudlow site II was close to the value calculated for the high-affinity binding site using

frontal analysis. This result might explain why there was a change in the apparent activity at these binding sites using the two-site frontal analysis model. Perhaps the model was starting to differentiate between these two high-affinity sites. Now that the K_a values were further from each other than with the gHSA1 column, this model might have been primarily detecting the interactions at Sudlow site II for the high-affinity site while the K_a value for Sudlow site I interaction was closer to the lower-affinity result. This would also explain why the lower-affinity site K_a value using the frontal analysis model was higher than expected for only non-specific binding interactions.

Acetohexamide Binding to gHSA3

The gHSA3 column contained the most glycation of the three tested columns, with almost double the value of mol hexose/mol HSA compared to the gHSA1 column. The determination of binding constants for this column again began with frontal analysis studies. The data were fit to a single-site binding model using Equation 5-1 and a double-reciprocal plot. This plot also had non-linear deviations at high concentrations, so Equation 5-5 was used to estimate the high-affinity binding constants using concentrations of 1-10 mM (r = 0.999, n = 5). The K_a value calculated using this model was 1.9 (± 0.1) x 10^5 M^{-1}. The corresponding m_L value was 1.6 (± 0.1) mol.

The two-site model was employed next, as was done for the previous columns, to further examine both the high- and lower-affinity binding sites. Using this model, K_a values of 2.0 (± 0.3) x 10^5 M^{-1} and 4.1 (± 0.7) x 10^3 M^{-1} were calculated for the high-affinity and low-affinity sites, with corresponding m_L values of 1.5 (± 0.1) x 10^{-8} mol and 3.0 (± 0.1) x 10^{-8} mol, respectively. As seen with the gHSA2 column, this model shows a

K_a value for the high-affinity sites in strong agreement with the one-site model when using Equation 5-5 and data at low concentrations. The binding capacities and the protein content of the column were again used to examine the relative activity of the binding sites. An activity of 0.80 (± 0.09) was calculated for the high-affinity binding sites, which was statistically identical to that found for the gHSA2 column, while the activity for the lower-affinity sites was higher and had a larger standard deviation, 1.6 (± 0.5). This result was explored more using zonal elution competition studies.

Competition studies were performed to examine the binding occurring at Sudlow sites I and II on HSA. Plots of 1/*k* vs. [acetohexamide] for L-tryptophan and *R*-warfarin both appeared to give linear results, with correlation coefficients of 0.999 and 0.971, respectively. The calculated retention factor at [I] = 0 for the competition of L-tryptophan and acetohexamide was 4.7 (± 0.1), while the predicted value was 4.5 (± 0.1). These values fell within two standard deviations of one another and there was only a 5.2% difference between these values.

R-Warfarin retention factors were also determined. The calculated retention factor at [I] = 0 for this interaction was 47 (± 1) and the predicted value was 44 (± 3) when no acetohexamide was present. These values were within 7.2% of one another and within two standard deviations. The warfarin data did not fit quite as neatly to a one-site model as was seen when using the gHSA1 and gHSA2 columns (Figure 5-6). It was observed that at low acetohexamide concentrations (1-10 μM), warfarin gave a linear fit with a correlation coefficient of 0.999; however, at the higher concentrations (15 and 20 μM), the retention factor for the probe increased (i.e., a decrease in 1/*k*). When linear

Figure 5-6. Determination of the R-warfarin retention on the gHSA3 column in the presence of acetohexamide, as analyzed using Equation 5-6. The solid line represents the best-fit line for the entire data set, while the dashed line represents the best-fit line for only the bottom four concentrations (1-10 μM acetohexamide). The best-fit line for the entire data set was y = 930 (± 100) x + 0.023 (± 0.001), r = 0.971, n = 6. The best-fit line for the lower four concentrations was y = 1400 (± 100) x + 0.021 (± 0.001), r = 0.999, n = 4. The error bars represent ± 1 SD.

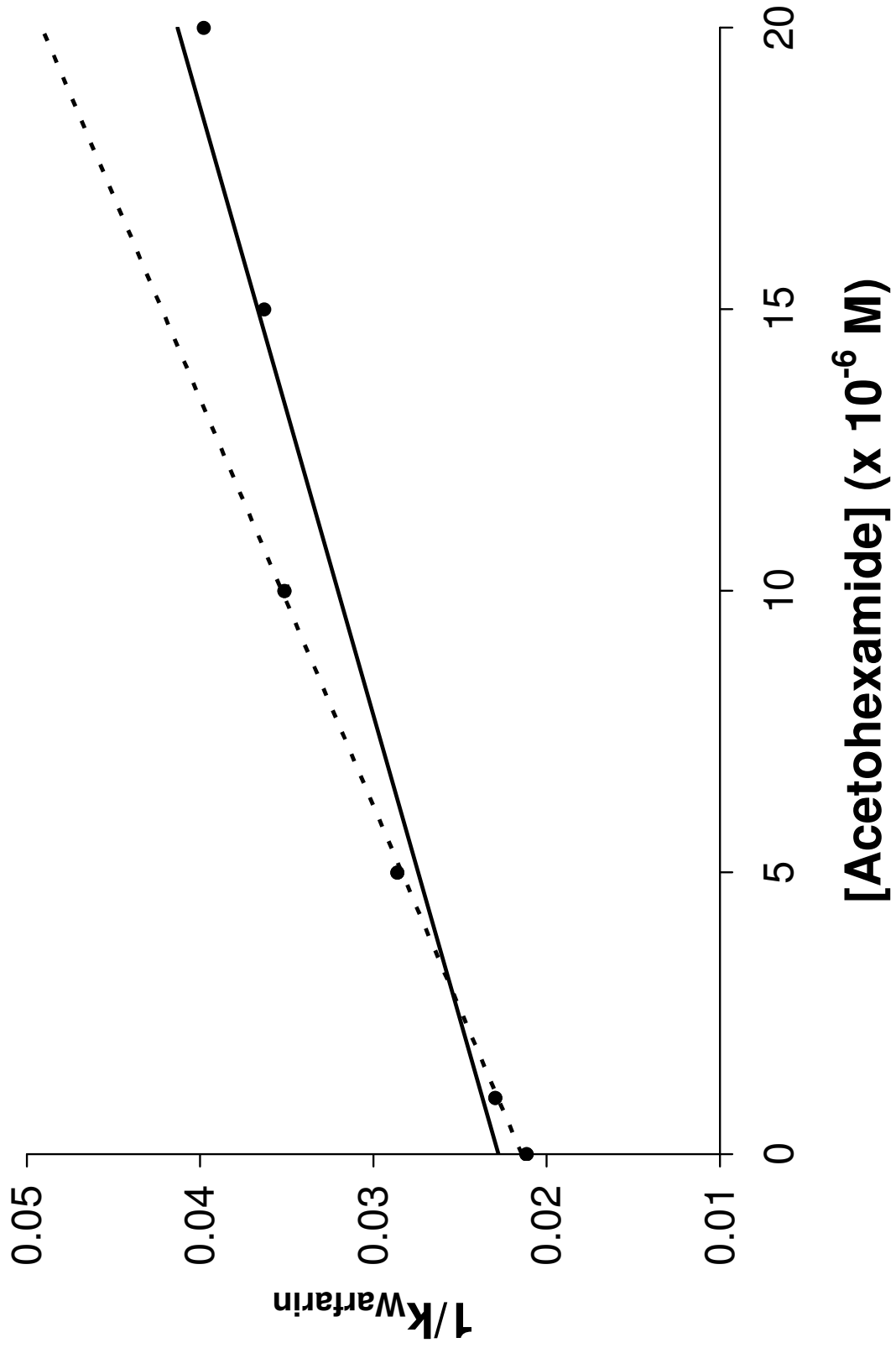
0.05
0.04
0.03
0.02
0.01
1/K Warfarin
0
5
10
15
20
[Acetohexamide] (x 10-6 M)

regression was performed on only the lower four concentrations, a predicted retention factor of 47 (± 1) was obtained at [I] = 0, which gave a 1.3% difference between this value and the experimental value.

Association equilibrium constants were calculated using the regression data from the competition studies. Acetohexamide was calculated to bind to gHSA3 with a K_a value of 1.2 (± 0.1) x 10^5 M^{-1} at Sudlow site II. This value was close to the one calculated for the high-affinity sites using the two-site frontal analysis model. Using the full concentration range for *R*-warfarin, a K_a value of 4.1 (± 0.6) x 10^4 M^{-1} was calculated for acetohexamide binding to Sudlow site I, with this value increasing to 6.5 (± 0.2) x 10^4 M^{-1} if only the lower acetohexamide concentrations were used. It appears as though the frontal model is able to detect the high-affinity region at site II but perhaps is not able to differentiate the lower-affinity site I interactions. It is also interesting to note that the K_a value at this binding site decreased for gHSA2 and increased for gHSA3, while the binding at Sudlow site II steadily increased as the level of glycation increased.

Tolbutamide Binding to gHSA1

Similar studies were performed using tolbutamide. Much like the acetohexamide studies, these studies started with the column containing HSA with the lowest level of glycation, gHSA1. The method of frontal analysis was used to gain information about the overall binding of tolbutamide to HSA, with increasing levels of glycation being present when using the three glycated HSA columns. Tolbutamide breakthrough curves began at a shorter timeframe than those obtained for acetohexamide, so initial experimental observations suggested that the association equilibrium constants should be

smaller than the K_a values calculated for acetohexamide. However, upon further investigation, the breakthrough times were only slightly lower for tolbutamide due to the slope of its breakthrough curves (see Figure 5-7). The initial data was fit to a one-site model using Equation 5-1. Using this model it was clear that linear deviations at high concentrations were present for this drug, indicating that binding to more than one binding site was occurring. This result was also seen for previous studies using HSA with no glycation. The apparent "double break" in the breakthrough curve seen in Figure 5-7 for tolbutamide also could elude to a two-site binding system. Equation 5-5 was employed to estimate the binding at the high-affinity site using concentrations of 1-10 μM. The resulting K_a value using this model was 9.1 (± 0.2) x 10^4 M^{-1}, with a corresponding m_L value of 1.7 (± 0.3) x 10^{-8} mol ($r = 0.999$, $n = 6$).

The two-site model was used next to see if more binding sites could be differentiated for this drug. This was accomplished using Equation 5-4 and non-linear regression. The calculated values for tolbutamide binding to gHSA1 were as follows: K_a = 1.2 (± 0.2) x 10^5 M^{-1} and m_L = 1.1 (± 0.2) x 10^{-8} mol for the high-affinity set of binding sites, and K_a = 9.5 (± 3.2) x 10^3 M^{-1} and m_L = 1.7 (± 0.1) x 10^{-8} mol for the lower-affinity binding sites. The first thing noted for these binding constants was the large K_a value for the high-affinity binding site. This K_a value was larger than the one calculated using Equation 5-5 but was also notably larger than the value calculated for a column with non-glycated HSA, which had a value of 8.7 (± 0.6) x 10^4 M^{-1} when using Equation 5-4.

The activity calculated for the high-affinity sites using the two-site model gives a value of 0.82 (± 0.18). This activity is lower than expected to include more than one binding region, but with the associated error it is difficult to determine if it is showing

Figure 5-7. Breakthrough curves for 100 μM tolbutamide and 100 μM acetohexamide on the gHSA3 column. Due to differences in absorbance values, the curves have been normalized to appear the same height.

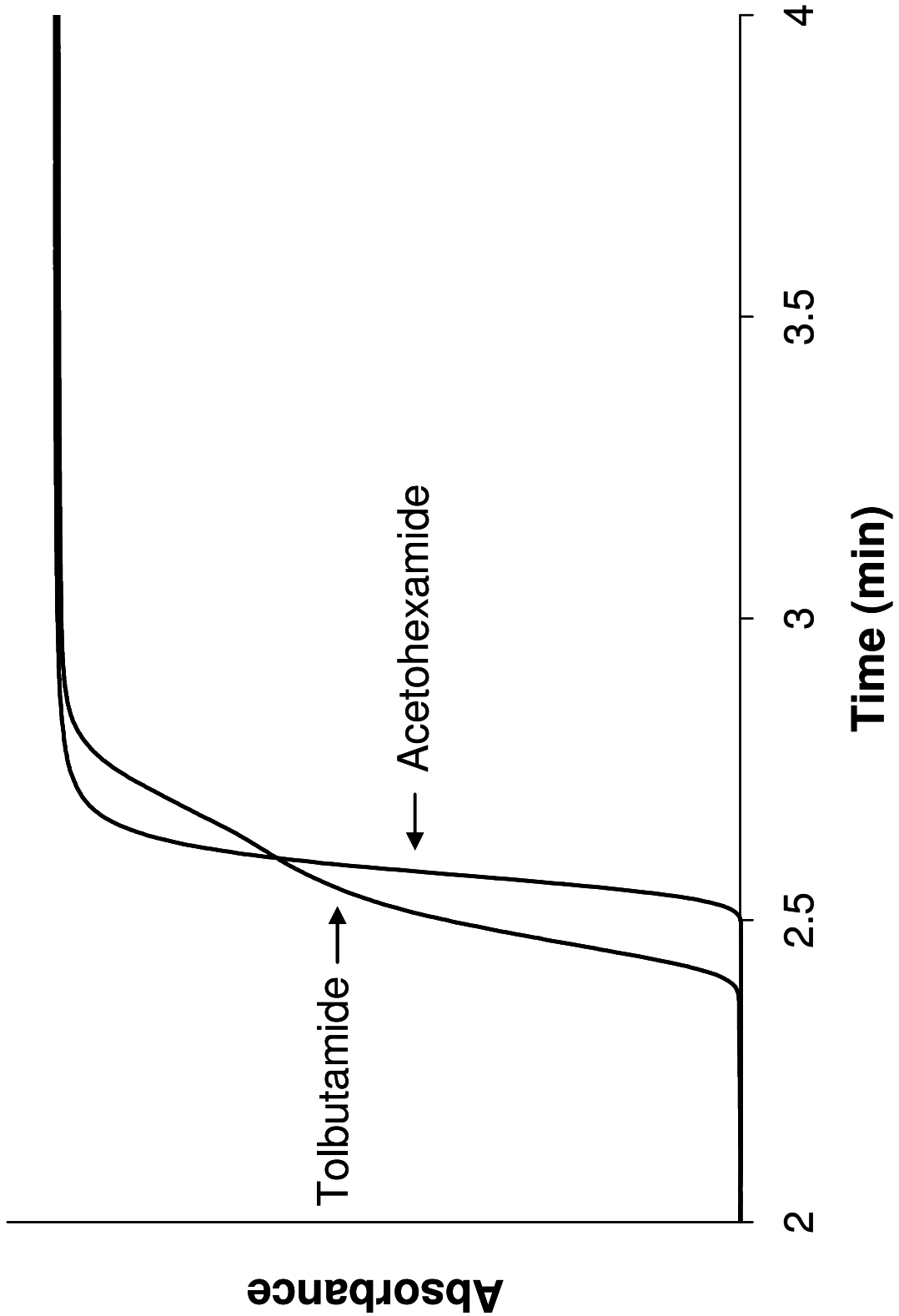
Absorbance
Tolbutamide
Acetohexamide
2
2.5
3
3.5
4
Time (min)

one binding region or two. The activity at the lower-affinity binding sites was 1.2 (± 0.2) suggesting tolbutamide was binding at more than one binding region within this group of sites.

Zonal elution competition studies were used to further examine the interactions at these binding sites. In these studies, concentrations of 0-20 μM tolbutamide were used, while the injections made using no competing agent in the mobile phase were collected from the acetohexamide competition studies. Unfortunately, it was determined later that the data collected using no competing agent in the mobile phase did not correspond well to the other data collected for this drug. Compared to the L-tryptophan data, this concentration had a lower retention factor (higher 1/*k*) than the data collected for the gHSA1 and gHSA2 columns, while *R*-warfarin data had a higher retention factor (lower 1/*k*) for these columns (Figure 5-8). This effect was present but not as drastic for the gHSA3 column. Therefore, the data when no competing agent was present in the mobile phase was removed for the tolbutamide studies.

A retention factor of 5.0 (± 0.2) was found for L-tryptophan on this column. The best-fit line for this model gave a correlation coefficient of 0.998. The calculated value (the zero concentration point that was disregarded from these studies to calculate the best-fit line) was 3.9 (± 0.1). The difference between the calculated and the predicted value was 23%. This difference was calculated to further explain why this concentration was not used in the linear regression of this model. *R*-Warfarin showed similar differences of 20% with a predicted retention factor of 47 (± 1) using the best-fit line with a correlation coefficient of 0.999 ($n = 5$), while the experimental *k* value was 59 (± 1).

The association constant of tolbutamide was also calculated using the method of

Figure 5-8. Determination of (a) *R*-warfarin and (b) L-tryptophan retention in the presence of tolbutamide, as analyzed using Equation 5-6. The best-fit line for *R*-warfarin was $y = 1500\ (\pm\ 100)\ x + 0.021\ (\pm\ 0.001)$, $r = 0.999$, $n = 5$. The best-fit line for L-tryptophan was $y = [1.2\ (\pm\ 0.1)\ \text{x}\ 10^4]\ x + 0.20\ (\pm\ 0.01)$, $r = 0.998$, $n = 5$. The error bars represent ± 1 SD.

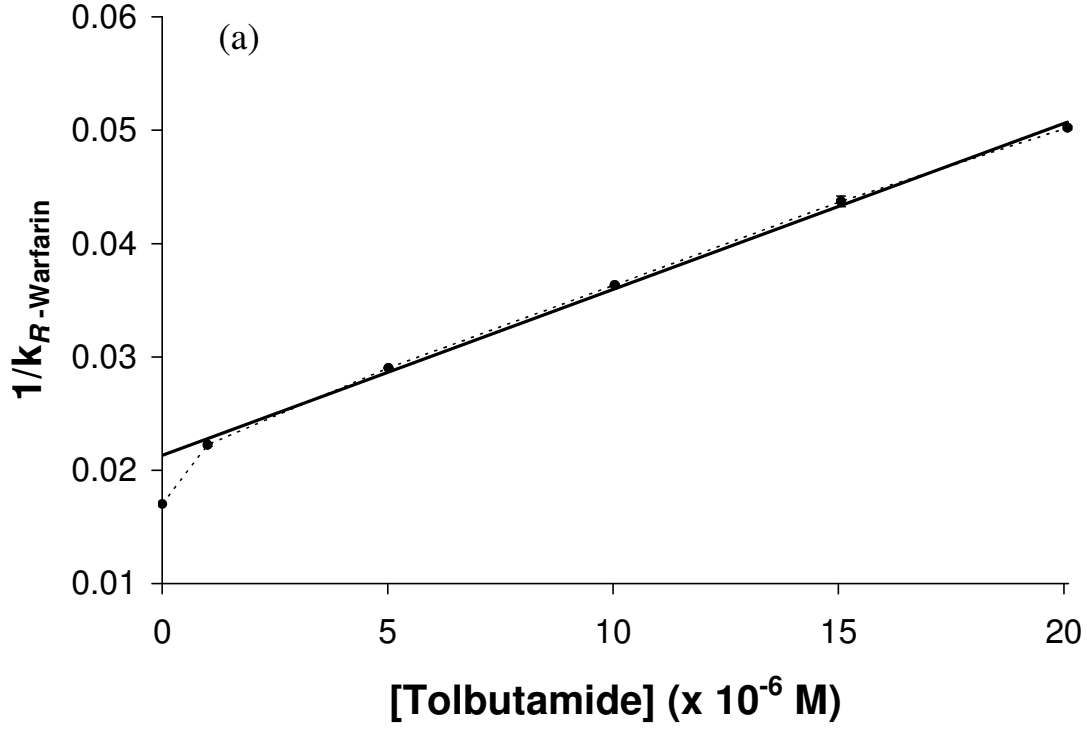
(a)
0.06
0.05
0.04
0.03
0.02
0.01
1/k_R-Warfarin
0
5
10
15
20
[Tolbutamide] (x 10^-6 M)

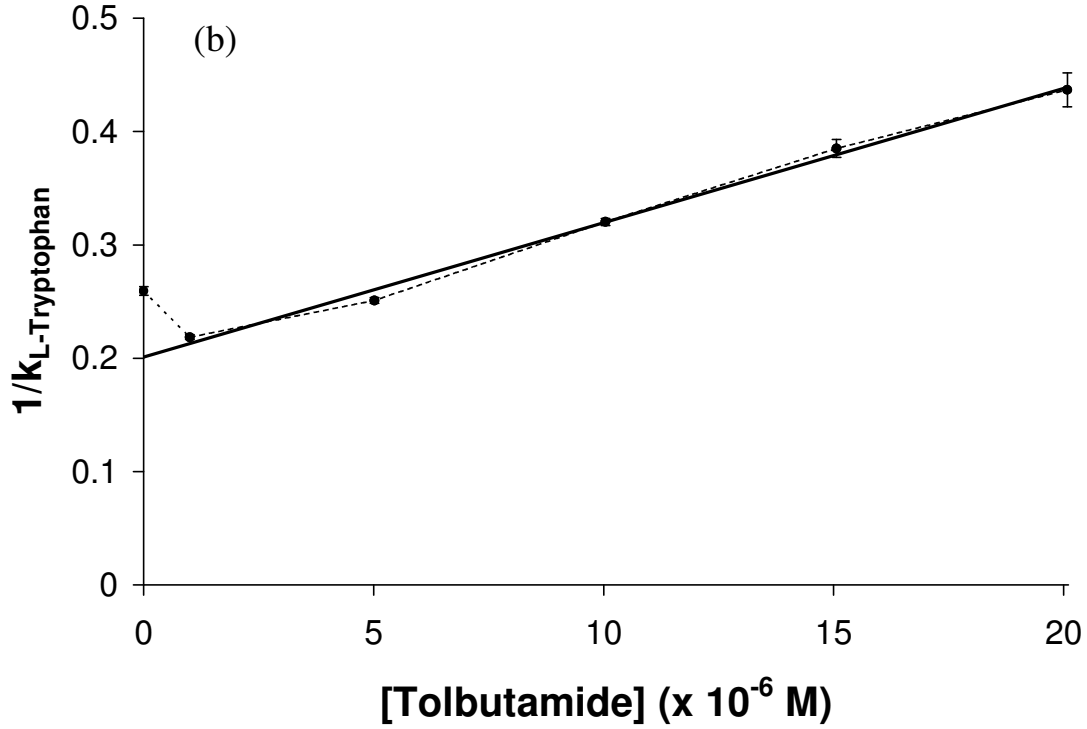
(b)
0.5
0.4
0.3
0.2
0.1
0
1/k_L-Tryptophan
0
5
10
15
20
[Tolbutamide] (x 10^-6 M)

zonal elution. The K_a value for tolbutamide binding at Sudlow site I was 5.9 (± 0.3) x 10^4 M^{-1} and the K_a value for the binding of tolbutamide at Sudlow site II was 6.9 (± 0.2) x 10^4 M^{-1}. These values were close to one another, showing a possibility of why the frontal analysis studies were unable to differentiate these binding constants at the high-affinity sites. Without running zonal elution studies, frontal analysis alone would have overestimated the high-affinity binding constant for tolbutamide due to an inability to separate such closely related binding constants for these two regions. This is a good example of why zonal elution and frontal analysis can be used to complement one another in gaining information about drug-protein interactions. Similar results were found for a normal HSA column, where the binding of tolbutamide at Sudlow site I gave a K_a of 5.5 (± 0.2) x 10^4 M^{-1} and at Sudlow site II gave a K_a of 5.3 (± 0.2) x 10^4 M^{-1}. The binding constants at both of these sites increased slightly on the gHSA1 column, perhaps attributing to the overall increase in the binding constant that was found when using frontal analysis.

Tolbutamide Binding to gHSA2

The gHSA2 column was used to examine the binding of tolbutamide at higher levels of glycation. Frontal analysis was performed and the data were fit to Equation 5-1 for a one-site model. The data deviated from linearity at high concentrations, so Equation 5-5 was used to calculate binding constants for the high-affinity sites using the lower analyte concentrations of 1-10 μM. This gave a K_a value of 1.1 (± 0.1) x 10^5 M^{-1} and an m_L value of 2.1 (± 0.3) x 10^{-8} mol with a correlation coefficient of 0.999 (n = 5).

The data were then fit to the two-site model. This model gave a lower K_a value of 8.4 (± 1.6) x 10^4 M^{-1} for the high-affinity binding site, which was similar to the K_a value calculated using the single-site model. The lower-affinity binding sites also seemed to have a larger standard error, giving a K_a value of 7.8 (± 5.1) x 10^3 M^{-1}. The binding capacities for these two sites are 2.2 (± 0.4) x 10^{-8} mol and 1.9 (± 0.2) x 10^{-8} mol, respectively. The binding capacities along with the protein content of the column gave activities of 1.0 (± 0.3) for the high-affinity binding sites and 0.87 (± 0.18) for the lower-affinity sites. These activities suggested more than one binding region was taking part in the interactions at these binding sites.

Zonal elution studies were performed to determine the retention factors and binding constants for tolbutamide at Sudlow sites I and II. In these studies, *R*-warfarin was used to examine Sudlow site I, where a retention factor of 58 (± 3) was calculated for the drug at [I] = 0. For consistency, the concentration at 0 μM tolbutamide was removed from the linear regression (r = 0.994, n = 5). This experimental value gave a retention factor of 64 (± 1), which was 10% different from the predicted value. L-Tryptophan was used to examine Sudlow site II, where a retention factor of 6.8 (± 0.2) at [I] = 0 was calculated for the compound, with a correlation coefficient of 0.999 for the best-fit line. Again, the data when no tolbutamide was present in solution was removed from the regression calculations but was found to be 5.8 (± 0.1) or a 14% difference from the predicted value.

Association equilibrium constants for tolbutamide were calculated to be 6.6 (± 0.5) x 10^4 M^{-1} for Sudlow site I and 7.2 (± 0.3) x 10^4 M^{-1} for Sudlow site II. The association equilibrium constant for Sudlow site I was statistically identical to the gHSA1

column when taking into account the standard deviation of this value. The association constant for Sudlow site II increased in this column compared to the gHSA1 column. The K_a values calculated using this model were both lower than the high-affinity K_a value calculated using either of the frontal analysis models, but considering the proximity of the values to one another the frontal analysis model might not have been able to differentiate these two values.

Tolbutamide Binding to gHSA3

The final study was performed using the third and most highly glycated HSA column. Frontal analysis was performed for this system with the data fit to a one-site model. As expected, the data deviated from linearity at high analyte concentrations, so the low analyte concentrations were used to estimate binding constants for the high-affinity binding sites. Using Equation 5-5, a K_a of 1.0 (± 0.2) x 10^5 M^{-1} and an m_L of 1.8 (± 0.3) x 10^{-8} mol was calculated for this set of sites. This association equilibrium constant was comparable to the K_a calculated for the gHSA2 column.

A two-site binding model was used to try and differentiate the high- and lower-affinity binding sites for this column. This model resulted in association equilibrium constants of 8.9 (± 0.6) x 10^4 M^{-1} and 1.7 (± 1.1) x 10^3 M^{-1} for the high- and lower-affinity binding sites, respectively. The corresponding m_L values for these sites were 1.9 (± 0.1) x 10^{-8} mol and 3.6 (± 1.4) x 10^{-8} mol, with activities of 1.0 (± 0.1) and 1.9 (± 0.8), respectively. The K_a and activity calculated for the high-affinity binding sites were similar to those for the gHSA2 column, possibly indicating that any binding changes for this drug had begun to level out. The lower-affinity binding constants gave values

expected for non-specific binding interactions, including lower K_a values with high associated errors and high activities.

Competition studies were performed to determine if changes were taking place at Sudlow sites I and II at this level of glycation (Note: although this column did not seem to give deviations when no tolbutamide was present in the mobile phase, as did the other two columns, the point at [I] = 0 was still removed to make the data analysis consistent). Linear regression performed on each data set resulted in responses with correlation coefficients of 0.998 for L-tryptophan and 0.999 for *R*-warfarin (n = 5). From these plots, *R*-warfarin had a predicted retention factor of 45 (± 1), or a value only 5% from the experimental retention factor of 47 (± 1) at [I] = 0. Likewise, L-tryptophan had a predicted retention factor of 5.3 (± 0.1) at [I] = 0, which was within 5% of the experimental value of 5.1 (± 0.1). The K_a value calculated for tolbutamide at Sudlow site I using this model was 6.5 (± 0.2) x 10^4 M^{-1}. This value was comparable to the binding constant determined for the gHSA2 column; the error associated with the gHSA2 column overlapped with this value, making the results statistically identical. The K_a value calculated for tolbutamide at Sudlow site II was 6.4 (± 0.3) x 10^4 M^{-1}. This value decreased from the gHSA2 column value, which had increased from the gHSA1 value.

Conclusion

These studies showed that as glycation levels increase on HSA, acetohexamide and tolbutamide continue to have access to and bind to Sudlow sites I and II on HSA. Frontal analysis using acetohexamide indicated that there was no appreciable change in going from normal HSA to mildly glycated HSA, but as the level of glycation was further

increased small increases in the association equilibrium constant were evident. Similar studies using tolbutamide showed an increase in the equilibrium constant for the high-affinity group of sites in going from normal to glycated HSA, which decreased for subsequent glycation levels.

Competition studies indicated that the association equilibrium constant of both tolbutamide and acetohexamide at Sudlow site I increased from normal HSA to glycated HSA but then decreased with increased glycation levels. At Sudlow site II, the K_a for acetohexamide decreased from normal to glycated HSA then increased with increased levels of glycation, while tolbutamide binding increased from normal HSA through gHSA2 but then decreased for gHSA3. Even small changes in drug-protein binding can affect the free fraction of the drug, which can have serious consequences on the blood sugar levels of an individual with diabetes. This is important when determining a patient's dosage level. Further studies can be done to examine the binding of these drugs in combination with other drugs.

References

1. Mendez, D. L.; Jensen, R. A.; McElroy, L. A.; Pena, J. M.; Esquerra, R. M., *Arch. Biochem. Biophys.* **2005,** *444*, 92-99.
2. Nakajou, K.; Watanabe, H.; Kragh-Hansen, U.; Maruyama, T.; Otagiri, M., *Biochim. Biophys. Acta* **2003,** *1623*, 88-97.
3. Ascenzi, P.; Bocedi, A.; Notari, S.; Fanali, G.; Fesce, R.; Fasano, M., *Mini-Rev. Med. Chem.* **2006,** *6*, 483-489.
4. Abou-Zied, O. K.; Al-Shihi, O. I. K., *J. Am. Chem. Soc.* **2008,** *130*, 10793-10801.
5. Petitpas, I.; Bhattacharya, A. A.; Twine, S.; East, M.; Curry, S., *J. Biol. Chem.* **2001,** *276* (25), 22804-22809.
6. Fasano, M.; Curry, S.; Terreno, E.; Galliano, M.; Fanali, G.; Narciso, P.; Notari, S.; Ascenzi, P., *IUBMB Life* **2005,** *57* (12), 787-796.
7. Dockal, M.; Carter, D. C.; Ruker, F., *J. Biol. Chem.* **1999,** *274* (41), 29303-29310.
8. Colmenarejo, G., *Med. Res. Rev.* **2003,** *23* (3), 275-301.
9. Dockal, M.; Chang, M.; Carter, D. C.; Ruker, F., *Protein Sci.* **2000,** *9*, 1455-1465.
10. Sudlow, G.; Birkett, D. J.; Wade, D. N., *Mol. Pharmacol.* **1975,** *11*, 824-832.
11. Sudlow, G.; Birkett, D. J.; Wade, D. N., *Mol. Pharmacol.* **1976,** *12*, 1052-1061.
12. Bertucci, C.; Andrisano, V.; Gotti, R.; Cavrini, V., *J. Chromatogr. B* **2002,** *768*, 147-155.
13. Herve, F.; Urien, S.; Albengres, E.; Duche, J.-C.; Tillement, J.-P., *Clin. Pharmacokinet.* **1994,** *26* (1), 44-58.
14. Ascoli, G. A.; Domenici, E.; Bertucci, C., *Chirality* **2006,** *18*, 667-679.

15. Iberg, N.; Fluckiger, R., *J. Biol. Chem.* **1986,** *261* (29), 13542-13545.

16. Garlick, R. L.; Mazer, J. S., *J. Biol. Chem.* **1983,** *258* (10), 6142-6146.

17. Loubatieres, A., *Ann. NY Acad. Sci.* **1957,** *71*, 4-11.

18. Green, J. B.; Feinglos, M. N., *Curr. Diabetes Rep.* **2006,** *6*, 373-377.

19. Skillman, T. G.; Feldman, J. M., *Am. J. Med.* **1981,** *70*, 361-372.

20. Jakoby, M. G.; Covey, D. F.; Cistola, D. P., *Biochem.* **1995,** *34*, 8780-8787.

21. Koyama, H.; Sugioka, N.; Uno, A.; Mori, S.; Nakajima, K., *Biopharm. Drug Dispos.* **1997,** *18* (9), 791-801.

22. Tsuchiya, S.; Sakurai, T.; Sekiguchi, S.-i., *Biochem. Pharmacol.* **1984,** *33* (19), 2967-2971.

23. Hage, D. S., *J. Chromatogr. B* **2002,** *768*, 3-30.

24. Schiel, J. E.; Joseph, K. S.; Hage, D. S., Biointeraction Affinity Chromatography. In *Adv. Chromatogr.*, Grinsberg, N.; Grushka, E., Eds. Taylor & Francis: New York, 2010; Vol. 48.

25. Tweed, S. A. Effects of Heterogeneity on the Characterization of Chromatographis Stationary Phases. Thesis, University of Nebraska, Lincoln, 1997.

26. Loun, B.; Hage, D. S., *J. Chromatogr.* **1992,** *579*, 225-235.

27. Ruhn, P. F.; Garver, S.; Hage, D. S., *J. Chromatogr. A* **1994,** *669* (1-2), 9-19.

28. Joseph, K. S.; Moser, A. C.; Basiaga, S.; Schiel, J. E.; Hage, D. S., *J. Chromatogr. A* **2009,** *1216* 3492-3500.

29. Lapolla, A.; Fedele, D.; Reitano, R.; Arico, N. C.; Seraglia, R.; Traldi, P.; Marotta, E.; Tonani, R., *J. Am. Soc. Mass Spectrom.* **2004,** *15*, 496-509.

30. Ney, K. A.; Colley, K. J.; Pizzo, S. V., *Anal. Biochem.* **1981,** *118*, 294-300.

31. Yang, J.; Hage, D. S., *J. Chromatogr. A* **1997,** *766*, 15-25.

32. Loun, B.; Hage, D. S., *Anal. Chem.* **1994,** *66* (21), 3814-3822.

33. Yang, J.; Hage, D. S., *J. Chromatogr.* **1993,** *645* (2), 241-250.

34. Conrad, M. L.; Moser, A. C.; Hage, D. S., *J. Sep. Sci.* **2009,** *32*, 1145-1155.

35. Moser, A. C.; Kingsbury, C.; Hage, D. S., *J. Pharm. Biomed. Anal.* **2006,** *41*, 1101-1109.

CHAPTER 6

THEORETICAL CONSIDERATIONS IN DRUG-PROTEIN BINDING

Introduction

Binding to serum proteins greatly influences the pharmacokinetics and pharmacodynamics of drugs.[1] Binding to such proteins affects the absorption, distribution, metabolism and excretion of these compounds.[2] In many situations, the binding of a drug to a serum transport protein can aid or impair the distribution of the drug to target tissues, which can affect the efficacy of the drug. Any modifications in the protein, such as structure or concentration, can also alter the binding of a drug to the protein.[3]

There are many proteins in human plasma, however, only a small number of these are considered transport proteins. The transport proteins that bind with the highest affinity are often specific for a particular compound, such as vitamin D (vitamin D-binding protein) or thyroxine (thyroxine-binding globulin).[3] The proteins with lower binding affinities are often less specific and bind a wider range of analytes. The two most important of these latter transport proteins are α_1-acid glycoprotein (AGP) and human serum albumin (HSA).[1, 3] The focus of this text will be on drug-protein binding with HSA.

HSA binds a wide variety of endogenous and exogenous compounds and is the most important nonspecific transport protein in the circulation. It is the most abundant protein in plasma, with a concentration of ~40 mg/mL, and accounts for almost 60% of total plasma proteins.[2] Although HSA binds and transports many endogenous

compounds (e.g. fatty acids, bilirubin, bile salts, and hormones) it is most studied for its startling ability to bind a wide variety of drugs.[2] HSA has two major binding sites for drugs: Sudlow site I, or the warfarin-azapropazone site, and Sudlow site II, or the indole-benzodiazepine site, as well as a number of minor binding sites.[4-6]

Equilibrium dialysis, ultrafiltration, and ultracentrifugation are the most widely used methods in drug-protein binding studies.[1] In these techniques, a drug-protein solution must reach equilibrium before the free fraction and bound fraction of the drug are separated and analyzed to determine the free fraction in solution. Typically these techniques require high sample and protein concentrations in order to allow detection of the free fraction. Another method used in these types of studies is high-performance affinity chromatography (HPAC). This method offers low sample requirements and does not require a prior separation step. It also offers good precision, reproducibility, and ease of automation.[7]

There are two main methods utilized with HPAC: zonal elution and frontal analysis. Zonal elution involves injecting a small plug of sample onto a column containing an immobilized ligand while monitoring the elution time or volume of an injected solute.[7, 8] Frontal analysis is performed by continuously applying a sample to the column and instead of a peak, like that obtained in zonal elution, a breakthrough curve will result and a measurement of the breakthrough time is then made. There are a number of practical considerations to consider when performing these studies; however, this text will focus primarily on determining the appropriate analyte concentration that should be used to ensure that all binding interactions are observed during drug-protein

binding studies. Also, optimization of these concentrations may allow use of a small analyte concentration range that will save time and money for such studies.

Theory

Frontal Analysis Theory

The frontal analysis data used in these theoretical studies were previously analyzed using Equations 6-1 and 6-2 for a single-site binding model (Note: derivations for Equations 6-1 and 6-2 can be found in Reference 9).[7-9]

$$\frac{1}{m_{Lapp}} = \frac{1}{(K_a m_L[\mathrm{A}])} + \frac{1}{m_L} \tag{6-1}$$

$$m_{Lapp} = \frac{m_L K_a[\mathrm{A}]}{(1 + K_a[\mathrm{A}])} \tag{6-2}$$

In these equations, m_{Lapp} is the apparent moles of analyte required to saturate the column at a given analyte concentration [A], while m_L is the binding capacity of the column. The value K_a is the association equilibrium constant for the analyte with the ligand. When $1/m_{Lapp}$ vs. 1/[A] is plotted, Equation 6-1 predicts a linear result if single-site binding is taking place between the analyte and the ligand. If linear deviations occur at high concentrations (low 1/[A] values), more than one binding site on the ligand is involved in analyte binding.

The above equations can be expanded to describe multiple binding sites. Equations 6-3, 6-4, and 6-5 are examples of such expansions for a two-site binding model.[7, 8, 10]

$$\frac{1}{m_{Lapp}} = \frac{1 + K_{a1}[\mathrm{A}] + \beta_2 K_{a1}[\mathrm{A}] + \beta_2 K_{a1}^2[\mathrm{A}]^2}{m_{Ltot}\{(\alpha_1 + \beta_2 - \alpha_1\beta_2)K_{a1}[\mathrm{A}] + \beta_2 K_{a1}^2[\mathrm{A}]^2\}} \tag{6-3}$$

$$\lim_{[A]\to 0} \frac{1}{m_{Lapp}} = \frac{1}{m_{Ltot}(\alpha_1 + \beta_2 - \alpha_1\beta_2)K_{a1}[A]} + \frac{\alpha_1 + \beta_2^{\,2} - \alpha_1\beta_2^{\,2}}{m_{Ltot}(\alpha_1 + \beta_2 - \alpha_1\beta_2)^2} \qquad (6\text{-}4)$$

$$m_{Lapp} = \frac{m_{L1}K_{a1}[A]}{(1 + K_{a1}[A])} + \frac{m_{L2}K_{a2}[A]}{(1 + K_{a2}[A])} \qquad (6\text{-}5)$$

In these equations, K_{a1} is the association equilibrium constant for the binding site with the highest affinity (L_1), while K_{a2} is the association equilibrium constant for the binding site with the lowest affinity (L_2). The term β_2 is the ratio of the association equilibrium constants, where $\beta_2 = K_{a2}/K_{a1}$ and $0 < K_{a2} < K_{a1}$. The values m_{L1} and m_{L2} correspond to the binding capacities at the high- and low-affinity binding sites, respectively, and the term α_1 represents the fraction of all binding regions that make up the high affinity binding sites (i.e., $\alpha_1 = m_{L1,tot}/m_{Ltot}$). Equation 6-4 is a linear approximation of Equation 6-3 as the concentration of the analyte goes to zero. Although a plot of data according to Equation 6-3 will be non-linear throughout a broad range of concentrations for multi-site binding, a plot using Equation 6-4 approaches linearity at low concentrations and can be used to estimate the binding constant and binding capacity at the high-affinity binding site in this situation.[10] A plot of m_{Lapp} vs. [A] based on Equation 6-5 can be used to find binding constants and binding capacities at both high- and low-affinity binding sites.

Concentration Effects

Some previous theoretical studies have already been conducted that can aid in determining a concentration range suitable for frontal analysis studies in a case with single-site binding.[7] As it turns out, this concentration range is primarily dependent on

the equilibrium constant of the analyte under investigation, as is shown in the following equation.[7]

$$\frac{m_{Lapp}}{m_L} = \frac{K_a[\mathrm{A}]}{1 + K_a[\mathrm{A}]} \qquad (6\text{-}6)$$

It can be seen from Equation 6-6 that the fraction of active ligand sites that are bound to the analyte (m_{Lapp}/m_L) is dependent only on the association equilibrium constant of the analyte (K_a) and the concentration of the analyte ([A]).[7] A plot made according to this equation can be seen in Figure 6-1. When no analyte is present in the system, m_{Lapp}/m_L is equal to zero. As the concentration of the analyte approaches infinity, the fraction m_{Lapp}/m_L will increase and approach a limit of one. The K_a[A] range between zero and infinity shows where m_{Lapp}/m_L has a detectable change in value. For a given 1:1 binding system where 10-90% of the binding sites are filled (i.e., a shift of ± 10% or an m_{Lapp}/m_L range of 0.1-0.9), a K_a[A] range between ~0.1 and 10 would be needed. For an analyte like *S*-warfarin that has a high K_a value of 2.5 x 10^5 M^{-1} on immobilized HSA, this would mean working with a concentration range of 0.5 to 35 μM to see this shift. On the other hand, L-tryptophan, which has a lower binding affinity of 1.1 x 10^4 M^{-1} for HSA, would need a concentration range that spans from 10 to 800 μM to produce similar shifts.

Theoretical determinations such as these found by using Equation 6-6 are important to ensure that a drug-protein system has been thoroughly examined. For instance, many compounds bind to HSA at more than one binding site, with initial preferences toward a higher affinity site at lower analyte concentrations. Typically a drug will bind to the highest affinity binding site at lower concentrations while binding to secondary or tertiary sites will become more important as the concentration increases. It

Figure 6-1. Change in m_{Lapp}/m_L vs. $K_a[A]$ for a frontal analysis experiment where the analyte-ligand system has single-site binding

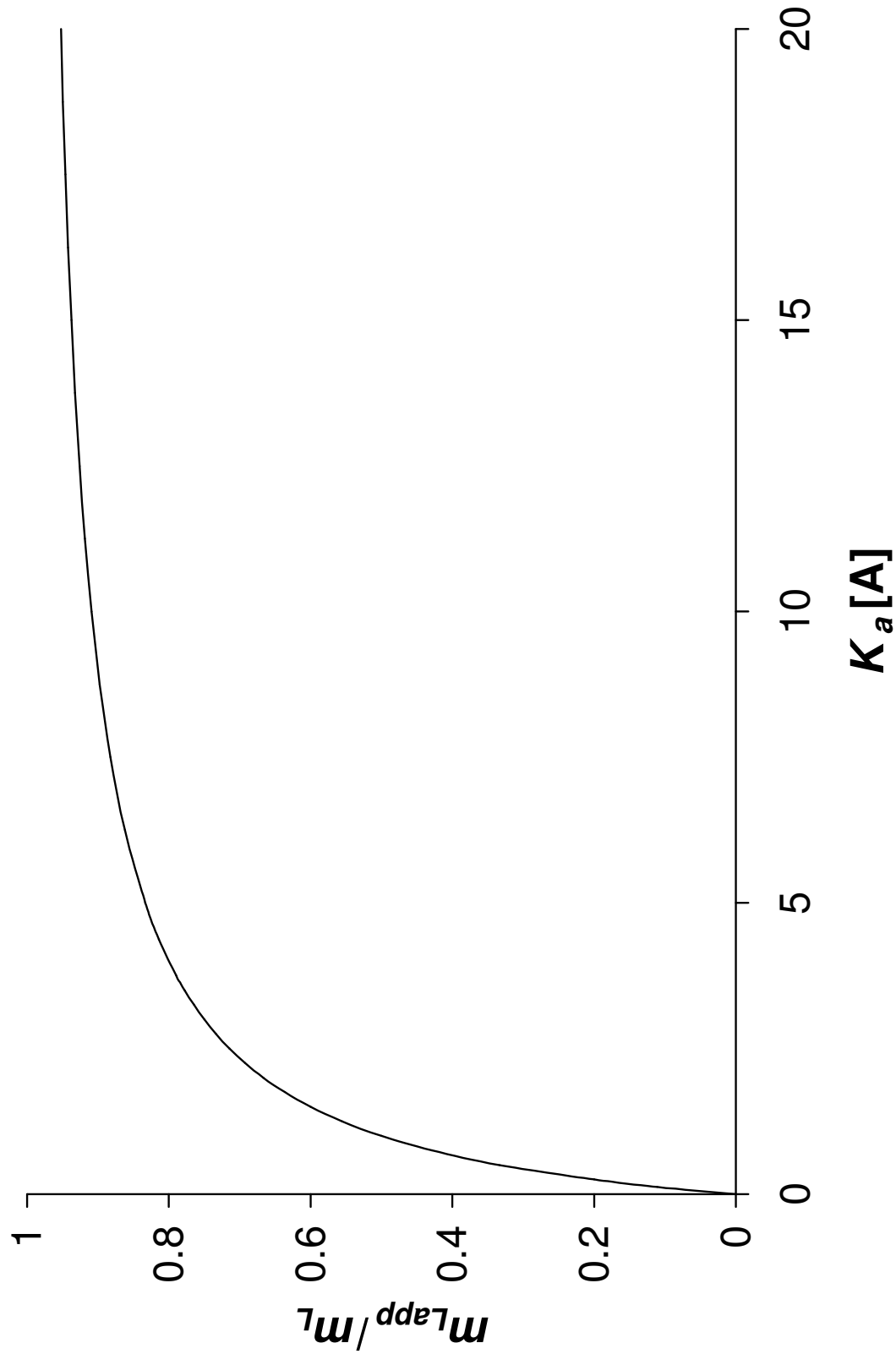
0
0.2
0.4
0.6
0.8
1
m_{Lapp}/m_L
0
5
10
15
20
K_a [A]

is essential to use a concentration range that is large enough to encompass these secondary interactions to ensure that a full representation of the drug-protein interactions is made. Such interactions were studied here using experimental data of compounds that have been previously shown to have interactions at more than one binding region on HSA.[11]

Concentration Determinations Using Confidence Intervals

In this work, confidence intervals are used to examine data from compounds that have multi-site interactions with HSA. Equation 6-4 was used to determine the best-fit line for the drug-protein binding data used in these studies. Confidence intervals were then used to investigate the linear deviations observed for each data set using the following equation at each data point.[12]

$$V_y = V_{res}\left(\frac{1}{n} + \frac{(x-\bar{x})^2}{S_{xx}}\right) \tag{6-7}$$

In Equation 6-7, V_y is the variance of the estimate of y for the best-fit line. V_{res} is the variance of the residuals as defined below,[12]

$$V_{res} = S_{res}^2 = \frac{\sum (y_i - y)^2}{n-2} \tag{6-8}$$

where S_{res}^2 is the standard deviation of the residuals squared, y_i is the calculated value of y at point i, while y is the predicted value for i from the best-fit line. The value n is the number of data points used in the calculation of the best-fit line. The value x was the concentration, while $\bar{x}$ was the average concentration for the data set. The value S_{xx} was the standard deviation, as calculated using Equation 6-9.[12]

$$S_{xx} = \sum (x_i^2) - (\sum x_i)^2 / n \quad (6\text{-}9)$$

Once the variance for *y* had been determined at a given data point, a confidence level for *y*, CL(*y*), was calculated using the following equation.[12]

$$CL(y) = a + b * x \pm t(f, p) * \sqrt{V_y} \quad (6\text{-}10)$$

In Equation 6-10, *a* is the intercept and *b* is the slope given by the best-fit line. The value *t* is taken from the *t*-test for the given number of data points and confidence level. The standard deviation of the mean ($SD_{\bar{y}} = SD/\sqrt{y}$) was then used along with the *t*-value to determine the 95% confidence interval (C.I.) at that data point.[12]

$$y \pm t * S_{\bar{y}} \quad (6\text{-}11)$$

This was repeated at all data points for the given drug-protein system and used to create a confidence interval at a 95% confidence level for the best-fit line.

Experimental

All experimental materials and methods for the frontal analysis studies can be found in Chapters 3 and 5 of this dissertation.

Results and Discussion

Acetohexamide has been investigated in previous binding studies with both normal and glycated HSA (see Chapters 3 and 5).[11] An initial fit of the normal HSA data to a one-site binding model using Equation 6-1 showed linear deviations at high concentrations, suggesting that acetohexamide was interacting with HSA at more than one binding site. In this instance, data at relatively low concentrations (i.e., 1-10 μM

acetohexamide) were used to estimate the association equilibrium constant for the high-affinity binding sites using Equation 6-4. This value was determined to be 2.0 (± 0.1) x 10^5 M^{-1}. The data was also fit to two- and three-site binding models, with the best fit determined to be to a two-site model. This drug was found to have an overall association equilibrium constant of 1.3 (± 0.2) x 10^5 M^{-1} for its high-affinity binding sites using a two-site model (Equation 6-5), as determined using a concentration range of 1-1000 μM acetohexamide.

Using the equilibrium constant from the single-site binding model with Equation 6-6, a concentration range of 1-50 μM acetohexamide would have been sufficient to perform these studies, while using the data from the two-site model and Equation 6-6 a concentration range of 1-70 μM would be needed. The difference in estimated equilibrium constants using Equation 6-4 and Equation 6-5 resulted in a 40% increase in the concentration range necessary to observe the full binding range for this drug. The general question that this leads to is what concentration range is necessary to gain reliable binding data from such a system?

Using the acetohexamide data and the single-site binding model, the best-fit line for the lower concentrations (1-5 μM) was analyzed to determine when the data deviated from this line at a 95% confidence level. Calculations were performed at each data point using Equations 6-7 to 6-11. The number of data points used to evaluate the best-fit line was determined using a series of residual plots. Concentrations 1 to 5 μM acetohexamide, $n = 5$, gave seemingly scattered residuals while adding two more data points (going up to 10 μM acetohexamide) started to show a pattern in the residual plot (Note: little variation was noted between the slope and intercept of these two plots;

however, it seemed prudent to use only the lower five concentrations when performing the fit for these studies due to the information gained from the residual plots). A *t* value of 3.18 was used in these calculations for a 95% confidence level.

Equations 6-7 to 6-11 were used to determine the confidence interval at each concentration from 1 to 1000 μM acetohexamide and plotted along with the best-fit line. The numerical results are shown in Table 6-1, with the graphical results seen in Figure 6-2. From these results, it appeared as though the results started to move out of the 95% confidence interval at 10 μM acetohexamide and were visibly outside of this interval at 20 μM acetohexamide. This theoretical model suggested that using a concentration range of 1-50 μM is more than adequate to see the binding heterogeneity that is present in multi-site binding models for acetohexamide when using plots made according to Equation 6-4.

The frontal analysis data for acetohexamide data were also fit to a two-site model using Equation 6-5. While theoretical calculations were not made using this type of model, simple visual observations were used to examine the results found using the linear-regression confidence interval calculations. The entire data set was originally fit to a two-site model to obtain a K_a value at the high-affinity binding site of 1.3×10^5 M^{-1}. A smaller data set was used to fit only concentrations of 1-50 μM acetohexamide to this model. This concentration range was used to examine both the one-site model (Equation 6-2) and the two-site model to determine if distinctions could be made using this concentration range (Figure 6-3). Deviations of the data from the one-site model are most evident at 20 and 50 μM acetohexamide shown in Figure 6-3(a), while the two-site model, shown in Figure 6-3(b) appears to have an improved fit for these data points.

Table 6-1. Confidence interval data calculated for acetohexamide according to Equations 6-7 through 6-11 at the 95% confidence level. The first three significant figures are underlined.

1/[Acetohexamide] (M^{-1})	Predicted	C.I. (+)	C.I. (-)	Experimental	SD (Experimental)
1.00E+06	305688241.6	312071164.5	299305318.8	305222354.5	380483.9206
8.00E+05	255819160.2	260334073.5	251304246.9	254595312.8	99898.50694
5.71E+05	198825924.3	202490150.3	195161698.3	200187021.9	364343.8178
4.00E+05	156080997.4	160510830.6	151651164.1	159088335.5	152574.2973
2.00E+05	106211915.9	112474476.6	99949355.27	103533214.7	417335.3436
1.33E+05	89588888.78	96568234.46	82609543.10	84483318.50	58417.05282
1.00E+05	81277375.21	88626659.25	73928091.17	73554876.54	228816.6904
5.00E+04	68810104.85	76725701.99	60894507.72	58312815.86	209566.7377
3.33E+04	64654348.07	72761333.65	56547362.49	50826782.33	159533.4508
2.00E+04	61329742.64	69590676.86	53068808.42	43722616.43	403027.2491
1.00E+04	58836288.57	67213146.10	50459431.03	36514118.79	671536.8986
3.33E+03	57172271.68	65626702.30	48717841.07	32113840.57	1182529.949
2.00E+03	56841525.31	65311394.30	48371656.33	25256511.44	508298.3995
1.33E+03	56675215.27	65152849.60	48197580.94	23582722.87	1565851.176
1.00E+03	56592120.08	65073634.89	48110605.26	20485137.35	1447220.635

Figure 6-2. Frontal analysis data for acetohexamide with low concentrations fit to a best-fit line according to Equation 6-4. Confidence intervals at a 95% confidence level are shown on either side of the best-fit line.

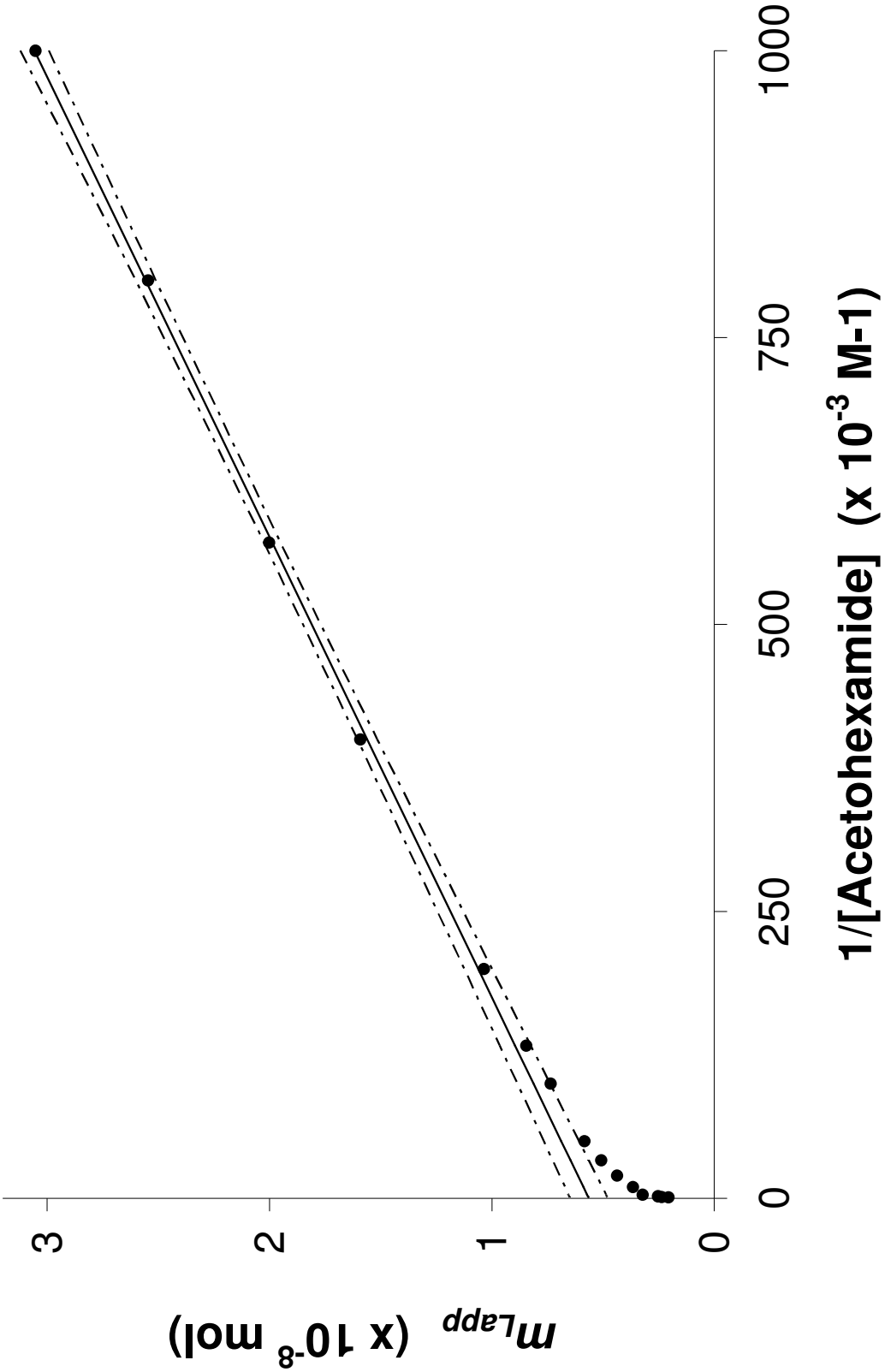
0
1
2
3
m_{Lapp} (x 10^{-8} mol)
0
250
500
750
1000
1/[Acetohexamide] (x 10^{-3} M-1)

Figure 6-3. Plot of m_{Lapp} vs. [acetohexamide] for concentrations 1-50 μM using (a) Equation 6-2 and (b) Equation 6-5.

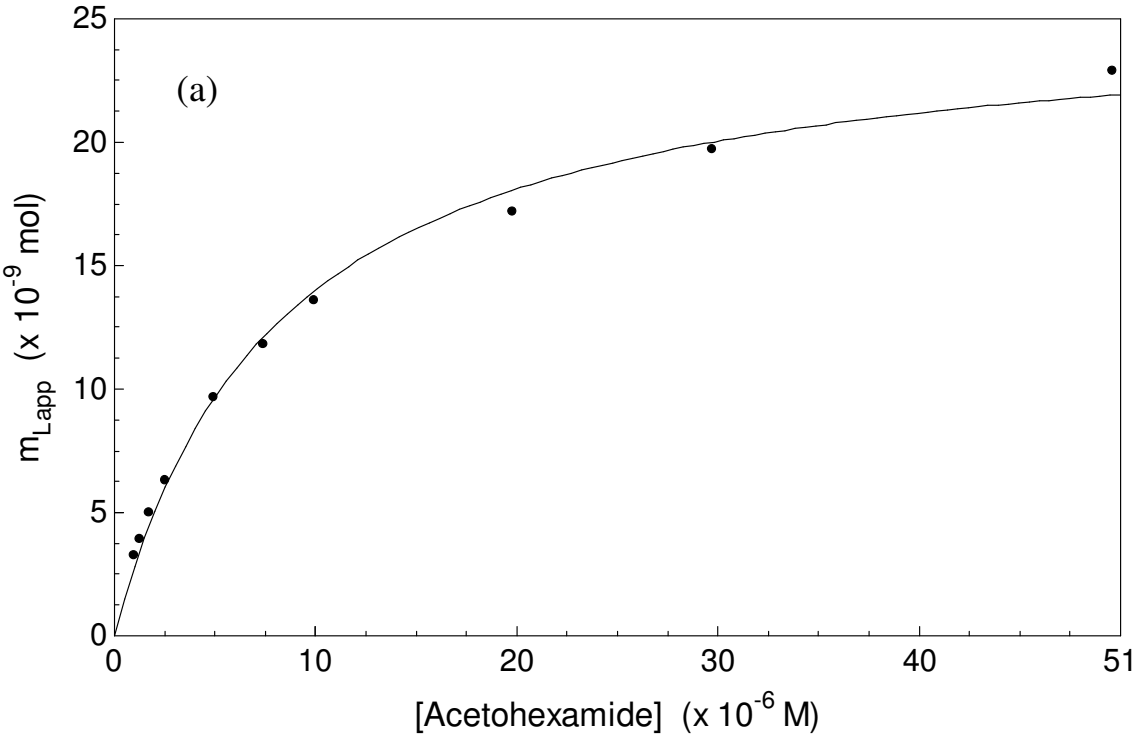
(a)
m_{Lapp} (x 10^{-9} mol)
[Acetohexamide] (x 10^{-6} M)
0
5
10
15
20
25
0
10
20
30
40
51

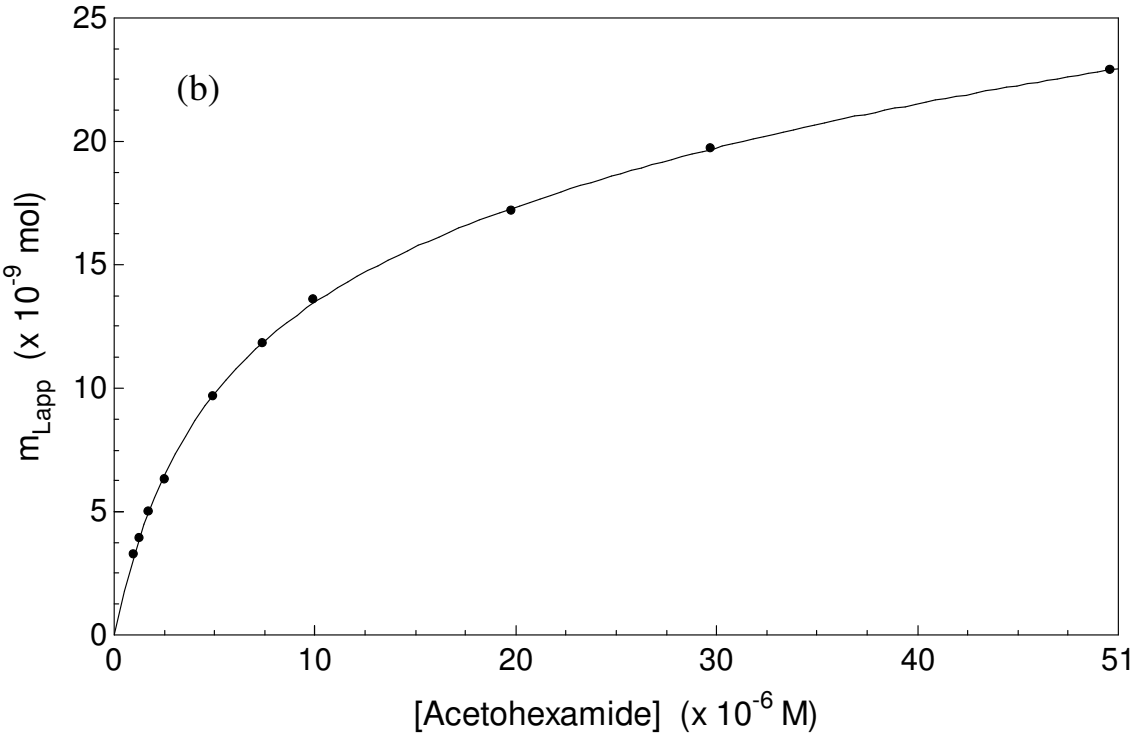
(b)
m_{Lapp} (x 10^{-9} mol)
[Acetohexamide] (x 10^{-6} M)
0
5
10
15
20
25
0
10
20
30
40
51

Using these concentrations, it was apparent that the data still fit best to the two-site binding model versus the one-site model. A K_a value of 2.2 (± 0.2) x 10^5 M^{-1} was obtained for the high-affinity binding site using the two-site model. This value was within one standard deviation of the K_a value calculated using only the low concentrations of the original linear one-site model and Equation 6-4. Similar results were shown for acetohexamide binding to glycated HSA (results not shown).

Theoretical calculations were performed using data gained from studies with tolbutamide and a normal HSA column. Using a concentration range of 1-10 μM tolbutamide, a best-fit line was made to the data. This concentration range was chosen after making a series of residual plots made for the data. Previous studies determined the K_a value of tolbutamide at the high-affinity binding site to be 8.7 (± 0.6) x 10^4 M^{-1}. Equation 6-1 predicts that a concentration range of 1-100 μM is necessary to see the entire interaction of tolbutamide with HSA for such a site. These studies originally used a concentration range of 1-200 μM tolbutamide which was more than sufficient for such work.

The previous studies performed with tolbutamide binding to normal HSA showed that tolbutamide binds to HSA at two high-affinity binding sites with statistically identical affinity. This made it especially difficult to separate the high-affinity binding site into two distinct binding sites. Analyzing the best-fit line for tolbutamide at the 95% confidence level gave the plot shown in Figure 6-4 and corresponding numerical values shown in Table 6-2. At the 95% confidence level, 100 μM tolbutamide is outside of the linear range of the data, as shown in Table 6-2. The plot shows that linear deviations are becoming apparent by 50 μM tolbutamide but the data, listed in Table 6-2, shows that the

Table 6-2. Confidence interval data calculated for tolbutamide according to Equations 6-7 through 6-11 at the 95% confidence level. The first three significant figures are underlined.

1/[Tolbutamide] (M^{-1})	Predicted	C.I. (+)	C.I. (-)	Experimental	SD (Experimental)
8.00E+05	572622265.9	583826460.1	561418071.7	574377438.9	1587647.500
5.71E+05	424893789.2	432119810.1	417667768.4	420005087.1	220492.0343
4.00E+05	314097431.7	320241095.4	307953768.1	316414774.3	969010.3201
2.00E+05	184835014.7	192882170.4	176787859.0	188643514.7	109449.3259
1.00E+05	120203806.1	130001227.7	110406384.5	117211492.6	248278.5945
5.00E+04	87888201.85	98660273.21	77116130.49	82705486.88	2022745.247
2.00E+04	68498839.29	79877964.40	57119714.17	57952437.24	542308.4366
1.00E+04	62035718.43	73620327.47	50451109.39	48320244.42	411295.4363
5.00E+03	58804158.00	70492050.14	47116265.87	41485039.78	1015414.310

Figure 6-4. Frontal analysis data for tolbutamide with low concentrations fit to a best-fit line according to Equation 6-4. Confidence intervals at a 95% confidence level are shown on either side of the best-fit line.

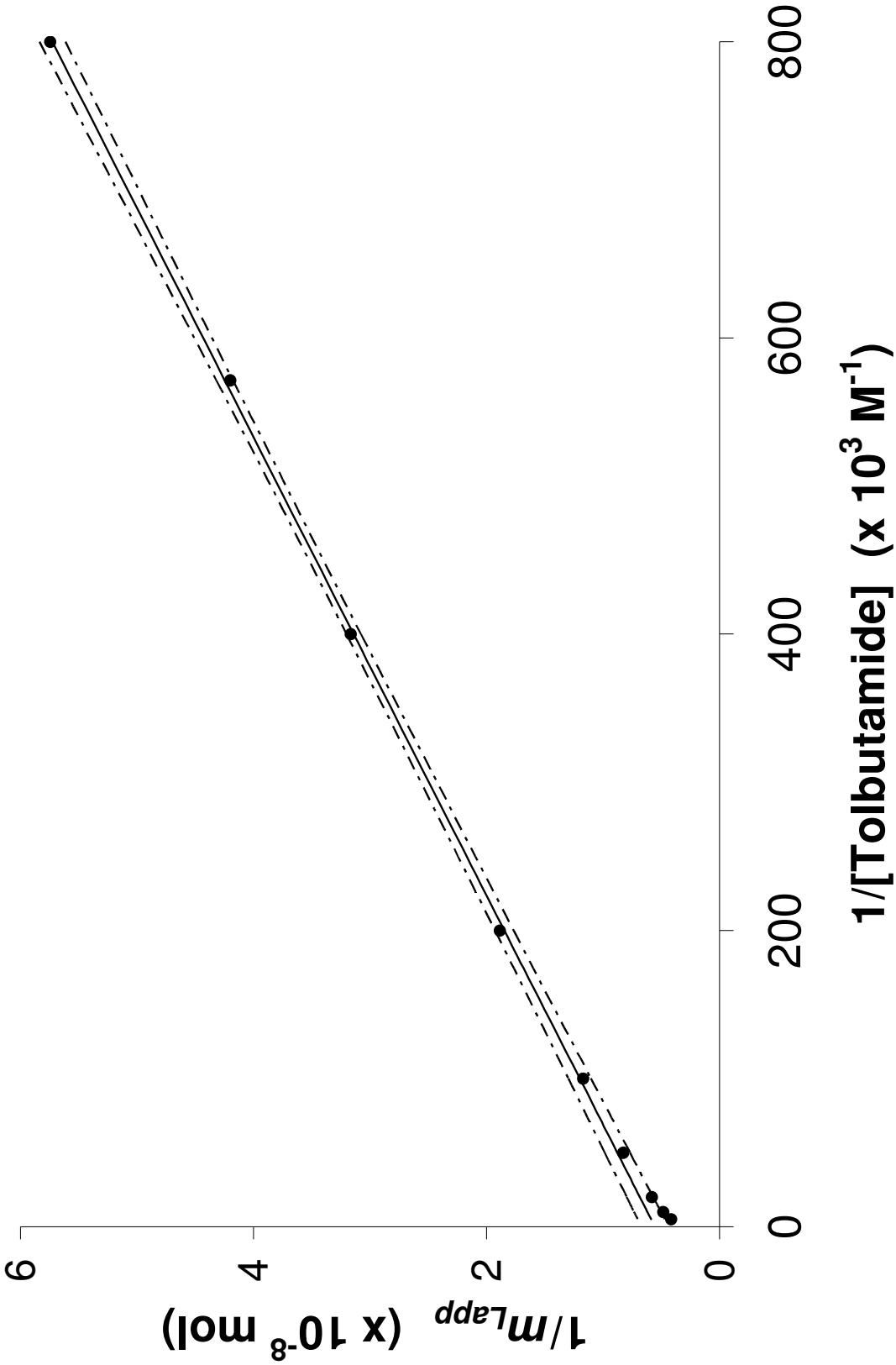
0
200
400
600
800
1/[Tolbutamide] (x 10^3 M^-1)
0
2
4
6
1/m_Lapp (x 10^-8 mol)

Figure 6-5. Plot of m_{Lapp} vs. [tolbutamide] using (a) Equation 6-2 and (b) Equation 6-5.

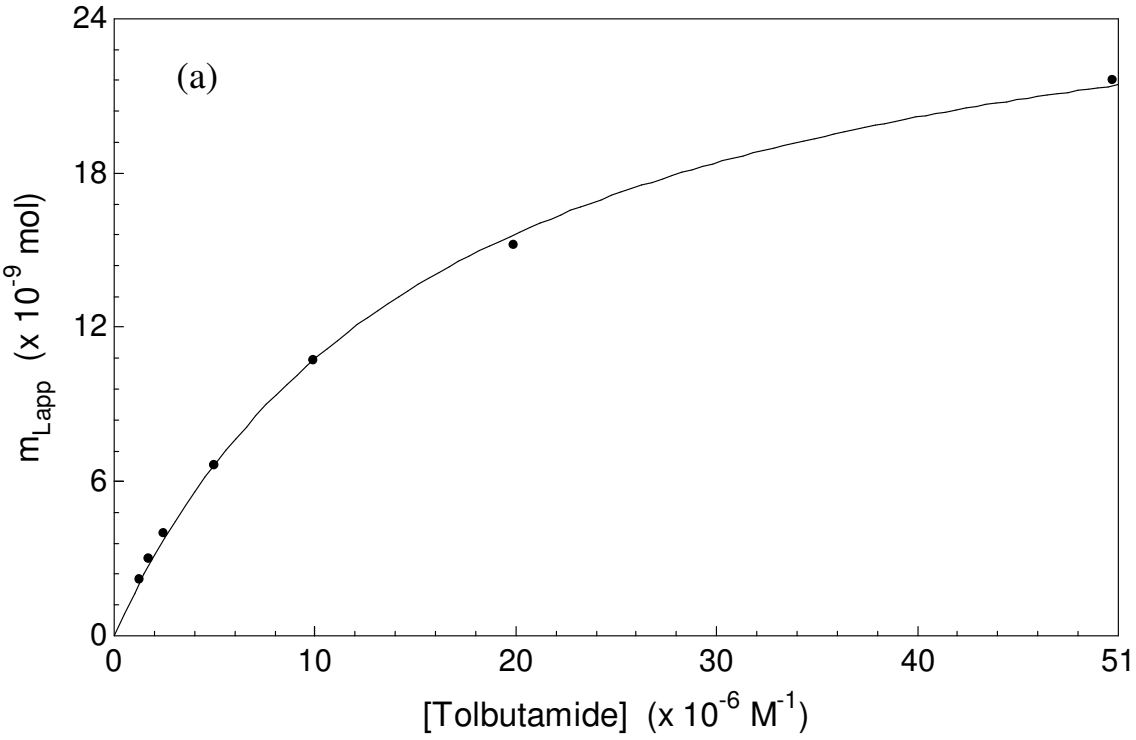
(a)
24
18
12
6
0
0
10
20
30
40
51
m_{Lapp} (x 10^{-9} mol)
[Tolbutamide] (x 10^{-6} M^{-1})

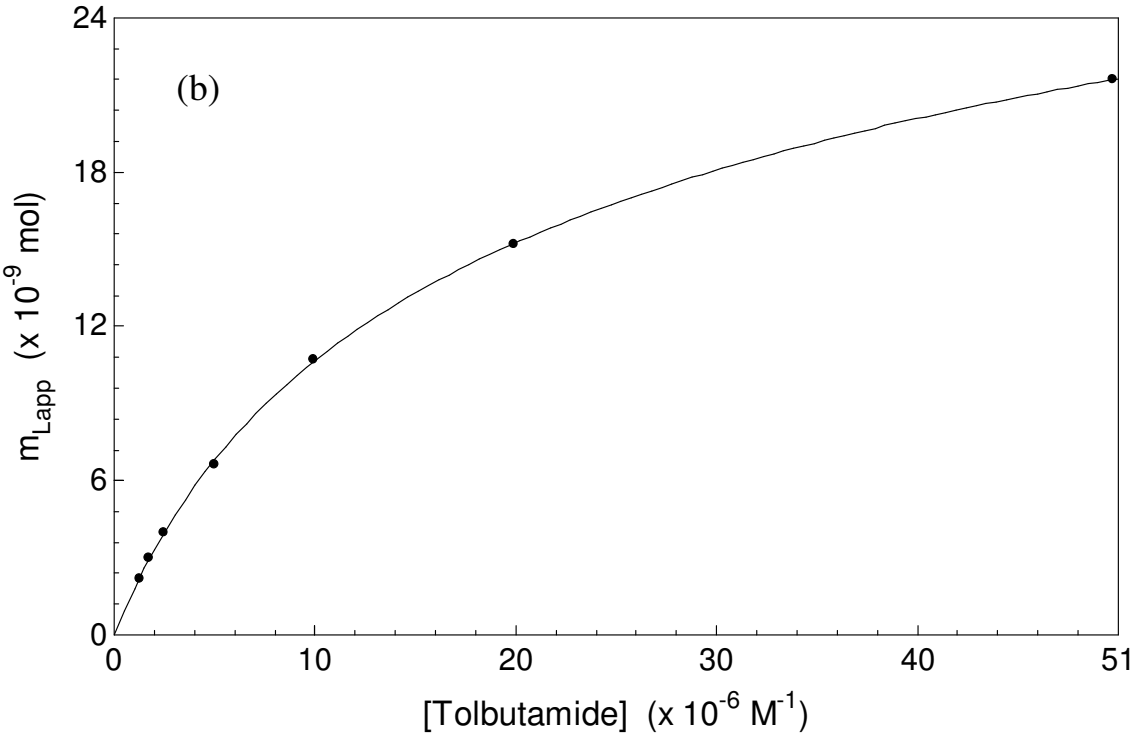
(b)
24
18
12
6
0
0
10
20
30
40
51
m_{Lapp} (x 10^{-9} mol)
[Tolbutamide] (x 10^{-6} M^{-1})

data is not quite outside the 95% confidence interval.

This smaller data set was tested by fitting the concentration range of 1-50 μM tolbutamide to non-linear models using Equation 6-5 (Figure 6-5). The data showed some deviations from the one-site model at 20 and 50 μM tolbutamide, much like acetohexamide. Similar to what was seen when using the full data set, this model had a noticeably better fit to a two-site binding model, giving a K_a of 9.6 (± 3.2) x 10^4 M^{-1} for the high-affinity binding site. This concentration range also produced a higher affinity secondary binding site of 1.2 (± 2.4) x 10^4 M^{-1}, but this site had a high associated standard error.

Conclusion

Theoretical studies examined the concentration ranges that should be used for frontal analysis studies. While the minimum concentration range recommended for acetohexamide, as determined from the experimental binding constant, was between 1 and 50 μM, the theoretical studies showed that linear deviations could actually be seen before reaching 50 μM. It was also shown that a smaller concentration range gave results statistically equivalent to previously determined binding constants using a two-site binding model. The same was true for tolbutamide. This later work is especially important for this study due to the lower experimental binding constant of tolbutamide compared to acetohexamide and two similar high-affinity binding sites. However, it was shown that the same binding constants could be calculated using a narrower concentration range, which will conserve solutions, decrease drug cost, and cut down experiment run times in the future.

References

1. Ascoli, G. A.; Domenici, E.; Bertucci, C., *Chirality* **2006,** *18*, 667-679.
2. Colmenarejo, G., *Med. Res. Rev.* **2003,** *23* (3), 275-301.
3. Herve, F.; Urien, S.; Albengres, E.; Duche, J.-C.; Tillement, J.-P., *Clin. Pharmacokinet.* **1994,** *26* (1), 44-58.
4. Sudlow, G.; Birkett, D. J.; Wade, D. N., *Mol. Pharmacol.* **1975,** *11*, 824-832.
5. Sudlow, G.; Birkett, D. J.; Wade, D. N., *Mol. Pharmacol.* **1976,** *12*, 1052-1061.
6. Sengupta, A.; Hage, D. S., *Anal. Chem.* **1999,** *71*, 3824-3827.
7. Hage, D. S., *J. Chrom. B* **2002,** *768*, 3-30.
8. Schiel, J. E.; Joseph, K. S.; Hage, D. S., Biointeraction Affinity Chromatography. In *Advances in Chromatography*, Grinsberg, N.; Grushka, E., Eds. Taylor & Francis: New York, 2010; Vol. 48.
9. Loun, B. Characterization of Drug-Protein Interactions Using High-Performance Affinity Chromatography. Dissertation, University of Nebraska, Lincoln, 1994.
10. Tweed, S. A. Effects of Heterogeneity on the Characterization of Chromatographis Stationary Phases. Thesis, University of Nebraska, Lincoln, 1997.
11. Joseph, K. S.; Hage, D. S., *J. Chrom. B* **2010,** *submitted*.
12. Meier, P. C.; Zund, R. E., *Statistical Methods in Analytical Chemistry*. John Wiley & Sons: Hoboken, NJ, 1993.

CHAPTER 7

SUMMARY AND FUTURE WORK

Summary of Work

Drug-protein interactions affect the transport and efficacy of the drug in the body. The work in this dissertation used the method of high-performance affinity chromatography to examine drug-protein binding. Frontal analysis was used to determine association equilibrium constants and binding capacity for various analytes with human serum albumin (HSA) and glycated human serum albumin (gHSA). Zonal elution competition studies were used to determine the specific binding location(s) on this protein for each of the analytes.

The first chapter gave a general introduction on the topics presented in this manuscript. It began with a background discussion on diabetes and lead into a brief summary of one specific class of drugs used to treat this disease. This chapter also highlighted the importance of HSA as a transporter protein within the human body and discussed the significance of drug-protein binding studies in determining the efficacy of drugs in the body. The method of high-performance affinity chromatography was also introduced, along with methods such as frontal analysis and zonal elution.

The work in chapter two examined four coumarin compounds as alternatives to warfarin as a probe for drug-protein binding studies using HSA. This study used frontal analysis and zonal elution to determine the binding constants and binding location of the compounds with HSA. All four compounds had interactions that fit a two-site binding model, and warfarin showed direct competition at the high-affinity site for each

compound. After taking into consideration non-specific binding, binding strength, and the number of binding sites on HSA, 4-hydroxycoumarin was determined to be the best alternative to warfarin as a site-selective probe for HSA.

Chapter 3 demonstrated the depth of information that can be gleaned when using both frontal analysis and zonal elution as complimentary methods to look at drug-protein binding. The binding of two sulfonylureas, acetohexamide and tolbutamide, to HSA was examined using high-performance affinity chromatography. Frontal analysis studies showed that acetohexamide and tolbutamide had interactions at two different classes of binding sites on HSA: a high-affinity group of sites and a lower-affinity class of sites. The data obtained using competition studies and zonal elution indicated that the both drugs bound to Sudlow sites I and II with relatively high affinity. It was determined that the combined binding at Sudlow sites I and II made up the high-affinity class of sites found using frontal analysis.

The overall goal of this research was to examine the binding of diabetes drugs to HSA during diabetes. Chapters 4 and 5 use glycated HSA columns to aid in the understanding of these interactions. In Chapter 4, the binding of warfarin and L-tryptophan to glycated HSA was studied. These compounds are often used in drug-HSA binding studies as probe compounds for Sudlow sites I and II, respectively. The association equilibrium constant for warfarin remained consistent as the levels of glycation were increased. The binding constant for L-tryptophan showed an increase with glycated HSA compared to literature values for normal HSA; however, the binding constant remained the same with increasing levels of glycation. These compounds were found to be suitable for use in drug-protein binding studies using glycated HSA.

The binding of acetohexamide and tolbutamide to gHSA was examined in Chapter 5 to determine if changes in binding were exhibited as the level of glycation on HSA was increased to levels typically seen in diabetic individuals. The association equilibrium constants and binding capacities were determined using frontal analysis for the overall drug-protein interactions, while competition studies were used to examine interactions at Sudlow sites I and II. The data obtained using frontal analysis showed little change in the overall binding constant when going from no glycation to mildly glycated HSA at the high-affinity site for acetohexamide; this was followed by a small increase in the association equilibrium constant as glycation levels were increased further. The binding constant for tolbutamide at the high-affinity binding site appeared to have an initial increase when glycation was introduced. However, this value decreased to levels seen for normal HSA as glycation was increased. Competition studies showed an increase in binding constants for both acetohexamide and tolbutamide at Sudlow site I in going from normal to minimally glycated HSA, followed by a decrease as glycated levels increased. The binding of these drugs differed at Sudlow site II, where the association equilibrium constant for acetohexamide decreased upon initial HSA glycation while the binding constant of tolbutamide increased.

Chapter 6 examined the range of analyte concentrations that should be used in frontal analysis studies when examining drug-protein binding for systems with multi-site interactions. Confidence intervals were used to examine data from two compounds that are known to bind to HSA at more than one type of binding site. Theoretical studies with various concentration ranges were compared to known experimental values. This data was used to determine the concentration range that could be used with the tested analytes.

Future Work

These studies primarily focused on the binding of one class of drugs to HSA as glycation levels were increased. The work involved in this dissertation used HSA that was glycated *in vitro* and immobilized via the Schiff base method onto silica. With this in mind, future work could lead in many directions.

More studies could be undertaken to examine the immobilization of the glycated HSA to the silica. Glycated HSA is a heterogeneous compound that can take on many forms. Initial glycation of HSA is actually reversible. It is not until the Amadori product is formed that a stable, covalent bond is made with a sugar molecule. Furthermore, this product can undergo subsequent glycation rearrangements to form advanced glycation endproducts. Therefore, when undertaking covalent immobilization to silica, stability studies would be a valuable tool in determining the length of time in which glycation levels of the proteins remain consistent upon immobilization. To further expand on this, it would also be valuable to look at glycation levels of HSA directly before and directly following immobilization to ensure that the same amount of glycated HSA was being immobilized to the silica without preference to more mildly glycated HSA. Other methods of protein immobilization are currently being explored in our group, including entrapment.

Diabetic patients are unfortunately afflicted with a myriad of illnesses brought on by diabetes. This often means that a large regiment of prescription medications are used to combat these multiple conditions. It is also common for diabetic patients to be on more than one medication for the control of diabetes. Future studies could include work with multiple drugs that are most commonly used for the treatment of diabetes and

diabetes-induced illnesses/symptoms. One relatively new treatment uses a synthetic, incretin mimetic, glucoregulatory peptide in combination with sulfonylureas to control type II diabetes.[1, 2] Future studies could include such drugs as competing agents in drug-protein binding studies.

Ongoing work in our group is looking at serum samples containing glycated HSA that have been collected from diabetic patients. The HSA from these samples has been separated from the serum and immobilized onto silica for use in similar studies as have been outlined in this work. Comparing such samples to the *in vitro* samples used in these studies will also be valuable in future work.

References

1. Cvetkovic, R. S.; Plosker, G. L., *Drugs* **2007,** *67* (6), 935-954.

2. Keating, G. M., *Drugs* **2005,** *65* (12), 1681-1692.